

**REGULATION OF DNA REPAIR IN RESPONSE TO OXIDATIVE STRESS
IN HUMAN CELLS**

By

Samantha Phillips BSc (Hons)

**A thesis submitted for the
degree of Doctor of Philosophy
at the University of Leicester
2003**

**Department of Pathology
Robert Kilpatrick/Clinical Sciences Building
University of Leicester
Leicester**

UMI Number: U186672

All rights reserved

INFORMATION TO ALL USERS

The quality of this reproduction is dependent upon the quality of the copy submitted.

In the unlikely event that the author did not send a complete manuscript and there are missing pages, these will be noted. Also, if material had to be removed, a note will indicate the deletion.



UMI U186672

Published by ProQuest LLC 2013. Copyright in the Dissertation held by the Author.
Microform Edition © ProQuest LLC.

All rights reserved. This work is protected against
unauthorized copying under Title 17, United States Code.



ProQuest LLC
789 East Eisenhower Parkway
P.O. Box 1346
Ann Arbor, MI 48106-1346

ABSTRACT

Discovering more about maintenance of DNA integrity, despite its continual exposure to both endogenous and exogenous damaging agents is essential. The research presented in this thesis examined the regulation of DNA repair pathways in response to agents shown to induce oxidative stress and oxidative damage to cellular DNA in human dermal fibroblasts. Non-cytotoxic doses of hydrogen peroxide (H₂O₂), UVB irradiation, hypochlorite (HOCl) and vitamin C were established. Measurement of base excision repair (BER) and nucleotide excision repair (NER) factors using a ribonuclease protection assay showed little modulation of gene transcript levels in response to treatment with H₂O₂, UVB, HOCl or vitamin C. Significant changes in protein expression of the BER factors 8-oxoguanine glycosylase (hOGG1) and human apurinic/aprimidinic endonuclease (hAPE) and of the NER factors human homologue of Rad23 (hHR23B) and Xeroderma pigmentosum protein A (XPA) in response to oxidative stress were not observed. Likewise, significant changes in endonuclease nicking activity (measured as the excision activity at a known site of oxidative DNA damage) were not observed. Studies in MCF-7, MDA-MB-468, MDA-MB-436, MDA-MB-231, T47-D, ZR-75.1 and HBL-100 human breast cancer cell lines revealed significantly elevated endonuclease nicking activity in the MDA-MB-436 cell line compared to human dermal fibroblasts. In contrast to the other breast cancer cell lines under investigation, MDA-MB-436 cells were found to have a relatively low gene expression of the nucleotide pool sanitiser, human MutT homologue (hMTH1). The other breast cancer cell lines possessed increased gene expression of hMTH1 relative to dermal fibroblasts, which may be as a response to increased oxidative stress generated as a consequence of the carcinogenesis process. In conclusion, regulation of DNA repair pathways in response to oxidative stress may be an important consequence in the carcinogenesis process. hMTH1 expression and endonuclease nicking activity may provide useful tools for investigations into carcinogenesis in the future.

Regulation of DNA repair in response to oxidative stress

For Grandma

x

ACKNOWLEDGEMENTS

I wish to thank Dr Karl Herbert and Professor Peter Farmer for their assistance, encouragement and enthusiasm throughout the completion of this thesis. I would also like to thank Drs Howard Pringle and Jacqui Shaw for their scientific input and advice.

I would like to acknowledge the Medical Research Council and Dr Karl Herbert, Department of Pathology, University of Leicester for their financial contributions.

I also wish to thank all of my friends and colleagues over the past three years for their much valued assistance and friendship.

And last but not least, I wish to give enormous thanks to my family and most especially my husband, Richard.

CONTENTS

	Page
Abstract	II
Dedication	III
Acknowledgements	IV
Contents	V
Index of Figures	VII
Index of Tables	IX
Abbreviations	X

CHAPTER ONE: Introduction	Page
1.1 Oxidative stress: causes and consequences	2
1.2 DNA damage mechanisms and damage detection	3
1.3 DNA damage and disease	6
1.4 DNA repair processes	8
1.4.1 Base excision repair (BER)	9
1.4.2 Nucleotide excision repair (NER)	13
1.5 Co-ordination of oxidative DNA damage repair	19
1.6 Modulation of BER and NER pathways	20
1.7 The importance of p53 in repair processes	21
1.8 Consequences of repair defects	22
1.9 Aims and objectives	23

CHAPTER TWO: Materials and Methods	Page
2.1 Materials	26
2.2 Equipment	32
2.3 Methods	34

CHAPTER THREE: Establishing a cellular model to study responses to oxidative stress	Page
3.1 Introduction	52
3.2 Aims	57
3.3 Methods	58
3.4 Results	66
3.5 Discussion	81

CHAPTER FOUR: Modulation of BER and NER gene expression during oxidative stress in human fibroblasts	Page
4.1 Introduction	91
4.2 Aims	95
4.3 Methods	96
4.4 Results	98
4.5 Discussion	116

CHAPTER FIVE: DNA repair activity in response to oxidative stress and in breast cancer		Page
5.1	Introduction	129
5.2	Aims	132
5.3	Methods	133
5.4	Results	139
5.5	Discussion	166
 CHAPTER SIX: General discussion and Future work		 Page
6.1	General discussion	177
6.2	Future work	184
 APPENDICES		 Page
Appendix I: Design of hMTH1 primers		186
Appendix II: Raw data from densitometric analysis of ribonuclease Protection assay (example)		187
Appendix III: hMTH1 PCR product sequencing data		190
Appendix IV: Emission spectrum of UVB lamp		194
Appendix V: Communications arising from this thesis		195
 REFERENCES		 196

INDEX OF FIGURES

	Page
1.1 The mechanism of formation of guanine products from radical attack of •OH at the C8 position	4
1.2 Fenton reaction and dismutation reaction	6
1.3 Spectrum of cellular responses produced by reactive oxygen species	7
1.4 Base excision repair pathways in mammalian cells	10
1.5 Proposed model for nucleotide excision repair pathways in mammalian cells	15
3.1 Cellular responses and consequences of oxidative stress	53
3.2 Mechanisms of UV-induced DNA damage mediated by photosensitisers and its sequence specificity	56
3.3 Flow diagram illustrating the steps involved in the alkaline unwinding assay of adherent cells	62
3.4 An overview of the Riboquant™ Multi-probe Ribonuclease Protection Assay	64
3.5 Integrity of RNA extracted from CCRF-HSB-2 cells using three separate RNA isolation kits	68
3.6 Human dermal fibroblast viability over time following treatment with a range of ROS generating agents and the antioxidant vitamin C	71
3.7 Dose-dependent increase in cell viability measurement following treatment of dermal fibroblasts with three doses of vitamin C	72
3.8 Dose-dependent increase in A492 readings following incubation of vitamin C with dermal fibroblasts and also in a cell-free environment	73
3.9 Percentage double-stranded DNA measured by alkaline unwinding following treatment of dermal fibroblasts with H ₂ O ₂ , HOCl, UVB and vitamin C	74
3.10 Measurement of strand breaks induced per cell in fibroblasts treated with H ₂ O ₂ , HOCl, UVB and vitamin C	75
3.11 Oxidative DNA damage in fibroblasts treated with H ₂ O ₂ , HOCl, UVB and vitamin C	77
3.12 Ribonuclease protection assay of CCRF-HSB-2 cells using hBER-1 multi-probe template set	79
3.13 Ribonuclease protection assay of CCRF-HSB-2 cells using hNER-2 multi-probe template set	80
4.1 Effects of H ₂ O ₂ on BER gene expression	99
4.2 Effects of H ₂ O ₂ , UVB, HOCl and vitamin C on BER gene expression in human dermal fibroblasts	101
4.3 Effects of vitamin C on NER gene expression	103
4.4 Effects of H ₂ O ₂ , UVB, HOCl and vitamin C on hNER-1 gene expression in human dermal fibroblasts	104
4.5 Effects of vitamin C on NER gene expression	107
4.6 Effects of H ₂ O ₂ , UVB, HOCl and vitamin C on hNER-2 gene expression	108
4.7 Western blot of mammalian DNA repair factors hAPE, hOGG1, hHR23B and XPA in human dermal fibroblasts	112
4.8 Effect of H ₂ O ₂ , UVB, HOCl and vitamin C on hAPE protein levels in human dermal fibroblasts	113
4.9 Effect of H ₂ O ₂ , UVB, HOCl and vitamin C on hHR23B protein levels in human dermal fibroblasts	113
4.10 Effect of H ₂ O ₂ , UVB, HOCl and vitamin C on hOGG1 protein levels in human dermal fibroblasts	114

Regulation of DNA repair in response to oxidative stress

4.11	Effect of H ₂ O ₂ , UVB, HOCl and vitamin C on hHR23B protein levels in human dermal fibroblasts	115
5.1	Schematic illustration of routes to remove and prevent 8-oxoguanine in nuclear DNA	131
5.2	An overview of the endonuclease nicking assay	136
5.3	Endonuclease nicking assay with two concentrations of purified Fpg protein	140
5.4	Endonuclease nicking assay of two concentrations of purified Fpg protein at different timepoints	141
5.5	Endonuclease nicking assays to determine optimum concentration of cell lysate and incubation time for analysis of dermal fibroblast repair activity	142
5.6	9mer product formation after two hours incubation at 37°C with different amounts of total cellular protein	143
5.7	Repair activity over time	143
5.8	Lack of endonuclease nicking activity with undamaged 24mer oligonucleotide	144
5.9	Endonuclease nicking activity of dermal fibroblast cell lysates following treatment with 400 µM and 800 µM H ₂ O ₂	145
5.10	Effect of hydrogen peroxide on repair activity in dermal fibroblasts	146
5.11	Endonuclease nicking activity of dermal fibroblast cell lysates following treatment with 600 J/m ² and 1200 J/m ² UVB	148
5.12	Effect of UVB on repair activity in dermal fibroblasts	149
5.13	Endonuclease nicking activity of dermal fibroblast cell lysates following treatment with 300 nM and 600 nM HOCl	150
5.14	Effect of HOCl on repair activity in dermal fibroblasts	151
5.15	Endonuclease nicking activity of dermal fibroblast cell lysates following treatment with 400 µM and 800 µM vitamin C	152
5.16	Effect of vitamin C on repair activity in dermal fibroblasts	153
5.17	Endonuclease nicking activity of breast cancer cell lysates	154
5.18	Baseline repair activity in a panel of seven breast cancer cell lines	156
5.19	RT-PCR analysis of hMTH1 and β-actin in breast cancer cell lines	158
5.20	Comparative expression level of hMTH1 in breast cancer cell lines measured by RT-PCR	159
5.21	Quantitative real-time RT-PCR analysis of hMTH1 and β-actin mRNA expression in breast cancer cell lines	160
5.22	Melt curve generated from quantitative real-time RT-PCR analysis of hMTH1 and β-actin mRNA expression in breast cancer cell lines	160
5.23	Comparative expression levels of hMTH1 in breast cancer cell lines as measured by quantitative real-time RT-PCR analysis	163

INDEX OF TABLES

	Page
1.1 Profiles of some human DNA glycosylases	11
1.2 Summary of repair factors involved in nucleotide excision repair	18
2.1 Primary and secondary antibodies used for Western blotting	28
3.1 Summary of RNA extraction from CCRF-HSB-2 cell line using three commercially available RNA isolation kits	67
3.2 Comparison of RNA extracted from primary lymphocytes and normal dermal fibroblasts	69
4.1 Summary of studies designed to investigate modulation of BER factors following treatment with oxidising agents	93
4.2 Summary of changes in BER and NER gene expression following treatment with H ₂ O ₂ , UVB, HOCl and vitamin C	110
5.1 Summary of mean percentage 9mer formation and relative induction factors of breast cancer cell lines compared to dermal fibroblasts	157
5.2 Calculations of comparative expression levels of hMTH1 in breast cancer cell lines produced by quantitative real-time RT-PCR analysis	162
5.3 Comparison of relative expression levels of hMTH1 in breast cancer cell lines calculated from RT-PCR and quantitative real-time RT-PCR analysis	164

LIST OF ABBREVIATIONS

AA	Ascorbic acid
AMPS	Ammonium persulphate
AP	Apurinic/Apyrimidinic
AP-1	Activator Protein-1
ARE	Antioxidant Responsive Element
ATP	Adenosine 5' triphosphate
BER	Base excision repair
BRCA	Breast Cancer
BSA	Bovine serum albumin
CAK	Cdk-Activating Kinase
CCRF-HSB-2	Human Caucasian Acute Human T-Lymphoblastic Leukaemia Cells
Cdk	Cyclin-dependant Protein Kinase
CDNA	Complementary Deoxyribonucleic Acid
CHO	Chinese hamster ovary cells
CO ₂	Carbon dioxide
CPD	Cyclopyrimidine Dimers
CS	Cockayne' Syndrome
CSA	Cockayne' Syndrome Complementation Group A
CSB	Cockayne' Syndrome Complementation Group B
C _T	Calculated threshold
DDB	DNA binding factor
DEP	Diesel exhaust particles
DEPC	Diethyl pyrocarbonate
dG	Deoxyguanosine
dGTP	Deoxyguanosine Triphosphate
DMEM	Dulbecco's Modified Eagles Medium
DMSO	Dimethylsulphoxide
DNA	Deoxyribonucleic acid
dNTP	Deoxynucleotide Triphosphate
DPBS	Dulbecco's phosphate buffered saline
DSB	Double Strand Break Repair
DTT	Dithioreitol
ECL	Enhanced chemiluminescence
E.coli	Escherichia Coli
EDTA	Ethylene diaminetetraacetic acid
ELISA	Enzyme Linked Immunoabsorbant Assay
ENTG	Human Homologue of <i>E.coli</i> Endonuclease III (Nth)
ERCC	Excision Repair Cross Complementation
ESCODD	European Standards Committee For Oxidative DNA Damage
Fapy-Ade	2,6-diamino-4-hydroxy-5-formamidopurine
Fapy-Gua	2,6-diamino-4-hydroxy-5-formamidopyrimidine
FEN-1	Flap structure-specific endonuclease 1
FCS	Foetal calf serum
GG-NER	Global Genome-Nucleotide Excision Repair
GST	Glutathione-S-Transferase
hAPE	Human Apurinic/Apyrimidinic Endonuclease
HBSS	Hank's Balanced Salt Solution
HCl	Hydrogen chloride

Regulation of DNA repair in response to oxidative stress

HCR	Host cell reactivation assay
HEPES	N-[2-hydroxyethyl]piperazine-N'-[ethanesulfonic acid]
hHR23B	Human Homologue to Rad23
HIF-1	Hypoxia-Inducible Factor-1
hMTH1	Human MutT Homologue
hMYH	Human Mut Y Homologue
hNEIL	Human Nei-Endonuclease VIII-Like
hNTH	Human Endonuclease III Homologue
H ₂ O ₂	Hydrogen peroxide
HOCl	Hypochlorite
hOGG1	Human 8-oxoguanine glycosylase 1
HPLC	High performance liquid chromatography
HRP	Horse radish peroxidase
HSF1	Heat Shock Transcription Factor 1
hSMUG1	Human 5-hydroxymethyluracil Glycosylase
hTDG	Human Thymine DNA Glycosylase
hUNG	Uracil DNA Glycosylase
IgG	Immunoglobulin G
LBB	Lysis binding buffer
MAT1	Ménage-a-trois protein 1
MGMT	O ⁶ -Methylguanine-DNA Methyl-Transferase
MMR	Mismatch Repair
MOPS	3-[N-morpholino]propanesulfonic acid
MPC	Magnetic particle concentrator
MPG	Methylpurine Glycosylase
mRNA	Messenger ribonucleic acid
mtDNA	Mitochondrial DNA
MTS	3-4,5-Dimethylthiazol-2-yl)-5-(3-carboxymethoxyphenyl)-2-(4-sulfophenyl)-2H-tetrazolium
NDF	Normal dermal fibroblasts
NER	Nucleotide excision repair
NIR	Nucleotide Incision Repair
NF-κB	Nuclear Factor-κB
NO	Nitric Oxide
NQO1	NAD(P)H:Quinone Oxidoreductase
8-oxodATP	7, 8-dihydro-8-oxo-2'-deoxyadenosine
8-oxodG	7, 8-dihydro-8-oxo-2'-deoxyguanosine
8-oxoG	8-oxoguanine
PAGE	Polyacrylamide gel electrophoresis
PARP	Poly (ADP)-ribose polymerase
PBMC	Peripheral blood mononuclear cells
PBS	Phosphate buffered saline
PCNA	Proliferating Cell Nuclear Antigen
PCR	Polymerase chain reaction
PIPES	Piperazine-N,N'-bis[2-ethanesulphonic acid],1,4-piperazinediethanesulphonic acid)
PMS	Phenazine methosulphate
PVDF	Polyvinylidene difluoride
RFC	Replication Factor C
RNA	Ribonucleic Acid

Regulation of DNA repair in response to oxidative stress

RNA	Ribonucleic acid
RNase	Ribonuclease
ROS	Reactive oxygen species
RPA	Replication Protein A
RPMI-1640	Roswell Park Memorial Institute medium-1640
rRNA	Ribosomal ribonucleic acid
RT-PCR	Reverse transcriptase polymerase chain reaction
<i>S.cerevisiae</i>	<i>Sacchromyces Cerevisiae</i>
SDS	Sodium dodecyl sulphate
SOD	Superoxide Dismutase
TAE	Tris acetate EDTA buffer
TBE	Tris borate EDTA buffer
TBS	Tris buffered saline
TBS-T	Tris buffered saline with Tween 20
TC-NER	Transcription Coupled-Nucleotide Excision Repair
TE	Tris EDTA buffer
T/E	Trypsin/EDTA
TEMED	N,N,N',N'-tetramethylethylenediamine
TFIIH	RNA Polymerase II Transcription Factor II H
TPA	12-O-tetradecanoylphorbol-13-acetate
Triton X-100	t-Octylphenoxypolyethoxyethanol
TRNA	Transfer RNA
TTD	Trichothiodystrophy
Tween 20	Olyoxyethylenesorbitan monolaurate
UP	Ultra pure
UV	Ultra violet
UVA	Ultraviolet A (320-400 nm)
UVB	Ultraviolet B (280-320 nm)
UVC	Ultraviolet C (100-280 nm)
XP	Xeroderma Pigmentosum
XPA	Xeroderma Pigmentosum Complementation Group A
XPB	Xeroderma Pigmentosum Complementation Group B
XPC	Xeroderma Pigmentosum Complementation Group C
XPD	Xeroderma Pigmentosum Complementation Group D
XPE	Xeroderma Pigmentosum Complementation Group E
XPF	Xeroderma Pigmentosum Complementation Group F
XPG	Xeroderma Pigmentosum Complementation Group G
XP-V	Xeroderma Pigmentosum-Variant
XRCC1	X-ray Repair Cross-Complementing Protein 1

CHAPTER ONE

Introduction

CHAPTER 1: INTRODUCTION

Deoxyribonucleic acid (DNA) is often referred to as ‘the building block’ of life. Within its double helical structure exist the genes capable of maintaining and controlling the development of life. Maintaining the integrity of DNA is essential for every cellular life form, in order to ensure that an intact and viable genome is passed on to the next generation. If any sustained damage is present then serious consequences may result. A number of processes exist that protect against the development of cancer, and other diseases, which may result from damage to the structure of DNA. Discovering more about how the integrity of DNA is maintained, despite the continual exposure to both endogenous and exogenous agents that threaten to alter the structure of DNA, is essential. It is hoped that increasing our knowledge of inherent protective systems will enable us to manage and prevent these diseases better in the future.

1.1 Oxidative stress: causes and consequences

Oxidative stress in cells occurs as a result of an imbalance in the production of harmful reactive oxygen species (ROS) and free radicals, such as nitric oxide (NO) and peroxy radicals (ROO[•]), and the actions of the antioxidant defense system. ROS and other species are able to react with biological macromolecules such as lipids, proteins and nucleic acids (Floyd, 1990). ROS species include oxygen free radicals such as superoxide (O₂^{•-}) and the hydroxyl radical (•OH), and non-radical oxidants such as hydrogen peroxide (H₂O₂) and singlet oxygen (¹O₂).

ROS are present in the body as a consequence of both endogenous and exogenous processes. The main endogenous source of ROS is as a byproduct of aerobic metabolism, caused by the partial reduction of O₂ in the electron transport chain to produce O₂^{•-}, which then subsequently forms H₂O₂ and •OH radicals (Henle & Linn, 1997). The fact that DNA adduct levels within different species correlates roughly with metabolic rate, suggests that this process is a very important cause of oxidative stress (Adelman *et al.*, 1998). Other endogenous sources of ROS include the ‘oxidative burst’ associated with phagocytes, neutrophils and macrophages, which are important in the immune response. Visible light, ultraviolet light, ionizing radiations and a range of reactive xenobiotics (e.g. quinines and

peroxides) add to the endogenous ROS sources, to ensure that the mammalian body is under constant exposure to these reactive species.

ROS can damage DNA directly by attacking any of its four bases (adenine, thymine, guanosine and cytosine) or the deoxyribose-phosphate backbone. Indirect damage occurs via propagation reactions due to the formation of reactive intermediates produced after attack on other cellular components such as lipids and proteins (Marnett, 2000).

1.2 DNA damage mechanisms and damage detection

Oxidative damage of cellular DNA has been detected by chemical, physical, enzymatic and immunochemical methods (Ames, 1989; Cadet *et al.*, 1997; Dizdaroglu *et al.*, 2002). Steady state levels of oxidative DNA adducts have been measured at one or more orders of magnitude greater compared to non-oxidative adducts such as methylated, deaminated and depurinated products (Beckman & Ames, 1997).

The four major classes of DNA damage are; strand breaks (either single-strand or double-strand breaks), abasic sites (apurinic/apyrimidinic or AP sites), base modifications and DNA-protein cross-links (Cadet *et al.*, 1997). As many as one hundred different DNA modifications have been observed after exposure to ROS (Cadet *et al.*, 1997). Guanine is the most easily oxidized of the four DNA bases due to its low oxidation potential (Kawanishi *et al.*, 2001). The most abundant and most studied oxidative lesion in mammalian DNA is the C-8 oxidation of guanine, which leads to the formation of 7,8-dihydro-8-oxoguanine, also called 8-oxoguanine (8-oxoG) (Boiteux & Laval, 1997) (**figure 1.1**).

8-oxoG and its deoxyribonucleosidase, 8-oxo-7,8-dihydro-2'-deoxyguanosine (8-oxodG) have been studied by various analytical techniques (HPLC-ECD, HPLC-MS/MS, GC-MS, ELISA) in order to determine background levels of oxidative damage and the consequences of subjecting cells to increased oxidative stress (Cadet *et al.*, 2000; Helbock *et al.*, 1999; Loft & Poulsen, 1999).

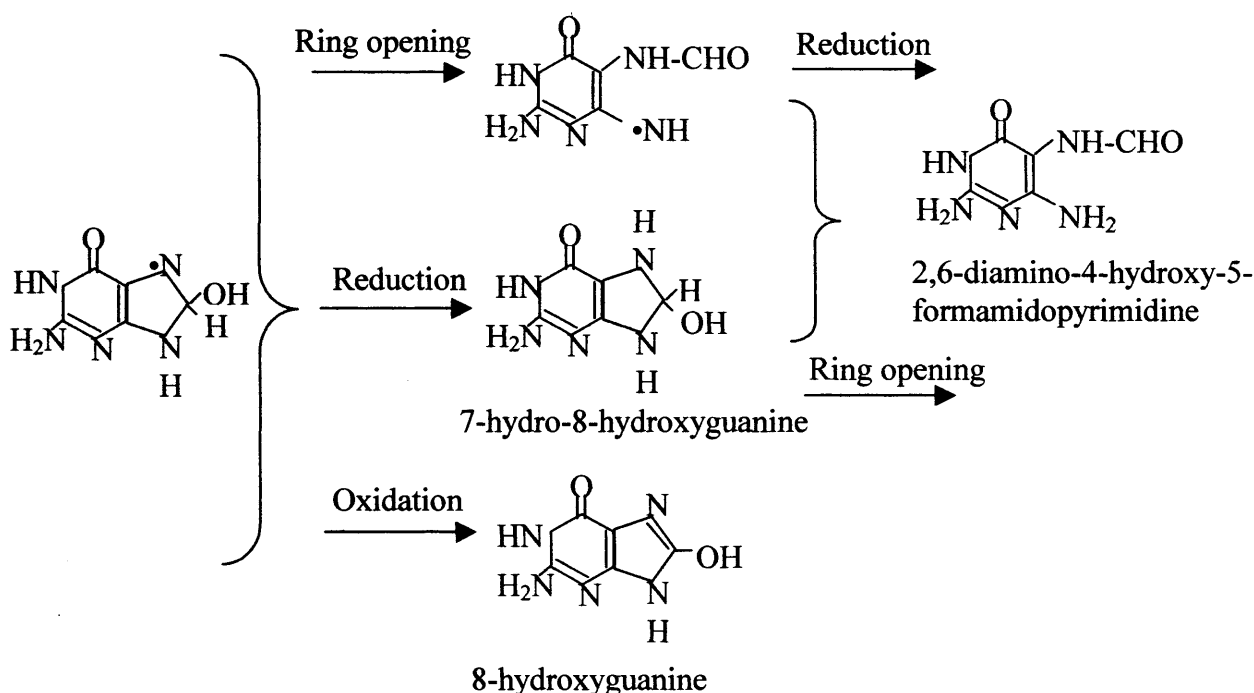


Figure 1.1: The mechanism of formation of guanine products from radical attack of $\cdot\text{OH}$ at the C8 position.

Adapted from Dizdaroglu *et al.*, 2002.

One report suggests that oxidised guanine is present in the human genome at the level of 0.1 8-oxodG lesions per 10^5 base pairs, making oxidised deoxyguanosine levels several times as great as those of classical aromatic carcinogens such as benzo[a]pyrene in lymphocytes or lung tissue DNA (Loft & Poulsen, 1996). However, considerable controversy has been generated concerning the accuracy of such methods due to problems with the artificial generation of adducts during sample preparation and analysis (Helbock *et al.*, 1998; Ravanat *et al.*, 2002). This is highlighted by considerable differences in measurements produced by different groups (Loft & Poulsen, 1999). In recent years, the European Standards Committee for Oxidative DNA Damage (ESCODD) has been formed, in an effort to standardise methods of oxidative DNA damage detection. This collaboration aims to ensure reliable, sensitive analysis of both endogenous and induced levels of oxidative damage to DNA (ESCODD, 2000; 2002; 2003). The latest findings report values of 8-oxodG present at 4.01 per 10^6 guanines as measured by chromatographic methods and 0.53 per 10^6 guanines for enzyme-based techniques as measured in HeLa cells (ESCODD, 2003).

Despite the high occurrence of 8-oxoG, AP sites are the most common form of DNA damage. It is estimated that 10,000 to 20,000 apurinic and 500 apyrimidinic sites are produced per cell each day under normal physiological conditions (Kreklau *et al.*, 2001), although many of these may be generated as intermediates of repair (see Base excision repair section 1.4.1). This compares to approximately 1000 8-oxodG lesions per cell per day (Capelli *et al.*, 2001). Base damage and strand breaks are repaired at different rates (Akman *et al.*, 2000); 8-oxoG is repaired at a quarter of the rate of uracil, produced in DNA by the deamination of cytosine, and uracil is repaired seven times slower than AP sites (Capelli *et al.*, 2001). Unrepaired AP sites halt mRNA and DNA synthesis or act as non-coding lesions, increasing the formation of mutations (Hsieh *et al.*, 2001). It is thought that 10,000 purines and 200 pyrimidines are lost spontaneously during each completed cell cycle (typically lasting twenty-four hours) of mammalian cells.

Damage to DNA is not homogeneous throughout the genome. The heterogeneous nature of DNA, exemplified by the presence of supercoiling and histones within DNA superstructure, also alters susceptibility to DNA damage. Histones present on nuclear DNA diminish the occurrence of the Fenton reaction (see **figure 1.2**). 8-oxodG is between ten and fifteen times more abundant in mitochondrial DNA (mtDNA) than in nuclear DNA (Loft & Poulsen, 1996). This may be as a consequence of the proximity of ROS generation at the site of oxidative phosphorylation in mitochondria, the lack of histones in mtDNA, different pathways and rates of DNA repair processes, or a combination of these factors.

The binding of metal ions to DNA also influences sites of DNA damage, as these ions may catalyse a reaction known as the Fenton reaction (**figure 1.2**). This reaction generates ROS in close proximity to DNA itself, including $\cdot\text{OH}$, which is the most reactive and therefore most damaging of all ROS. Oxidative stress may also liberate iron ions from their sites of sequestration within the cell so that they can bind to DNA (Halliwell & Gutteridge, 1990). Metal ions bind to GG with greater preference than to any other G containing sequences, making the formation of purine adducts even more likely (Kawanishi *et al.* 2001).

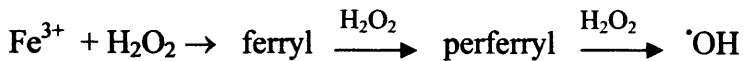
As shown in **figure 1.1**, the creation of such oxidised products as 8-oxoG can lead to subsequent formation of numerous more products depending on the experimental

conditions, the redox status of the surrounding cells and the availability of metal ions (Dizdaroglu *et al.*, 2002).

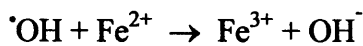
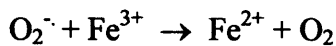
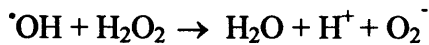
Fenton Reaction



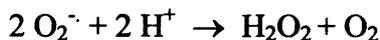
Some Fe^{3+} complexes can react further with H_2O_2 in a multi stage process e.g.



Additional reactions can then occur:



Dismutation Reaction



At physiological pH it is largely the sum of the following two stages:

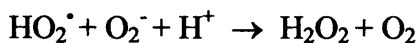
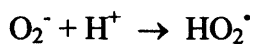


Figure 1.2: Fenton Reaction and Dismutation Reaction

(Adapted from Halliwell & Gutteridge, 1990).

1.3 DNA damage and disease

Biological consequences of ROS damage to DNA include chromosome alterations, gene mutations, cell transformation and cell death (Martins & Meneghini, 1990; Hoeijmakers, 2001). DNA lesions may be genotoxic and lead to mutations such as those commonly observed in mutated protooncogenes and tumour suppressor genes such as p53 (Hainaut *et al.*, 1998; Lengauer *et al.*, 1998) but ROS are not only genotoxic, they may also modulate gene expression via activation of transcription factors. For example, nuclear factor- κ B (NF- κ B) and heat shock transcription factor 1 (HSF1) are both activated by ROS

(Martindale & Holbrook, 2002; Michiels *et al.*, 2002). ROS damage is also known to alter cell cycle kinetics, induce apoptosis (programmed cell death) (Marnett, 2000) and influence second messengers such as calcium (Epe, 1995).

Low levels of oxidative stress have been suggested to induce cellular proliferation instead of inducing apoptosis and necrosis (Kondo *et al.*, 2000), whilst growth arrest/senescence have been reported in cells exposed to intermediate levels (**figure 1.3**).

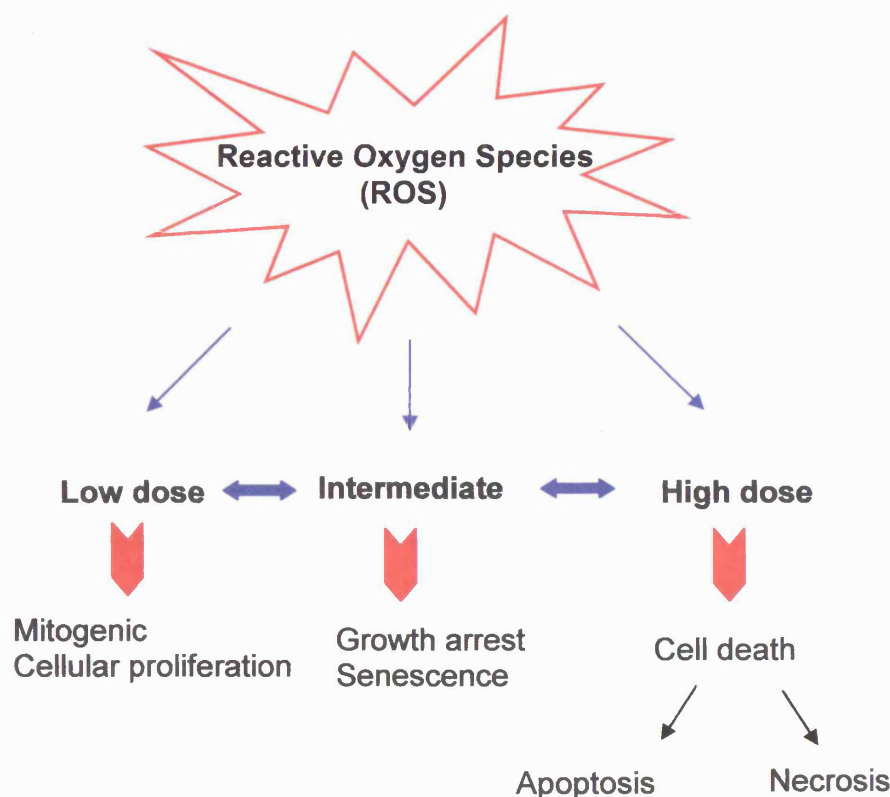


Figure 1.3: Spectrum of cellular responses produced by reactive oxygen species. Responses produced depend on the severity of the damage, which is influenced by the cell type, magnitude of the dose and duration of the exposure. Typically low doses of ROS are mitogenic and promote cellular proliferation. Intermediate doses may result in either temporary or permanent growth arrest. Severe oxidative stress may cause cell death, either via apoptosis or necrosis.

The ROS-generating chemicals H_2O_2 and paraquat have been shown capable of increasing spontaneous mutation frequencies by up to 27-fold in human lung cancer cell lines (Zienoldding *et al.*, 2000), with the actual sites of DNA damage reportedly affecting mutation frequencies (Kawanishi *et al.*, 2001). Evidence for a role of ROS in carcinogenesis has been found in mouse models (Floyd, 1990) and, as exemplified below,

clinical studies have been performed to determine the extent that oxidative stress contributes to carcinogenesis and other disorders in humans.

Malins and Haimanot (1991) associated oxidised DNA bases with breast cancer, showing a nine-fold increase in the levels of 8-oxoG, 8-hydroxyadenine (8-oxoA) and a formidopyrimidine in breast tumour tissue compared with surrounding normal tissue. Increased levels of 8-oxodG in breast cancer were also measured by Li *et al.*, (2001), whilst Okamoto *et al.*, (1994) demonstrated high levels in tumours of the kidney. Shimoda *et al.*, (1994) showed an increase of 8-oxodG in the liver tissue of sufferers of chronic inflammatory diseases such as cirrhosis and hepatitis. Smokers and personnel exposed to ionising radiations and transition metals have also been reported to have increased levels of 8-oxodG (Kondo *et al.*, 2000). Recently, elevated levels of 8-oxodG have also been reported in human atherosclerotic plaques (Martinet *et al.*, 2002) and ROS have also been associated with the pathogenesis of chronic obstructive pulmonary disease (Langen *et al.*, 2003).

1.4 DNA repair processes

In order to limit the damage caused by oxidative stress a number of intricate antioxidant defence systems have evolved. These include enzymes such as superoxide dismutase (SOD), catalase, glutathione peroxidase and peroxyredoxins, as well as low-molecular mass scavengers such as glutathione. Increased expression of some of these antioxidants has been recorded in response to oxidative stress mediated by what is known as the antioxidant responsive elements (ARE) of genes. Antioxidant-inducible genes include glutathione-S-transferase (GSTs) and NAD(P)H:quinine oxidoreductase (NQO1) (Loft & Poulsen, 2000). It is when these antioxidant defences can no longer cope with the damage inflicted from ROS, that oxidative stress is generated. In order to combat damage inflicted by excess ROS, DNA is also continuously repaired by a variety of enzymes in a number of distinct repair processes. Of these, base excision repair (BER) and nucleotide repair (NER), play a major role. Other repair processes, such as double strand break (DSB) and mismatch repair (MMR) also contribute to conserving the integrity of the genome (Wood *et al.*, 2001).

1.4.1 Base excision repair (BER)

BER is a multistep process largely responsible for the removal of small, non-bulky base adducts including oxidative lesions. In human cells BER proceeds via a number of alternative pathways (**figure 1.4**); the ‘short-patch’ DNA polymerase β -dependent pathway (left hand pathway in **figure 1.4**) involves the excision and replacement of a single damaged nucleotide, whilst the ‘long-patch’ proliferating cell nuclear antigen (PCNA)-dependent pathway (centre pathway in **figure 1.4**) involves the replacement of up to eight nucleotides (Prasad *et al.*, 2001). More recently, an alternative pathway to classic BER has been described and termed nucleotide incision repair (NIR) (right hand pathway in **figure 1.4**) (Ischenko & Saporbaev, 2002).

‘Short-patch’ and ‘long-patch’ BER processes involve the recognition of a modified base by a DNA glycosylase. The damaged base is released by hydrolytic cleavage of the N-glycosyl bond connecting the base to the deoxyribose, leaving an apurinic/apyrimidinic (AP) site. The phosphodiester DNA backbone is then cleaved on the 5’ side of the AP site by an AP endonuclease, generating 3’-OH and 5’deoxyribose phosphate ends. In ‘short-patch’ repair, the 5’deoxyribose phosphate termini is excised to leave a single nucleotide gap which is filled by a DNA polymerase before the nick is sealed by a DNA ligase (Hickson, 1997). ‘Long-patch’ repair involves the excision of 2-8 nucleotides that are removed by flap endonuclease (FEN-1) before DNA synthesis and ligation can occur. This general scheme is commonly used by all organisms, although in some cases the initial DNA glycosylase may also have lyase activity (Bouziane *et al.*, 2000). The type of glycosylase initiating repair, along with possibly the cell cycle status of the cell, governs which BER pathway is followed (Krokan *et al.*, 2000).

Glycosylases

A number of DNA glycosylases have been identified in humans; each excises a specific subset of damaged bases, although there seems to be an extensive redundancy of function for some enzymes (**table 1.1**). For oxidized DNA bases in humans, 8-oxoG DNA glycosylase (hOGG1) is the best studied. This is a bifunctional enzyme, possessing lyase activity as well as a glycosylase function, which is known to excise 8-oxoG.

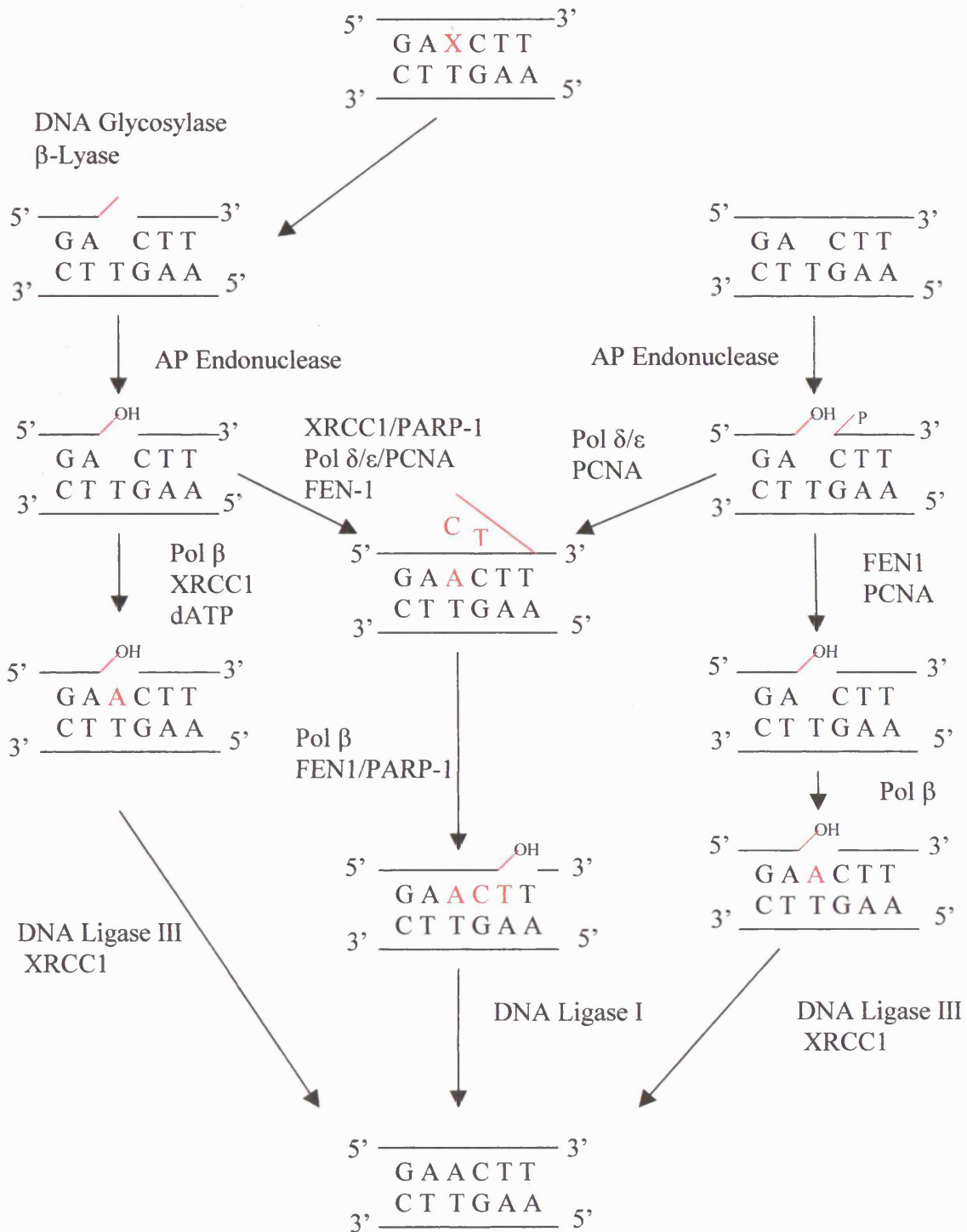


Figure 1.4: BER Pathways in mammalian cells. Left pathway represents bases removed by monofunctional, and bifunctional DNA glycosylases with AP lyase activity (short patch repair). Centre pathway shows long patch repair. Right hand pathway is a minor pathway in mammalian cells, probably associated with the repair of modified abasic sites not recognized by the APE protein.

Adapted from Akman, et al., 2000.

Glycosylase	Lyase Activity	Cellular Localisation	Substrate Specificity
hOGG1	Yes	Nuclear(α) Mitochondrial (β)	MefapyG:C>>fapyG:C>>8-oxoG:C>>8-oxoG:T
hNTH1	Yes	Nuclear Mitochondrial?	T/C-glycol, fapy, dihydrouracil
hMYH	Possibly.	Nuclear Mitochondrial.	Misincorporated A:8-oxoG, A:G, A:C
hNEIL1	Yes	Nuclear	Stalled replication. T-glycol.
hNEIL2	Yes	Nuclear	Oxidised cytosine & 5-hydroxyuracil
hNEIL3	Yes	Nuclear	Removes fragmented/oxidized pyrimidines
hMPG	No	-	3-meA, 7-meA, 3-meG, 7-meG, 8-oxoG, hypoxanthine, ϵ A, ϵ G
hTDG	No	Nuclear	U:G> ϵ C:G>T:G
hSMUG1	No	-	ssU>U:A, U:G
hUNG1	No	Mitochondrial	ssU>U:G>U:A, 5-FU, poor
hUNG2	No	Nuclear	repair of 5-hydroxyU, isodialuric acid, alloxan

Table 1.1: Profiles of some human DNA glycosylases. Substrate specificities are described for the nucleotide bases adenine (A), cytosine (C), guanine (G), thymine (T), uracil (U) and single-stranded (ss), methyl (me) and etheno (ϵ) adducts. Human DNA glycosylases listed are 8-oxoguanine glycosylase (hOGG1), endonuclease III homologue (hNTH1), Mut Y homologue (hMYH), nei endonuclease VIII-like 1, 2 and 3 (hNEIL1, 2 & 3), methylpurine DNA glycosylase (hMPG), thymine DNA glycosylase (hTDG), 5-hydroxymethyluracil glycosylase (hSMUG1), uracil DNA glycosylase 1 and 2 (hUNG1 & 2).

Adapted from Neilson & Krokan, 2001.

Chapter 1: Introduction

It has been suggested that hOGG1 is the rate-limiting step in human BER of 8-oxoG because of its high affinity for the damaged site (Vidal *et al.*, 2001). The half-life of the hOGG1 complex has been measured at greater than two hours, thus leading to a lack of hOGG1 turnover.

The presence of the major human endonuclease hAPE1 stimulates the glycosylase activity of OGG1 and increases the efficiency of the process. It has been suggested that under physiological conditions hOGG1 is in fact a monofunctional enzyme, perhaps with lyase activity simply acting as a back up system (Vidal *et al.*, 2001). In fact the rate of the *in vitro* reaction only partly depends on cellular levels; addition of the hOGG1 enzyme to cellular extracts does not always produce a proportional increase in activity (Capelli *et al.*, 2001).

Other bifunctional DNA glycosylases include hNTH1 (human Nth homolog 1) and hNEH1, 2 and 3 (human Nei Homolog 1, 2 & 3). hNTH1 acts primarily on damaged pyrimidine derivatives resulting from ring saturation, ring fragmentation, ring contraction and unexpectedly ring-opened purine residues (Fapy) (Dizdaroglu *et al.*, 1999). hNTH1 acts preferentially on 5-hydroxycytosines and AP sites when they are situated opposite to guanine (Eide *et al.*, 2001) and also removes 8-oxoG when it is situated opposite to G (Matsumoto *et al.*, 2001). Meanwhile, hNEH1 excises Fapy, oxidised purines and also 8-oxoG, whilst hNEIL2 appears to have a rather limited substrate range, preferring only cytosine-derived lesions, with 5-hydroxyuracil as the preferred substrate (Hazra *et al.*, 2002; Hazra *et al.*, 2003). Initial characterization of the enzymic activity of hNEIL3 has shown that it removes fragmented and oxidized pyrimidines (www.cgal.icnet.uk/DNA_Repair_Genes.html). Tissue specific mRNA levels of hOGG1 and NEILs are distinct (Gros *et al.*, 2002). It is thought that hNEILs may account for the lack of phenotype in hOGG1 *-/-* knockout mice, perhaps being present as a backup system to oxidative damage.

The monofunctional DNA glycosylases single-strand mismatch-specific uracil-DNA glycosylase (SMUG1), human thymine DNA glycosylase (hTDG) and human MutY homolog (hMYH) all have differing specificities for the wide range of damaged bases occurring in DNA.

Endonucleases

The major human AP endonuclease hAPE (also known as HAP-1, Ref-1, Apex, Ape1) incises the phosphodiester backbone of DNA immediately 5' to the lesion and is involved in both 'short-patch' and 'long-patch' repair (Frosina *et al.*, 1996; Wilson & Barsky, 2001). This action produces a single-strand break with a normal 3'-hydroxyl group and an abnormal 5'-abasic terminus. Recently a second AP endonuclease, APE2, was identified in mammals (Hadi & Wilson, 2000) and was found to be localised in both nucleus and mitochondria (Tsuchimoto *et al.*, 2001). hAPE is a multi-functional protein that also has roles in the redox activation of transcription factors, redox activation of bioreductive drugs, redox activation of p53 and the negative response element of the parathyroid hormone gene (Evans *et al.*, 2000).

Ligation

In the 'short-patch' repair pathway the 5'-abasic residue is removed and the single nucleotide gap filled by PCNA-independent DNA polymerase β (DNA pol- β) before the nick is then sealed by a complex of XRCC1/DNA ligase III (Wilson & Thompson, 1997). 'Long-patch' repair involves PCNA-dependent DNA pol- β as well as Pol δ/ϵ in a PARP-1 and FEN-1 stimulated reaction (Klungland & Lindahl, 1997; Prasad *et al.*, 2001). The scaffold protein XRCC1 is involved in both pathways. It is thought that 8-oxoG repair is thought to be carried out almost exclusively via the short patch repair pathway of BER. The recently described polynucleotide kinase (Whitehouse *et al.*, 2001) is believed to be important during repair synthesis following BER of single-strand breaks.

1.4.2 Nucleotide excision repair (NER)

NER removes large, bulky lesions capable of distorting both the helical conformation and chemical properties of DNA (Batty & Wood, 2000). This complex process involves the actions of at least 30 proteins (de Boer & Hoeijmakers, 2000).

Following damage recognition, the DNA helix is opened up around the damaged site and the two phosphodiester bonds either side of the lesion are hydrolysed to generate an oligonucleotide containing the damaged DNA. Usually, the 5th phosphodiester bond on the 3' side and 24th phosphodiester bond on the 5' side are hydrolysed to generate an

oligonucleotide in the range of 24 to 32 nucleotides with an average length of 27 nucleotides.

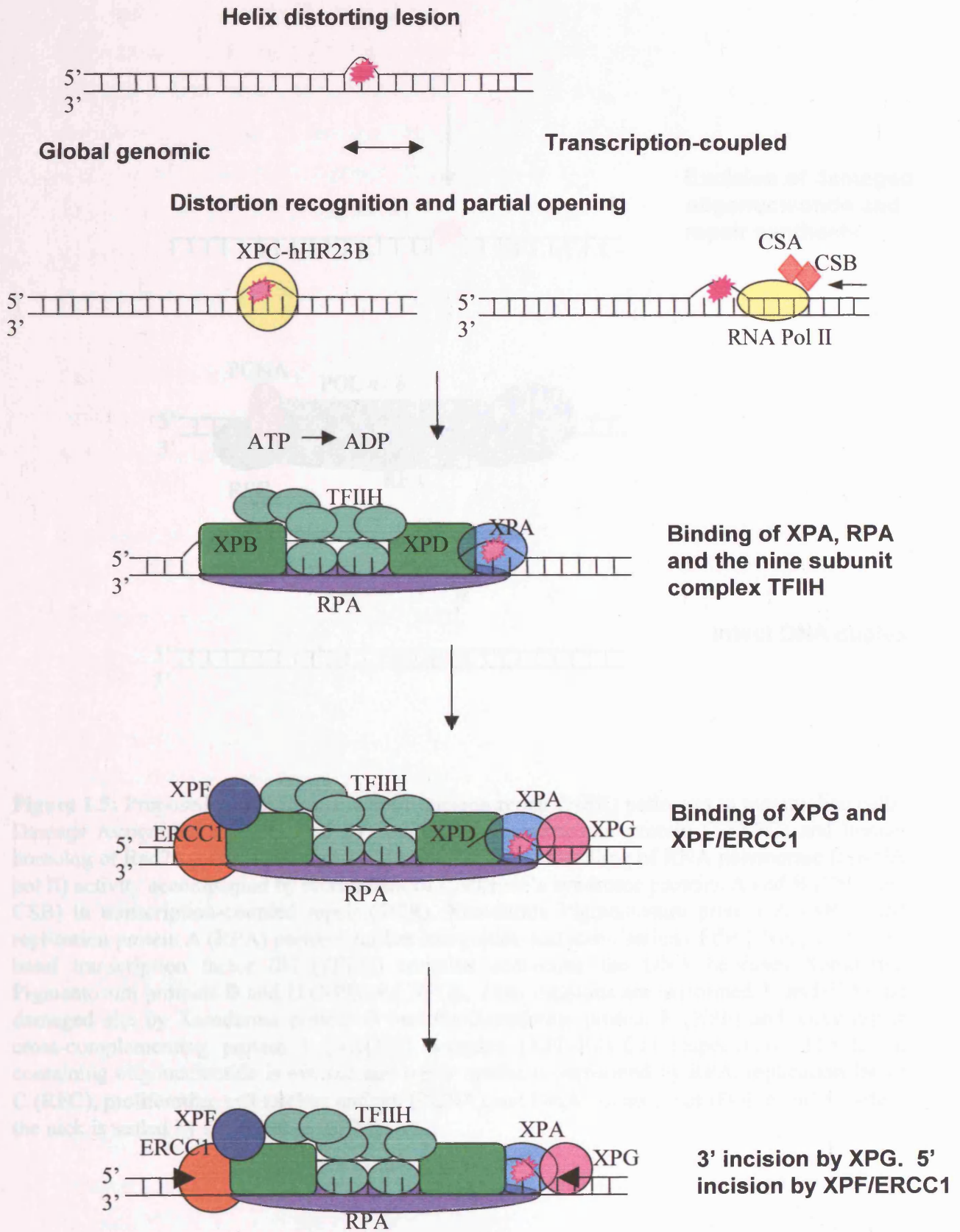
The incisions produced each side of the lesion are produced by a multisubunit ATP-dependent nuclease exinuclease, which in humans is composed of 16 polypeptides. The ATP dependent reaction is needed to 'deform' the DNA so that it kinks and unwinds to allow access to further repair complexes (Sancar, 1994). One or more of the proteins remains bound to the DNA, before being dissociated by replication and repair enzymes so that ligation can occur (Sancar, 1996).

The location of the lesion affects the rate of repair, as the greater the distortion of the DNA helix the easier it is to recognize the damage and the faster the repair can be carried out (Batty & Wood, 2000). Active genes are repaired far more efficiently than inactive ones (Hanawalt, 1995) and lesions within the template strand of a transcriptionally active gene are repaired more rapidly than lesions in the non-transcribing (coding) strand (Friedberg, 1996). The slow and inefficient repair of inactive genes is termed global genome repair (GGR), whilst the efficient repair of the transcribing strand of transcriptionally active genes is termed transcription coupled repair (TCR) (**figure 1.5**). This process also helps to resume transcription after DNA damage (Balajee *et al.*, 1998).

Global genome repair

The heterodimer XPC-hHR23B is the first component to recognize the damage in GGR. Its binding to the lesion site may lead to further distortion (Janićijević *et al.*, 2001), and aid the recruitment of RPA, XPA and the transcription factor II (TFIIH) (Batty & Wood, 2000).

XPA plays a crucial role at the early stages of both GGR and TCR. It is a DNA binding protein with marked preference for damaged DNA. In general the affinity of XPA correlates with the extent of the helical distortion caused by the DNA damage. It seems to act in verifying the NER lesion and plays a central role in positioning the repair machinery correctly around the injury.



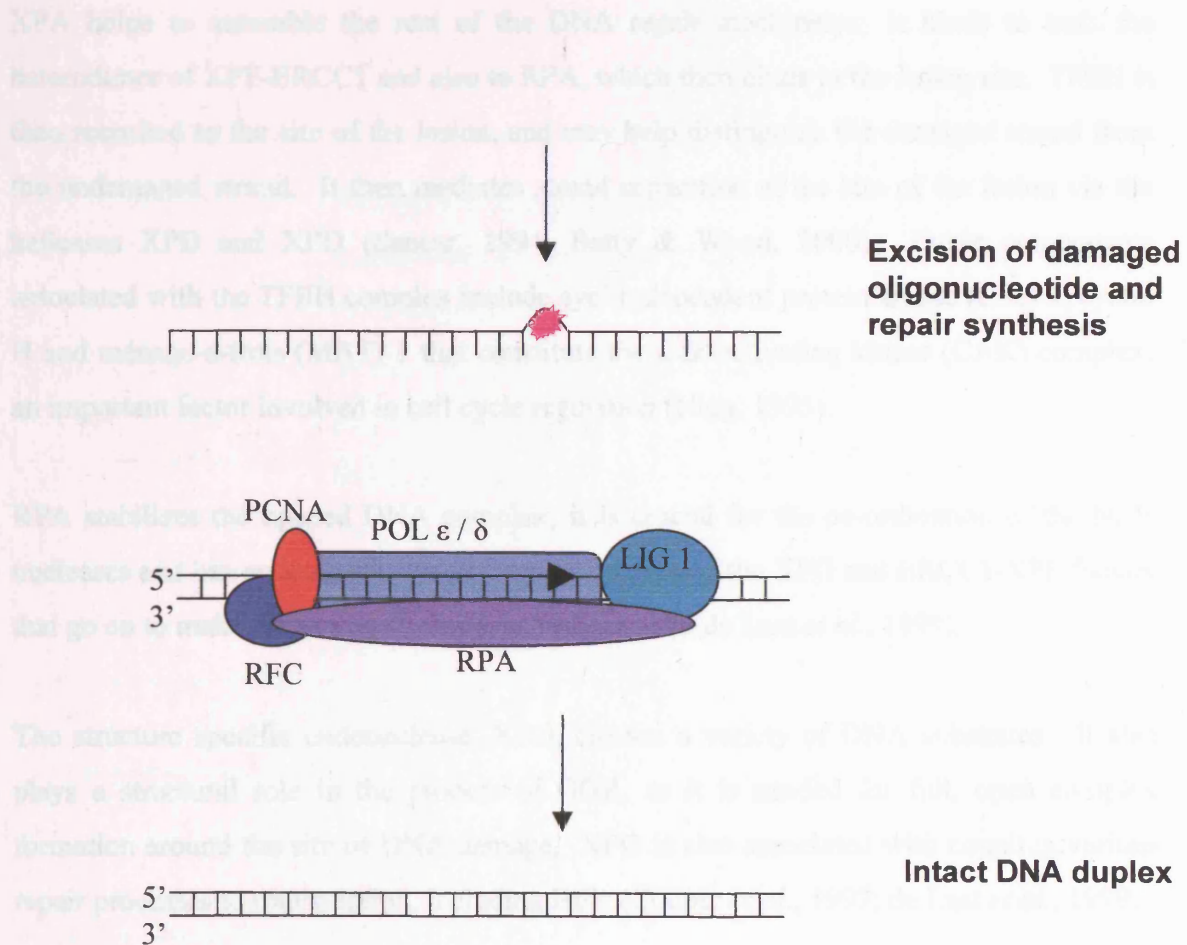


Figure 1.5: Proposed model for nucleotide excision repair (NER) pathways in mammalian cells. Damage recognition is performed by Xeroderma Pigmentosum protein C (XPC) and human homolog of Rad23 (hHR23B) in global genomic repair and stalling of RNA polymerase II (RNA pol II) activity accompanied by recruitment of Cockayne's syndrome proteins A and B (CSA and CSB) in transcription-coupled repair (TCR). Xeroderma Pigmentosum protein A (XPA) and replication protein A (RPA) perform further recognition and stabilisation of the RNA polymerase basal transcription factor IIIH (TFIIH) complex containing the DNA helicases Xeroderma Pigmentosum proteins B and D (XPB and XPD). Dual incisions are performed 3' and 5' to the damaged site by Xeroderma protein G and the Xeroderma protein F (XPF) and x-ray repair cross-complementing protein 1 (XRCC1) complex (XPF-ERCC1) respectively. The lesion containing oligonucleotide is excised and repair synthesis performed by RPA, replication factor C (RFC), proliferating cell nuclear antigen (PCNA) and DNA polymerases (POL ϵ and δ) before the nick is sealed by DNA ligase (LIG I).

XPA helps to assemble the rest of the DNA repair machinery. It binds to both the heterodimer of XPF-ERCC1 and also to RPA, which then binds to the lesion site. TFIIH is then recruited to the site of the lesion, and may help distinguish the damaged strand from the undamaged strand. It then mediates strand separation at the site of the lesion via the helicases XPB and XPD (Sancar, 1994; Batty & Wood, 2000). Other components associated with the TFIIH complex include cyclin-dependent protein kinase (Cdk) 7, cyclin H and ménage-a-trois (MAT) 1 that constitute the Cdk-activating kinase (CAK) complex, an important factor involved in cell cycle regulation (Nigg, 1995).

RPA stabilizes the opened DNA complex; it is crucial for the co-ordination of the NER nucleases and has an important role in the positioning of the XPG and ERCC1-XPF factors that go on to make the 3' and 5' incisions respectively (de Laat *et al.*, 1999).

The structure specific endonuclease, XPG, cleaves a variety of DNA substrates. It also plays a structural role in the process of GGR, as it is needed for full, open complex formation around the site of DNA damage. XPG is also associated with coupling various repair processes to transcription, including BER (Cooper *et al.*, 1997; de Laat *et al.*, 1999).

The catalytic turnover of the repair process is facilitated by PCNA, which releases the damage-containing oligomer and repair exonuclease subunits from the initial site of damage. The resulting gap is then filled by DNA polymerases δ or ϵ and ligated to form an intact strand of DNA by ligase I (Sancar, 1994). A summary of the factors involved in NER can be seen in **table 1.2**.

Transcription coupled repair

In TCR, damage recognition is performed when RNA polymerase II stalls at the site of a DNA lesion as it moves along a transcribing strand. The CSA/CSB heterodimer is recruited to the site of the stalled RNA polymerase II and, perhaps with the aid of TFIIH, backs off the RNA polymerase without dissociating it, so that other repair proteins may access the damaged site. CSA/CSB also recruits XPA to the lesion site, in order to increase the rate of assembly of the nuclease. CSA is thought to act as a general mediator, recruiting repair proteins to the damaged site, whilst CSB is a putative helicase that acts to unwind the DNA

helix, thus allowing access to other complexes. Excision and then repair synthesis then follow

Human Protein	Proposed Function
XPC-hHR23B	Recognises damage in non-transcribed DNA. Recruits other NER proteins.
CSA-CSB	Binds to stalled RNA polymerase II and initiates TCR-GGR.
XPA	Binds damaged DNA after XPC or RNA polymerase II.
RPA (p70, p32, p14)	Stabilises open complex with XPA and positions nucleases.
XPB	3' to 5' helicase.
TFIIHp62	?
TFIIHp52	?
TFIIHp44	DNA binding?
TFIIHp34	DNA binding?
XPD	5' to 3' helicase.
XPG	Endonuclease (3' incision). Stabilises full open complex.
XPF	Part of endonuclease (5' incision).
ERCC1	Part of endonuclease (5' incision).

Table 1.2: Summary of repair factors involved in NER. XP refers to the complementation groups of the human disease Xeroderma Pigmentosum. Abbreviations: human homolog of Rad 23 (hHR23B), replication protein A (RPA), RNA polymerase II basal transcription factor IIIH (TFIIH), x-ray repair cross-complementing protein 1 (XRCC1), Xeroderma pigmentosum complementation groups (XPA, XPB, XPC, XPD, XPF and XPG).

as in the GGR process. After the ligase dissociates, RNA polymerase is able to resume transcription along the repaired transcript (Sancar, 1996). The XPC-hHR23B complex helps to detect the lesion and recruit the rest of the repair machinery in GGR but it is the sole factor dispensable for TCR-NER, whilst both CSA and CSB are essential for TCR.

1.5 Co-ordination of oxidative DNA damage repair

Considerable overlap exists in the substrate specificity of the two excision repair pathways and certain proteins are involved in more than one pathway. BER is considered to be the main process involved in the removal of minor base damage induced by oxidising agents with NER acting as a backup system (de Boer & Hoeijmakers, 2000). NER has recently been shown to excise cyclopurine and pyrimidopurione oxidative lesions (Gros *et al.*, 2002) amongst others. Recently, the CSB protein has been linked to the repair of 8-oxoG through an interaction with hOGG1 in both nuclear (Tuo *et al.*, 2001; 2002) and mitochondrial DNA (Stevsner *et al.*, 2002). The interaction of these two processes requires further investigation to determine exactly how they cooperate to produce efficient DNA repair.

The TCR of thymine glycols (a type of oxidized pyrimidine) has been demonstrated in yeast cells exposed to H₂O₂. TCR of oxidative damage requires a function of the XPG protein distinct from that generally associated with its action in GGR-NER and is thought to involve the BER pathway (Cooper *et al.*, 1997; de Laat *et al.*, 1999; Klungland & Lindahl, 1997). BRCA1, a tumour suppressor gene linked to certain types of breast cancer, has also been linked with the TCR of oxidative damage (Gowan *et al.*, 1998; Leadon, 1999). However, there is currently some debate over the published evidence for such a role (Brinkley, 2003 [<http://www.biomedcentral.com/news/20030618/04>]), resulting in a retraction of the original paper (Gowan *et al.*, 2003).

In addition to repair pathways able to excise lesion-containing DNA, exists a protein able to remove oxidised bases from the nucleotide pool. Damaged nucleotides present in the nucleotide pool could be introduced into DNA and RNA during their synthesis. Mammalian cells contain MutT homolog (MTH1 or NUDT1), an 8-oxo-GTPase, which

hydrolyses 8-oxoGTP, 8-oxoGTP and 2-hydroxy(OH)-dATP and 8-oxodATP, preventing their misincorporation into RNA and DNA (Nakabeppu, 2001).

1.6 Modulation of BER and NER pathways

Evidence in the literature suggests that both BER and NER may be subject to regulation following exposure to potentially damaging agents. In *E.coli*, the presence of ROS such as O_2^- and H_2O_2 , rather than actual damage to the cellular DNA, is enough to elicit a protective response (the SoxRS and OxyR responses, respectively) (Volkert & Landini, 2001). Responses to direct damage to DNA are also activated following exposure to UV and methylation damage through the RecA and Ada regulatory proteins, respectively (Volkert & Landini, 2001).

Ribonuclease protection assay analysis of mRNA expression demonstrated an increase in transcript levels of the glycosylase genes *fpg*, *mutY*, *nth* and *nei* when *E.coli* were shifted from anaerobic to aerobic growth. Higher transcript levels of these DNA repair genes were also expressed when cells were in exponential growth phase compared to stationary phase (Gifford *et al.*, 2000).

In mammalian cells regulation of the *APE* gene was not observed following exposure to the DNA damaging agents 12-O-tetradecanoylphorbol-13-acetate (TPA), dimethyl sulphoxide, dexamethasone, bleomycin, paraquat or heat shock treatment (Harrison *et al.*, 1995). A number of studies have reported *APE* modulation post-treatment with the oxidative stress inducing agents H_2O_2 and HOCl (Grösch *et al.*, 1998; Ramana *et al.*, 1998; Saitoh *et al.*, 2001), crocodylite asbestos (Fung *et al.*, 1998) and peroxisome proliferators (Kim *et al.*, 2001). However, conflicting results for the different agents are also found in the literature (Hsieh *et al.*, 2001).

Reports suggest that NER may be subject to regulation following exposure to UV irradiation (Ye *et al.*, 1999; Maeda *et al.*, 2001; Adimoolam & Ford, 2002). However, there are no reports of modulation following oxidative stress, despite the involvement of TCR, and specifically CSB, in the repair of some oxidative lesions (Tuo *et al.*, 2001; Tuo *et al.*, 2002).

Small molecule antioxidants (vitamins E/C) have evolved to prevent membrane oxidation or to minimize the damage by removing it (Marnett, 2000) but there is still much controversy concerning their mechanisms of action and level of benefit gained. One possibility is that these molecules could act by up-regulating some of the enzymes involved in the removal of oxidative adducts from DNA (Cooke *et al.*, 2000).

Considering the wide ranging implications for a role of oxidative stress and ROS in carcinogenesis, other diseases and the aging process, it is very important that the exact regulatory mechanisms for the processes involved in dealing with such stresses are determined. Presently, there is much debate as to the presence of any adaptive response in mammalian cells following exposure to these damaging agents.

1.7 *The importance of p53 in repair processes*

The tumour suppressor p53 is the most commonly altered gene in human cancer. It is lost or contains mutation in approximately half of all human cancers (May & May, 1999). Following DNA damage the latent form of the protein is up regulated and converted to the active tetramer. It then performs important functions in G₁ cell cycle arrest or apoptosis and more recently has been indicated as performing a number of roles in the repair processes described above. The decision of which path to follow may be determined by the extent of the DNA damage (May & May, 1999).

Exact details of how p53 helps to regulate repair are not known as yet. p53 null cells show a partial defect in NER, suggesting an important role for p53 in this repair process (Ford & Hanawalt, 1997; Wani *et al.*, 1999). It is known that p53 binds directly to a number of GGR (XPB, XPD and RPA) and TCR (XPB, XPD, CSB and RPA) factors. p53 complexes with PCNA and also to RPA, converting it from its replication form to repair form (Sancar, 1996). p53 also modulates DNA polymerase δ or ϵ of the NER pathway (Offer *et al.*, 1999). The C-terminus of p53 binds XPB and XPD, constituents of the TFIIH complex, to inhibit their helicase activity. NER-TCR is still active in the absence of p53 activity (Therrien *et al.*, 1999) indicating that although p53 may interact with a number of repair proteins it may be more important in apoptosis than in the process of DNA repair itself (McKay *et al.*, 1999).

Evidence for a link between p53 and NER has been observed for the p48 regulatory subunit of XPE (Hwang *et al.*, 1999; Nospikel & Hanawalt, 2002). As p53 does not localise to sites of DNA damage, it is thought to act as a transcriptional regulator of DNA binding factor 2 (*DDB2*) (encoding the p48 protein) and XPC (Fitch *et al.*, 2003; Wang *et al.*, 2003).

In the BER process, APE acts on p53 to convert it from the latent to active form (Hsieh *et al.*, 2001). In one study cell extracts over expressing p53 exhibited an augmented BER activity *in vitro* that was abolished by the depletion of p53 from nuclear extracts (Offer *et al.*, 1999).

The numerous possible roles of p53 in DNA damage and repair mechanisms highlight the complexity of such processes. However, they also indicate that any model system being used to study the impact of BER and NER on repair of oxidative damage should be wild-type for p53 (in respect to the numerous functions of p53 in these different pathways) to ensure that the repair processes are being studied as near to *in vivo* conditions as possible.

1.8 Consequences of repair defects

The importance of DNA repair processes for survival has been highlighted by the generation of repair deficient animals. These animals present with defective embryogenesis, tissue specific dysfunction, hypersensitivity to DNA damaging agents, premature senescence, genetic instability and increased cancer rates (Wilson & Thompson, 1997).

Animals deficient in APE are non-viable, often not surviving through embryogenesis (Grösch *et al.*, 1998). However, those with single glycosylase mutations show normal development and surprisingly, only a moderate increase in mutation frequency (Klungland *et al.*, 1999), this may be as a consequence of the overlapping substrate ranges of DNA glycosylases. There are no major diseases in humans characterized by defects in the BER system.

In contrast to BER, a number of diseases have been identified in which deficiency in a NER factor leads to an absence or greatly reduced ability of DNA repair. Xeroderma pigmentosum (XP) is a rare, autosomal recessive disease. It is characterized by severe

photosensitivity, an extremely high incidence of skin cancers, greater risk to internal cancers and also neurological abnormalities (Sancar, 1996; Batty & Wood, 2000).

XP patients have been classified into seven complementation groups, XP-A through XP-G, corresponding to a defect in a single protein involved in the incision stage of NER. XP-variants (XP-V) suffer from an increased risk of skin cancer but present with no neurological conditions. They are not defective in NER and have near normal UV resistance at the cellular and biochemical level but are thought to lack a mechanism to bypass DNA damage during replication (Batty & Wood, 2000). Cockayne syndrome (CS) is also an inherited, recessive disorder. Patients present with photosensitivity, growth and mental retardation but no predisposition to cancer. This disease is caused by defects in TCR-NER and most patients belong to groups CS-A and CS-B, being deficient in the TCR factors CSA and CSB respectively (Le Page *et al.*, 2000). The exact mechanisms behind the different phenotypes of these diseases are not yet known.

Trichothiodystrophy (TTD) patients suffer from the symptoms of brittle hair, short stature, mental underdevelopment and neuroskeletal abnormalities. They are thought to be deficient in the NER factors XPB, XPD and XPG (Hanawalt, 1994).

Decreased levels of repair factors and decreased repair capabilities may be important in susceptibility to carcinogenesis. mRNA levels of several NER factors have been found to vary by three- to seven-fold between individuals (Vogel *et al.*, 2000). The impact of such variations on an individual's susceptibility to certain cancers has not yet been assessed.

From the examples above it can be seen how important these repair processes are in normal development and disease prevention. It highlights the importance of finding out more about how all of these pathways interact and exactly how each of the components is regulated.

1.9 Aims and objectives

This project aimed to discover more about how DNA repair processes may interact in order to combat the deleterious effects of oxidative stress. It is hoped that finding out more about how these processes are regulated at the cellular level may help to increase our

ability to prevent and treat those disorders that are produced either by the lack of specific components of the repair pathways or by insufficient DNA repair.

Cultured human cell lines were used to determine whether an adaptive response to oxidative stress is co-ordinated by BER and NER, and how these two processes may interact to combat such stress. Initial investigations focused on regulation of BER and NER at both transcriptional and functional levels. This involved the following experimental aims:

- ❖ To establish a mammalian cell culture model suitable for studying 'normal' DNA repair responses.
- ❖ To determine adequate doses of damaging agents capable of inducing oxidative DNA damage without affecting other cellular processes.
- ❖ To develop methods to measure gene, protein and activity levels of BER and NER repair pathways.
- ❖ To assess potential modulation of these pathways following exposure to changes in cellular oxidative stress.
- ❖ To measure DNA repair activity in human breast cancer cell lines to establish a role for ROS in carcinogenesis.
- ❖ To measure transcript levels of the nucleotide pool sanitiser hMTH1 in breast cancer cell lines to provide more evidence for a role of ROS in carcinogenesis and as a potential biomarker for breast cancer susceptibility and cancer progression.

CHAPTER TWO

Materials and Methods

CHAPTER 2: MATERIALS AND METHODS

2.1 MATERIALS

2.1.1 Cell Culture and Treatment Reagents

2.1.1.1 Cell Lines and Primary Cells

Human Caucasian acute T-lymphoblastic leukaemia cell line (CCRF-HSB-2) was purchased from the European Collection of Cell Cultures, Salisbury, UK. Mycoplasma Experience, Surrey, UK, screened the CCRF-HSB-2 cell line for mycoplasma contamination.

MCF-7, MDA-MB-468, MDA-MB-436, MDA-MB-231, T47-D, ZR-75.1, HBL-100 and HCC1937 human mammary epithelial-like cells were all purchased from American Type Culture Collection (ATCC), Rockville, MD, USA.

Human dermal fibroblasts were isolated from mammary reduction of female adult human skin by Angie Gillies, Department of Pathology, University of Leicester, UK.

Primary lymphocytes were separated from peripheral whole blood with Histopaque from Sigma, Poole, UK.

2.1.1.2 Cell Culture Media

Roswell Park Memorial Institute medium (RPMI-1640) without glutamine was purchased from Gibco Life Technologies, Paisley, UK. Dulbecco's Modified Eagles Medium (DMEM) with 1000 mg glucose/L without l-glutamine was purchased from Sigma.

Foetal calf serum (FCS) (Batch No. 1999) was obtained from Labtech International, East Sussex, UK. Trypsin (EC 3.4.21.4), ethylenediaminetetraacetic acid (EDTA) 1 × solution in Hank's Balanced Salt Solution (HBSS) without calcium and magnesium and GlutaMAX™-1 were obtained from Gibco Life Technologies. Dulbecco's phosphate buffered saline solution (DPBS, pH 7.3) was from Cambrex

BioScience Wokingham Limited, Wokingham, UK. Gentamicin solution (10 mg/mL) was purchased from Sigma.

2.1.1.3 Cell Treatment Reagents

Ascorbic acid (AA) and hydrogen peroxide (H₂O₂) (30% w/w) solution were purchased from Sigma; sodium hypochlorite (5.63 % chlorine availability) was obtained from Sigma-Aldrich, MO, U.S.A.

2.1.1.4 Markers of Cell Viability

0.4% (w/v) trypan blue solution was purchased from Sigma. The CellTiter 96[®] Aqueous Non-Radioactive Cell Proliferation Assay was obtained from Promega UK Limited, Southampton, UK.

2.1.2 Extraction Methods

2.1.2.1 Total Cellular RNA Extraction

The different kits used for the extraction of total RNA from cultured cells were; the SV Total RNA Isolation System from Promega, RNazol[™] B and its replacement, RNA-Bee[™] from Biogenesis Limited, Poole, UK and Purescript[®] from Gentra Systems, MN, U.S.A. Absolute ethanol was purchased from Merck Limited, Lutterworth, UK. All other agents for RNA extraction; isopropanol, chloroform and nuclease-free water, were purchased from Sigma.

2.1.2.2 mRNA Extraction

The magnetic particle concentrator (MPC) and Dynabeads[®] mRNA direct[™] kit consisting of Dynabeads[®] oligo(dT)25 at a suspension of 5 mg beads/mL in PBS, containing 0.05% Tween-20 and 0.02 % sodium trinitrate were from Dynal Biotech UK, Wirral, UK. Diethyl pyrocarbonate (DEPC) and dithiothreitol (DTT) were from Acros Organics, U.S.A, and proteinase K was from Roche Diagnostics, Basel, Switzerland. Other constituents of the lysis binding buffer (LBB): tris-HCl, lithium chloride, EDTA and sodium dodecyl sulphate (SDS) were all from Sigma.

2.1.2.3 Cellular Lysate Extraction

The protease inhibitors antipain, chymostatin, leupeptin and pepstatin A were purchased from Sigma, as were all the other reagents; EDTA, magnesium acetate, β -mercaptoethanol, potassium chloride and Trizma[®] - HCl. Bradford-based BioRad protein assay solution, used for cell lysate protein quantitation, was purchased from BioRad, Hemel Hempstead, UK. Bovine serum albumin (BSA) was from ICN Biomedicals Incorporated, Ohio, U.S.A.

2.1.3 Immunochemical Methods

All of the primary and secondary antibodies used in Western blotting are listed in **Table 2.1**.

Antibody	Source
Primary	
Monoclonal anti-Ref-1 (clone 15)	BD Transduction Laboratories, CA, U.S.A
Monoclonal anti-hHR23B (clone 16)	BD Transduction Laboratories
Polyclonal anti-hOGG1 (Ab808)	Dr. P. Mistry, University of Leicester, UK
Monoclonal anti- β -actin (clone AC-15)	Sigma
Monoclonal anti-XPA (clone 12F5)	BD Transduction Laboratories
Secondary	
Sheep anti-mouse IgG–Horseradish peroxidase conjugated (HRP)	Sigma
Goat anti-rabbit IgG - HRP	Sigma

Table 2.1: Primary and secondary antibodies used for Western blotting.

2.1.3.1 Western Blotting

The following were obtained from Sigma; ECL Immobilon-P polyvinylidene difluoride (PVDF) membrane (0.45 μ M pore size), Ponceau S, glycine, sodium chloride, sodium hydroxide, Trizma[®]-base and olyoxyethylenesorbitan monolaurate (Tween-20). ECL[™] reagents and Hyperfilm[™] were from Amersham, Little Chalfont, UK and methanol and hydrochloric acid were from Fisher Scientific UK,

Loughborough, UK. Also purchased were dried skimmed milk powder; sample bags for use with 1450 Microbeta™ counter from Perkin Elmer, Beaconsfield, UK and Whatman® 3 MM filter paper from Whatman International Ltd., Maidstone, UK. Primary and secondary antibodies are detailed in **Table 2.1**.

2.1.4 Molecular Biology Reagents

2.1.4.1 Reverse Transcription-Polymerase Chain Reaction (RT-PCR)

Taq DNA polymerase (5 U/μL), RNasin® RNase inhibitor (40 U/μL) and AMV reverse transcriptase (10 U/μL) were all purchased from Promega. Trizma®-base, ammonium sulphate, magnesium chloride, β-mercaptoethanol and EDTA were all from Sigma; dATP, dGTP, dTTP and dCTP were all purchased from Boehringer Mannheim, Mannheim, Germany and BSA was from ICN Biomedicals Inc. Sterile light paraffin oil was purchased from South Devon Health Care, Paignton, UK. β-actin primers (forward: 5'-TCATCACCATTGGCAATGAGCG-3' and reverse: 5'-CTAGAAGCATTTGCGGTGGACG-3') were designed by Lindsay Primrose, Department of Pathology, University of Leicester. hMTH1 primers (forward: 5';TGCAAGAAGGAGAGACCATC-3' and reverse: 5'-TCTGAAGCAGGAGTGGAAAC-3') were designed using Primer3 Output (www.genome.wi.mit.edu/cgi-bin/primer/primer3_www_results.cgi) accessed through www.pubmed.com (**Appendix I**). All PCR primers were synthesized by Sigma-Genosys Limited, TX, USA.

2.1.4.2 Quantitative real-time RT-PCR

iQ™ SYBR® Green Supermix was purchased from Bio-Rad. All other materials were obtained as for RT-PCR (section 2.1.4.1).

2.1.4.3 Ribonuclease Protection Assay

The RiboQuant™ Multi-Probe Ribonuclease Protection Assay System, consisting of the *In Vitro* Transcription Kit and Ribonuclease Protection Assay Kit, along with Multi-Probe Template Sets hBER-1, hBER-2 and hNER-1 were obtained from PharMingen International, San Diego, CA, U.S.A. Tris-saturated phenol, nuclease-free water, isoamyl alcohol and chloroform were purchased from Sigma. Ethanol was from Merck and the [α-³²P] UTP (3000 Ci/mmol) was purchased from

Amersham. RiboGreen[®] RNA Quantitation Reagent was purchased from Molecular Probes, Cambridge Bioscience, Cambridge, UK.

2.1.4.4 Endonuclease Nicking Assay

The 8-oxoG containing oligonucleotide, where **O** represents 8-oxoG, (5'-GAACTAGTGOATCCCCGGGCTGC-3') (100 pmol), and the accompanying complimentary A oligonucleotide (5'-GCAGCCCGGGGGATCCACTAGTTC-3') (100 pmol) were purchased from R & D Systems, MN, U.S.A. T4 polynucleotide kinase and 10 × T4 polynucleotide kinase buffer were obtained from New England BioLabs Inc., MA, U.S.A. [γ -³²P] ATP was purchased from Amersham. The undamaged oligonucleotide control (5'-GAACTAGTGGATCCCCGGGCTGC-3') and complimentary undamaged oligonucleotide (5'-CGAGCCCGGGGGATCCACTAGTTC-3'), together with the random 9-mer oligonucleotide (5'-GAACTAGTG-3') used for a size marker, were prepared by Sigma-Genosys Limited. The QIAquick Nucleotide Removal Kit was purchased from QIAGEN Limited, Crawley, UK and ethanol was purchased from Merck. Agents used to prepare the 3 × denaturing buffer were 97% de-ionizing formamide and bromophenol blue, both from Sigma and sodium hydroxide purchased from Fisher.

2.1.4.5 Big-Dye DNA Sequencing

The QIAquick PCR Purification Kit, used to purify the DNA fragments from RT-PCR reaction products, was from QIAGEN Limited. The Big Dye mix was purchased from Applied Biosystems, Warrington, UK and the Centri-sep spin columns were from Princeton Separations, Inc., NJ, USA. Thin walled 0.5 mL microcentrifuge tubes were purchased from Techne Incorporated, N.J, USA.

2.1.5 DNA Damage Measurement

2.1.5.1 Alkaline Unwinding

Potassium dihydrogen orthophosphate, sodium chloride, EDTA, sodium hydroxide and hydrochloric acid (36%), were all obtained from Fisher. Sodium phosphate, potassium chloride, SDS, peroxide free t-octylphenoxypolyethoxyethanol (Triton

X-100) and Trizma[®]-base were all purchased from Sigma. Purified Fpg protein was a kind gift from Professor A. Collins, Rowett Research Institute, Aberdeen, UK.

2.1.5.2 Hydroxyapatite Chromatography

Sodium dihydrogen orthophosphate and potassium dihydrogen orthophosphate were both from Fisher. Sodium phosphate, potassium phosphate and Hoechst 33258 were purchased from Sigma.

2.1.6 Electrophoresis

2.1.6.1 Agarose Gel Electrophoresis and Photography

Agarose, ethidium bromide tablets, boric acid, EDTA, trizma[®]-base, sodium sulfite, 3-[N-morpholino]propanesulfonic acid (MOPS), sodium acetate (trihydrate), bromophenol blue, nuclease-free water, glycerol, 97% deionised formamide and 37% formaldehyde were all from Sigma. 0.28-6.58 kb RNA markers were from Promega. Xylene-cyanol FF was purchased from Merck.

2.1.6.2 Polyacrylamide Gel Electrophoresis (PAGE)

Trizma[®]-base, urea, boric acid, EDTA, ammonium persulfate (AMPS), N, N, N',N'- tetramethylethylenediamine (TEMED), glycine, formamide, bromophenol blue and SDS were all purchased from Sigma. DTT was purchased from Acros Organics. Prestained Precision Protein Standards, 30% (w/v) acrylamide/bisacrylamide solution (29:1) and 40% (w/v) acrylamide/bisacrylamide solution (19:1) were all obtained from BioRad. Sequencing grade 30% (w/v) acrylamide/0.8% (w/v) bisacrylamide, for use in the endonuclease nicking assay, was purchased from Flowgen, Ashby de la Zouch, UK. Whatman[®] 3 MM and 1 Chr filter paper were from Whatman International Ltd.

2.2 EQUIPMENT

2.2.1 UV Source and Radiometer

UV irradiations were performed using a UVB lamp (Model UVM-57 Chromatovue® Lamp 302 nm, UVP Inc, Knight Optical Technologies, Leatherhead, UK) (emission spectrum is given in **Appendix IV**). The energy output from the UV source was assessed with an Optical Radiometer with a UVB sensor (Micropulse Technology, Knight Optical Technologies).

2.2.2 Spectrophotometry and Spectrofluorimetry

Spectrophotometric measurements of 96-well plates using 630 nm (protein quantitation) and 492 nm (CellTiter 96® Aqueous Non-Radioactive Cell Proliferation Assay) filters were performed on a Wellscan plate reader (Denley, UK). Fluorescence detection of RiboGreen® labelled RNA in 96-well plates was performed on a Cary Eclipse fluorescence spectrophotometer (Varian Limited, Walton-on-Thames, Surrey, UK). Fluorescence detection of Hoescht 33258 binding to single and double-stranded DNA was performed on a CytoFluor® Series 4000 multi well plate reader using CytoFluor® software, both from Perseptive Biosystems, MA, U.S.A. RNA samples were quantified and the purities verified on a Lambda 2 UV/VIS Spectrophotometer, Perkin Elmer with Perkin Elmer Computerised Spectroscopy Software, version 4.3.

2.2.3 Electrophoresis

All PAGE and Western blotting apparatus as well as Powerpacs (models 300 and 1000) were purchased from BioRad, UK. RT-PCR and RNA integrity gels were performed using agarose gel cask tanks produced and designed by Leicester University Workshop, Leicester, UK. Ribonuclease protection assay products were run on sequencing gel tanks using a Consort E432 power pac from Flowgen.

2.2.4 Imaging

RNA integrity agarose gels were photographed under UV light using a Polaroid MP4⁺ Instant Camera System (model 44-16, Wheathampstead, UK) using Type 55 Polaroids. RT-PCR agarose gels were captured using a Chromato-Vue® TM-40 UV

Transilluminator from UVP, Incorporated, CA, USA with UVP VisionWorks 3.1 software. Western blotting Hyperfilm™ ECL™ was developed on a Compact X4 Automatic X-ray Film Processor, X-ograph Imaging Systems, Malmesbury, UK. Type 55 Polaroid negatives, Hyperfilm™ ECL™, Ribonuclease protection assay and endonuclease nicking assay Kodak X-Omat negatives were analysed and quantified using a β -Imaging Computing Densitometer (Molecular Dynamics, Little Chalfont, UK) with MD Image Quant Software version 3.3.

2.2.5 Miscellaneous Equipment

Radioactivity monitoring was carried out with a Mini-monitor g.m Meter type 5.10, Mini Instruments Ltd., Essex, UK. Ribonuclease protection assay gels were dried on a GF10 Gel Dryer from Jouan Incorporated, Virginia, USA. RT reactions were performed on Thermo Electron Hybaid Px2 thermal cyclers (Fisher), PCR reactions were performed on Perkin Elmer PE 9600 thermal cyclers (Perkin Elmer) and sequencing reactions were performed in a Techne Unit Progene Thermal Cycler (Techne Ltd., Cambridge, UK). Purified PCR products were sequenced on an ABI 377 XL Automated DNA Sequencer and data analysis performed using Sequence Analysis Software (Applied Biosystems). All cells were incubated at 37°C in Sanyo incubators (Sanyo Gallenkamp, Leicestershire, UK).

2.3 METHODS

2.3.1 Cell Culture and Treatments

2.3.1.1 Cell Culture

All cells were cultured and experiments performed in a Sanyo incubator in a 5% CO₂ atmosphere and routinely passaged. Adherent cells were detached in trypsin-EDTA solution (0.05% (w/v) trypsin, 0.02% (w/v) EDTA and 145 mM sodium chloride) at 37° for 4 minutes.

CCRF-HSB-2 cells were grown in RPMI-1640 with 2 mM GlutaMAX™-1 and 10% FCS. Cultures were maintained up to passage 20 between $2-3 \times 10^5$ cells/mL and not allowed to exceed a cell density of $2-3 \times 10^6$ cells/mL.

Human dermal fibroblasts (passage < 18) were grown to 80% confluence in DMEM supplemented with 2 mM GlutaMAX™-1, 10% FCS and 5 µg/mL gentamicin.

Primary lymphocytes were obtained from 30 mL peripheral blood of healthy donors by isolation of peripheral blood mononuclear cells (PBMC). AN equal amount of sterile PBS was added to the blood sample and 10 mL aliquots carefully layered onto 3 mL aliquots of Histopaque. Samples were centrifuged at 400 g for 30 minutes at 20°C. The plasma/platelet layer was removed using a Pasteur pipette and the white PBMC layer removed to a fresh tube. 10 mL RPMI-1640 medium supplemented with 10% FCS was added to each sample and the tubes mixed by inversion to wash the cells before centrifugation at 250 g for 10 minutes at 20°C. The supernatant was discarded before the pellet was dislodged by gentle shaking and then resuspended in 10 mL fresh medium. The wash steps were repeated twice more before the cells were resuspended in 10 mL RPMI-1640 and incubated at 37°C for 1 hour. After 1 hour, the medium containing the lymphocytes, was removed to a fresh cell culture flask, leaving monocytes attached to the original discarded flask. Lymphocytes were maintained at 37°C in RPMI-1640 supplemented with 10% FCS and 2 mM GlutaMAX™-1 until required for RNA extraction.

MCF-7, MDA-MB-231, MDA-MB-468, HBL-100 and T47-D cell lines were grown in DMEM without phenol red supplemented with 2 mM l-glutamine. MDA-MB-

436, ZR75-1 and HCC1937 cells were grown in RPMI-1640 supplemented with 10% FCS and 2 mM l-glutamine. All breast cancer cell lines were maintained in culture by Peter Goodrem, Department of Pathology, University of Leicester.

2.3.1.2 Cell Treatments

H₂O₂, sodium hypochlorite and ascorbic acid were diluted in prewarmed DMEM and then filter sterilized through a 0.2 µM filter. Cells were treated with doses of either 0 µM, 400 µM or 800 µM H₂O₂ or ascorbic acid or 0 nM, 300 nM or 600 nM sodium hypochlorite, mixed gently and incubated at 37°C for up to 24 hours. UV irradiations were performed in sterile PBS in 6-well plates. Cells were exposed to 600 J/m² or 1200 J/m² UVB and then incubated at 37°C for up to 24 hours in fresh medium. Control samples were sham treated.

2.3.1.3 Measurement of Cell viability Following Treatments

CellTiter 96[®] Aqueous Non-Radioactive Cell Proliferation Assay

The CellTiter 96[®] Aqueous Non-Radioactive Cell Proliferation Assay (Promega) is a spectrophotometric method for determining the number of viable cells within a given population. The assay is based on the conversion of the tetrazolium salt compound, 3-(4,5-dimethylthiazol-2-yl)-5-(3-carboxymethoxyphenyl)-2-(4-sulfophenyl)-2H-tetrazolium, inner salt) (MTS) to a soluble formazan, in the presence of an electron coupling reagent, phenazine methosulphate (PMS), by cellular dehydrogenases. The MTS is thus bioreduced by metabolically active cells to produce the water soluble, brown coloured formazan. Absorbance of this compound can then be measured at 492 nm. The absorbance of the formazan product at 492 nm is directly proportional to the number of living cells in culture and so can be used to quantify the cell viability and cell death in a given population of cells. The assay does not distinguish between apoptosis and necrosis. Percentage cell viability was calculated using the following equation:

$$\% \text{ cell viability} = \frac{\text{absorbance of treated cells (- blank)}}{\text{absorbance of control cells (- blank)}} \times 100$$

Dermal fibroblasts were seeded at 5000 cells/well in a 96-well plate and incubated at 37°C for 24 hours to allow population doubling. The MTS/PMS solution was prepared by adding 100 µL PMS solution (0.92 mg/mL in PBS) to 2000 µL MTS solution (2 mg/mL in PBS). The cells were then treated in triplicate with the appropriate agents. 20 µL MTS/PMS solution were added to each well 1 hour before the absorbance readings were taken at 492 nm on a Wellscan plate reader. As a blank, 20 µL MTS/PMS solution was added to 100 µL of complete medium without any cells present. Control cells had 20 µL complete medium added.

2.3.2 Extraction and Quantitation Methods

2.3.2.1 Total RNA Extraction

Three separate RNA extraction kits were assessed for RNA yield, purity and integrity using CCRF-HSB-2 cells.

SV Total RNA Kit (Promega)

5×10^6 CCRF-HSB-2 cells were collected by centrifugation at 200 g for 3 minutes. The cell pellet was then washed with 10 mL ice-cold PBS and the centrifugation step repeated. After discarding the supernatant, the pellet was lysed in 175 µL ice-cold SV RNA Lysis Buffer by gentle pipetting. The lysate was then passed through a 21 G needle 4-5 times before being expelled in to a 1.5 mL microfuge tube. 350 µL SV RNA Dilution Buffer was added and the sample mixed by inversion 3-4 times. Samples were then heated to 70°C for 3 minutes and then centrifuged at 1500 g for 30 minutes at room temperature. The resulting supernatant, approximately 350 µL, was then transferred to a fresh tube and 200 µL ice-cold 95% ethanol were added. The samples were mixed by pipetting and then transferred to the Spin Column Assembly (consisting of the Spin Basket and Collection Tube) before centrifugation at 1500 g for 2 minutes at room temperature. 600 µL SV RNA Wash Solution were added and samples centrifuged at 1500 g for 2 minutes. DNase I solution was prepared by adding 40 µL yellow core buffer, 5 µL 0.09 M magnesium chloride and 5 µL DNase I enzyme to a microfuge tube. 50 µL of the freshly prepared DNase I solution was then applied to the Spin Basket membrane, ensuring that the surface was completely covered. Samples were incubated for 15 minutes at 20 - 25°C and then 200 µL SV DNase Stop Solution

were applied. Samples were centrifuged at 1500 g and then washed by adding 600 μL SV RNA wash solution and centrifuging at 1500 g for 3 minutes. The Collection Tube was then emptied before washing again with 250 μL SV RNA Wash solution and centrifugation at 1500 g for 3 minutes. The cap was removed from the Spin Basket and it was transferred from the Collection Tube to an Elution Tube. RNA was eluted by completely covering the membrane with 100 μL nuclease-free water and centrifuging at 1500 g for 1 minute. The Spin Baskets were then removed; the Elution Tubes capped and extracted RNA stored at -20°C overnight or at -80°C for long-term storage.

Purescript[®] Kit (Gentra Systems)

1 mL of CCRF-HSB-2 cell suspension at a concentration of $1-2 \times 10^6$ cells/mL in RPMI-1640 was pipetted into a microfuge tube and placed on ice. Samples were centrifuged at 1500 g for 30 seconds at 4°C and the supernatant then removed. The cells were resuspended in the residual supernatant by vortexing before the addition of 300 μL Cell Lysis Solution, followed by mixing by pipetting up and down 2-3 times. 100 μL ice-cold Protein-DNA Precipitation Solution were added and samples mixed by inversion 10 times and then incubated on ice for 5 minutes. Following incubation, samples were centrifuged at 1500 g for 30 minutes at 4°C until a tight white pellet was formed. The supernatant was removed to a fresh microfuge tube containing 300 μL ice-cold isopropanol, and mixed by inversion 50 times before being centrifuged at 1500 g for 15 minutes at 4°C to form the RNA pellet. The supernatant was carefully removed and the pellet washed by the addition of 300 μL ice-cold 70 % ethanol and centrifugation at 1500 g for 5 minutes at 4°C . The ethanol supernatant was pipetted off and the pellet left to air dry for 10-15 minutes, taking care not to over dry. The RNA pellets were then resuspended in 20 μL ice-cold Hydration Solution and mixed by vortexing. Samples were stored at -20°C overnight before RNA quantitation and then at -80°C for long-term storage.

RNAzol[™] B Isolation of RNA (Biogenesis Ltd)

$10-20 \times 10^6$ cells in 10 mL cell culture medium were centrifuged at 200 g for 3 minutes and the supernatant discarded. The cell pellets were washed twice in sterile PBS, by centrifugation at 200 g for 3 minutes, and the final cell pellets were lysed in

1 mL ice-cold RNAzol™ B solution by gentle pipetting. The lysate was expelled into a 1.5 mL microfuge tube and then placed on ice. 100 µL chloroform were added to the lysates and the samples mixed by vortexing for 10 seconds. After 10 minutes incubation on ice the samples were centrifuged at 1500 g for 10 minutes at 4°C. After centrifugation, 400 µL of the upper, clear aqueous layer, were added to 500 µL of isopropanol on ice, and vortexed for 5 seconds before being incubated for 1 hour at -20°C (samples could also be left overnight at this stage) to precipitate the RNA. After incubation, the samples were centrifuged at 1500 g for 10 minutes at 4°C to obtain the RNA pellet. The supernatant was carefully pipetted off and 1 mL ice-cold 75% ethanol added. The pellet was washed by centrifugation at 1500 g for 10 minutes, and then the supernatant was removed and the pellet air-dried for 10-15 minutes. The RNA was resuspended in 20 µL nuclease-free water and then stored at -20°C overnight before quantitation by UV spectrophotometry and long-term storage at -80°C.

RNA-Bee™ Isolation of RNA (Biogenesis Limited)

The new formulation of RNA isolation reagent obtained from Biogenesis Limited was used in exactly the same way as the RNAzol™ B reagent except that RNA quantitation was performed by fluorescence analysis using the RiboGreen® method. The values obtained compared favourably with those obtained via UV spectrophotometry.

2.3.2.2 Total RNA Quantitation and Integrity

RiboGreen® RNA Quantitation Reagent (Molecular Probes)

RiboGreen® is a highly sensitive fluorescent nucleic acid stain for quantitating RNA in solution. When added to RNA in solution a large fluorescent enhancement is produced which can be measured by excitation at 500 nm and emission at 525 nm. The amount of RNA in a given sample is determined by comparison between the amount of fluorescence produced in the sample upon addition of the RiboGreen® RNA quantitation reagent, when compared to the RiboGreen® RNA quantitation reagent prepared with known amounts of standard ribosomal RNA (16S and 23S rRNA from *E. coli*).

RNA samples were diluted 1:100 000 in Tris-EDTA (TE buffer) (200 mM Tris-HCl, 20 mM EDTA, pH 7.5). The standard curve was produced by diluting the standard ribosomal RNA (100 ng/mL) 1:1000 in TE buffer and then performing serial dilutions in TE buffer to produce a range from 5 to 50 ng/mL ribosomal RNA in 500 μ L volumes. The RiboGreen[®] RNA quantitation reagent was diluted 1:2000 in TE buffer and 500 μ L added to each standard and each RNA sample. Triplicate 300 μ L aliquots of standard and RNA sample were pipetted in to a 96-well plate before excitation and emission readings were taken in a Cary Eclipse fluorescence spectrophotometer. A reagent blank was prepared without any ribosomal RNA standard present and the value of fluorescence produced subtracted from that of each of the samples. Corrected data was used to generate a standard curve of fluorescence versus RNA concentration in order to determine the amount of RNA in each sample.

RNA Quantitation by UV Spectrophotometry

RNA samples were thawed on ice and diluted 1 in 1000 with nuclease-free water. UV readings were taken at 260 nm, 280 nm and for samples extracted with the SV Total RNA System additionally at 230 nm. The 260:280 ratio was then determined to indicate the amount and purity of the RNA present.

The A₂₆₀ gives a reading of RNA content where 1 A₂₆₀ unit of single stranded RNA is equivalent to 40 μ g/mL. The A₂₆₀:A₂₈₀ ratio should be approximately 2.0 for pure RNA (1.7-2.1 is the acceptable range). The 230:260 ratio for SV Total RNA samples was used to indicate the presence of any contaminating guanidinium thiocyanate reagent. Samples free of reagent contamination should have a ratio of approximately 1.5.

RNA integrity

The integrity of the RNA samples was assessed by denaturing gel electrophoresis on 1.5% (w/v) agarose gels run at 75V for 110 minutes. Gels were stained with ethidium bromide (0.5 μ g/mL). Samples were denatured by the use of a formaldehyde/formamide sample buffer (10 mL deionised formamide, 3.5 mL 37% formaldehyde, 2 mL 3-[N-morpholino]propane sulphonic acid (MOPS buffer)). Briefly, 18 μ L sample buffer and 2 μ L loading buffer (1 mM

ethylenediaminetetraacetic acid (EDTA), 0.4% bromophenol blue, 1 mg/mL ethidium bromide in 50% (v/v) nuclease free water, 50% (v/v) glycerol) were added to 2-3 µg RNA samples on ice. Samples were vortexed and heated at 65°C for 12 minutes and then placed on ice before being loaded on to the gel.

RNA markers (0.28-6.58 kb) were used to identify 28S rRNA (4,800 bp) and 18S rRNA (1,900 bp) bands which should appear in a 2:1 ratio for an intact RNA sample. Results were visualised using a BioRad MultiImager and bands quantified, taking into account background interference. Initial integrity results were obtained using the RNAzo1™ B reagent. Following the replacement of this reagent with the new formulation of RNA-Bee™ further integrity gels were run.

2.3.2.3 mRNA Extraction

Dermal fibroblasts and breast cancer cell lines were grown to near confluence (90 %) before being trypsinised, washed in 10 mL HBSS and then counted using a haemocytometer and Trypan Blue exclusion (section 2.3.1.3). Cells were lysed in 100 µL lysis binding buffer (composition) per 1×10^5 cells. 5 µL of 1 mg/mL proteinase K solution was added to 100 µL aliquots of lysate and incubated at 37°C for 30 minutes. DNA was then sheared by passing the lysate through a 21G, followed by a 25G sterile needle in a 1 mL syringe, 3 to 5 times each.

The oligo(dT)₂₅ Dynabeads were reconditioned, by washing twice in lysis binding buffer, before being added to the lysate. Samples were left at room temperature for 5 minutes to allow the mRNA to bind to the beads and then the Dynabeads were pelleted in the MPC. The supernatant was discarded and the pellets washed twice in wash buffer (10 mM Tris-HCl (pH 8.0), 0.15 M lithium chloride, 1 mM EDTA) containing 0.1% SDS and then twice in wash buffer without SDS. The Dynabeads were finally resuspended in 30 µL DEPC treated water and stored at 4°C until the reverse transcriptase reaction was performed (section 2.3.4.3)

2.3.2.4 Preparation of Cellular Lysates

At the appropriate time points, $5 - 10 \times 10^6$ dermal fibroblasts were trypsinised and then washed twice in PBS before being lysed in 50 µL ice-cold cell lysis buffer (5

mM magnesium acetate, 50 mM potassium chloride, 50 mM Tris-HCl (pH 7.4), 3 mM EDTA, 5 µg/mL leupeptin, 5 µg/mL pepstatin A, 5 µg/mL chymostatin, 5 µg/mL antipain, 3 mM β-mercaptoethanol), and then stored at -80°C until required for Western blotting.

2.3.3 Immunochemical Methods

2.3.3.1 Western Blotting

Levels of various DNA repair proteins in human dermal fibroblasts were measured using SDS-PAGE and Western Blotting.

Cellular lysates (section 2.3.2.4) were thawed on ice before being homogenised using 20 strokes of a manual pestle and centrifuged at 1500 g for 15 minutes at 4°C. Protein concentrations were determined using the BCA Bradford based protein assay using BSA as standard. Aliquoted lysates were stored at -80 °C until required for Western Blotting.

40 µg of total cellular protein were loaded on to 12% SDS-polyacrylamide gels in 1 × running buffer (25 mM Trizma base, 192 mM glycine, 3.5 mM SDS) at 100V for 15 minutes, followed by 120V for a further 90 minutes, before electroblotting to PVDF membranes in transfer buffer (0.2 M glycine, 25 mM Trizma-base, 10 % (v/v) methanol) at 100V for 1 hour. Ponceau S staining (0.1% (w/v) Ponceau S, 5% acetic acid) for 5 minutes at room temperature was used to detect transferral of total cellular protein. Membranes were destained using 0.1 M sodium hydroxide for 30 seconds. Membranes were washed for 5 minutes in UP water before being blocked in tris-buffered saline (5mM Trizma-base, 15 mM sodium chloride) containing 0.1% (v/v) Tween 20 (TBS-T) with 10% milk. Membranes were washed for 15 minutes in TBS-T and then washed twice more for 10 minutes each in TBS-T, before being incubated in primary antibody at 4°C overnight. Membranes were then washed twice for 15 minutes and twice for 5 minutes in TBS-T before incubation with the appropriate secondary antibody for 1 hour at room temperature. Two 15 minute washes and four 5 minute washes followed before ECL™ detection and autoradiography.

XPA mouse monoclonal antibody (BD Pharmingen) was used at 1:500 diluted in TBS-T. Ref-1 mouse monoclonal antibody (BD Pharmingen) was used at 1:100 diluted in TBS-T. hHR23B mouse monoclonal antibody (BD Pharmingen) was used at 1:250 dilution in TBS-T. β -actin mouse monoclonal antibody (Sigma) was used at 1:3000 dilution in TBS-T. HRP-conjugated anti-mouse secondary antibody (Sigma) was used at 1:5000 dilution in TBS-T. hOGG1 rabbit IgG antibody was prepared 'in-house' and used at a dilution of 1:1250 in TBS-T. HRP-conjugated anti-rabbit secondary antibody (Sigma) was used at a 1:10 000 dilution in TBS-T.

Blots were stripped by incubation at 50°C for 30 minutes in 50 mL stripping buffer (6.25 mM Tris-HCl (pH 6.8), 2% SDS) with 350 μ L β -mercaptoethanol added and agitation every 10 minutes. Blots were rinsed with UP water before being washed three times for 10 minutes in TBS-T, rinsed once again in UP water and then subjected to Ponceau S staining before reprobing with the appropriate antibodies.

2.3.4 Molecular Biology Techniques

2.3.4.1 RNase Protection Assay

The Ribonuclease Protection Assay was performed as per manufacturers instructions. The assay involves the *in vitro* synthesis of a radioactively labelled anti-sense RNA probe transcribed from a DNA template. The probe anneals to complementary mRNA species present in a sample of total RNA, which is extracted from the samples under investigation, in an overnight hybridisation reaction. Any single-stranded RNA or free anti-sense probe is then digested by RNase treatment and the protected double-stranded species are extracted from the reaction mixture and then resolved on a denaturing polyacrylamide gel and quantified by autoradiography.

***In vitro* probe synthesis**

The probe synthesis was performed using [α -³²P]-UTP and either hBER-1, hNER-1 or hNER-2 template sets. The [α -³²P]-UTP, GACU nucleotide pool, DTT, 5 x transcription buffer and appropriate template set were brought to room temperature prior to adding to a 1.5 mL screw lid microfuge tube in the following order: 1 μ L RNasin, 1 μ L GACU nucleotide pool, 2 μ L DTT, 4 μ L 5 x transcription buffer, 1 μ L template set, 10 μ L [α -³²P] UTP and 1 μ L T7 RNA polymerase. The reagents

were mixed by pipetting, followed by a quick spin in a microfuge. The sample was then incubated at 37°C for 1 hour.

2 µL DNase was added to terminate the transcription reaction by incubation at 37°C for 30 minutes. 26 µL 20 mM EDTA, 25 µL tris-saturated phenol, 25 µL chloroform:isoamyl alcohol (50:1) and 2 µL yeast tRNA were then added, and the sample mixed by vortexing. The sample was centrifuged at 1500 g for 5 minutes at room temperature, and the upper aqueous layer was transferred to a fresh tube. 50 µL chloroform:isoamyl alcohol (50:1) was added and the sample vortexed and then centrifuged at 1500 g for 2 minutes in a microfuge at room temperature. The upper aqueous phase was again transferred to a fresh tube, and 50 µL 4 M ammonium acetate and 250 µL ice-cold 100 % ethanol added. The tubes were inverted to mix and incubated for 45 minutes at -80°C in order to precipitate the RNA. The sample was then centrifuged at 1500 g for 15 minutes at 4°C, the resulting supernatant was removed and 100 µL 90 % ice-cold ethanol was added to wash the pellet. The sample was centrifuged at 1500 g for 5 minutes at 4°C, the supernatant was removed and the pellet was air-dried for 5 to 10 minutes. The pellet was resuspended in 50 µL Hybridisation buffer and solubilised by gentle vortexing and stored at -20°C until required.

RNA preparation

Human control RNA-2 and yeast tRNA (both supplied by BD PharMingen), used as integrity and non-specific controls, were treated exactly the same as the other samples. RNA samples extracted from treated cells were removed from storage at -80°C and precipitated as follows; 50 µL 4 M ammonium acetate and 250 µL ice-cold ethanol were added and the tubes inverted to mix. The samples were then incubated on dry ice for 45 minutes and centrifuged at 1500 g for 15 minutes at 4°C. The supernatant was removed and 100 µL 90% ice-cold ethanol were added. Samples were then centrifuged at 1500 g for 5 minutes at 4°C, the supernatant was removed and the pellet air-dried, to remove any traces of ethanol, before being resuspended in 8 µL hybridisation buffer.

Hybridisation

2 μL of the synthesized probe (a total of 8.0×10^5 cpm/ μL for hBER-1 template set, 2.3×10^5 cpm/ μL for hNER-1 template set and 8.6×10^5 cpm for hNER-2 template set as described in Chapter 3) were added to each RNA sample and mixed by pipetting. A drop of mineral oil was added to each sample to prevent evaporation, and the samples were placed in a heat block preheated to 90°C . Immediately after the samples were placed in the heat block the temperature was turned down to 56°C and the temperature allowed to ramp down slowly overnight. After 15 hours the temperature was turned to 37°C , 15 minutes prior to the RNase treatments.

RNase treatments

The RNA samples were removed from the heat block and 100 μL of RNase cocktail (2.5 mL RNase buffer, 6 μL RNase A + T1 mix per 20 samples) pipetted underneath the oil in to the aqueous layer. Samples were centrifuged in a microfuge for 10 seconds and then incubated at 30°C for 45 minutes. The RNase digests were extracted from underneath the oil and transferred to tubes containing 18 μL aliquots of proteinase cocktail (390 μL proteinase K buffer, 30 μL proteinase K, 30 μL yeast tRNA per 20 samples). The samples were vortexed and spun briefly in a microfuge before being incubated at 37°C for 15 minutes.

RNA extraction

65 μL tris-saturated phenol and 65 μL chloroform:isoamyl alcohol (50:1) were added and samples spun into an emulsion before centrifugation at 1500 g for 5 minutes at room temperature. The upper aqueous layer was removed to a fresh tube and extracted once again with 65 μL tris-saturated phenol and 65 μL chloroform:isoamyl alcohol (50:1). After transferring the aqueous layer to a fresh tube, 120 μL 4 M ammonium acetate and 650 μL ice-cold 100% ethanol were added and samples mixed by inversion before being incubated for 45 minutes on dry ice. Samples were then centrifuged at 1500 g for 15 minutes at 4°C , the supernatant was removed, and 100 μL ice-cold 90% ethanol was added. The samples were centrifuged at 1500 g for 5 minutes at 4°C , the supernatant was completely removed and the pellet was air-dried. 5 μL 1 x loading buffer was added to the dry pellets and resuspended by vortexing. Samples were then denatured by heating to 90°C for 3 minutes and then placed immediately on ice. 2 μL were loaded on to a 5%

denaturing polyacrylamide gel that had been pre-run at 40 Watts constant power for 45 minutes. 2 μL of a probe set diluted in loading buffer (1×10^3 cpm/ μL) was loaded on to the gel to act as an unprotected probe marker. The gel was run at 50 Watts constant power for approximately 90 minutes, then dried down under vacuum at 80°C for 1 hour and autoradiography performed. Densitometry was performed on a PDSI Densitometer (Molecular Dynamics) and bands normalised to GAPDH expression in each lane.

2.3.4.2 Endonuclease Nicking Assay

Trypsinised dermal fibroblasts were washed twice in 10 mL sterile PBS by centrifugation at 200 g for 5 minutes and then lysed in 50 μL ice-cold Cell Lysis Buffer. Samples were then stored at -80°C until protein concentration could be determined using the Bradford assay (Bradford, 1976).

Oligonucleotide labelling reaction

To label the 8-oxoG containing oligonucleotide, 5 μL oligonucleotide (10 pmol), 5 μL $10 \times$ polynucleotide kinase buffer, 5 μL $\gamma^{32}\text{P}$ -ATP (3000 Ci/mmol), 34 μL distilled water and 1 μL T4 polynucleotide kinase were pipetted into a 1.5 mL screw cap microfuge tube and incubated at 37°C for 30 minutes. The labelling reaction was heated to 75°C for 10 minutes before being placed on ice. 1 μL (10 pmol) complimentary oligonucleotide was then added and the reaction heated to 95°C for 10 minutes before cooling to room temperature.

Single-stranded oligonucleotide was removed using the QIAquick[®] Nucleotide Removal Kit as follows. 500 μL Buffer PN was added to the reaction before transferring to a fresh Spin Column and Collection Tube assembly. The sample was then centrifuged at 750 g for 1 minute. The wash through was discarded and the Spin Column transferred to a new collection tube. 500 μL Buffer PE was added and then the assembly was centrifuged at 750 g for 1 minute. The flow-thru was discarded and 500 μL more Buffer PE was added to the Spin Column before centrifuging at 750 g for 1 minute. The flow-thru was again discarded and the Spin Column was then centrifuged for 1 minute at 1500 g without adding any more buffer. The Spin Column was then transferred to a fresh Collection Tube and

210 μL Elution Buffer added to it before centrifugation at 1500 g for 1 minute. The labelled probe was then stored at -20°C until required for the oligonucleotide reaction.

The random 9-mer and undamaged oligonucleotide were labelled as above except the random 9-mer was not annealed to a complementary strand.

Oligonucleotide reaction

Once protein concentrations had been determined by the Bradford assay 50 μg total protein was used to assess repair activity. 6 μL labelled oligonucleotide were added to each sample and reaction volumes made up to 20 μL with cell lysis buffer where necessary. The samples were then incubated at 37°C for 2 hours. At the end of the incubation 10 μL 3 \times denaturing buffer (97% de-ionising formamide, 300 mM sodium hydroxide, 0.2% bromophenol blue) were added to each reaction and samples heated to 95°C for 10 minutes before being placed on ice for 5 minutes. Samples were then stored overnight at -20°C .

Electrophoresis

Size markers were prepared by adding 1.5 μL 3 \times denaturing buffer to 3 μL of the oligonucleotide and 3 μL random 9-mer and heating them to 95°C for 10 minutes before cooling on ice for at least 5 minutes. 4.5 μL of the markers and 8 μL of the samples were loaded on to a gel, which had been pre-run at 15 mA for 30 minutes. The gels were then run at 15 mA for 90 minutes. Gels were then washed in 500 mL UP water for 2 minutes at room temperature, wrapped in Saran wrap and then subjected to autoradiography.

2.3.4.3 Reverse Transcriptase- Polymerase Chain Reaction (RT-PCR)

Reverse Transcriptase (RT) reactions were set up using mRNA extracted onto Dynabeads as described in section 2.3.2.3. The RT reactions were performed on the same day as the mRNA extractions. +RT and -RT reactions were set up using mastermixes containing the following: 10 μL mRNA/Dynabeads preparation; 5 μL 5 \times AMV buffer, 2.5 μL 10 mM dNTPs in DEPC treated water and 0.62 μL (25 units) RNasin. + RT reactions contained 0.5 μL (5 units) AMV-RT. Both reaction

volumes were made up to 25 μL with DEPC treated water. Reactions were then performed at 42°C for 1 hour using a Hybaid thermal cycler.

Polymerase chain reactions (PCR) were set up using a mastermix containing 1 \times AJ buffer, 0.2 pmol of both sense and anti-sense primer and 1 μL cDNA. Reactions were performed in a Perkin Elmer thermal cycler. Initial denaturation was performed at 98°C for 3 minutes before the addition of 1 Unit of Taq polymerase at the annealing temperature of 60°C, which was held for 3 minutes before extension at 72°C for 1 minute. The DNA was then amplified for a further 29 cycles for the β -actin primers, or 31 cycles for the hMTH1 primers using the following conditions:

94°C	30 seconds	denaturation
60°C	30 seconds	annealing of primers
72°C	60 seconds	extension of primers

PCR products were then stored at 4°C until analysed on a 3% agarose gel.

2.3.4.4 Big-Dye DNA Sequencing

PCR products were firstly purified using the QIAquick PCR Purification Kit as follows: 150 μL Buffer PB were added to 30 μL PCR product and mixed; the sample was then applied to a QIAquick column and centrifuged at 1500 g for 30 to 60 seconds; the resulting flow-thru was discarded from the collection tube and 750 μL Buffer PE was used to wash the column by repeating the centrifugation; flow-thru was again removed and the column spun for 1 minute at 1500 g, to completely remove any residual wash buffer. DNA was then eluted in 30 μL Buffer EB by centrifugation at 1500 g for a further minute.

The sequencing reaction was set up by adding 8 μL Big Dye (Applied Biosystems), 3.5 μL of primer (at 1 pmol/ μL) and 6.5 μL UP water to 2 μL of the PCR product. Reactions were then covered with 50 μL paraffin oil and the sequencing reaction performed in a Progene thermal cycler under the following conditions:

96°C	10 seconds
50°C	5 seconds
60°C	4 minutes

This was performed for a total of 35 cycles.

Unincorporated Big Dye terminators were then removed using the Centri-Sep spin columns according to the manufacturer's instructions. Firstly the dry gel within the column was reconstituted by the addition of 800 µL UP water and left to rehydrate for an hour at room temperature. Any air bubbles were then removed from the column by gentle tapping. After removal of the column end stopper, excess fluid was allowed to drain into a wash tube. The column and wash tube were then centrifuged at 750 g for 2 minutes to remove the remainder of the fluid. The 20 µL sample was then applied directly to the centre of the column and centrifuged at 750 g for 2 minutes. The purified sample was thus collected in a fresh sample collection tube and sent for sequencing by PNAOL, University of Leicester.

Briefly, sequencing reactions were performed using ABI BigDye terminator sequencing chemistry (version 3.1). Unincorporated dye terminators were removed using DyeEx™ 2.0 Spin Columns and the resulting products analysed on an Applied Biosystems 377 XL DNA Sequencer. The resulting chromatogram files were viewed on CHROMAS software viewed at <http://www.technelysium.com.au/chromas.html>.

2.3.5 DNA Damage Detection

2.3.5.1 Alkaline Unwinding Assay

3×10^5 dermal fibroblasts were seeded in 6-well plates and allowed to attach for 24 hours before treatment. At the appropriate time point cell culture medium was removed and cells were washed twice in 5 mL cold PBS. To control cell number one plate was trypsinised and a cell count performed. The alkaline unwinding procedure was then performed in a darkened environment. Firstly, the cells were lysed by incubation with 500 µL lysis buffer (6 mM sodium phosphate, 1 mM potassium dihydrogen orthophosphate, 137 mM sodium chloride, 3 mM potassium

chloride, 0.1% Triton X-100) for 5 minutes on ice. After incubation the lysis buffer was removed and discarded. Histones were then removed by adding 500 μ L salt solution (2 M sodium chloride, 0.01 M EDTA, 0.002 M Tris) and incubation for 2 minutes. The salt solution was then discarded and the cells remained on ice for a further 8 minutes. 760 μ L Fpg-buffer (0.05 M sodium phosphate, 0.01 M EDTA) (pH 7.5), either with or without 1 μ g/mL Fpg-protein, were added and samples incubated at 37°C for 30 minutes. To perform the unwinding step, 775 μ L alkaline solution I (0.1075 M sodium hydroxide, 0.02 M EDTA, 0.69 M sodium chloride) (pH 12.3), were added for exactly 30 minutes at room temperature in the dark. Neutralisation, to stop the reaction, was then performed by adding 450 μ L 0.2 M HCl to a final pH of 6.8 and mixing immediately. Samples were then sonicated on ice for 15 seconds and SDS (from a 5% SDS stock) added to a final concentration of 0.05%. Samples were stored at -20°C until hydroxyapatite chromatography was performed.

2.3.5.2 Hydroxyapatite Chromatography

Separation of single- and double-stranded DNA was performed on 0.5 mL hydroxyapatite columns at 60°C. Single- and double-stranded DNA were eluted with 1.5 mL of 0.15 M and 0.35 M potassium phosphate buffer respectively. The DNA content of both fractions was then determined by adding Hoechst 33258 (final concentration of 7.5×10^{-7} M) to 1.5 mL of each sample and measuring the fluorescence with a spectrofluorometer (Ex 360 nm, Em 455 nm).

2.3.6 Data Analysis and Statistical Testing

Sequencing results were viewed and analysed using Chromus Version 1.45 software (Conor McCarthy School of Health Science, Griffith University, Queensland, Australia) and compared to published cDNA sequences using BLAST 2.2.6 software (<http://www.ncbi.nlm.nih.gov/blast/>) accessed through www.pubmed.com.

All statistical testing was performed using Statistical Package for Social Sciences (SPSS) version 10.1.01 and graphical presentations produced using Microsoft Excel 2000.

2.3.7 Safety

All hazardous chemicals were handled as according to the manufacturer's safety guidelines including the use of eye protection, chemical fume cupboards and method of disposal. Experiments performed with radioactive material were performed in a designated area and in accordance with the University of Leicester regulations.

CHAPTER THREE

Establishing a Cellular Model to Study Responses to Oxidative Stress

CHAPTER 3: ESTABLISHING A CELLULAR MODEL TO STUDY RESPONSES TO OXIDATIVE STRESS

3.1 INTRODUCTION

Oxidative stress is an important contributory factor in genetic instability and tumour progression (Zienoldding *et al.*, 2000). It has also been implicated in a wide variety of disease processes including atherosclerosis, diabetes, pulmonary fibrosis, neurodegenerative disorders and arthritis, and is believed to be a major factor in ageing (Martindale & Holbrook, 2002).

Cells are constantly exposed to oxidants produced from both physiological processes, such as mitochondrial aerobic respiration, and also pathophysiological conditions such as inflammation, ischemia-reperfusion, chemical metabolism and exposure to radiation (Loft & Poulsen, 1999). Because of the associations between oxidative stress, oxidative DNA damage and carcinogenesis, much interest has been generated into investigating the effects of ROS and oxidative stress on DNA homeostasis in cellular systems.

Oxidant injury is capable of eliciting a wide spectrum of cellular responses ranging from cellular proliferation to growth arrest, senescence and even cell death. The observed outcome varies between cell types and also depends on the damaging agent, its dosage and the duration of treatment. A variety of intracellular stress signalling pathways are activated in response to an oxidative insult and these pathways will exert their effects via modulation of transcription factors that affect changes in patterns of gene expression (Bernstein *et al.*, 2002; Martindale & Holbrook, 2002) (**figure 3.1**).

ROS may directly regulate the activity of transcription factors. Redox regulation has been described for NF- κ B, AP-1, Sp-1 and p53 (Michiels *et al.*, 2002). In contrast, decreased oxygen tension is also deleterious to cellular functions due to decreased energy availability leading to cell death. For this reason, strategies to overcome states of hypoxia have also developed. The most studied transcription factor in this pathway is hypoxia-inducible factor-1 (HIF-1) (Michiels *et al.*, 2002).

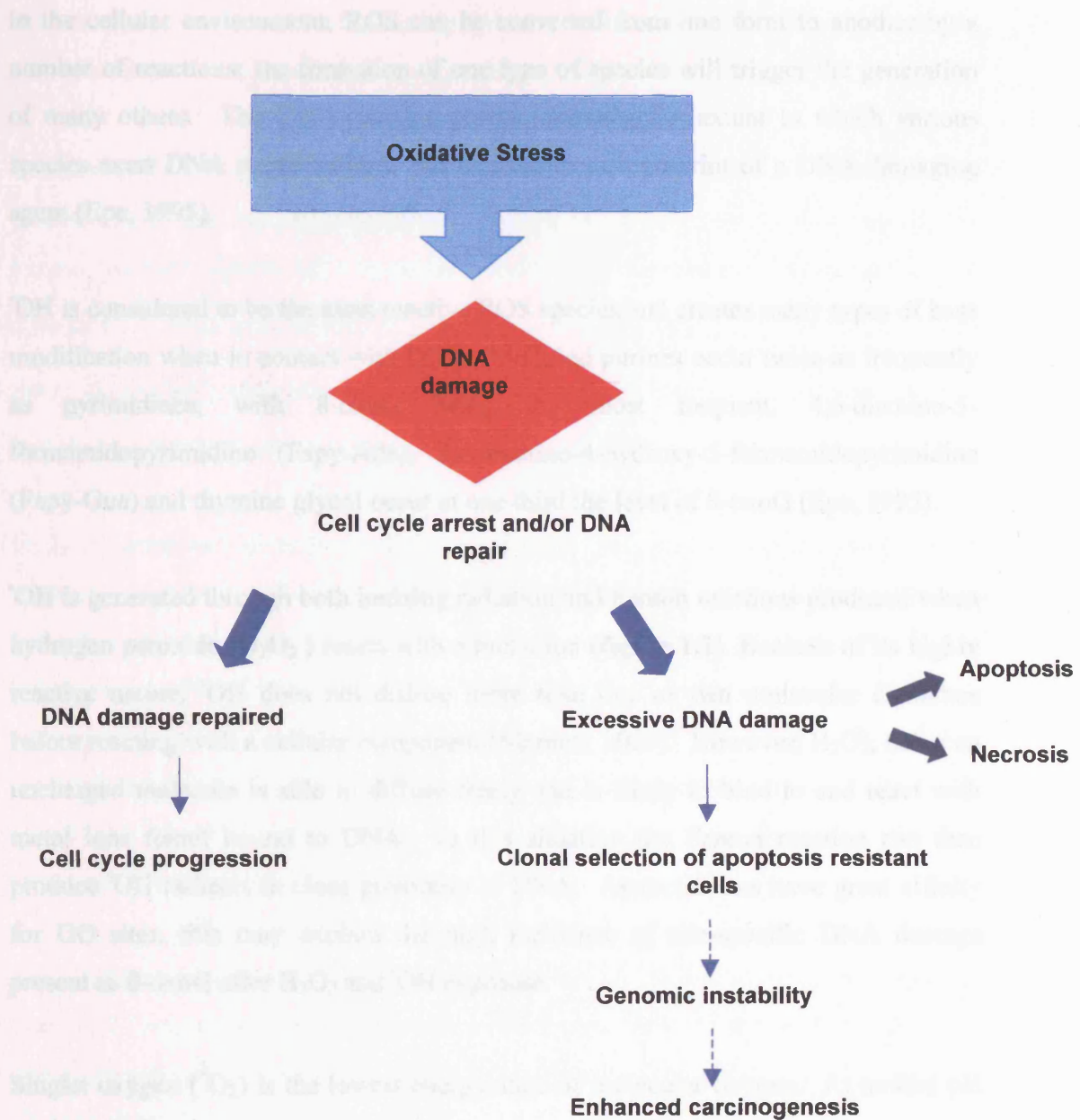


Figure 3.1: Cellular responses and consequences of oxidative stress. Oxidative stress results in oxidative DNA damage, which may result in cell cycle arrest and initiation of DNA repair mechanisms. If DNA is repaired then the cell cycle will resume and cells will proliferate as normal. Excessive DNA damage may be too severe for efficient repair and results in cell death either via apoptotic or necrotic mechanisms. Cells that do not undergo cell death but retain an amount of DNA damage may be resistant to apoptosis and introduce genomic instability leading to enhanced carcinogenesis.

In the cellular environment, ROS can be converted from one form to another by a number of reactions; the formation of one type of species will trigger the generation of many others. The DNA damage profile, showing the extent to which various species exert DNA modifications, can be used as a fingerprint of a DNA damaging agent (Epe, 1995).

$\cdot\text{OH}$ is considered to be the most reactive ROS species and creates many types of base modification when in contact with DNA. Modified purines occur twice as frequently as pyrimidines, with 8-oxoG being the most frequent. 4,6-diamino-5-formamidopyrimidine (Fapy-Ade), 2,6-diamino-4-hydroxy-5-formamidopyrimidine (Fapy-Gua) and thymine glycol occur at one third the level of 8-oxoG (Epe, 1995).

$\cdot\text{OH}$ is generated through both ionizing radiation and Fenton reactions produced when hydrogen peroxide (H_2O_2) reacts with a metal ion (**figure 1.2**). Because of its highly reactive nature, $\cdot\text{OH}$ does not diffuse more than one or two molecular diameters before reacting with a cellular component (Marnett, 2000). However, H_2O_2 , being an uncharged molecule is able to diffuse freely and is likely to bind to and react with metal ions found bound to DNA. In this situation the Fenton reaction can then produce $\cdot\text{OH}$ radicals in close proximity to DNA. As metal ions have great affinity for GG sites, this may explain the high incidence of site-specific DNA damage present as 8-oxoG after H_2O_2 and $\cdot\text{OH}$ exposure.

Singlet oxygen ($^1\text{O}_2$) is the lowest energy state of molecular oxygen. At neutral pH guanine is the only substrate of $^1\text{O}_2$, which predominantly generates 8-oxoG in mammalian cells (Epe, 1995; Cadet *et al.*, 1997). $^1\text{O}_2$ is generated both in photoreactions and dark reactions. In photoreactions, a photosensitiser molecule absorbs light and reacts with molecular oxygen in energy transfer reactions (type II reactions). The transfer reaction with oxygen is very efficient and so is able to compete with type I reactions in which the photosensitiser reacts directly with molecules such as DNA (Epe, 1995). Cellular constituents such as porphyrins and flavins are potential photosensitisers. In dark reactions $^1\text{O}_2$ is formed from the interactions of peroxy radicals and hypochlorite and peroxynitrite plus H_2O_2 . Such

reactions are of potential biological significance under conditions of oxidative stress, particularly at sites of inflammation (Epe, 1995; Cadet *et al.*, 1997).

Superoxide ($O_2^{\cdot-}$) is relatively unreactive with DNA by itself but dismutates to produce H_2O_2 that, in the presence of transition metal ions, forms $\cdot OH$ through the Fenton reaction (**figure 1.2**). It can also reduce and liberate Fe^{3+} from ferritin and liberate Fe^{2+} from iron-sulphur clusters (Henle & Linn, 1997). $O_2^{\cdot-}$ also reacts with nitric oxide ($NO\cdot$) to produce peroxynitrite ($ONOO^-$). Endogenous sources of $O_2^{\cdot-}$ include macrophages and neutrophils (Cadet *et al.*, 1997).

H_2O_2 is generated directly in many enzymatic and non-enzymatic reactions of molecular oxygen in cells (Epe, 1995). It is often assumed not to react directly with DNA but some evidence has been presented for the formation of adenine-1-oxide in both isolated and cellular DNA (Epe, 1995). However, Fenton reactions appear to play a major role in the biological effects mediated by H_2O_2 in cells. The damage profile is similar to $\cdot OH$, the highly reactive product of the Fenton reaction, but the *in vivo* repair of up to eleven different base adducts has been detected after H_2O_2 treatment (Jaruga & Dizdaroglu, 1996).

Solar light contains both UVA (320-380 nm, 95%) and UVB (280-320, 5%) radiation. The UVB component is primarily responsible for induction of skin cancer and causes direct photoactivation of DNA to form cyclopyrimidine dimers (CPD) and 6-4 photoproducts (Kawanishi *et al.*, 2001).

Oxidative adducts such as 8-oxodG can also be induced through type I and type II photoreactions mediated via UVA induced mechanisms that can also involve the generation of ROS (**figure 3.2**) (Kawanishi *et al.* 2001). The damage profile produced by treatment of cells with visible light (400-500 nm) is described as being similar to those of 1O_2 and type I photosensitisers, purine base adducts being generated in high excess to strand breaks, AP sites and pyrimidine modifications (Epe, 1995; Pflaum *et al.*, 1998).

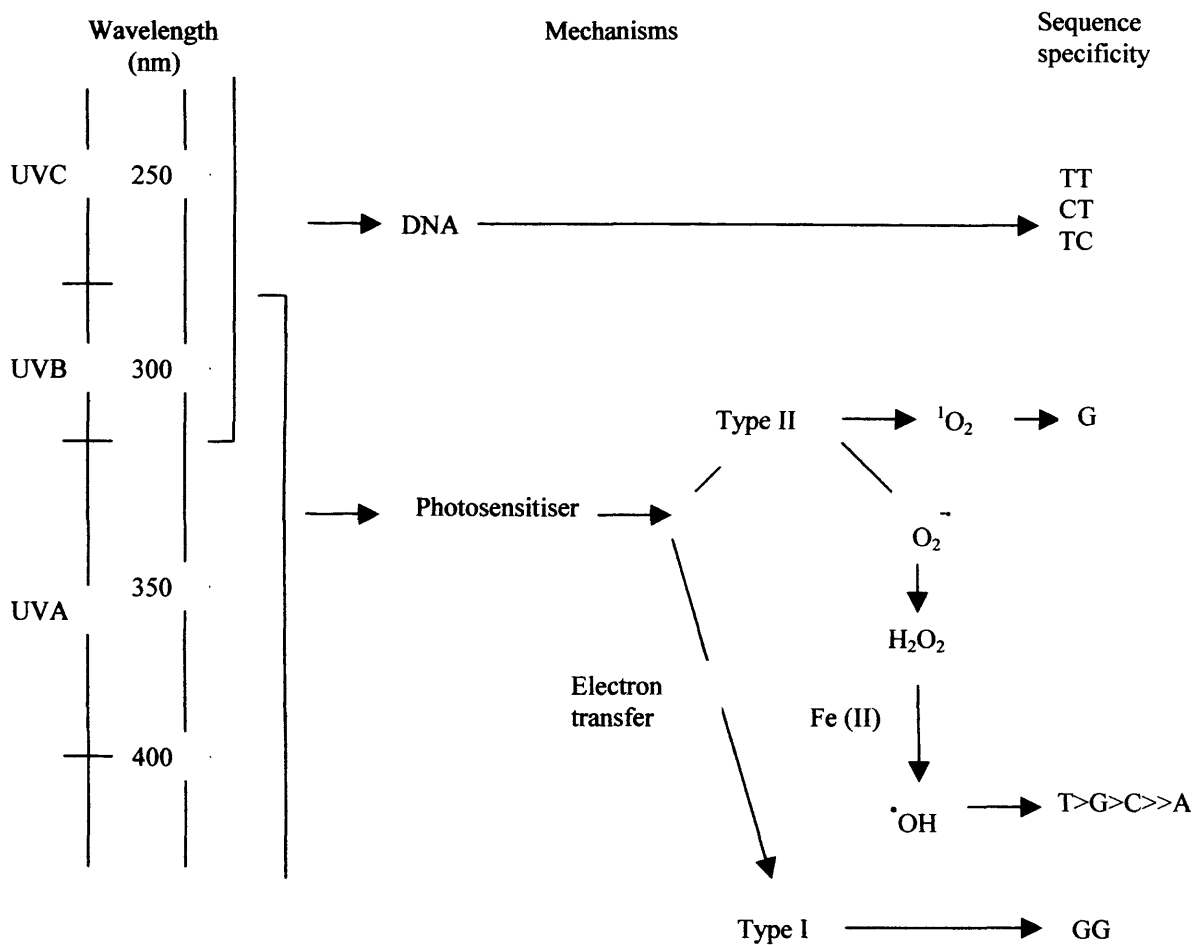


Figure 3.2: Mechanisms of UV-induced DNA damage mediated by photosensitisers and its sequence specificity

Taken from Kawanishi *et al.* (2001).

Oxidative DNA damage has been measured by a number of different techniques (Ames, 1989; Cadet *et al.*, 1997; Dizdaroglu *et al.*, 2002, ESCODD, 2003). Despite the prevalence of such methods, there is still debate over the sensitivity and accuracy of many of these measurements. The European Standards Committee on Oxidative DNA Damage (ESCODD) has been established to resolve these problems. In its most recent report (ESCODD, 2003) measurements taken using the chromatographic methods of GC-MS, HPLC-MS/MS and HPLC-ECD were assessed in comparison with the enzymatic methods of alkaline unwinding, alkaline elution and single cell gel electrophoresis (comet assay). The enzymatic techniques were found to be highly sensitive and reported levels of 8-oxodG in untreated HeLa cells of 0.53 lesions per 10^6 guanines compared to 4.01 per 10^6 for chromatographic methods (ESCODD, 2003).

3.2 AIMS

The aims of the work in this chapter were to establish a suitable model system in which to study the effects of cellular oxidative stress on modulation of DNA repair factors and their activity. This model must be capable of inducing oxidative DNA damage at levels that are in excess to those produced during normal metabolic processes, but not at sufficient levels to lead to the activation of cell death signalling and apoptosis. Different agents will be studied (H_2O_2 , HOCl, UVB and the antioxidant vitamin C) in order to ascertain whether the different DNA damage profiles produced by such agents will result in different DNA repair responses. The type of cell studied should also be capable of damage detection and DNA repair responses typical of those produced *in vivo*.

Different methods of RNA isolation will be investigated to determine the most suitable protocol for the isolation of pure and intact RNA for use in the ribonuclease protection assay in future studies (chapter 4). Preliminary ribonuclease protection assays will be performed in order to establish optimal conditions for analysis of gene transcript levels in cells exposed to oxidative stress. Cell viability following treatment with the selected oxidative stress inducing agents will be assessed in order to establish suitable non-cytotoxic concentrations for use in further studies. DNA damage induced by the oxidative stress generating agents will also be measured to ensure that adequate damage is occurring for any DNA repair processing to become necessary.

3.3 METHODS

3.3.1 Cell culture

Normal dermal fibroblasts were obtained (with informed consent) from a patient undergoing mammary reduction at the Leicester Royal Infirmary, Leicester, UK and processed by Angie Gillies (Dept. Pathology, University of Leicester, Leicester, UK). They were maintained in culture as described in section 2.3.1.1. Aliquots of 1×10^6 cells of low passage were frozen down and stored in liquid nitrogen until required. Cells were not used once they had reached passage 20.

The CCRF-HSB-2 cell line used to assess the three RNA isolation kits was cultured as described in section 2.3.1.1. Cells were grown to a confluence of $1-2 \times 10^6$ cells/mL and not used after passage 20.

Primary lymphocytes were obtained from PBMC separated from whole blood of healthy donors as described in section 2.3.1.1. The isolated PBMCs were incubated at 37°C for 1 hour to allow any monocytes to adhere to the cell culture flask before removing the cell culture medium containing the lymphocytes to a fresh flask. Isolated lymphocytes were maintained in culture as described in section 2.3.1.1.

3.3.2 Cellular viability

Normal dermal fibroblast cell viability was assessed using the CellTiter 96® Aqueous Non-Radioactive Cell Proliferation Assay as described in section 2.3.1.3. Cells were seeded at 5000 cells/well in a 96-well plate and incubated at 37°C to allow population doubling. Cells were treated in triplicate with each of the four agents being tested: 400 μ M H₂O₂, 600 J/M² UVB, 300 nM HOCl or 400 μ M vitamin C at 4, 8 and 24 hours. Absorbance at 492 nm was measured 1 hour following the addition of 20 μ L of MTS/PMS solution. Control, untreated, cells had 20 μ L blank medium added. A blank control contained 100 μ L complete medium without any cells present.

3.3.3 RNA isolation procedures

RNA extractions with three separate kits were performed as detailed in section 2.3.2. For the SV Total RNA kit a total of 5×10^6 CCRF-HSB-2 cells were used per sample; the Purescript® RNA Isolation Kit was performed using 1 mL of cells at $1-2 \times 10^6$ cells/mL per sample and the RNazol™ B extraction was performed on a total of $10-20 \times 10^6$ cells per sample. Before each extraction procedure, cell counts were performed in triplicate using a haemocytometer (section 2.3.1.3).

RNA Quantitation

Once isolated, total RNA was quantitated spectrophotometrically by analysis at 260 nm, 280 nm and 230 nm, in order to check RNA purity and determine yield. The A260:A280 ratio gives a measure of purity and indicates contamination due to the presence of proteins or phenol (as used in the RNazol™ B procedure). The A260:A280 ratio should be approximately 2.0 for pure RNA but 1.7-2.1 is the acceptable range. The A260:A230 ratio indicates possible contamination by guanidinium thiocyanate (as used in the SV Total RNA Kit) and should be approximately 1.5 for an uncontaminated sample. The A260 value gives a reading of RNA content, where one A260 unit of single stranded RNA is equivalent to 40 µg/mL.

RNA integrity

The integrity of the RNA samples was assessed by denaturing gel electrophoresis on a 1.5% (w/v) agarose gel at 75V for 110 minutes and stained with ethidium bromide (0.5 µg/mL) (section 2.3.2.2). Samples (2-3 µg RNA) were denatured on ice in 18 µL of a formaldehyde/formamide sample buffer and 2 µL loading buffer added. Samples were vortexed and then heated at 65°C for 12 minutes before being loaded on to the gel.

RNA markers (0.28-6.58 kb) were used to identify 28S rRNA (4,800 bp) and 18S rRNA (1,900 bp) bands which should appear in a 2:1 ratio for an intact RNA sample. Results were visualised using the BioRad MultiImager and bands quantified, taking into account background interference.

3.3.4 Determining suitable cellular model

The suitability of different cell types for the investigations was assessed. Peripheral blood mononuclear cells (PBMC) were separated from whole blood using Histopaque 1077 (section 2.3.1.1). In an attempt to obtain a pure population of lymphocytes the PBMC layer was plated out for 1 hour to allow monocytes present to adhere to the cell culture flask. Lymphocytes were then obtained by removing the culture medium from the flask and centrifuging at 200 g for 5 minutes. RNA was extracted from the final lymphocyte pellet using 1 mL RNAzol™ B per 5×10^6 cells.

Normal dermal fibroblasts were obtained as described in section 2.3.1.1. RNA was extracted from approximately 10×10^6 cells using 1 mL RNAzol™ B and final RNA pellets stored at -80°C until RNA quantitation and integrity could be assessed (section 2.3.2.2). CCRF-HSB-2 cells were not considered suitable to be used as a cellular model due to their leukaemic status.

3.3.5 DNA damage measurement

3×10^5 normal dermal fibroblasts were seeded in 6-well plates and allowed to attach for 24 hours prior to treatment with $400 \mu\text{M H}_2\text{O}_2$, 600 J/M^2 UVB, 300 nM HOCl or $400 \mu\text{M}$ vitamin C for 2 hours at 37°C . One 6-well plate was used per treatment so that + and – Fpg treatment was performed in triplicate for each agent. The alkaline unwinding technique was then performed (under subdued lighting) as detailed in section 2.3.5.1. Attached cells were firstly rinsed with sterile PBS, then lysed on ice and histones removed by a brief incubation with a salt solution. Fpg buffer, with or without Fpg protein ($1 \mu\text{g/mL}$) was added for 30 minutes at 37°C in order to produce ‘nicks’ in the cells DNA at sites of oxidative damage (primarily 8-oxoG). Alkaline solution I (pH 12.3) was added to perform unwinding of the DNA and the reaction stopped by neutralisation using 0.2 M HCl to a final pH of 6.8. Samples were sonicated on ice and SDS added to a final concentration of 0.05%.

The separation of single- and double-stranded DNA was performed on 0.5 mL hydroxyapatite columns constantly heated to 60°C (section 2.3.5.2). 1.5 mL of 0.15 M and 0.35 M potassium phosphate buffer was used for the elution of single- and double-stranded DNA respectively. DNA content of both fractions was then

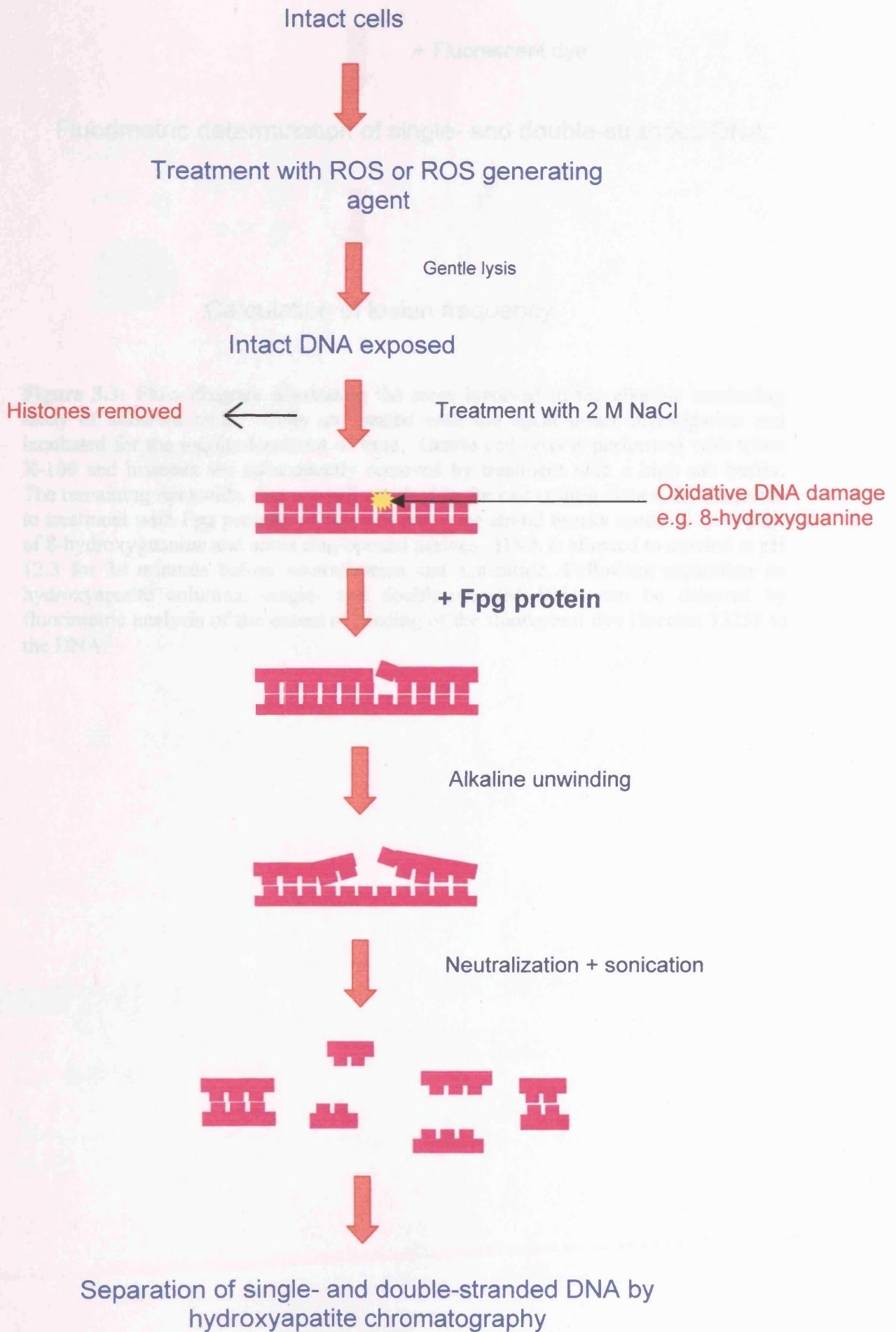
determined by adding Hoechst 33258 to a final concentration of 7.5×10^{-7} M. Fluorescence was then measured (Ex 360 nm, Em 455 nm) and the percentage of double- and single-stranded DNA content determined. The number of Fpg-sensitive lesions per cell was then calculated using the methods of Hartwig *et al.*, 1996. A brief summary of the technique is shown in **figure 3.3**.

3.3.6 Optimising conditions for the ribonuclease protection assay

The ribonuclease protection assay involves the *in vitro* synthesis of a radioactively labelled anti-sense RNA probe transcribed from a DNA template. The probe anneals to complementary mRNA species present in a sample of total RNA, which is extracted from the samples under investigation, in an overnight hybridization reaction. Any single-stranded RNA or free anti-sense probe is then digested by RNase treatment and the protected double-stranded species are extracted from the reaction mixture and then resolved on a denaturing polyacrylamide gel and subjected to autoradiography followed by densitometric analysis. An overview of the procedure is shown in **figure 3.4**.

The ribonuclease protection assay procedure is detailed in section 2.3.4.1. The use of 10 μ g, 15 μ g and 20 μ g total RNA was assessed. Optimal concentrations of [α - 32 P] UTP were also investigated based on the manufacturer's recommendations of 3.1×10^5 cpm/ μ L, 3.9×10^5 cpm/ μ L and 2.3×10^5 cpm/ μ L for the hBER-1, hNER-1 and hNER-2 kits respectively. Dried gels were exposed to autoradiography film for different lengths of time in order to establish the most suitable exposure time for densitometric analysis.

Chapter 3: Establishing a cellular model



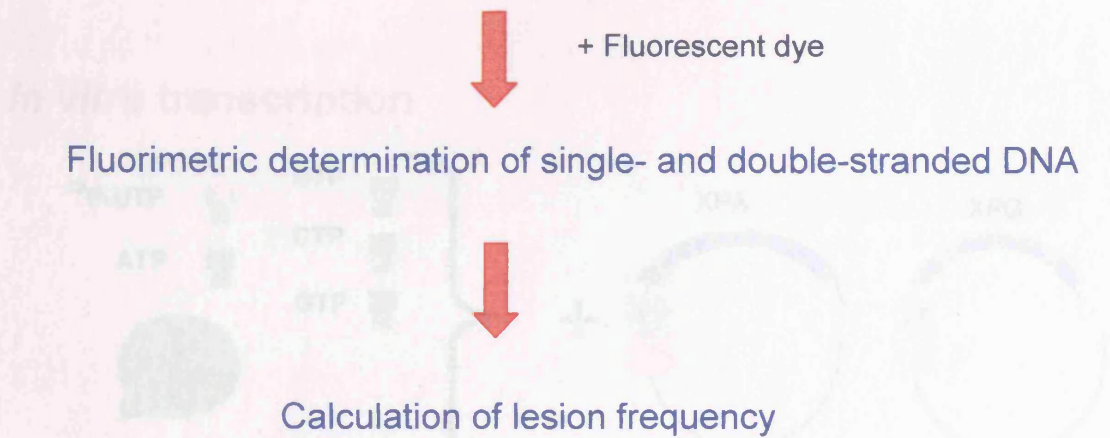
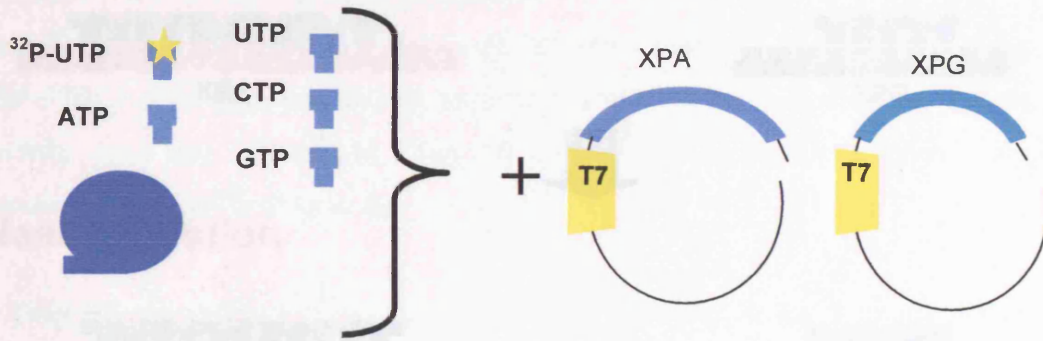
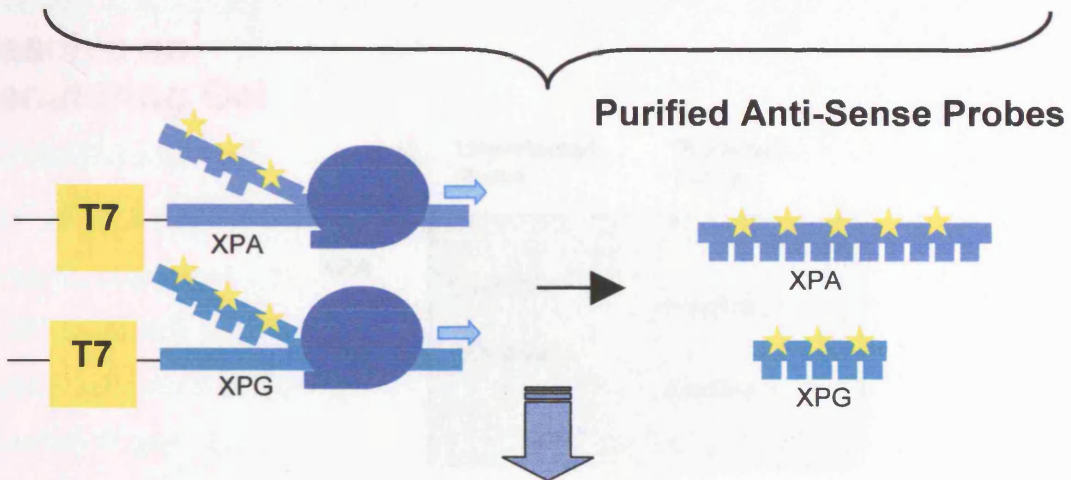


Figure 3.3: Flow diagram illustrating the steps involved in the alkaline unwinding assay of adherent cells. Cells are treated with the agent under investigation and incubated for the required amount of time. Gentle cell lysis is performed with triton X-100 and histones are subsequently removed by treatment with a high salt buffer. The remaining nucleoids, that are still attached to the cell culture dishes, are subjected to treatment with Fpg protein, which will introduce strand breaks specifically at sites of 8-hydroxyguanine and some ring-opened purines. DNA is allowed to unwind at pH 12.3 for 30 minutes before neutralization and sonication. Following separation on hydroxyapatite columns, single- and double-stranded DNA can be detected by fluorimetric analysis of the extent of binding of the fluorescent dye Hoechst 33258 to the DNA.

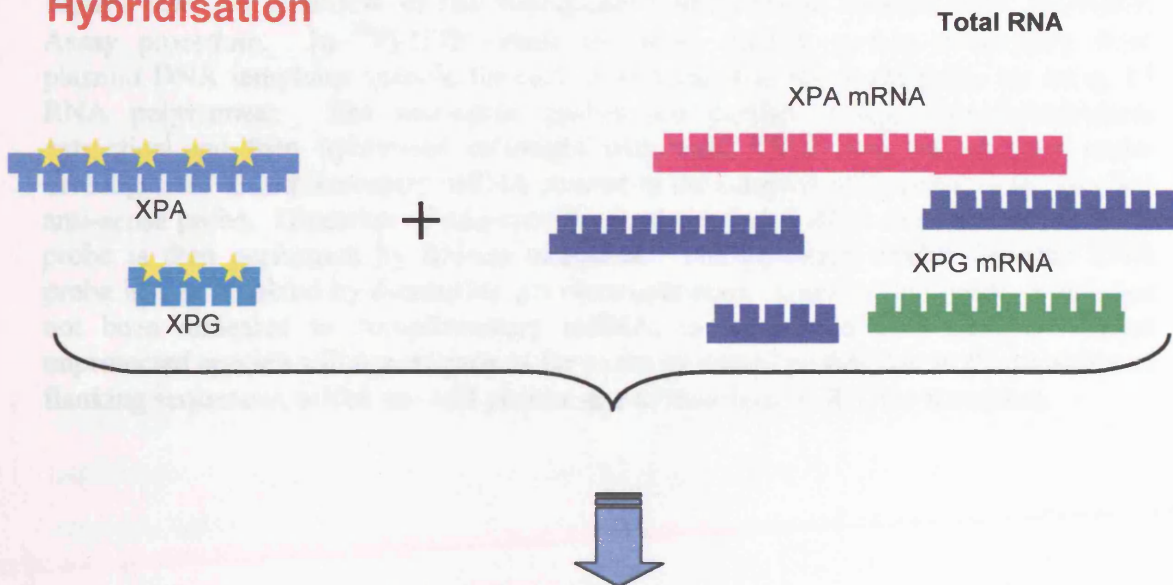
In vitro transcription



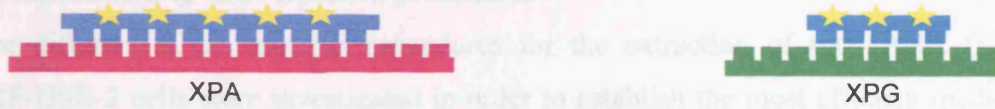
T7 RNA Polymerase



Hybridisation



Annealing of complimentary mRNA



RNase Digestion



Resolve on Denaturing Gel

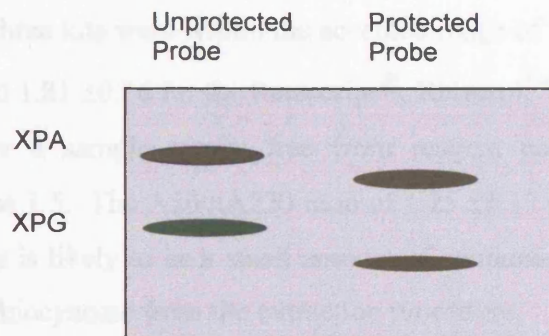


Figure 3.4: An overview of the Riboquant™ Multi-Probe Ribonuclease Protection Assay procedure. [α - 32 P]-UTP labels anti-sense mRNA probes transcribed from plasmid DNA templates specific for each gene present in the multi-probe kit using T7 RNA polymerase. The anti-sense probes are purified using phenol:chloroform extraction and then hybridised overnight with total RNA from the samples under investigation. Complementary mRNA present in the samples will anneal to the labelled anti-sense probe. Digestion of non-specific single-stranded RNA and excess anti-sense probe is then performed by RNase treatment. The protected double-stranded RNA probe is then resolved by denaturing gel electrophoresis. Unprotected probe, which has not been annealed to complimentary mRNA, is used as a size marker. These unprotected species will not migrate as far as the protected probes due to the presence of flanking sequences, which are still present due to their lack of RNase treatment.

3.4 RESULTS

3.4.1 Assessment of RNA isolation procedures

Three different RNA isolation procedures for the extraction of total RNA from CCRF-HSB-2 cells were investigated in order to establish the most efficient method to obtain pure and intact total RNA for use in ribonuclease protection assay experiments (detailed in chapter 4).

The three RNA isolation kits were chosen because of their differing methods of total RNA isolation. The SV Total RNA System uses a guanidinium thiocyanate membrane based procedure, Purescript® is based on cell lysis and precipitation using an anionic detergent and RNAzol™ B uses a phenol:chloroform extraction. A summary of the results produced with each of the three RNA isolation kits is shown in **table 3.1**.

A260:A280 ratios for all three kits were within the accepted range of 1.7 to 2.1, being 2.09 ± 0.22 , 1.67 ± 0.19 and 1.81 ± 0.16 for the Purescript®, RNAzol™ B and SV Total Systems respectively. For a sample totally free from reagent contamination the A260:A230 ratio should be 1.5. The A260:A230 ratio of 1.25 ± 0.17 for the SV Total system indicates that there is likely to be a small amount of contamination due to the presence of guanidinium thiocyanate from the extraction procedure.

The total yields produced by each sample ranged from a mean of $9.97 \pm 3.50 \mu\text{g}$ for the SV Total System to $15.45 \pm 13.98 \mu\text{g}$ for Purescript® and $77.11 \pm 27.46 \mu\text{g}$ for RNAzol™ B. Yield was calculated using the A260 reading, where 1 A260 unit of single-stranded RNA is equivalent to $40 \mu\text{g/mL}$. Figures adjusted for yield of RNA produced per 1×10^6 cells revealed that the kits are comparable when assessed in this way. The SV Total System and RNAzol™ B adjusted figures showed yields per 1×10^6 cells of $2.46 \pm 0.81 \mu\text{g}$ and $5.03 \pm 2.59 \mu\text{g}$ respectively. The Purescript® kit gave a mean yield per 1×10^6 cells of $8.00 \pm 7.30 \mu\text{g}$ but both the standard deviation and coefficient of variation (91.25 %) showed high variability indicating very poor reproducibility.

Kit	260:280	260:230 ^a	Total Yield (µg)	Yield (µg/ 10 ⁶ cells)	Starting Material	RNA Integrity Ratio ^b	Extraction Time	Extraction Method	Cost
Purescript® n = 43	2.09 ±0.22 10.48%	N/A	15.45 ±13.98 90.49%	8.00 ±7.30 91.25%	1 - 2 × 10 ⁶ cells	2.08 ±0.31 14.93%	2.5 - 3.0 hours	Anionic detergent	£88.50 (100 samples)
RNAzol™ B n = 19	1.67 ±0.19 11.32%	N/A	77.11 ±27.46 35.62%	5.03 ±2.59 51.50%	10 - 20 × 10 ⁶ cells	2.24 ±0.09 4.11%	3.0 - 3.5 hours	phenol:chloroform	£139 (100 samples)
SV Total System n = 21	1.81 ±0.16 8.96%	1.25 ±0.17 14.05%	9.97 ±3.50 35.11%	2.46 ±0.81 32.78%	5 × 10 ⁶ cells	1.87 ±0.35 18.49%	3.0 - 3.5 hours	guanidinium thiocyanate	£125 (100 samples)

Table 3.1: Summary of RNA extraction from CCRF-HSB-2 cell line using three commercially available RNA isolation kits.

Figures shown are mean ± standard deviation and % coefficient of variation.

^a A260:A230 ratio gives an indication of contamination by guanidinium thiocyanate and is not applicable to Purescript® and RNAzol™ B.

^bn = 8. Intact RNA should have an integrity ratio of 2.0. Less than 2.0 indicates degradation of RNA.

Integrity results, determined by denaturing agarose gel electrophoresis, indicated that all three kits produced intact RNA. An example of an integrity gel is shown in **figure 3.5**.

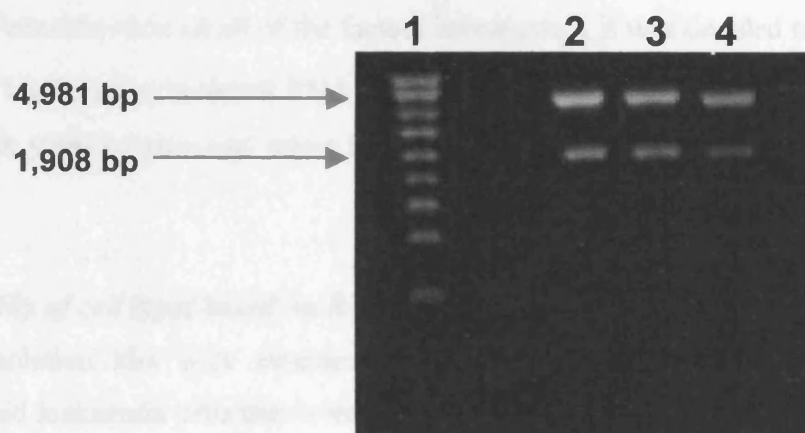


Figure 3.5: Integrity of RNA extracted from CCRF-HSB-2 cells using three separate RNA isolation kits. CCRF-HSB-2 RNA was extracted and quantitated using RNAzol™ B, SV Total RNA System or the Purescript® kit as described in section 3.3.3. 2-3 μg RNA was denatured in sample buffer and loading buffer, heated at 65°C for 12 minutes and loaded on to a 1.5% (w/v) agarose gel with 0.5 $\mu\text{g}/\text{mL}$ ethidium bromide. Samples and 0.28 – 6.58 kb RNA marker were run at 75V for 110 minutes then visualised using a UV transilluminator. Integrity ratios were determined by densitometric analysis of 28S (4,800 bp) and 18S (1,900 bp) rRNA bands. **Lane 1;** 0.28 – 6.58 kb RNA marker. **Lanes 2-4;** RNA extracted using RNAzol™ B, SV Total RNA System and the Purescript® kit respectively.

Integrity ratios for the three kits were 2.24 ± 0.09 , 1.87 ± 0.35 and 2.08 ± 0.31 for the RNAzol™ B kit, SV Total System and Purescript® kit respectively (**table 3.1**). However, the SV Total System and Purescript® kit had much higher coefficients of variation compared to that of the RNAzol™ B kit being 18.49% and 14.93% compared to 4.11% respectively.

The three kits each took between 2 – 3 hours for complete extraction. They also did not vary greatly in cost. The RNAzol™ B and the SV Total System cost £139 and £125 per 100 samples respectively and the Purescript® kit cost £88.50 per 100 samples. The number of replicates for each kit varied due to the amount of starting

material needed; limiting the number of samples that could be extracted in one batch for RNAzol™ B and the SV Total System.

After careful consideration of all of the factors investigated, it was decided to use the RNAzol™ B kit for all subsequent RNA extractions. This decision was based on its relatively high yield of pure and intact RNA and low degree of variability between extractions.

3.4.2 Suitability of cell types based on RNA yield

The RNA isolation kits were assessed using highly proliferative CCRF-HSB-2 lymphoblastoid leukaemia cells that were easily grown to high density in suspension. The use of this cell line for further investigations was not suitable due to their leukaemic status. Primary lymphocytes obtained from peripheral blood of healthy donors and primary dermal fibroblasts obtained from mammary reduction were assessed for their suitability for use in further studies. The RNAzol™ B kit was used for total RNA isolation.

Table 3.2 shows RNA integrity and purity values, along with yield of total RNA for primary lymphocytes and fibroblasts using RNAzol™ B.

Cell Type	A260:A280	RNA Integrity Ratio	Yield (µg/10⁶ cells)
Primary lymphocytes (n=5)	1.58 ±0.03	1.69 ±0.13	1.73 ±0.52
Primary fibroblasts (n=6)	1.69 ±0.10	1.48 ±0.11	12.60 ±6.72

Table 3.2: Comparison of RNA extraction from primary lymphocytes and normal dermal fibroblasts. RNA was extracted using RNAzol™ B as detailed in section 3.3.3. RNA purity, integrity and yield were also determined as described in section 3.3.3.

Chapter 3: Establishing a cellular model

The primary lymphocytes and dermal fibroblasts gave similar A260:A280 ratios, 1.58 ± 0.03 and 1.69 ± 0.10 respectively. The slightly higher value for the dermal fibroblasts indicates that RNA of a slightly higher purity is present. RNA integrity ratios for both cell types were quite low, 1.69 ± 0.13 and 1.48 ± 0.11 for the primary lymphocytes and dermal fibroblasts respectively, indicating slightly more intact RNA in the primary lymphocytes total RNA. The yield of total RNA per 1×10^6 cells was quite different between the two types of cell, being 1.73 ± 0.52 and 12.60 ± 6.72 for the lymphocytes and fibroblasts respectively, indicating that a much greater yield of total RNA was obtainable from the fibroblasts compared to the primary lymphocytes. Due to the comparable A260:A280 and integrity ratios, the much greater yield of total RNA from the dermal fibroblasts and better reproducibility (since different donors would be needed to obtain sufficient amounts of RNA from lymphocytes), it was decided to use dermal fibroblasts for further investigations to be shown in this thesis.

3.4.3 Viability following cell treatments

Viability experiments were performed in order to establish concentrations of ROS and ROS generating agents that would induce oxidative stress in human dermal fibroblasts without producing extensive cell death. The CellTiter 96[®] Aqueous Non-Radioactive Cell Proliferation Assay was used to measure viability of the normal dermal fibroblasts over a 24 hour time period following treatment with the agents used in the study (**figure 3.6**).

The A492 of control cells was taken as the baseline for each time point, and so control cells were measured as 100% viable throughout the time course. H₂O₂ and HOCl treatments both gave a slight loss in viability over the 24 hour time period. At 24 hours post treatment the H₂O₂ and HOCl treated fibroblasts showed mean viabilities of 96.3% and 99.6% viable respectively over three repeats.

600 J/M² UVB treatment seemed to increase the absorbance at 492 nm over the time course. The peak in 492 nm absorbance was reached 4 hours after treatment; absorbance then declined over the next 20 hours so that by 24 hours post treatment the absorbance readings were equivalent to those recorded in the control cells. Vitamin C treatment also gave an increase in absorbance after 4 hours, which again had

decreased to levels similar to those recorded in the control cells by 24 hours. This increase produced by vitamin C treatment was much more marked than that of treatment with UVB and reached a maximum of 170% of control.

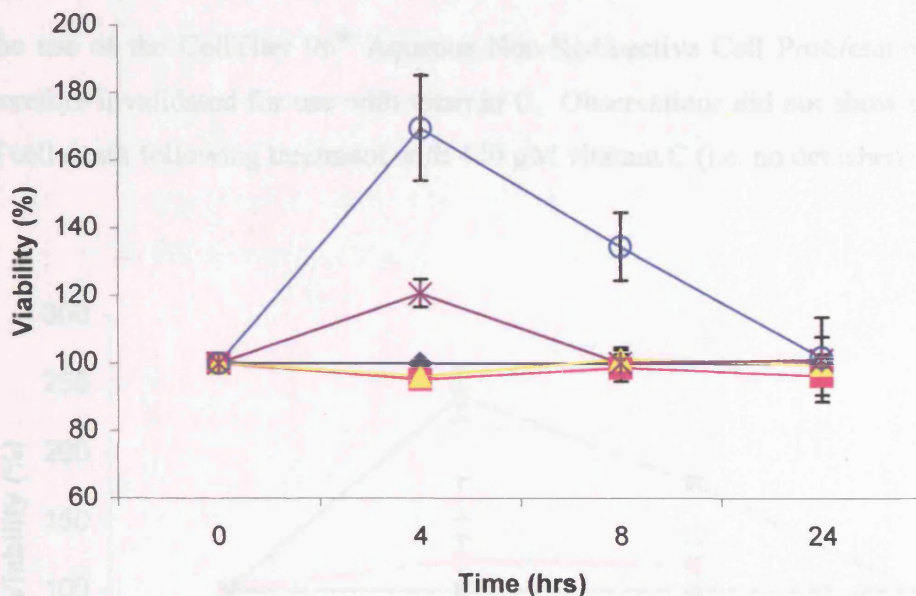


Figure 3.6: Human dermal fibroblast viability over time following treatment with a range of ROS generating agents and the antioxidant vitamin C. Human dermal fibroblasts were seeded at 5000 cells/well in a 96-well plate and incubated at 37°C for 24 hours prior to treatment with no agent (◆), 600 J/M² UVB (×), 400 μM H₂O₂ (■), 300 nM HOCl (▲) or 400 μM vitamin C (○) in triplicate. At the indicated time intervals cells were assessed for viability using the CellTiter 96® Aqueous Non-Radioactive Cell Proliferation Assay. Each treatment was performed in triplicate. Data is the mean of three independent experiments. Data ± SD.

The increase in absorbance following treatment with 400 μM vitamin C was investigated further. Fibroblasts were treated with three doses of vitamin C (100, 200 and 400 μM) in conditions identical to those previously described, and also in a cell free environment. The increase in A492 observed following treatment with vitamin C was dose-dependent, with a higher concentration of vitamin C producing a greater increase in absorbance at 492 nm. Cell viability was calculated as previously to show the dose-dependent relationship in A492 absorbance and is produced in **figure 3.7**.

Similar increases in A492 were also observed in the control experiment, which did not contain fibroblasts (**figure 3.8A**), indicating that the increased A492 is not due to a cellular effect (**figure 3.8B**) but a direct reaction between vitamin C and MTS.

The use of the CellTiter 96[®] Aqueous Non-Radioactive Cell Proliferation Assay is therefore invalidated for use with vitamin C. Observations did not show any amount of cell death following treatment with 400 μ M vitamin C (i.e. no detached cells).

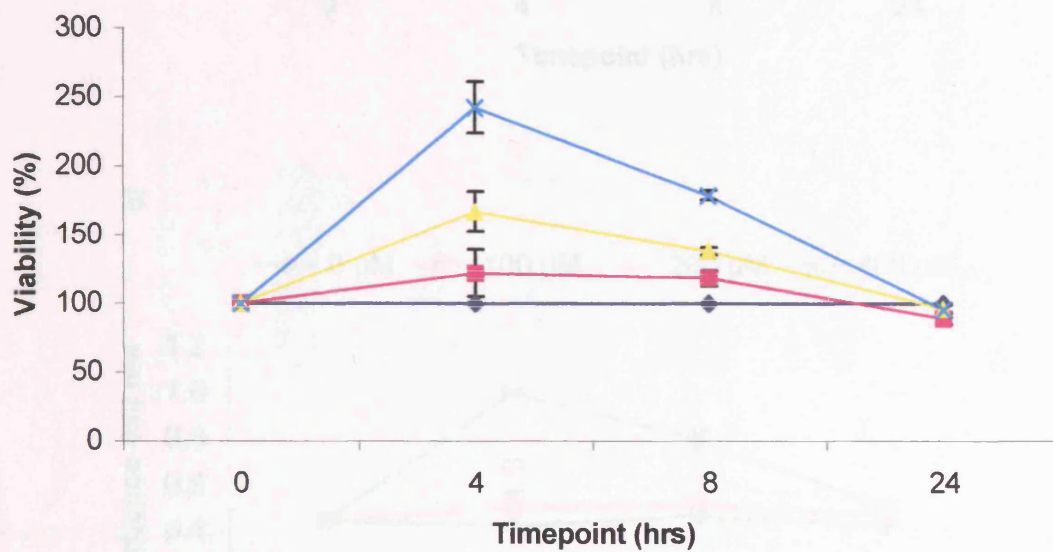


Figure 3.7: Dose dependent increase in cell viability measurement following treatment of dermal fibroblasts with three doses of vitamin C. Human dermal fibroblasts were seeded at 5000 cells/well in a 96-well plate and incubated at 37°C for 24 hours prior to treatment with no agent (◆), 100 μ M vitamin C (■), 200 μ M vitamin C (▲) or 400 μ M vitamin C (×) in triplicate. At the indicated time intervals (0, 4, 8 and 24 hours) cells were assessed for viability using the CellTiter 96[®] Aqueous Non-Radioactive Cell Proliferation Assay. Each treatment was performed in triplicate. Data is the mean of three independent experiments. Data \pm SD.

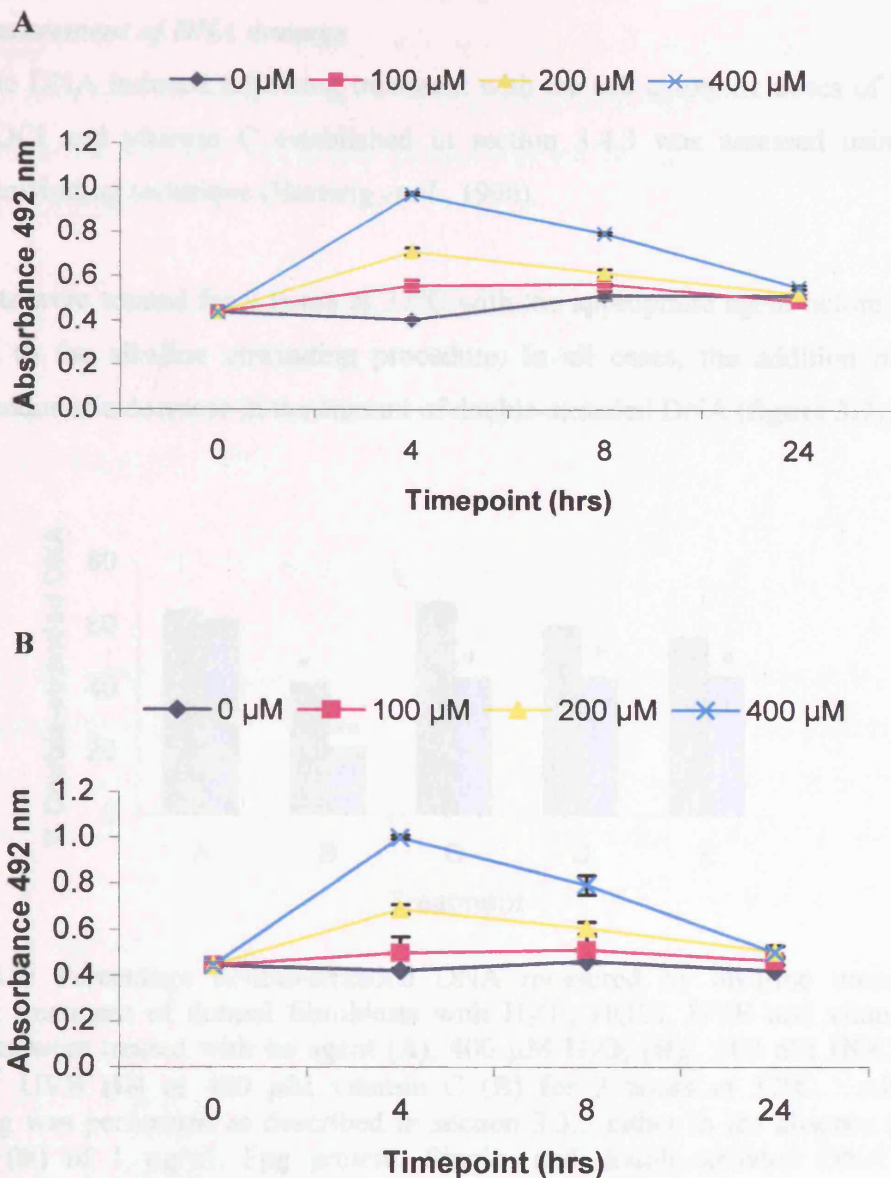


Figure 3.8: Dose-dependent increase in A492 readings following incubation of vitamin C with dermal fibroblasts and also in a cell-free environment. 5000 cells/well dermal fibroblasts were seeded into a 96-well plate in a volume of 100 μ L complete medium and incubated at 37°C for 24 hours prior to treatment with no agent (\blacklozenge), 100 μ M vitamin C (\blacksquare), 200 μ M vitamin C (\blacktriangle) or 400 μ M vitamin C (\times) in triplicate. At the indicated time intervals (0, 4, 8 and 24 hours) 20 μ L MTS/PMS solution was added and absorbance at 492 nm measured using a Denley Wellscan spectrophotometer. **A;** Experiment performed in complete medium, without dermal fibroblasts present. **B;** Experiment performed with dermal fibroblasts present. Each treatment was performed in triplicate. Data is the mean of three independent experiments. Data \pm SD.

3.4.4 Measurement of DNA damage

Damage to DNA induced following treatment with the sub cytotoxic doses of H₂O₂, UVB, HOCl and vitamin C established in section 3.4.3 was assessed using the alkaline unwinding technique (Hartwig *et al.*, 1996).

Fibroblasts were treated for 2 hours at 37°C with the appropriate agent before being subjected to the alkaline unwinding procedure. In all cases, the addition of Fpg protein produced a decrease in the amount of double-stranded DNA (**figure 3.9**).

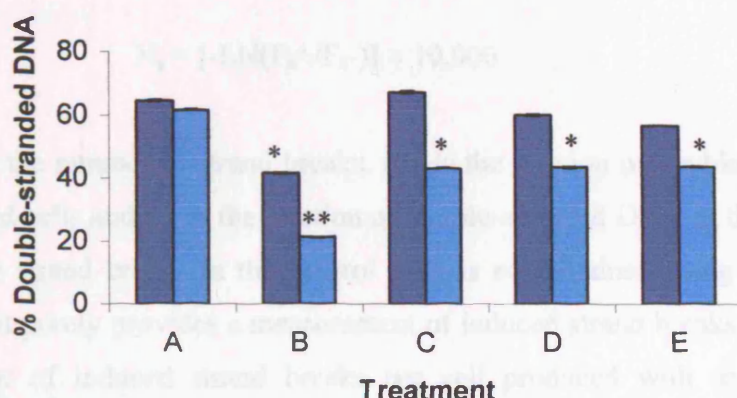


Figure 3.9: Percentage double-stranded DNA measured by alkaline unwinding following treatment of dermal fibroblasts with H₂O₂, HOCl, UVB and vitamin C. Fibroblasts were treated with no agent (A), 400 μM H₂O₂ (B), 300 nM HOCl (C), 600 J/M² UVB (D) or 400 μM vitamin C (E) for 2 hours at 37°C. Alkaline unwinding was performed as described in section 3.3.5 either in the absence (■) or presence (▒) of 1 μg/μL Fpg protein. Single- and double-stranded DNA were separated using hydroxyapatite chromatography (section 3.3.5) and percentage double-stranded DNA calculated. Results are expressed as triplicate readings from three independent experiments. Data ± SD. Means were compared using ANOVA and LSD post test; statistically significant differences between control and treated samples are highlighted as * and ** representing p<0.05 and p<0.02 respectively.

Treatment with 400 μM H₂O₂ significantly decreased the presence of double-stranded DNA from 61.5% ±0.1 in untreated control cells, to 21.2% ±0.1 (p<0.02). Treatment with 300 nM HOCl, 600 J/M² UVB and 400 μM vitamin C also produced significant decreases in percentage of DNA present as double-stranded to 43.2% ±0.1, 43.6% ±0.2 and 43.7% ±0.1 respectively (p<0.05). Samples not treated with Fpg protein showed similar percentages of double-stranded DNA to the control level of 64.4%

± 0.2 for treatment with 300 nM HOCl, 600 J/M² UVB and 400 μ M vitamin C, being 67.3% ± 0.3 , 60.0% ± 0.2 and 56.8% ± 0.1 respectively. The treatment of dermal fibroblasts with 400 μ M H₂O₂ produced a significant decrease in the percentage of double-stranded DNA even when Fpg protein was not added, the percentage being 41.6% ± 0.2 ($p < 0.05$).

The fraction of double-stranded DNA in the treated cells compared to that of the control cells was used to determine the relative number of strand breaks per cell produced by treatment with the DNA damaging agents according to the following equation (Hartwig *et al.*, 1996):

$$N_s = [-\text{LN}(F_{s+}/F_{s-})] \times 10,000$$

where N_s is the number of strand breaks, F_{s+} is the fraction of double-stranded DNA in the treated cells and F_{s-} is the fraction of double-stranded DNA in the control cells. A value for strand breaks in the control cells is not obtained using this method of analysis as it purely provides a measurement of induced strand breaks in treated cells. The number of induced strand breaks per cell produced with each of the four treatments is shown in **figure 3.10**.

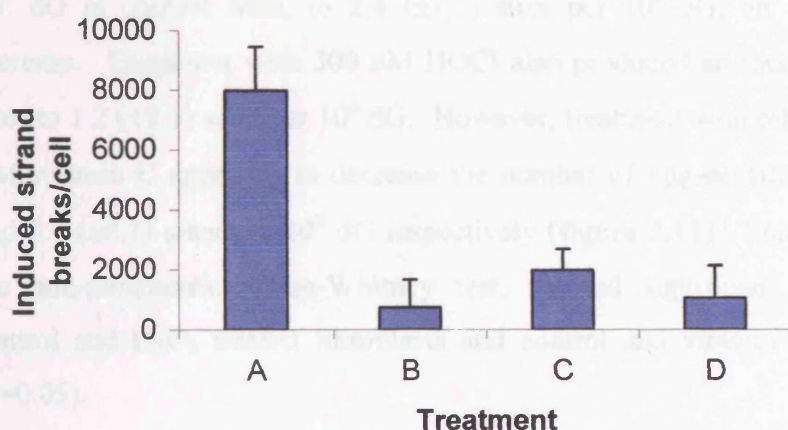


Figure 3.10: Measurement of strand breaks induced per cell in fibroblasts treated with H₂O₂, HOCl, UVB and vitamin C. Fibroblasts were treated with 400 μ M H₂O₂ (A), 300 nM HOCl (B), 600 J/M² UVB (C) or 400 μ M vitamin C (D) for 2 hours at 37°C. Alkaline unwinding and hydroxyapatite chromatography were performed as described in section 3.3.5. The number of induced strand breaks with each treatment was calculated as described in section 3.4.4. The data represent the mean (\pm SD) of triplicate measurements taken from three independent experiments.

Chapter 3: Establishing a cellular model

Treatment with 400 μM H_2O_2 induced the greatest number of strand breaks per cell of the four separate treatments with a value of 7975.8 (± 1465.3) compared to 735.7 (± 924.1), 1981.8 (± 688.5) and 1046.9 (± 1084.8) for treatment with 300 nM HOCl, 600 J/M^2 UVB and 400 μM vitamin C respectively.

The percentage of double-stranded DNA present in the samples after incubation either with or without Fpg protein was then used to calculate the number of Fpg-sensitive sites following treatment with the four agents as previously described (Hartwig *et al.*, 1996; Hartwig, 1998). The fraction of double-stranded DNA decreases logarithmically with increasing numbers of DNA strand breaks according to the following equation:

$$N = [-\text{LN} (F+/F-)] \times 16666$$

where N is the number of Fpg-sensitive sites, F+ is the fraction of double-stranded DNA of the Fpg treated cells, F- is the fraction of double-stranded DNA in cells not treated with Fpg (**figure 3.9**).

When this equation was applied to the treated fibroblasts the number of Fpg-sensitive sites in cells treated for 2 hours with 400 μM H_2O_2 increased from 0.5 (± 0.3) sites per 10^6 dG in control cells, to 2.4 (± 1.5) sites per 10^6 dG; an approximate 4.8-fold increase. Treatment with 300 nM HOCl also produced an increase in Fpg-sensitive sites to 1.2 (± 0.1) sites per 10^6 dG. However, treatment with 600 J/M^2 UVB and 400 μM vitamin C appeared to decrease the number of Fpg-sensitive sites to 0.3 (± 0.1) and 0.0 (± 0.1) sites per 10^6 dG respectively (**figure 3.11**). Statistical analysis using the non-parametric Mann-Whitney test, showed significant differences between control and H_2O_2 treated fibroblasts and control and vitamin C treated fibroblasts ($p=0.05$).

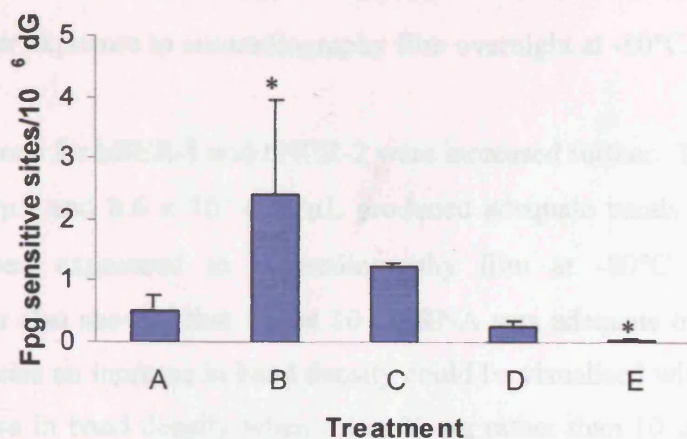


Figure 3.11: Oxidative DNA damage in fibroblasts treated with H₂O₂, HOCl, UVB and vitamin C. Fibroblasts were treated with 400 μM H₂O₂ (B), 300nM HOCl (C), 600 J/M² UVB (D) or 400 μM vitamin C (E) for 2 hours at 37°C. Control cells (A) were sham treated. Alkaline unwinding and hydroxyapatite chromatography were then performed as explained in section 3.3.5. DNA damage is expressed as the number of Fpg-sensitive sites per 10⁶ dG calculated as detailed in section 3.4.4. The data represent the mean (± standard deviation) of triplicate measurements taken from three independent experiments. Data were compared using the Mann-Whitney nonparametric test; statistically significant differences between control and treated samples are highlighted as * representing p=0.05.

3.4.5 Optimisation of ribonuclease protection assay

In the ribonuclease protection assay, the unprotected marker probes do not migrate as far as the protected fragments due to the presence of flanking sequences in the probes that are derived from the plasmids used in the transcription reaction. These flanking sequences do not hybridise with target mRNA and so are digested in the RNase reactions. However, the unprotected marker probes are not subjected to RNase treatments and so the flanking sequences are still present. (This is highlighted later in figure 3.13.)

The manufacturer's recommended probe concentrations of 3.1×10^5 cpm/μL, 3.9×10^5 cpm/μL and 2.3×10^5 cpm/μL for the hBER-1, hNER-1 and hNER-2 kits respectively, were not high enough to enable bands to be detected for each mRNA species in the samples even after up to 48 hours exposure to autoradiography film. In order to combat this, the recommended concentrations were doubled; this proved to

be adequate for the hNER-2 kit, which produced measurable bands with 4.6×10^5 cpm/ μ L after exposure to autoradiography film overnight at -80°C .

Concentrations for hBER-1 and hNER-2 were increased further. It was found that 8.0×10^5 cpm/ μ L and 8.6×10^5 cpm/ μ L produced adequate bands for detection of all species when exposed to autoradiography film at -80°C overnight. These experiments also showed that whilst 10 μ g RNA was adequate to detect most of the mRNA species an increase in band density could be visualised with 20 μ g total RNA. This increase in band density when using 20 μ g rather than 10 μ g total RNA whilst using the hBER-1 kit is shown in lanes 2 (10 μ g) and 3 (20 μ g) of **figure 3.12**. In this example the probe markers are not indicated, as they have not been resolved adequately by the electrophoresis.

As 20 μ g of total RNA was a substantial amount of the RNA which was extracted from the treated samples, it was decided to try using 15 μ g total RNA for the ribonuclease protection assay in order to ensure that enough RNA would be obtained for each sample. As shown by the example in **figure 3.13**, 15 μ g total RNA was adequate for the hNER-2 template set, and was also found to be adequate for use with the other two kits (data not shown).

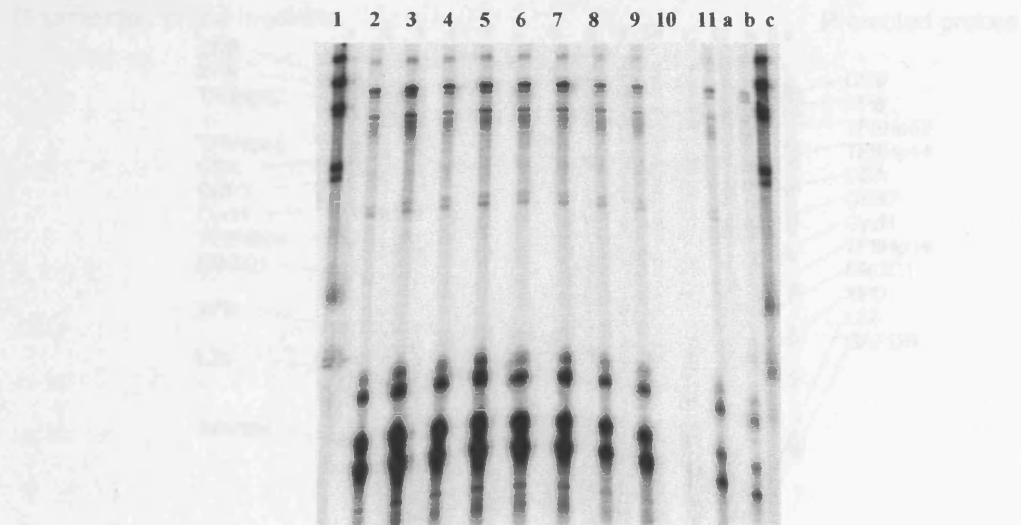


Figure 3.12: Ribonuclease Protection Assay of CCRF-HSB-2 cells using hBER-1 template multi-probe template set. Hybridisation was performed with either 10 µg or 20 µg of total RNA and a total of 8.0×10^5 cpm [α - 32 P] UTP labeled synthesized anti-sense probe. Samples were treated with RNase to digest any single-stranded RNA and free probe. RNase protected double-stranded RNA was extracted by phenol:chloroform:isoamyl alcohol extraction before resolution on a 5% polyacrylamide gel for 2 hours at 50 watts constant power. Lanes 1 and c; unprotected hBER-1 probe marker. Lanes 2 and 3; baseline RNA, 10 µg and 20 µg respectively. Lanes 4, 5, 6 and 7; 20 µg H₂O₂ treated RNA (0 µM, 10 µM, 100 µM and 400 µM respectively) after 2 hours exposure. Lanes 8, 9, 10 and 11; 20 µg H₂O₂ treated RNA (0 µM, 10 µM, 100 µM and 400 µM respectively) after 24 hours exposure. Lane a; yeast tRNA non-specific control (2 µg). Lane b; Human control-RNA-2 (1 µg) integrity control.

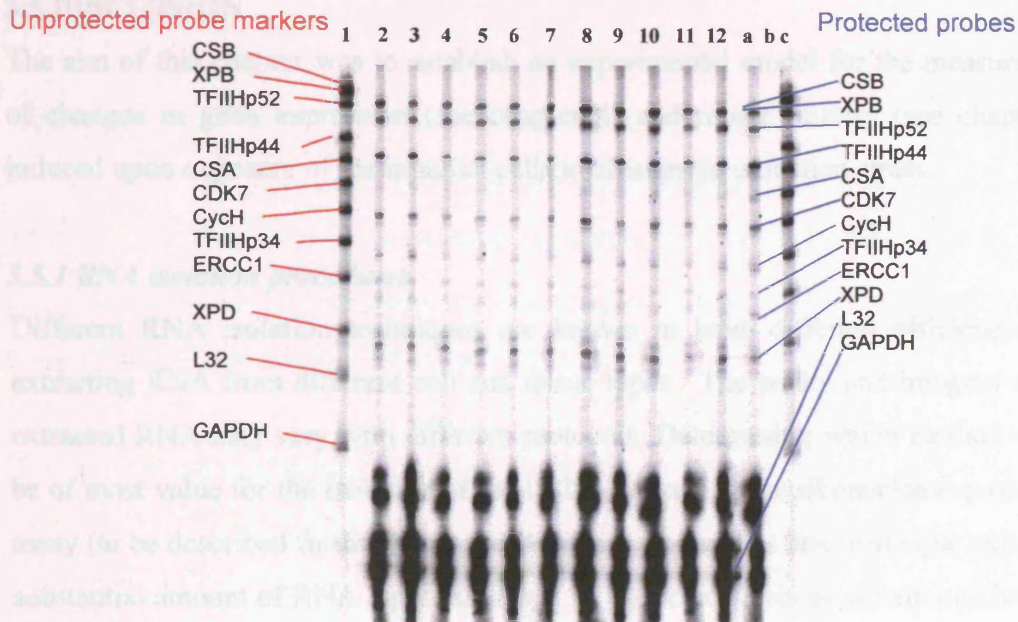


Figure 3.13: Ribonuclease Protection Assay of CCRF-HSB-2 cells using hNER-2 multi-probe template set. 15 μg of total RNA samples were hybridized with a total of 8.6×10^5 cpm [α - ^{32}P] UTP labeled synthesized anti-sense probe and RNase and proteinase treatments performed as described in section 3.3.6 before resolution on a 5% polyacrylamide gel for 2 hours at 50 watts constant power. Lanes 1 and c; unprotected hNER-2 probe marker. Lane 2; baseline RNA. Lane 3; control 0.5 hours post treatment. Lanes 4, 5, 6 and 7; H_2O_2 treated RNA (0 μM , 10 μM , 100 μM and 400 μM respectively) after 0.5 hours exposure. Lane 8; control RNA 1 hour post treatment. Lanes 9, 10, 11 and 12; H_2O_2 treated RNA (0 μM , 10 μM , 100 μM and 400 μM respectively) after 1 hour exposure. Lane a; Human control-RNA-2 (1 μg) integrity control. Lane b; yeast tRNA non-specific control (2 μg).

3.5 DISCUSSION

The aim of this chapter was to establish an experimental model for the measurement of changes in gene expression (see chapter 4) and repair activity (see chapter 5) induced upon exposure of mammalian cells to changes in oxidative stress.

3.5.1 RNA isolation procedures

Different RNA isolation techniques are known to have different efficiencies for extracting RNA from different cell and tissue types. The purity and integrity of the extracted RNA may vary with different protocols. Determining which method would be of most value for the isolation of total RNA for use in the ribonuclease protection assay (to be described further in chapter 4) was important, as this technique requires a substantial amount of RNA (approximately 15 µg per analysis as determined here) of good purity and integrity.

Three RNA isolation kits were chosen on account of their differing methods of extraction. The Purescript® kit used cell lysis and precipitation by an anionic detergent, RNAzol™ B a phenol:chloroform extraction and the SV Total System guanidium thiocyanate. Both phenol and guanidium thiocyanate are hazardous chemicals; the anionic detergent used in the Purescript® kit resulted in a far less hazardous method.

The three kits each took between 2 – 3 hours for complete extraction. The number of extractions performed with each kit varied due to the amount of starting material needed. RNAzol™ B and the SV Total RNA system required 2.5 to 10 times as many cells as the Purescript® RNA isolation kit.

The total yield of RNA obtained with the RNAzol™ B kit was approximately 5 times greater than for the Purescript® kit and almost 8 times greater than with the SV Total System. Although it showed the most reproducibility, the SV Total System did not produce a very substantial yield of RNA considering the amount of starting material

(5×10^6 cells). However, whilst the Purescript® kit produced a greater yield of RNA, it did not provide very reproducible results.

Figures adjusted for yield of RNA produced per 1×10^6 cells revealed that the Purescript® kit produced a slightly greater yield compared to the RNAzol™ B kit, whilst the SV Total System produced the smallest yield, being less than half the yield of the other two kits. Once again the poor reproducibility of the Purescript® kit was highlighted by a very poor coefficient of variation.

Reasons for variability in RNA yield could have been due to the inexperience of handling of RNA and also by the inaccuracy of cell counts produced using a haemocytometer. This would be of particular relevance when the amount of starting material was low, as in the extractions performed with the Purescript® kit. The aliquoting of 1 mL of cellular suspensions for extraction by the Purescript® kit was also more inaccurate than using 10 mL for the RNAzol™ B and SV Total System. The use of differing pipettes for the different volumes may have contributed to inaccuracies.

A260:A280 ratios for all three RNA isolation kits were within the accepted range of 1.7 to 2.1. This indicated that the samples generated from each of the kits were free from contamination by proteins, and in the case of RNAzol™ B, phenol as well. The A260:A230 ratio for the SV Total System was very reproducible, and showed that very little contamination from guanidinium thiocyanate was present.

The integrity ratios of the RNA produced by each kit are indicative of intact RNA. Intact RNA will have a 28S rRNA to 18S rRNA ratio of 2.0. The greater the percentage of 18S rRNA present in a given sample, the smaller the ratio will be, indicating degradation of RNA into smaller fragments. The presence of intact RNA is important for RNA to be used in a ribonuclease protection assay to ensure that mRNA transcripts are reliably measured. The Purescript® kit and RNAzol™ B extraction produced RNA of high integrity, although the lower coefficient of variation for the

RNAzol™ B kit indicated better reproducibility. The SV Total System had a lower integrity ratio and a greater coefficient of variation.

The actual amount of RNA that is required for the ribonuclease protection assay is 10-20 µg per sample. Taking into account all of the above factors such as yield, purity and integrity of the RNA, together with the reproducibility and time taken for extraction, it was decided to use RNAzol™ B for the further extraction of RNA to be used in the ribonuclease protection assay. This is due to its high yield of pure and intact RNA with a lot less variability compared to the Purescript® kit, perhaps due to the larger amount of starting material. The SV Total System was discounted because it produced a much lower yield of slightly less intact RNA.

3.5.2 Identification of suitable cell type for further investigations

As DNA repair is associated with a number of other processes (the p53 response and apoptosis, cellular proliferation and the cell cycle) it is essential that any cellular model used to study DNA repair will produce cellular responses to such treatments similar to those provoked *in vivo*. The T lymphoblastoid CCRF-HSB-2 cell line used for assessment of the RNA isolation kits was not suitable for such experiments as it is derived from a patient with acute lymphoblastoid leukaemia. Many cell lines that are derived from cancerous tissues are mutated for the tumour suppresser gene *p53* (Hainaut *et al.*, 1998; IARC TP53 mutation database, <http://www.iarc.fr/p53/>). As this gene is known to play a pivotal role in the DNA damage response it was decided to use primary cells from healthy donors which would be wild-type for *p53*. The two cell types that were investigated for their suitability were, primary lymphocytes obtained from whole blood, and dermal fibroblasts isolated from breast tissue following mammary reduction.

To assess the potential use of these two cell types, RNA extraction was performed on each type in order to ascertain which would provide a sufficient yield of pure and intact RNA for use in the ribonuclease protection assay. This would also show whether the cell type was easy to obtain and maintain in culture in sufficient quantities for the planned experiments.

The primary lymphocytes and dermal fibroblasts gave similar A260:A280 ratios. Integrity of the RNA extracted from the primary lymphocytes was greater than that extracted from the dermal fibroblasts, however the yield of RNA produced from the dermal fibroblasts was substantially greater compared to that from the primary lymphocytes, even considering the less reproducible results obtained with the dermal fibroblasts. As a much greater yield of RNA of a similar purity and integrity was obtained from the dermal fibroblasts, it was decided that these cells would be used for further studies.

3.5.3 Investigating cell viability in response to oxidative stress

The agents chosen for the investigations into responses produced by mammalian cells exposed to oxidative stress were H₂O₂, HOCl, UVB and vitamin C. Exposure of cells to H₂O₂ and HOCl has previously been suggested to modulate DNA repair in different cell types (Grösch *et al.*, 1998; Ramana *et al.*, 1998). However, more studies are needed to determine the exact mechanisms of such adaptive responses. UVB has been shown to induce oxidative lesions through interactions with photosensitisers (**figure 3.2**) (Cadet *et al.*, 1997; Kielbassa *et al.*, 1997; Kawanishi *et al.*, 2001) but little investigation in to the repair of such lesions has been performed.

NER appears to play a minor role in the repair of oxidative lesions (Reardon *et al.*, 1997) and the TCR factor, *CSB*, has recently been shown to play a role in BER via an interaction with the DNA glycosylase hOGG1 (Tuo *et al.*, 2001; Tuo *et al.*, 2002). Investigating responses produced in mammalian cells exposed to oxidative stress may therefore provide more information regarding the co-ordination of BER and NER in response to oxidative DNA damage.

The antioxidant capacities of vitamin C are not fully understood. Suggestions have been made that some of its antioxidant actions may be mediated via a role in the regulation of DNA repair pathways that are known to be involved in the repair of oxidative damage to DNA (Cooke *et al.*, 1998; Cooke *et al.*, 2003). One scheme suggests that vitamin C may ultimately affect DNA repair through redox pathways and activation of the transcription factor AP-1, possibly leading to enhanced NER (Lunec *et al.*, 2002).

Chapter 3: Establishing a cellular model

Doses of each of the agents chosen for the studies in this thesis were based on values reported in the literature, although care was also taken to use concentrations of agents which were likely to be physiological. High doses of some of these agents may produce modulation of cellular responses but for this study concentrations which may be produced *in vivo* were required.

Cytotoxicity studies performed using the CellTiter 96® Aqueous Non-Radioactive Cell Proliferation Assay showed that neither 400 µM H₂O₂, 300 nM HOCl nor 600 J/M² UVB produced high levels of cell death. A slight increase in measurement of absorbance at 492 nm 4 hours following treatment with 600 J/M² UVB may be explained by an increase in mitochondrial activity produced by the treatment, suggesting that a stress response is generated by this treatment. The slight loss in cell viability following treatment with these agents compared to the untreated control cells indicated that the agents were affecting cellular processes.

Treatment of the dermal fibroblasts with 400 µM vitamin C produced increased absorbance at 492 nm. Further investigations, using three different doses of vitamin C and also experiments without dermal fibroblasts present, showed that vitamin C was capable of reducing MTS to the formazan compound in a dose dependent manner in a cell free environment. This reducing activity of vitamin C has been described for the related compound MTT (Chakrabarti *et al.*, 2000) but not for the tetrazolium salt MTS before. This effect therefore invalidates the use of the CellTiter 96® Aqueous Non-Radioactive Cell Proliferation Assay in studies using vitamin C. Although a measurement of cell viability following treatment with vitamin C was not produced using the the CellTiter 96® Aqueous Non-Radioactive Cell Proliferation Assay, the lack of any cells detaching from the cell culture flasks indicated that vitamin C treatments were not inducing high levels of cell death. The concentration used (400 µM) has also previously been shown to produce very little cytotoxicity in other human cell types (personal communication Dr P. Mistry, Department of Biochemistry, University of Leicester).

3.5.4 Measurement of DNA damage using the alkaline unwinding technique

Indirect measurement of oxidative DNA damage performed using the alkaline unwinding technique showed very similar values for Fpg-sensitive sites in control cells to those reported in the literature, although this is the first time that this assay has been applied to primary fibroblasts. ESCODD (2003) reported 0.53 lesions per 10^6 dG in HeLa cells, Mistry & Herbert (2003) reported approximately 0.50 lesions per 10^6 dG in CCRF-HSB-2 cells and this study measured 0.50 lesions per 10^6 dG in dermal fibroblasts. In addition, all four of the treatments showed an induction in the number of strand breaks present in the DNA.

Treatment with 400 μ M H_2O_2 induced the greatest number of strand breaks of the four treatments. There is some evidence for a direct effect of H_2O_2 on DNA (Epe, 1995) but its main mechanism of DNA damage is through the actions of more reactive species produced as products of the Fenton reaction (**figure 1.2**). The hydroxyl radical product of the Fenton reaction is highly reactive and able to oxidise both base and sugar moieties of DNA, it is also capable of inducing strand breaks (Cadet *et al.*, 1997), which may explain the high incidence of induced strand breaks following H_2O_2 treatment even when Fpg protein was not added. Eleven different modified bases have been identified in human lymphoblasts following non-cytotoxic treatment with H_2O_2 (Jaruga & Dizdaroglu, 1996), and repair of Fapy-guanine and 8-oxoG were commenced within 2 hours of treatment. It is therefore possible that some strand breaks may have been induced as a consequence of intrinsic DNA repair activity produced by endonuclease activation.

Fpg-sensitive sites were induced in the dermal fibroblasts following treatment with 400 μ M H_2O_2 and 300 nM HOCl. Treatment with 300 nM HOCl produced a 2.5-fold induction in Fpg-sensitive sites, and the 4.8-fold induction of Fpg-sensitive sites measured following treatment with 400 μ M H_2O_2 was similar to levels reported following similar treatment of CCRF-HSB-2 cells (7.6-fold induction) (Mistry & Herbert, 2003). Again, the main mechanism was likely to be due to hydroxyl radicals, which are able to react with purines (e.g. guanine) to produce C4-OH, C5-OH and C8-OH-adduct radicals that can give rise the hydroxypurine (including 8-oxoG) and formamidopyrimidine substrates of the Fpg protein.

Chapter 3: Establishing a cellular model

Treatment of dermal fibroblasts with 600 J/M² UVB reduced the calculated number of Fpg-sensitive sites but also significantly decreased the percentage of double-stranded DNA present and produced a slight induction of strand breaks. The reduction in double-stranded DNA and induction of strand breaks present in cells incubated both with Fpg protein and also without it, shows that UVB treatment induced DNA strand breaks. Singlet oxygen induced DNA damage, produced as a result of UVB irradiation, would be expected to produce guanine modifications (sensitive to the Fpg protein) in high excess to single-strand breaks and other types of DNA damage (Epe, 1995). Although such a profile was not observed here, it was shown that the dose of UVB irradiation used was sufficient to induce DNA damage. DNA strand breaks may also be produced as a product of repair processes and therefore could indicate that DNA repair is being induced. However, the lack of Fpg-sensitive sites following UVB irradiation may also indicate a lack of photosensitisers in the fibroblasts, and hence site-specific oxidative DNA damage. It could also possibly indicate that DNA damage and repair are in a state of balance.

The reduction in Fpg-sensitive sites produced with 400 µM vitamin C treatment, combined with a decrease in the percentage of double-stranded DNA may also indicate that DNA repair intermediates are being generated. This would concur with suggestions that vitamin C may exert some of its effects via modulation of DNA repair processes (Cooke *et al.*, 1998; Lunec *et al.*, 2002; Cooke *et al.*, 2003).

All four of the treatments were shown to induce DNA strand breaks. The induction of Fpg-sensitive sites following treatment with 400 µM H₂O₂ and 300 nM HOCl also indicated that these treatments increased oxidative damage to DNA. The statistically significant decrease in Fpg-sensitive sites produced following treatment with 400 µM vitamin C indicated that this agent may decrease oxidative DNA damage, consistent with its role as an antioxidant. Overall, the results produced with the alkaline unwinding assay showed that the doses of H₂O₂, HOCl and UVB that were investigated with this technique were sufficient to elicit damage to DNA, and that vitamin C may act to decrease oxidative DNA damage.

3.5.5 Optimisation of ribonuclease protection assay

The ribonuclease protection assay is a method used to measure gene expression of a number of related genes simultaneously in a single sample. Other methods to do this include DNA microarrays. The ribonuclease protection assay offers a much more affordable and specific assay, as a small set of related genes can be assessed without generating an immense amount of data that is not related to the area of investigation.

Optimisation of the conditions for hBER-1, hNER-1 and hNER-2 multi-probe kits determined that 15 µg total RNA were adequate to observe bands for all genes in each of the three kits. 15 µg were chosen instead of 20 µg to ensure that sufficient RNA would be obtainable for replicate experiments.

CONCLUSIONS

In this chapter:

- RNAzol B™ was determined to be the most suitable RNA extraction procedure for use in future studies using a ribonuclease protection assay.
- Normal dermal fibroblasts isolated from mammary reduction were identified as a suitable cellular model for investigations into cellular DNA repair responses to oxidative stress.
- Sub lethal concentrations, over a twenty-four hour timecourse, of the ROS and ROS generating agents H₂O₂, HOCl and UVB to be used in work described in chapter 4 were determined.
- For the first time the alkaline unwinding assay was applied to a primary human cell line in order to measure DNA strand breaks and Fpg-sensitive sites.
- The alkaline unwinding technique showed that DNA damage was induced by treatment of the dermal fibroblasts with H₂O₂, HOCl and UVB. Induction of strand breaks following treatment with the four agents was observed along with the induction of Fpg-sensitive oxidative DNA damage following treatment with H₂O₂ and HOCl. Results obtained with UVB and vitamin C may also imply that repair is subject to modulation following these treatments. Further studies are required to confirm this. Nevertheless, all four treatments resulted in conditions for the potential modulation of DNA repair systems in these cells.
- Conditions for the use of a ribonuclease protection assay to measure changes in BER and NER gene expression in fibroblasts exposed to H₂O₂, HOCl, UVB and vitamin C were optimised for future studies described in chapter 4.

CHAPTER FOUR

Modulation of BER and NER Gene Expression During Oxidative Stress in Human Fibroblasts

CHAPTER 4: MODULATION OF BER AND NER GENE EXPRESSION DURING OXIDATIVE STRESS IN HUMAN FIBROBLASTS

4.1 INTRODUCTION

It has been suggested that an 'adaptive response' to oxidative stress exists and is coordinated through the BER pathway (Grösch *et al.*, 1998; Ramana *et al.*, 1998; Izumi *et al.*, 2000). Such a mechanism would act as a protective guard against damage inflicted by redox changes in the cellular environment. This may be damage due to either endogenous or exogenous sources; there may even be different responses according to the source of the inflicted damage.

Evidence for such a response to DNA damage is well documented in *E.Coli*, where DNA repair and protective responses to DNA damaging agents are known to be regulated at both the transcriptional and posttranslational level (Volkert & Landini, 2001). In this organism, sensory and regulatory circuits have evolved that recognise the presence of a DNA damaging agent or the consequences of its action on DNA and induce the appropriate DNA repair or protective responses. A number of distinct responses exist to deal with differing damaging species and DNA lesions. Damage produced by oxidizing agents is typically repaired by BER mechanisms (McCullough *et al.*, 1999). In *E.coli*, most of the genes encoding the DNA repair enzymes that act on oxidative damage appear to be expressed constitutively in actively growing cells, presumably because of the continuous production of ROS as by products of aerobic metabolism.

Of the *E.coli* genes that respond to oxidative damage most act to prevent, rather than actually repair the damage. The induction of these 'prevention' genes is triggered by the presence of ROS, rather than damage to the cellular DNA itself. Two key protective responses have been described in *E.coli*, one controlled by *oxyR* and the other by the *soxRS* genes (Volkert & Landini, 2001). They are both transcriptional activators; activated following exposure to hydrogen peroxide and superoxide respectively. One inducible repair enzyme that actually acts to repair the sites of damage however, is endonuclease IV, an AP endonuclease that is capable of repairing

3' phosphate residues to 3'OH groups that can then prime DNA synthesis (Chaudhry *et al.*, 1999; Izumi *et al.*, 2000).

As such protective mechanisms exist in *E.coli*, it may be that similar responses to ROS are generated by other organisms. A number of DNA damaging agents have been assessed for their abilities to induce an adaptive response in mammalian cells. Most of these studies have focused on APE and OGG1 and are summarised in **table 4.1**.

Fung *et al.*, (1998) reported increased APE mRNA, protein and activity following the treatment of rat mesothelial cells with the 8-oxodG inducing agent crocidolite asbestos. However, they did not find any significant increases in any of these when measured following treatment with concentrations of 10 – 500 μM H_2O_2 . In a study using Chinese hamster ovary (CHO) cells however, Grösch *et al.*, (1998), showed that concentrations of 300 μM H_2O_2 transcriptionally activated the *APE* gene approximately five hours after treatment. Corresponding upregulation of the APE protein, which was inhibited by treatment with cycloheximide and anisomycin, indicated that *de novo* protein synthesis was involved. This paper also reported the induction of the APE promoter by H_2O_2 and 0.05 mM sodium hypochlorite.

In a different study, H_2O_2 concentrations of 50 μM were found to activate the up-regulation of APE at polypeptide and mRNA levels in a HeLa S3 tumour cell line and WI 38 primary lung fibroblasts. These results were measured by Western and Northern blotting respectively (Ramana *et al.*, 1998). This paper also reported an increase in APE activity following treatment with 260 nM HOCl. However, such responses were not observed by Hsieh *et al.*, (2001), when they tried to repeat the same studies in human myeloid leukaemia cells. Ramana *et al.*, (1998) reported that *APE* is also activated by ionizing radiation and other ROS generators, but not by UV radiation or by alkylating agents.

Other BER factors have been investigated to see if they are also modulated upon exposure to DNA damaging agents. In a study by Kim *et al.*, (2001), human alveolar epithelial cells (A549) were treated with the oxidative stress inducing agent,

crocidolite asbestos. This agent, known to induce lung cancer, was shown to cause an increase in 8-oxoG levels, followed by increases in 8-oxoG repair enzyme activity and *hOGG1* and *hMTH1* gene expression, as measured by RT-PCR.

Repair Factor	Tissue/Cells	Treatment	Results	Reference
APE	Rat mesothelial cells	Asbestos H ₂ O ₂	↑mRNA, ↑protein No change	Fung <i>et al.</i> , 1998
APE	Chinese hamster ovary (CHO)	H ₂ O ₂	↑mRNA ↑ protein	Grösch <i>et al.</i> , 1998
hAPE	HeLa S3 & WI38 cells	H ₂ O ₂	↑mRNA ↑ protein	Ramana <i>et al.</i> , 1998
hAPE	Myeloid leukaemia (K562) cells	H ₂ O ₂	No change	Hsieh <i>et al.</i> , 2001
hOGG1 hMTH1	Epithelial (A549) cells	Crocidolite asbestos	↑mRNA ↑mRNA	Kim <i>et al.</i> , 2001
OGG1	Rat lung tissue	Diesel exhaust particles	↑mRNA	Tsurudome <i>et al.</i> , 1999
OGG1 APE	HeLa S3 cells HeLa S3 cells	HOCl HOCl	No change ↑mRNA ↑protein	Saitoh <i>et al.</i> , 2001
OGG1 APE MPG β polymerase	Rat tissue	Peroxisome proliferator	↑mRNA	Rusyn <i>et al.</i> , 2000

Table 4.1: Summary of studies designed to investigate modulation of BER factors following treatment with oxidizing agents. 8-oxoguanine glycosylase (OGG1) methylpurine DNA glycosylase (MPG), MutT homolog (MTH1), AP endonuclease (APE).

In an *in vivo* study by Rusyn *et al.*, (2000), rats were fed a diet containing the peroxisome proliferator, WY-14,643 (1000 p.p.m) for up to 22 weeks. A time-dependent 3- to 12- fold increase in mRNA for *OGG1*, *APE*, *MPG* and *polymerase β* were observed using a ribonuclease protection assay detection system. These data were used to suggest that the carcinogenic properties of peroxisome proliferators might be due to their ability to generate oxidative stress. Changes in levels of 8-oxoG, its rate of repair and *OGG1* mRNA were also measured in rat lungs following intratracheal administration of diesel exhaust particles (Tsurudome *et al.*, 1999). These results showed an increase in 8-oxoG levels present in the DNA of rat lung tissue, together with an increase in gene transcript level of *OGG1*.

Most of the studies mentioned above have focused on proteins involved in the BER pathway but NER modulation in response to oxidative stress and DNA damage has also been studied. A priming dose of UV radiation was shown to stimulate GGR, and recently, host cell reactivation (HCR) results have suggested that the TCR pathway is also inducible (McKay *et al.*, 1999).

In order to assess the effects of damaging agents on the levels of NER mRNA levels, Maeda *et al.*, (2001), used a ribonuclease protection assay approach. They reported a decrease of 10 to 60% in all genes present in Riboquant™ Multi-probe Ribonuclease protection assay hNER-1 and hNER-2 kits, following irradiation with 600 J/M² UVB in normal human keratinocytes

Suggestions that NER is not up-regulated to the same extent under the same conditions, suggests that BER is the main repair pathway for repair of these types of lesion (Ramana *et al.*, 1998). Studying a number of repair factors involved in both pathways in cells exposed to a number of different damaging agents will hopefully shed more light on this area.

4.2 AIMS

There is some debate at the moment as to how any 'adaptive response' to changes in cellular oxidative stress may be regulated, and whether it is a constitutive part of all cellular systems. This chapter aimed to study the affects of changes in cellular oxidative stress on the expression of individual DNA repair factors at both mRNA and protein level. Treatments with H₂O₂, HOCl, UVB and vitamin C were performed in order to assess whether the repair activities associated with the elimination of oxidative adducts in DNA were modulated following these treatments, which were shown to induce different DNA damage profiles (chapter 3).

mRNA levels of a number of genes known to be involved in BER and NER were measured using a ribonuclease protection assay. Any adaptive response to oxidative stress may be initiated at protein level as well as, or as opposed to at mRNA level; therefore, several important BER (hOGG1 & hAPE) and NER (hHR23B & XPA) repair factors were also assessed at protein level using the Western blotting technique.

4.3 METHODS

4.3.1 RNA isolation

As detailed in chapter 3, the RNAzol™ B kit was chosen as the most suitable extraction kit for use in the ribonuclease protection assay experiments. The manufacturers changed the formulation of this reagent and renamed it RNA-Bee™. The same extraction method was used as for the original kit and is described in section 2.3.2.1.

Due to laboratory relocation, RNA quantitation via UV spectrophotometry was no longer possible. For all ribonuclease protection assays, RNA quantitation was performed using a RiboGreen® RNA Quantitation reagent as described in section 2.3.2.2. The reagent contains a highly sensitive nucleic acid stain that produces a large fluorescent enhancement in the presence of RNA in solution (Ex 500 nm, Em 525 nm). When the fluorescence is compared to that of a known rRNA standard then the amount of RNA in a given sample can be determined.

RNA samples were diluted 1:100,000 in TE buffer and compared to a standard curve produced using 5 to 50 ng/mL ribosomal RNA in 500 µL aliquots. The RiboGreen® RNA Quantitation reagent was diluted 1:2000 in TE buffer and 500 µL added to each standard and RNA sample. Fluorescence readings were taken from triplicate 300 µL aliquots pipetted into 96-well plates. A reagent blank prepared without rRNA standard was used to correct for background readings. The standard curve and calculations were performed using Microsoft Excel 2000.

4.3.2 Treatment of human dermal fibroblasts

Human dermal fibroblasts (passage < 18) were grown to 80 % confluence (section 2.3.1.1), in 75 cm² cell culture flasks, and then treated with the appropriate agents. H₂O₂ and vitamin C were used at 400 µM, HOCl at 300 nM and UVB irradiations were performed with 600 J/m². H₂O₂, HOCl and vitamin C were all prepared in DMEM media and filter sterilised prior to treatments. UVB irradiations were performed in 6-well plates in sterile PBS. All controls were sham treated. Following

treatment, cells were incubated at 37°C for the appropriate amount of time (8, 12 or 24 hours) and then prepared for the ribonuclease protection assay or Western blotting as appropriate.

4.3.3 BER and NER gene expression

BER and NER gene expression were assessed following treatment with ROS and ROS generators by the use of a ribonuclease protection assay. The full methodology is described in section 2.3.4.1. Optimisation of the procedure for use in this thesis is shown in section 3.4.5 and an overview of the procedure is shown in **figure 3.4**. The preparative studies revealed that the optimal amount of RNA to use in the assay was 15 µg of total RNA. Optimal concentration of [α -³²P]-UTP labelled synthesised anti-sense probe to use for each of the kits was 8.0×10^5 cpm, 4.6×10^5 cpm and 8.6×10^5 cpm for the hBER-1, hNER-1 and hNER-2 kits respectively.

Each ribonuclease protection assay kit was repeated three times using RNA that was extracted from separate experiments. Bands were quantified using a PDSI densitometer (Molecular Dynamics) and background levels were taken in to account. Intersample differences were accounted for by comparison to levels of the housekeeping gene GAPDH. Results were expressed as a ratio to GAPDH in each sample and then corrected to control levels to eliminate effects of cell cycle changes. Examples of data analysis calculations are shown in **Appendix II**.

4.3.4 Measurement of DNA repair protein levels by Western blotting

Following treatment with the four damaging agents, protein levels of the BER factors hOGG1 and hAPE, and the NER factors XPA and hHR23B were assessed by Western blotting (sections 2.3.2.4 & 2.3.3.1). The housekeeping gene β -actin was used as a loading control. Optimal conditions for both primary and secondary antibodies were determined using untreated cellular lysates before treated samples were analysed.

4.4 RESULTS

4.4.1 BER and NER gene expression in normal dermal fibroblasts following exposure to changes in levels of oxidative stress

The ribonuclease protection assay was used to detect and quantify changes in expression of a specific set of genes at one time. This technique was used to highlight any changes in the mRNA expression of genes involved in the processes of NER and BER in human dermal fibroblasts following changes in the levels of cellular oxidative stress. H₂O₂, UVB and HOCl, along with the antioxidant vitamin C, were used to modulate levels of cellular oxidative stress.

The concentrations of the agents used were established using the CellTiter 96[®] Aqueous Non-Radioactive Cell Proliferation Assay (section 3.4.3) and the alkaline unwinding technique (section 3.4.4). As previously detailed in chapter 3, the CellTiter 96[®] Aqueous Non-Radioactive Cell Proliferation Assay showed that none of the agents reduced the viability of dermal fibroblasts below acceptable levels (i.e. 85%).

The alkaline unwinding technique showed that a stress response was produced, indicated by the induction of Fpg-sensitive sites and strand breaks. Together, the cell viability studies and alkaline unwinding technique suggested that any modulation of mRNA levels were more likely due to cellular responses to a change in the oxidative stress levels of the cells and/or DNA damage, as opposed to the initiation of cell death pathways.

4.4.2 Effects of H₂O₂, HOCl, UVB and vitamin C on BER gene expression

The effects of H₂O₂, UVB, HOCl and vitamin C on gene expression of the BER factors *OGG1*, *TDG*, *APE*, *UDG*, *MPG*, *ENTG*, *RPA4* and *MGMT* were assessed using the hBER-1 multi-probe kit and the housekeeping genes *L32* and *GAPDH*. An example of a gel produced using the hBER-1 kit with RNA extracted from fibroblasts treated with 400 μM H₂O₂ for 8 and 24 hours is shown in **figure 4.1**. **Figure 4.2** shows the results obtained from three independent experiments using the hBER-1 multi-probe kit. Results produced with 400 μM H₂O₂, 600 J/M² UVB, 300 nM HOCl and 400 μM vitamin C are shown in **figure 4.2 A, B, C and D** respectively.

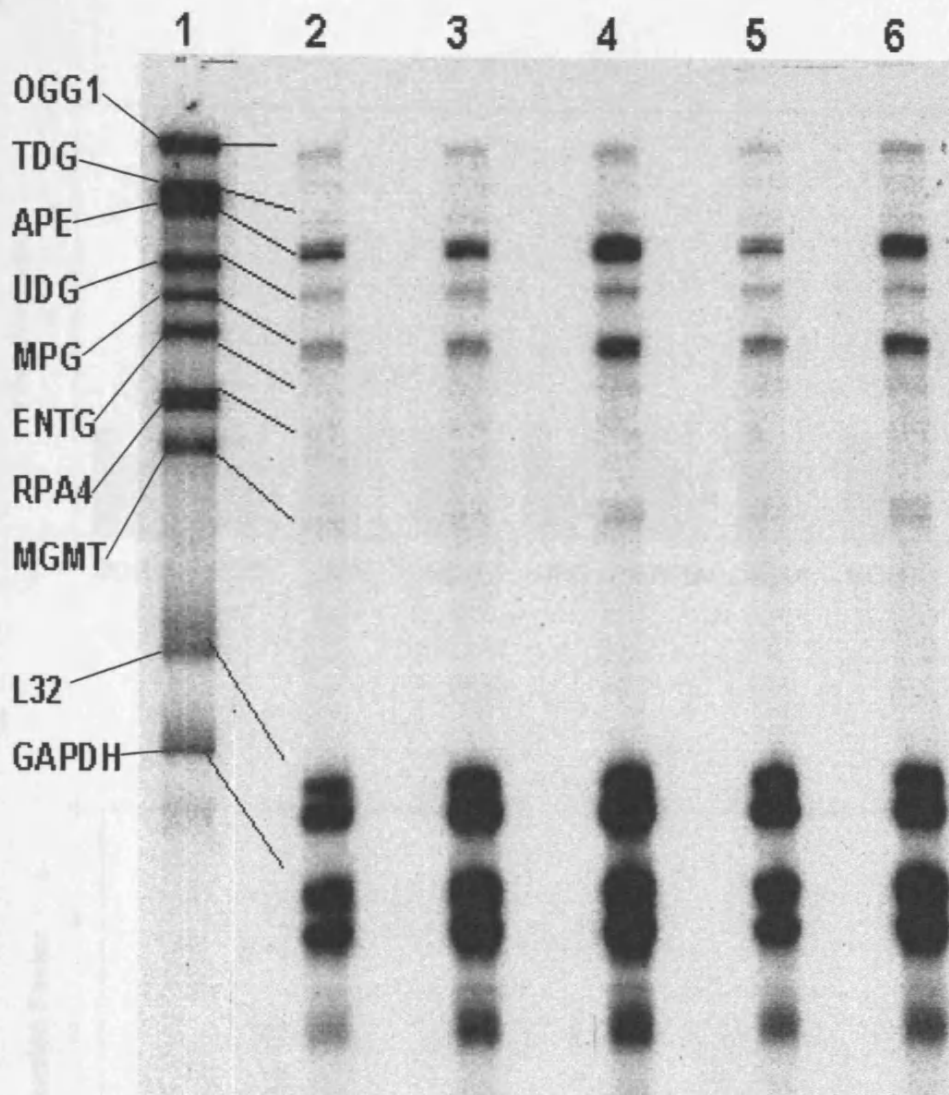
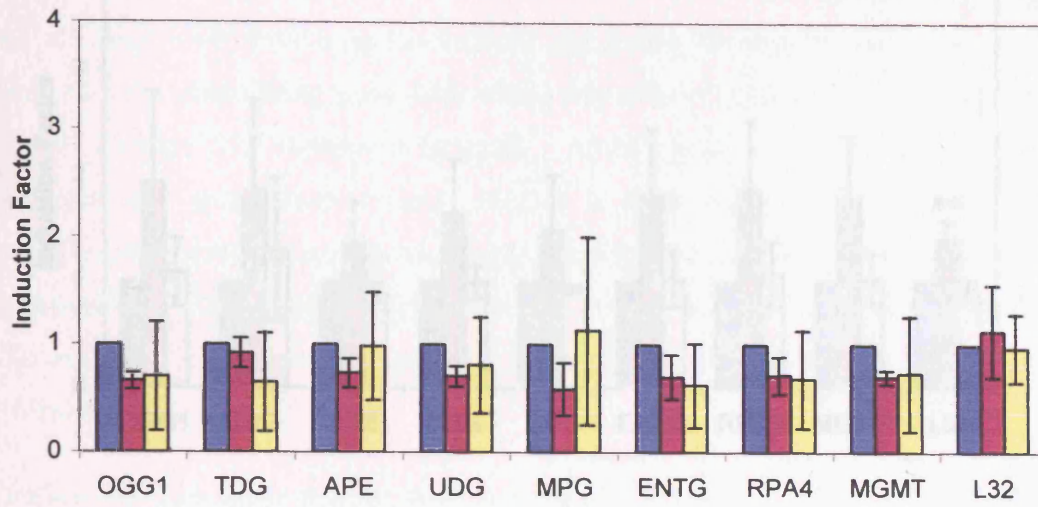


Figure 4.1: Effects of H_2O_2 on BER gene expression. Example of a ribonuclease protection assay hBER-1 gel. Hybridisation was performed with $15 \mu\text{g}$ of total RNA and a total of $8.0 \times 10^5 \text{cpm}$ [$\alpha\text{-}^{32}\text{P}$] UTP labelled synthesised anti-sense probe. RNase digestion, phenol:chloroform:isoamyl alcohol purification, polyacrylamide gel electrophoresis and autoradiography were performed as detailed in section 2.3.4.1. **Lane 1;** unprotected hBER-1 probe marker. **Lanes 2-4;** control normal dermal fibroblasts extracted at baseline, 8 hours and 24 hours respectively. **Lanes 5 & 6;** normal dermal fibroblasts treated with $400 \mu\text{M}$ H_2O_2 after 8 hours and 24 hours respectively. Bands were quantified using a PDSI densitometer (Molecular Dynamics) and background levels were taken in to account.

A



B

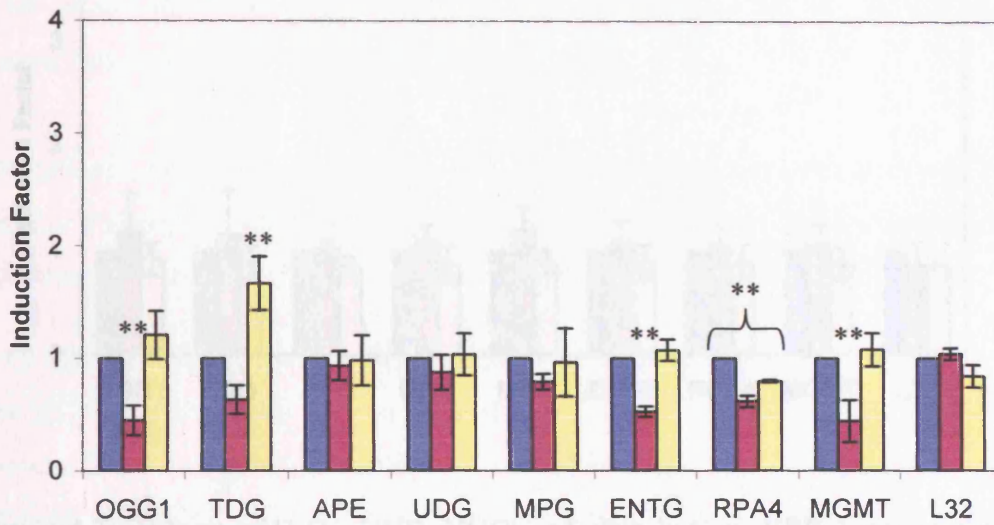


Figure 4.7. Effects of PAF, UVB, H₂O₂, and vitamin C on ribonuclease gene expression in human dental fibroblasts. In ribonuclease gene expression assay using the RT-PCR, RNA was prepared on 15 µg total RNA extracted from human dental fibroblasts treated with A) 400 µM H₂O₂, B) 400 µM UVB, C) 400 µM H₂O₂ + 400 µM vitamin C. Total RNA was extracted at 15 min (15), 2 hours (2h), and 24 hours (24h) post-treatment. Ribonuclease protein levels were determined as described in section 2.1.1, and data analysis as described in section 4.3.3. Data represent the mean (± SD) of triplicate independent experiments. Means were compared using ANOVA and Tukey HSD post test; statistically significant differences between control and treated samples are highlighted as ** representing p < 0.01.

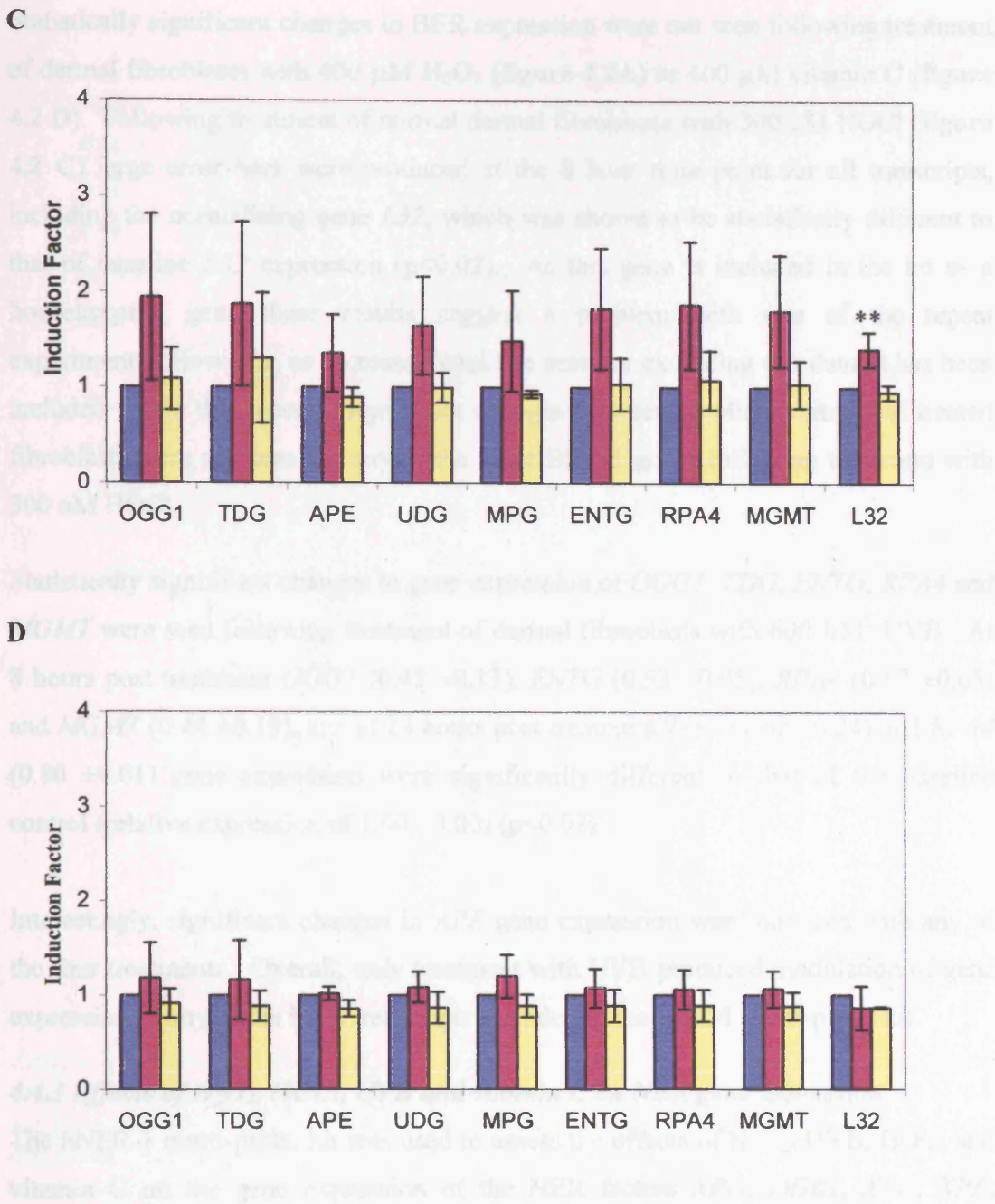


Figure 4.2: Effects of H_2O_2 , UVB, HOCl and vitamin C on BER-1 gene expression in human dermal fibroblasts. A ribonuclease protection assay using the hBER-1 kit was performed on 15 μg total RNA extracted from human dermal fibroblasts treated with **A**; 400 μM H_2O_2 , **B**; 600 J/M^2 UVB, **C**; 300 nM HOCl or **D**; 400 μM vitamin C. RNA was extracted at baseline (■), 8 hours (■) and 24 hours (■) post treatment. Ribonuclease protection assays were performed as described in section 2.3.4.1. and data analysis as described in section 4.3.3. Data represent the mean (\pm SD) of triplicate independent experiments. Means were compared using ANOVA and Tukey HSD post test; statistically significant differences between control and treated samples are highlighted as **, representing $p \leq 0.02$.

Statistically significant changes in BER expression were not seen following treatment of dermal fibroblasts with 400 μM H_2O_2 (**figure 4.2A**) or 400 μM vitamin C (**figure 4.2 D**). Following treatment of normal dermal fibroblasts with 300 nM HOCl (**figure 4.2 C**) large error bars were produced at the 8 hour time point for all transcripts, including the normalising gene *L32*, which was shown to be statistically different to that of baseline *L32* expression ($p < 0.02$). As this gene is included in the kit as a housekeeping gene these results suggest a problem with one of the repeat experiments. However, as no reason could be seen for excluding this data, it has been included within this report. Significant changes between baseline control and treated fibroblasts were not seen for any of the other BER-1 genes following treatment with 300 nM HOCl.

Statistically significant changes in gene expression of *OGG1*, *TDG*, *ENTG*, *RPA4* and *MGMT* were seen following treatment of dermal fibroblasts with 600 J/M^2 UVB. At 8 hours post treatment *OGG1* (0.45 ± 0.13), *ENTG* (0.53 ± 0.05), *RPA4* (0.62 ± 0.05) and *MGMT* (0.44 ± 0.19), and at 24 hours post treatment *TDG* (1.67 ± 0.24) and *RPA4* (0.80 ± 0.01) gene expression were significantly different to that of the baseline control (relative expression of 1.00 ± 0.00) ($p < 0.02$).

Interestingly, significant changes in *APE* gene expression were not seen with any of the four treatments. Overall, only treatment with UVB produced modulation of gene expression of any of the BER transcripts included in the BER-1 multi-probe kit.

4.4.3 Effects of H_2O_2 , HOCl, UVB and vitamin C on NER gene expression

The hNER-1 multi-probe kit was used to assess the effects of H_2O_2 , UVB, HOCl and vitamin C on the gene expression of the NER factors *XPG*, *DDB1*, *XPC*, *XPF*, *RPAp70*, *DDB2*, *hHR23B*, *XPA*, *RPAp32* and *RPAp14*. An example of a gel produced using RNA extracted from dermal fibroblasts treated with 400 μM vitamin C is shown in **figure 4.3**.

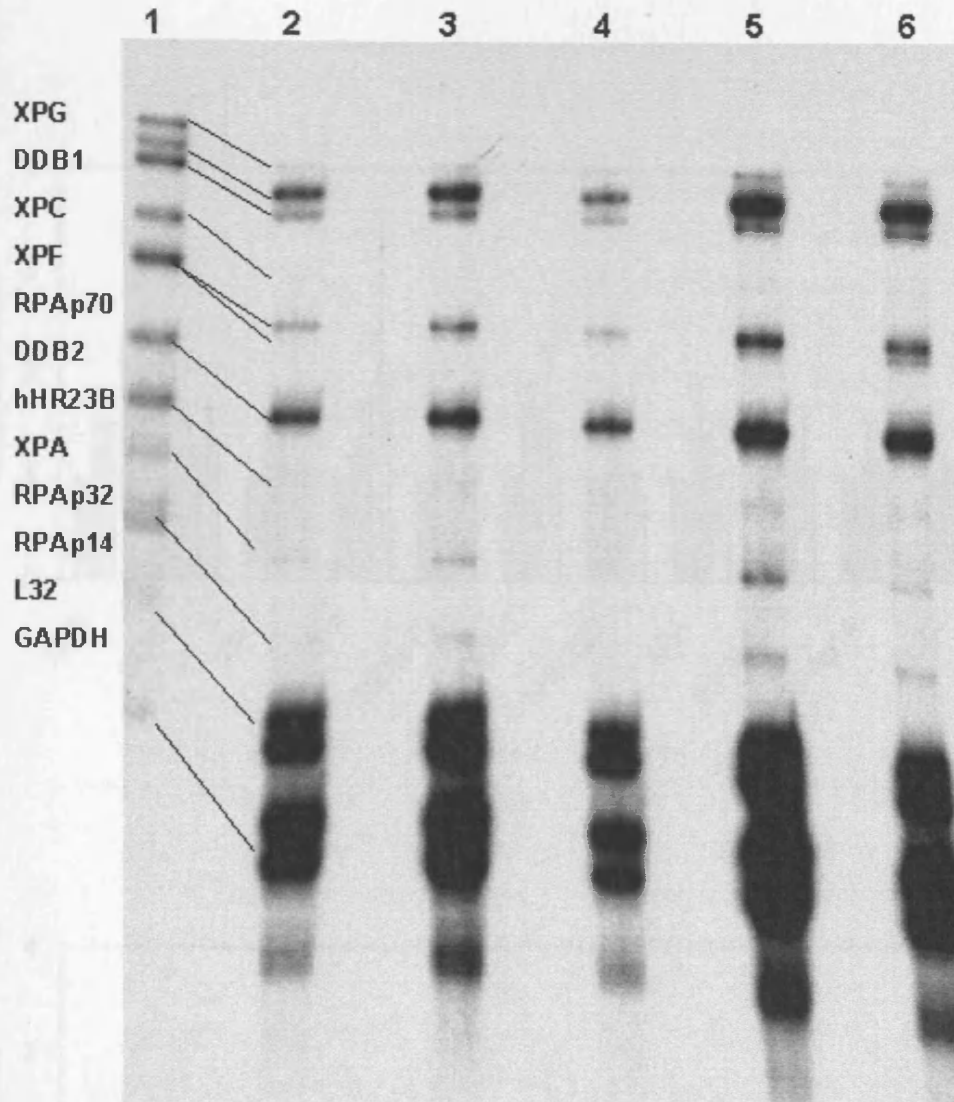
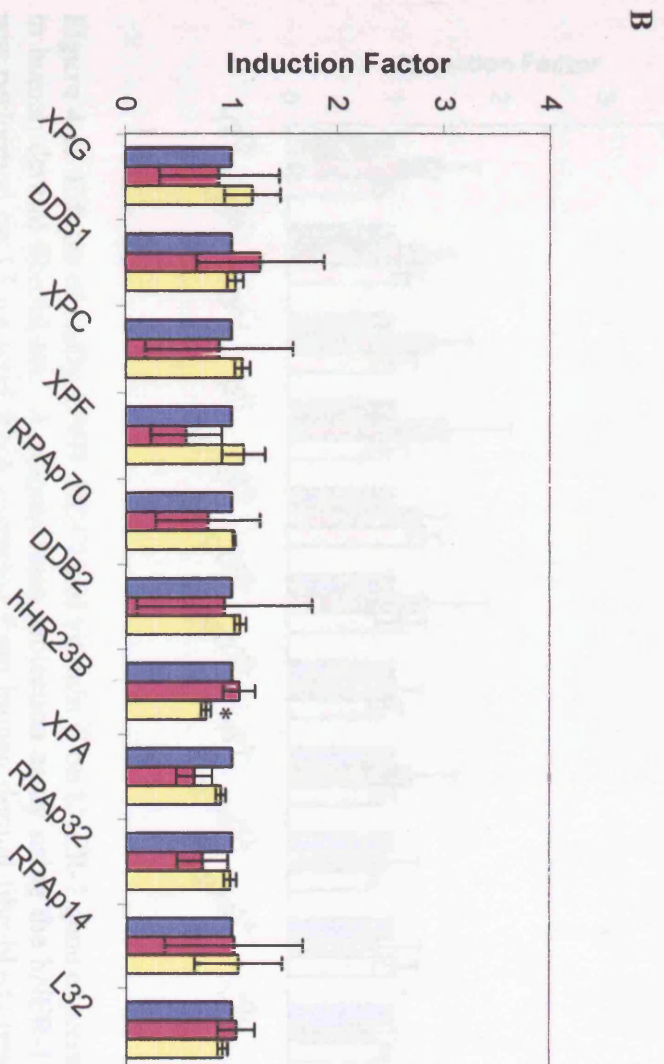
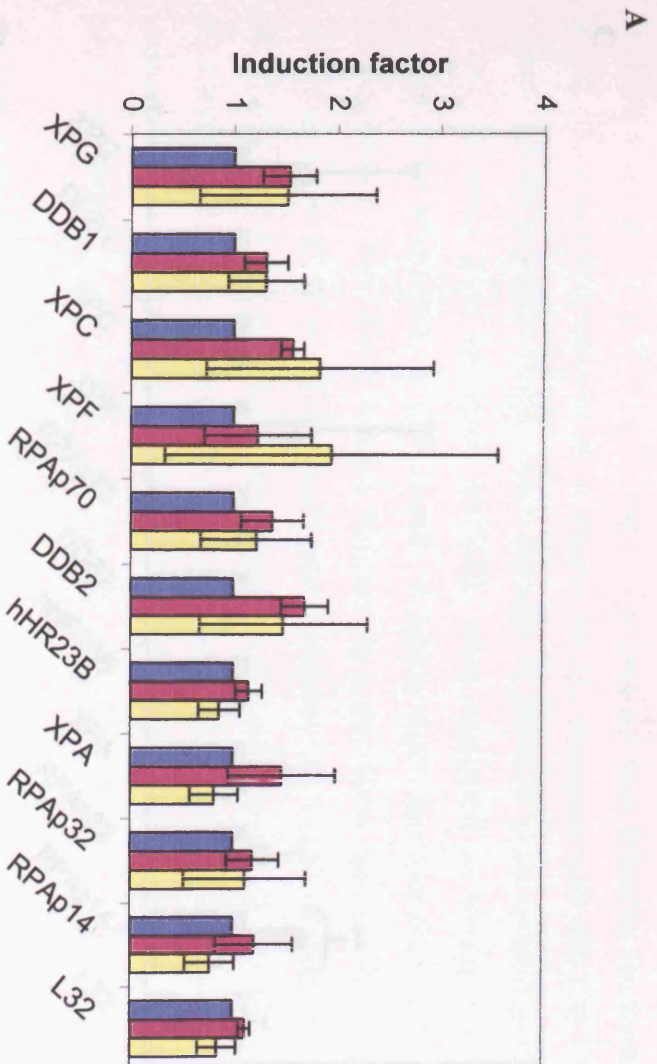


Figure 4.3: Effects of vitamin C on NER gene expression. Example of a ribonuclease protection assay hNER-1 gel. Hybridisation was performed with 15 μg of total RNA and a total of $8.0 \times 10^5 \text{cpm}$ [$\alpha\text{-}^{32}\text{P}$] UTP labelled synthesised anti-sense probe. RNase digestion, phenol:chloroform:isoamyl alcohol purification, polyacrylamide gel electrophoresis and autoradiography were performed as detailed in section 2.3.4.1. **Lane 1;** unprotected hNER-1 probe marker. **Lanes 2-4;** control normal dermal fibroblasts extracted at baseline, 8 hours and 24 hours respectively. **Lanes 5 & 6;** normal dermal fibroblasts treated with 400 μM vitamin C after 8 hours and 24 hours respectively. Bands were quantified using a PDSI densitometer (Molecular Dynamics) and background levels were taken in to account.

Figure 4.4 shows the results obtained from three independent experiments using the hNER-1 multi-probe kit. Results produced with 400 μM H_2O_2 , 600 J/M^2 UVB, 300 nM HOCl and 400 μM vitamin C are shown in **figure 4.4 A, B, C and D** respectively.



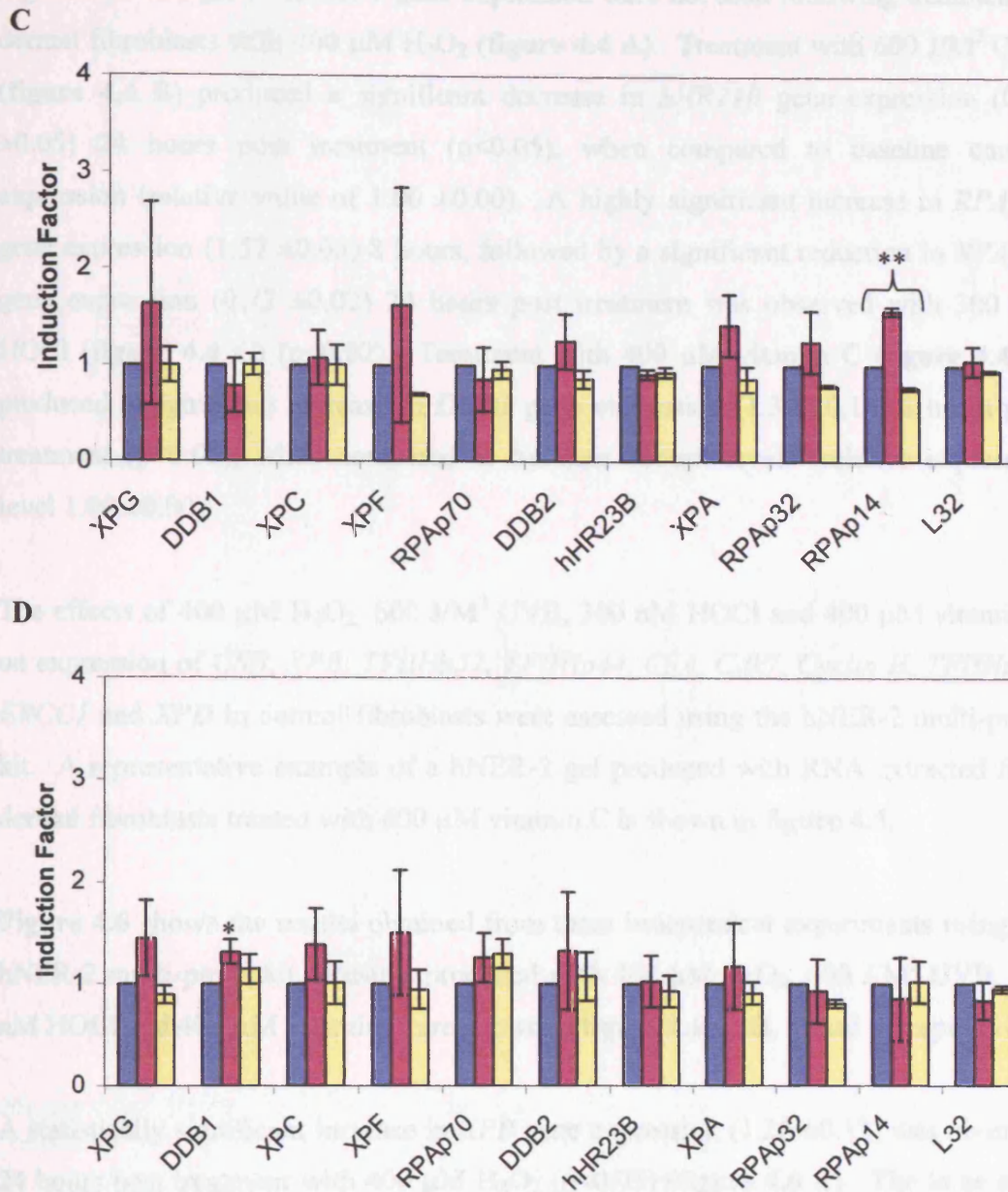


Figure 4.4: Effects of H₂O₂, UVB, HOCl and vitamin C on hNER-1 gene expression in human dermal fibroblasts. A ribonuclease protection assay using the hNER-1 kit was performed on 15 µg total RNA extracted from human dermal fibroblasts treated with **A**; 400 µM H₂O₂, **B**; 600 J/M² UVB, **C**; 300 nM HOCl or **D**; 400 µM vitamin C. RNA was extracted at baseline (■), 8 hours (■) and 24 hours (■) post treatment. Ribonuclease protection assays were performed as described in section 2.3.4.1. and data analysis as described in section 4.3.3. Data represent the mean (± SD) of triplicate independent experiments. Means were compared using ANOVA and Tukey HSD post test; statistically significant differences between control and treated samples are highlighted as * and **, representing p<0.05 and p<0.02 respectively.

Significant changes in hNER-1 gene expression were not seen following treatment of dermal fibroblasts with 400 μM H_2O_2 (**figure 4.4 A**). Treatment with 600 J/M^2 UVB (**figure 4.4 B**) produced a significant decrease in *hHR23B* gene expression (0.75 ± 0.05) 24 hours post treatment ($p < 0.05$), when compared to baseline control expression (relative value of 1.00 ± 0.00). A highly significant increase in *RPAp14* gene expression (1.57 ± 0.05) 8 hours, followed by a significant reduction in *RPAp14* gene expression (0.77 ± 0.02) 24 hours post treatment was observed with 300 nM HOCl (**figure 4.4 C**) ($p < 0.02$). Treatment with 400 μM vitamin C (**figure 4.4 D**) produced a significant increase in *DDB1* gene expression (1.32 ± 0.12) 8 hours post treatment ($p < 0.05$), when compared to baseline control levels (relative expression level 1.00 ± 0.00).

The effects of 400 μM H_2O_2 , 600 J/M^2 UVB, 300 nM HOCl and 400 μM vitamin C on expression of *CSB*, *XPB*, *TFIIHp52*, *TFIIHp44*, *CSA*, *Cdk7*, *Cyclin H*, *TFIIHp34*, *ERCC1* and *XPB* in dermal fibroblasts were assessed using the hNER-2 multi-probe kit. A representative example of a hNER-2 gel produced with RNA extracted from dermal fibroblasts treated with 400 μM vitamin C is shown in **figure 4.5**.

Figure 4.6 shows the results obtained from three independent experiments using the hNER-2 multi-probe kit. Results produced with 400 μM H_2O_2 , 600 J/M^2 UVB, 300 nM HOCl and 400 μM vitamin C are shown in **figure 4.6 A, B, C** and **D** respectively.

A statistically significant increase in *XPB* gene expression (1.26 ± 0.13) was observed 24 hours post treatment with 400 μM H_2O_2 ($p < 0.05$) (**figure 4.6 A**). The large error bars and statistically significant changes in gene expression of the house keeping gene *L32* 8 hours post treatment with 600 J/M^2 UVB (0.75 ± 0.13) and 300 nM HOCl (1.28 ± 0.15) (**figure 4.6 B & C**) indicate that experimental error may have led to inconsistent results. Statistically significant changes in gene expression of the hNER-2 factors were not produced following treatment of dermal fibroblasts with 400 μM vitamin C (**figure 4.6 D**).

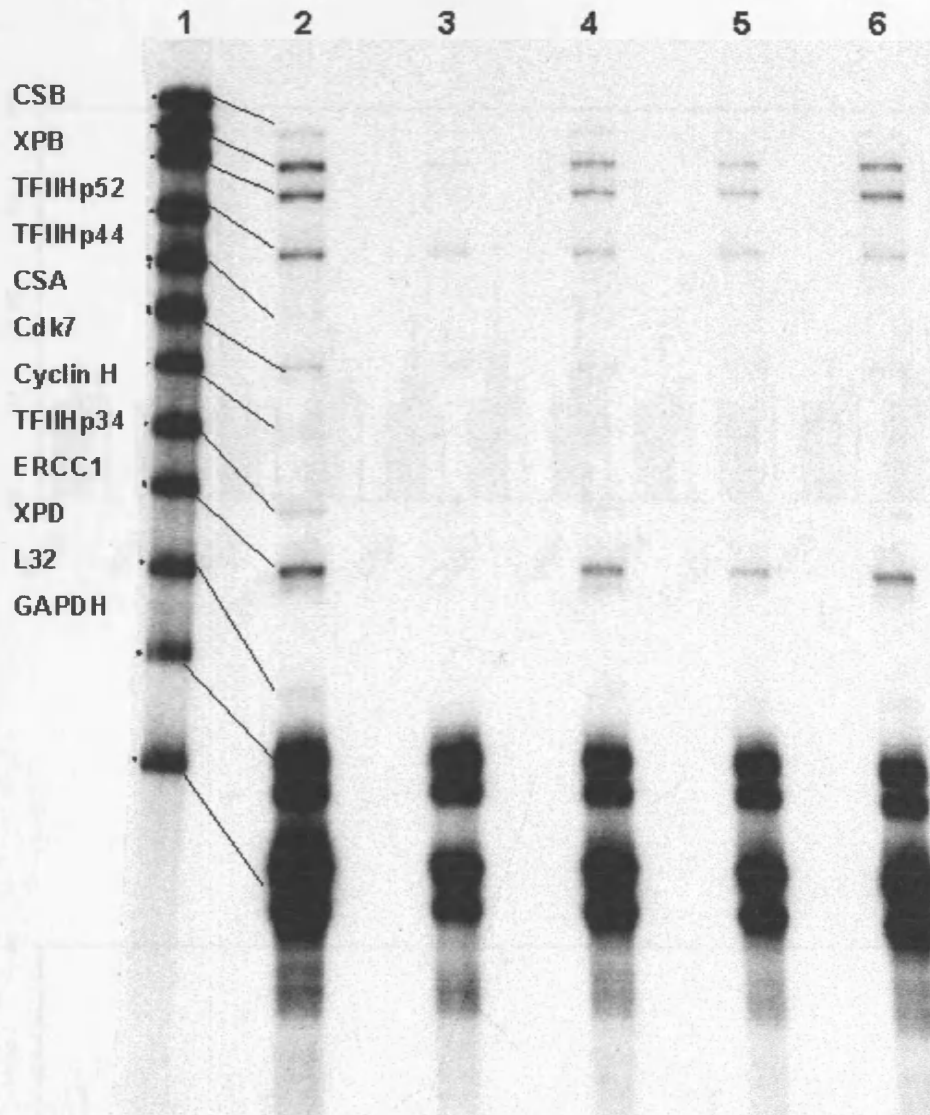
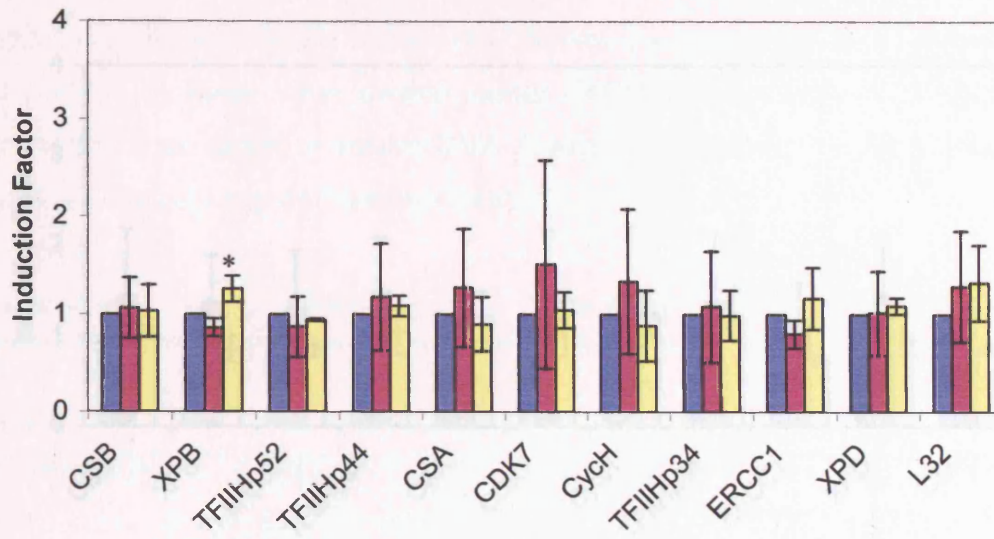
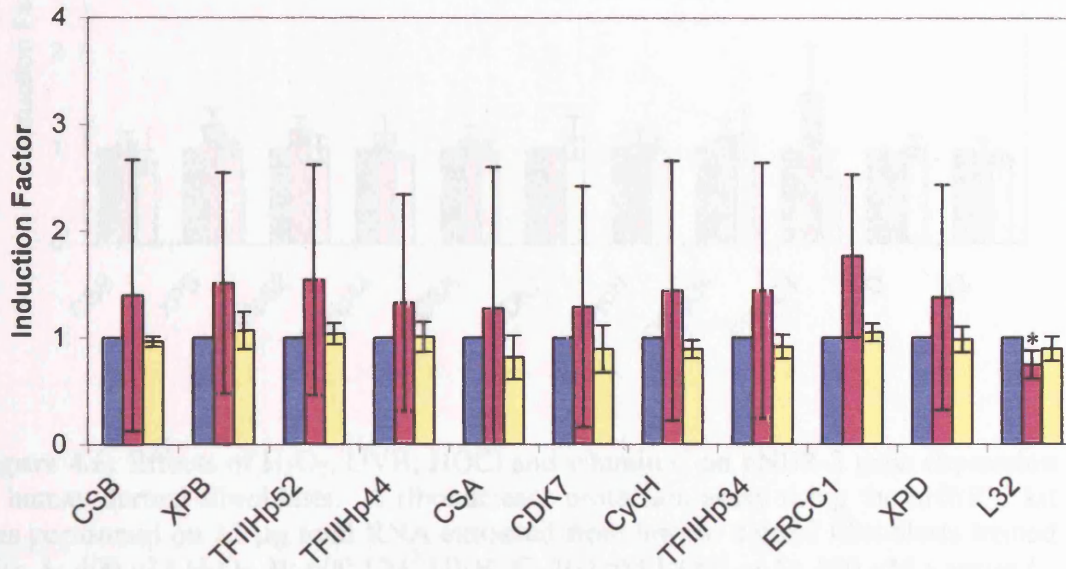


Figure 4.5: Effects of vitamin C on NER gene expression. Example of a ribonuclease protection assay hNER-2 gel. Hybridisation was performed with 15 μg of total RNA and a total of 8.0×10^5 cpm [α - ^{32}P] UTP labelled synthesised anti-sense probe. RNase digestion, phenol:chloroform:isoamyl alcohol purification, polyacrylamide gel electrophoresis and autoradiography were performed as detailed in section 2.3.4.1. **Lane 1;** unprotected hNER-2 probe marker. **Lanes 2-4;** control normal dermal fibroblasts extracted at baseline, 8 hours and 24 hours respectively. **Lanes 5 & 6;** normal dermal fibroblasts treated with 400 μM vitamin C after 8 hours and 24 hours respectively. Bands were quantified using a PDSI densitometer (Molecular Dynamics) and background levels were taken in to account.

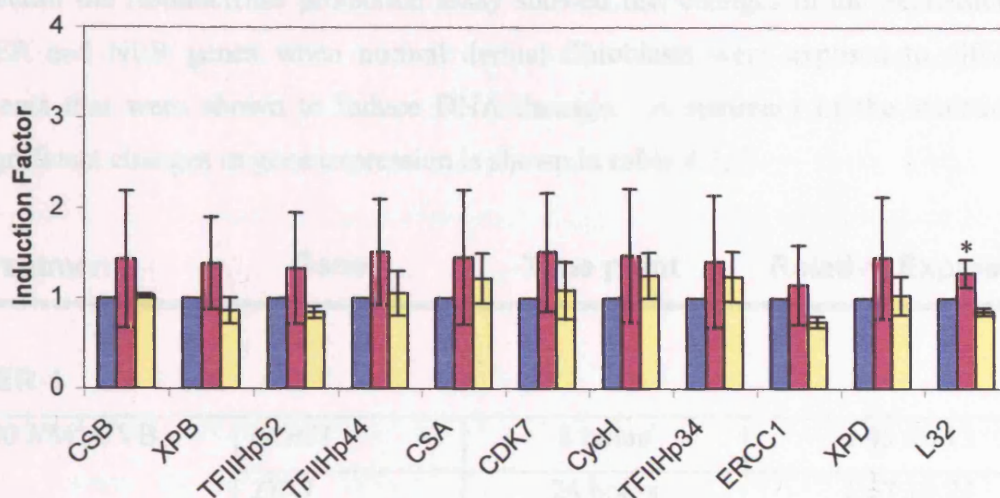
A



B



C



D

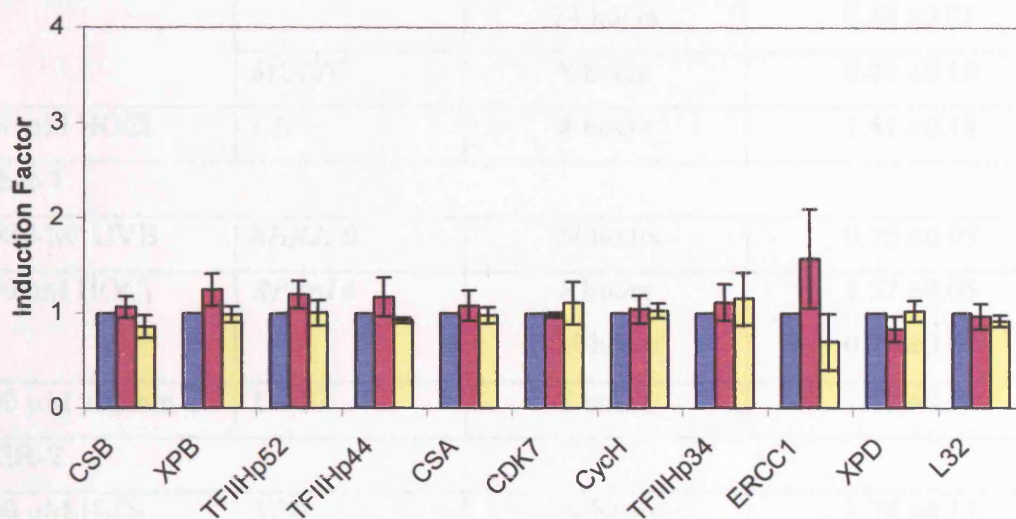


Figure 4.6: Effects of H₂O₂, UVB, HOCl and vitamin C on hNER-2 gene expression in human dermal fibroblasts. A ribonuclease protection assay using the hNER-2 kit was performed on 15 μ g total RNA extracted from human dermal fibroblasts treated with **A**; 400 μ M H₂O₂, **B**; 600 J/M² UVB, **C**; 300 nM HOCl or **D**; 400 μ M vitamin C. RNA was extracted at baseline (■), 8 hours (■) and 24 hours (■) post treatment. Ribonuclease protection assays were performed as described in section 2.3.4.1. and data analysis as described in section 4.3.3. Data represent the mean (\pm SD) of triplicate independent experiments. Means were compared using ANOVA and Tukey HSD post test; statistically significant differences between control and treated samples are highlighted as * representing $p < 0.05$.

4.4.4 Modulation of BER and NER gene expression measured by ribonuclease protection assay

Overall the ribonuclease protection assay showed few changes in the expression of BER and NER genes when normal dermal fibroblasts were exposed to different agents that were shown to induce DNA damage. A summary of the statistically significant changes in gene expression is shown in **table 4.2**.

Treatment	Gene	Time point	Relative Expression
BER-1			
600 J/M ² UVB	<i>OGG1</i>	8 hours	0.45 ±0.13
	<i>TDG</i>	24 hours	1.67 ±0.24
	<i>ENTG</i>	8 hours	0.53 ±0.05
	<i>RPA4</i>	8 hours	0.62 ±0.05
		24 hours	0.80 ±0.01
<i>MGMT</i>	8 hours	0.44 ±0.19	
300 nM HOCl	<i>L32</i>	8 hours	1.41 ±0.18
NER-1			
600 J/M ² UVB	<i>hHR23B</i>	24 hours	0.75 ±0.05
300 nM HOCl	<i>RPAp14</i>	8 hours	1.57 ±0.05
		24 hours	0.77 ±0.02
400 µM vitamin C	<i>DDB1</i>	8 hours	1.32 ±0.12
NER-2			
400 µM H ₂ O ₂	<i>XPB</i>	24 hours	1.26 ±0.13
600 J/M ² UVB	<i>L32</i>	8 hours	0.75 ±0.13
300 nM HOCl	<i>L32</i>	8 hours	1.28 ±0.15

Table 4.2: Summary of changes in BER and NER gene expression relative to baseline values in dermal fibroblasts following treatment with H₂O₂, UVB, HOCl and vitamin C. Dermal fibroblasts were treated with 400 µM H₂O₂, 600 J/M² UVB, 300 nM HOCl or 400 µM vitamin C and RNA extracted at 0, 8 and 24 hours. Ribonuclease protection assays were performed in triplicate with 15 µg total RNA as described in section 2.3.4.1.

4.4.5 Protein expression of APE, hOGG1, XPA and hHR23B

Western Blotting was performed using several antibodies raised against DNA repair proteins that are known to be involved in the repair of oxidative DNA damage. These proteins may be subject to posttranslational modification, independent of any modulation of their transcription level. If so, a lack of modulation at the mRNA level shown by the ribonuclease protection assay, may not necessarily indicate that the protein levels of these factors do not change.

The repair proteins that were investigated by Western blotting included the BER factors hAPE and hOGG1. These are both important factors in the repair of oxidative base lesions via the base excision repair pathway and are both reported to be modulated by exposure of cells to oxidative stress (Grösch *et al.*, 1998; Ramana *et al.*, 1998). The gene expression of *hOGG1* was shown to decrease 8 hours after treatment with 600 J/M² UVB in the ribonuclease protection assay experiments. Western blotting with antibodies raised against this protein was used to reveal whether a corresponding change in protein levels was produced as a result of the same treatment.

The NER factors hHR23B and XPA are both involved in the early damage recognition stages of nucleotide excision repair. It was thought that they might be subject to upregulation in a system where an increased state of oxidative stress is induced. However, ribonuclease protection assay results showed a statistically significant decrease in *hHR23B* mRNA 24 hours post treatment with 600 J/M² UVB. Studying protein levels of this repair factor in response to oxidative treatment may reveal more about its regulation.

To account for differences in gel loading and electroblotting efficiency the bands for each of the individual repair factors being investigated were normalised to the bands produced for the housekeeping gene β -actin. The β -actin normalised ratios for each treated sample were then compared to those for the untreated control samples at each time point in order to determine whether any changes in repair factor protein level had been induced by treatment.

Example blots for each of the repair factors investigated are shown in **figure 4.7**.

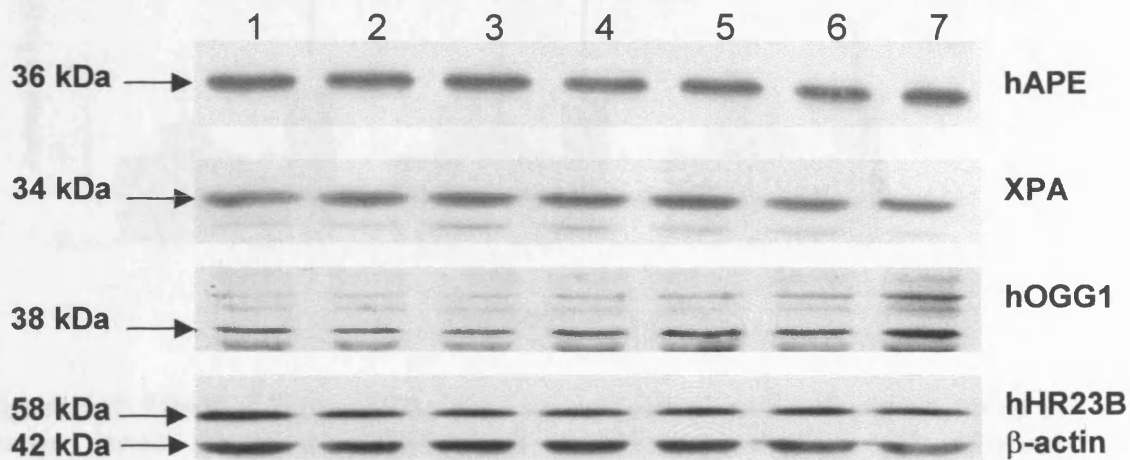


Figure 4.7: Western blot of mammalian DNA repair factors hAPE, hOGG1, hHR23B and XPA in human dermal fibroblasts. Fibroblasts were treated with 400 μM H₂O₂ and cultured for the appropriate time periods before cell harvesting. **Lanes 1-4;** control cells at 0, 8, 12 and 24 hours respectively. **Lanes 5-7;** Cells treated with 400 μM H₂O₂ after 8, 12 and 24 hours.

Statistically significant changes in hAPE protein were not measured following treatment with either 400 μM H₂O₂, 300 nM HOCl, 600 J/M² UVB or 400 μM vitamin C (**figure 4.8**). The large error bars produced following treatment with 300 nM HOCl showed that one experiment measured an approximate 3-fold induction in hAPE protein over the timecourse. However, three independent experiments did not produce such an induction. As no reason is known for excluding any of the results produced with 300 nM HOCl, they are all included in this thesis.

All four agents consistently showed no change in levels of hHR23B protein over the twenty-four hour time period (**figure 4.9**). Treatment of dermal fibroblasts with 400 μM H₂O₂, 600 J/M² UVB, 300 nM HOCl or 400 μM vitamin C did not produce any statistically significant changes in hOGG1 protein levels at either 8, 12 or 24 hours post treatment (**figure 4.10**). Of note there was no significant effect of UVB to reduce hOGG1 protein levels, although there was a trend for slightly lower levels at 8 and 12 hours post treatment.

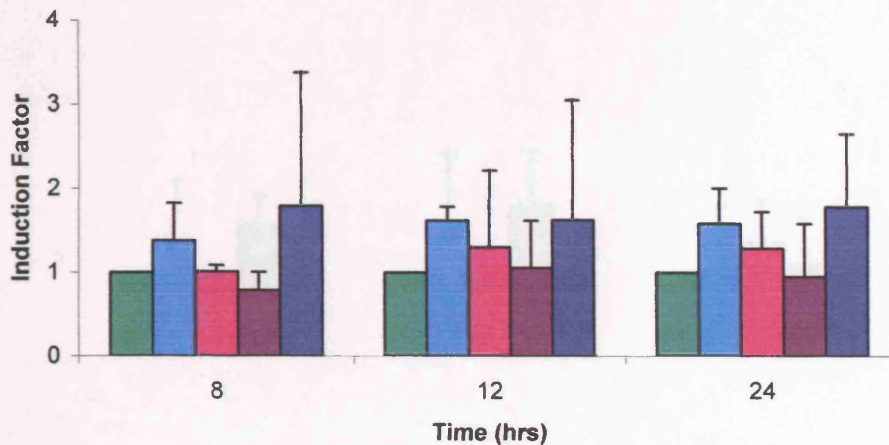


Figure 4.8: Effect of H₂O₂, UVB, HOCl and vitamin C on hAPE protein levels in human dermal fibroblasts. SDS-PAGE and Western Blotting with enhanced chemiluminescence detection was performed on 40 μg total cellular protein after treatment of human fibroblasts with either 400 μM H₂O₂ (■), 600 J/M² UVB (■), 400 μM vitamin C (■) or 300 nM HOCl (■). Control (■) represents fibroblasts sham treated. Intersample differences were accounted for by comparison to levels of the housekeeping gene β-actin and then compared to control samples to account for changes in gene expression induced by the cell cycle. Data represent the mean ± SD of three independent experiments for H₂O₂, UVB and vitamin C and four independent experiments for HOCl.

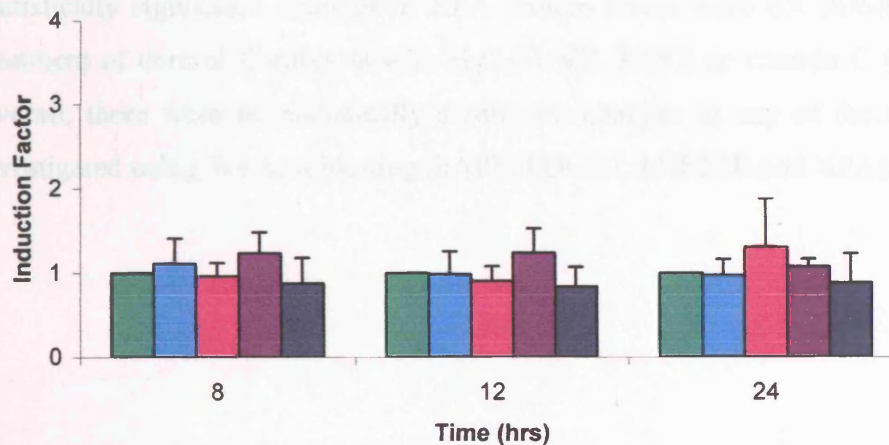


Figure 4.9: Effect of H₂O₂, UVB, HOCl and vitamin C on hHR23B protein levels in human dermal fibroblasts. SDS-PAGE and Western Blotting with enhanced chemiluminescence detection was performed on 40 μg total cellular protein after treatment of human fibroblasts with either 400 μM H₂O₂ (■), 600 J/M² UVB (■), 400 μM vitamin C (■) or 300 nM HOCl (■). Control (■) represents fibroblasts sham treated. Intersample differences were accounted for by comparison to levels of the housekeeping gene β-actin and then compared to control samples to account for changes in gene expression induced by the cell cycle. Data represent the mean ± SD of three independent experiments.

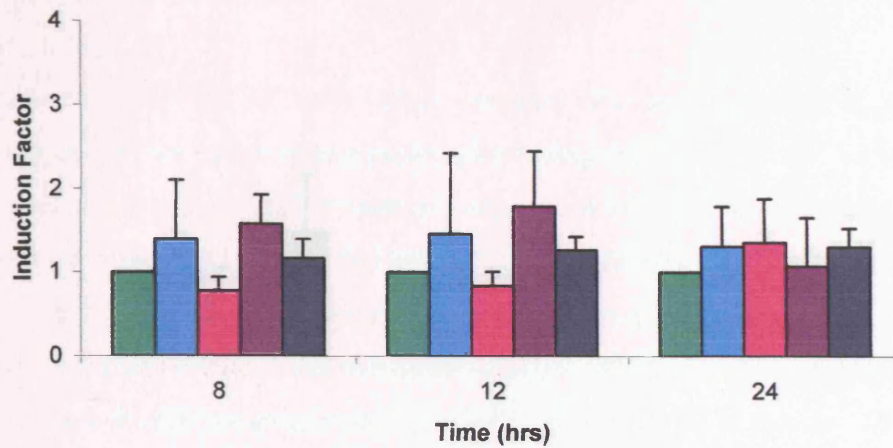


Figure 4.10: Effect of H_2O_2 , UVB, HOCl and vitamin C on hOGG1 protein levels in human dermal fibroblasts. SDS-PAGE and Western Blotting with enhanced chemiluminescence detection was performed on 40 μg total cellular protein after treatment of human fibroblasts with either 400 μM H_2O_2 (█), 600 J/M^2 UVB (█), 400 μM vitamin C (█) or 300 nM HOCl (█). Control (█) represents fibroblasts sham treated. Intersample differences were accounted for by comparison to levels of the housekeeping gene β -actin and then compared to control samples to account for changes in gene expression induced by the cell cycle. Data represent the mean \pm SD of three independent experiments.

Statistically significant changes in XPA protein levels were not detected following treatment of dermal fibroblasts with H_2O_2 , UVB, HOCl or vitamin C (**figure 4.11**). Overall, there were no statistically significant changes in any of the repair factors investigated using Western blotting (hAPE, hOGG1, hHR23B and XPA).

4.5 DISCUSSION

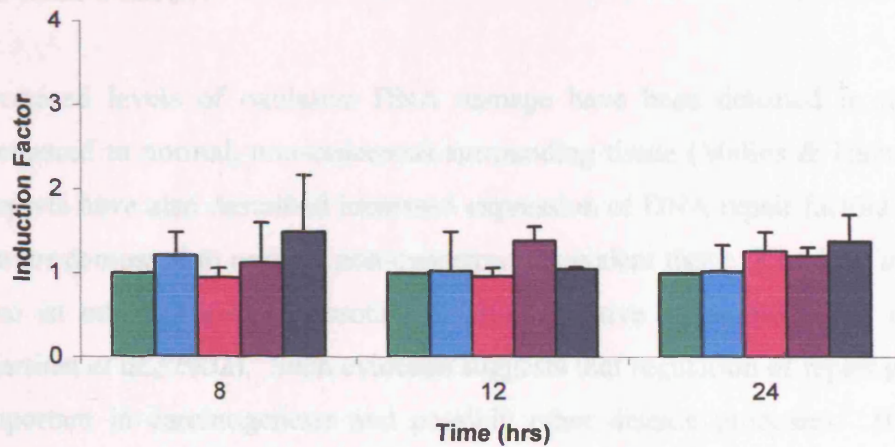


Figure 4.11: Effect of H_2O_2 , UVB, HOCl and vitamin C on XPA protein levels in human dermal fibroblasts. SDS-PAGE and Western Blotting with enhanced chemiluminescence detection was performed on 40 μg total cellular protein after treatment of human fibroblasts with either 400 μM H_2O_2 (█), 600 J/M^2 UVB (█), 400 μM vitamin C (█) or 300 nM HOCl (█). Control (█) represents fibroblasts sham treated. Intersample differences were accounted for by comparison to levels of the housekeeping gene β -actin and then compared to control samples to account for changes in gene expression induced by the cell cycle. Data represent the mean \pm SD of three independent experiments.

Data from the previous chapter show that the induction of XPA protein levels, although noted at low-dose UVB, was still able to induce DNA damage in the case of vitamin C deficiency and DNA damage. This result suggests that DNA repair pathways were active in these cells and therefore any modulation of these pathways was more than likely to be a net loss of repair capacity and not a gain. Mechanisms allowing the measurement of BER and NER gene expression, at both mRNA and protein level, were established and responses to changes in relative mRNA and protein levels.

4.5.1 BER and NER mRNA expression

The abundance of protein-coding genes can be determined by the presence of multiple-expressed low-copy genes, which are often found in a single gene. This allowed comparison of the level of mRNA in whole cells and between samples. This highly sensitive and specific approach allowed the detection and quantitation of gene expression at the mRNA level. Expression of BER and NER genes β and γ and δ hours and 24 hours post-treatment with H_2O_2 , HOCl and UVB and the antioxidant vitamin C was investigated. These data provide a clear picture of the

4.5 DISCUSSION

Increased levels of oxidative DNA damage have been detected in tumour tissue compared to normal, non-cancerous surrounding tissue (Malins & Haimanot, 1991). Reports have also described increased expression of DNA repair factors in cancerous tissues compared to normal, non-cancerous equivalent tissue (Kondo *et al.*, 2000) and also in other conditions associated with oxidative stress (Shimoda *et al.*, 1994; Martinet *et al.*, 2002). Such evidence suggests that regulation of repair genes may be important in carcinogenesis and possibly other disease processes. It is therefore important to establish the exact methods of regulation of DNA repair in order to understand more about how these processes may become deregulated in diseases such as cancer.

The aim of this chapter was to establish whether BER and NER repair factors are modulated by changes in cellular oxidative stress. To do this, non-cytotoxic doses of ROS and ROS generating agents were established as reported in the previous chapter. Data from the previous chapter also showed that the agents under investigation, although used at non-cytotoxic doses, were still able to induce DNA damage and in the case of vitamin C reduce oxidative DNA damage. This would suggest that DNA repair pathways were active in these cells and therefore, any modulation of these pathways was more than likely to be a response to oxidative stress and not cell death mechanisms. Methodologies allowing the measurement of BER and NER gene expression, at both mRNA and polypeptide level, were established and responses to changes in oxidative stress were measured.

4.5.1 BER and NER mRNA expression

The ribonuclease protection assay approach was used to distinguish the presence of multiply expressed DNA repair genes simultaneously in a single sample. This allowed comparative analysis of different mRNA products both within and between samples. This highly sensitive and specific approach allowed the detection and quantitation of gene expression at the mRNA level. Modulation of BER and NER genes 8 hours and 24 hours post treatment with H₂O₂, HOCl and UVB and the antioxidant vitamin C was investigated. These time points were chosen because

previous reports have shown that DNA repair enzymes may be modulated over this time period.

The data produced by the ribonuclease protection assay in this system showed few statistically significant differences in the transcript levels of the genes investigated with the three multi-probe kits. Expression of the BER factors *hOGG1*, *ENTG*, *MGMT* and *RPA4* showed small decreases 8 hours post treatment with UVB. A very small, but reproducible decrease of *RPA4* transcript level was also seen 24 hours following UVB treatment and a statistically significant increase in *TDG* mRNA was measured 24 hours post irradiation with UVB. No other studies have reported data on changes in BER gene expression following treatment with UVB irradiation. The BER pathway is not generally considered as a major route for the repair of damage induced by UVB radiation, although some of the DNA lesions induced e.g. 8-oxoG, are likely to be subject to repair by BER.

ENTG (human homologue of *E.coli* endonuclease III (Nth)) (Hilbert *et al.*, 1997), now more commonly termed *hNTH1*, is a bifunctional DNA glycosylase which removes oxidised pyrimidines from DNA (Marenstein *et al.*, 2003). Interestingly, both of the bifunctional glycosylases, *hOGG1*, which removes oxidised purines and *hNTH1* were slightly down regulated 8 hours post treatment with UVB. In both cases transcript level had returned to baseline level by 24 hours post treatment. There have been reports of *OGG1* induction following treatment with oxidising agents but no reports of modulation following UVB irradiation. No studies investigating a modulation of *hNTH1* following oxidative treatment have been reported.

RPA4 is a homologue of the 34-kDa subunit of replication protein A (RPA2). Little is reported about this individual subunit, but RPA is associated with PCNA-dependent long patch BER (Dianov *et al.*, 1999; Otterlei *et al.*, 1999). There have been no reports of its modulation in response to oxidative stress, although here, slight down regulation was observed 8 hours post UVB treatment, which was still statistically significant, although less so, by 24 hours post treatment.

TDG (thymine DNA glycosylase) removes bases mispaired with guanine (see **table 1.1**). A conservative upregulation of *hTDG* transcript was observed 24 hours post UVB treatment; no other studies have reported such findings.

MGMT (O⁶-methylguanine-DNA methyl-transferase) or ATase (O⁶-alkylguanine-DNA alkyltransferase) reverses O⁶-alkylation damage in DNA via covalent transfer of the alkyl group to the ATase protein before inactivating it and targeting it for ubiquitination and proteasome-mediated degradation (reviewed in Margison *et al.*, 2003). It is not involved in the repair of oxidative damage to DNA and so its down regulation following UVB irradiation may be due to other types of UVB damage.

The increase in A492 absorbance at 4 hours post treatment with UVB, using the CellTiter 96® Aqueous Non-Radioactive Cell Proliferation Assay in the previous chapter, suggested that a possible stress response was occurring. This could explain the transient changes in gene expression observed using the ribonuclease protection assay.

A very small, but statistically significant, down regulation of *hHR23B* was observed 24 hours post UVB treatment. No other studies have shown any modulation of this repair factor (part of the XPC-hHR23B heterodimer) that is involved in damage recognition in GGR-NER. Small increases in the DNA damage-binding protein complex subunit *DDB1* (Wittschieben & Wood, 2003) and the DNA helicase *XPB* were also observed 8 hours post treatment with the antioxidant vitamin C and 24 hours after treatment with H₂O₂ respectively. A small increase at 8 hours and then decrease at 24 hours post treatment with HOCl was observed in transcript level of the p14 subunit of RPA (*RPAp14*).

The very small changes observed in gene transcript level, although statistically significant, are not thought to be biologically significant and may merely be products of experimental error produced by the ribonuclease protection assay. The only gene involved in repair of oxidative damage to DNA that showed a two-fold or more change in transcript level (which may be considered biologically relevant) was *OGG1*, which showed a 2.2-fold decrease 8 hours post treatment with UVB.

The ribonuclease protection assay was used as a screening tool to highlight genes of interest that showed modulation following treatment with the agents being investigated. Significant up or down regulation of any of the individual DNA repair genes involved in the processing of oxidative damage would have been investigated further using the very sensitive method of quantitative real time RT-PCR. Genes that produced changes in mRNA levels would then also have been assessed at the polypeptide level, to see if the mRNA changes were reflected in changes at polypeptide level too.

The DNA repair factor *hOGG1* was shown by the ribonuclease protection assay to be down regulated in response to treatment with UVB. *hOGG1* has previously been investigated in a number of cellular models by both RT-PCR and quantitative real-time RT-PCR following treatment with damaging agents. Little regulation was observed at mRNA level with these techniques (personal communications Dr. P Mistry, Department of Biochemistry, University of Leicester and Mr. Peter Goodrem, Department of Pathology, University of Leicester respectively).

4.5.2 *hOGG1* & *hAPE* protein expression

It was decided to investigate the regulation of *hOGG1* at polypeptide level to see if the down regulation in mRNA level with UVB was also observed at polypeptide level. The AP endonuclease *hAPE*, was also chosen to be studied at polypeptide level in case modulation of this integral repair enzyme was occurring at posttranslational levels, without changes in transcription. Changes in *hAPE* have been suggested in previous studies (Ramana *et al.*, 1998; Saitoh *et al.*, 1998).

The Western blotting results showed no significant modulation of either *hOGG1* or *hAPE* following treatment of dermal fibroblasts with H₂O₂, UVB, HOCl or vitamin C. The nature of this assay relies on accurate protein quantification by use of the Bradford assay, as well as even loading of gels and transfer of proteins onto PVDF membranes, a two-fold or more change in signal would be expected to indicate any significant alterations in polypeptide levels between samples. However, a slight trend for decreased levels of *hOGG1* protein was observed at both 8 and 12 hours following treatment with 600 J/m² UVB, corresponding to the statistically significant decrease at

mRNA level at 8 hours post treatment. Both mRNA and protein levels had recovered to normal levels by 24 hours post treatment.

Harrison *et al.*, (1995) did not observe any significant regulation of the APE gene in response to DNA damaging agents such as: 12-*O*-tetradecanoylphorbol-13-acetate (TPA); dimethyl sulphoxide; dexamethasone; bleomycin; the free radical generator, paraquat or heat shock treatments. There was a report however, (Yao *et al.*, 1994) that APE expression was increased in colon cancer cells under hypoxic conditions; suggesting that modulation of APE is possible under certain circumstances.

Evidence for a modulation of APE in response to oxidative stress has been previously described. Grösch *et al.*, (1998) reported that APE is transiently inducible at mRNA, polypeptide and activity levels following treatment with the oxidising agents H₂O₂ and sodium hypochlorite (NaOCl) between 3 to 9 hours following treatment. This study used doses of 50 µM of NaOCl and 300 µM H₂O₂ but did not provide any details of cell viability following such treatment. The induction of APE mRNA following treatment with 300 µM H₂O₂ was inhibited with cycloheximide/anisomycin, indicating that *de novo* protein synthesis was required for eliciting this response.

The induction of APE protein levels produced up to a maximum 3.9 fold increase 11 hours following treatment with 50 µM NaOCl. The increase seen with 300 µM H₂O₂ treatment peaked at a level of 4-fold, 15 hours post treatment. However, the qualities of the bands produced in the Western blot were not sufficient to substantiate this claim, especially as band intensities were related purely to that of the mock treated control. Gel loading and protein transfer efficiency was not controlled by the inclusion of a probe for a housekeeping gene such as β-actin and no evidence is shown of repetition of the results.

Ramana *et al.*, (1998) also described a selective activation of APE by nontoxic levels of a variety of ROS and ROS generators, including ionizing radiation, HOCl, bleomycin, phenazine methosulphate and H₂O₂. However, these studies also provided

no evidence of repetition and as noted in this report, these assays are subject to a number of different factors which may produce inaccurate results.

In agreement with the observations in this thesis, an induction of APE was not observed by Hsieh *et al.*, (2001) at either mRNA or protein level when they tried to reproduce the same conditions as Ramana *et al.*, (1998). They did however, report that the conditions of Ramana *et al.*, produced increases in PKC activity, increased phosphorylation of APE and thus increased APE redox activity without a change in the amount of APE protein. Such studies into the phosphorylation of the APE protein may thus be an interesting area for future investigation.

It is known that APE possesses redox activity and promotes the binding of Jun/Jun homodimers or Fos/Jun heterodimers (Xanthoudakis *et al.*, 1992; 1994). APE is also known to stimulate the DNA binding of other classes of redox-regulated transcription factors, including the p50 subunit of NF- κ B, CREB, Myb, HIF-1 α and Pax-8 (reviewed in Evans *et al.*, 2000; Wilson & Barsky, 2001). APE has also been shown to interact with the tumour suppressor protein, p53 (Offer *et al.* 1999; Gaiddon *et al.*, 1999; Offer *et al.* 2001).

Recently, stimulation of APE endonuclease activity upon binding of heat shock protein 70 (HSP70) (Mendez *et al.*, 2003) and the Y box-binding protein 1 (DNA binding protein B) (Marenstein *et al.*, 2001), which is involved in transcription, have been described. These results provide more detail as to the complexity of the DNA damage response that APE is involved in.

The other DNA repair factor that has been reported to respond to changes in oxidative stress levels is the DNA glycosylase, OGG1. Tsurudome *et al.*, (1999) reported that *OGG1* mRNA was induced in rats exposed to intratracheal administration of diesel exhaust particles (DEP). The *OGG1* mRNA levels were measured in rat lung tissue 5 to 7 days following exposure to 2 mg and 4 mg DEP using the RT-PCR technique. It was reported that 4 mg DEP produced a clear induction of *OGG1* mRNA and that this was maximal at 7 days following treatment. However, numerical data of fold induction were not presented. Suitable non-treated and vehicle controls were also

analysed and repeat experiments were performed. These findings were used to suggest that DEP might induce its carcinogenic effects via the generation of oxidative stress.

In a similar study, investigating the mechanism of carcinogenesis of peroxisome proliferators, Rusyn *et al.*, (2000) reported 3- to 12- fold induction of the BER factors *OGG1*, *APE*, *MPG* and *polymerase β* in rat liver as measured by a ribonuclease protection assay, following treatment with 1000 p.p.m. of the agent WY-14,643. The agent was fed to the rats for up to 22 weeks before analysis. Experiments were performed in triplicate and representative ribonuclease protection assay gels were presented, but graphical data is only produced for a single experiment and no statistical data of mean levels of induction or standard deviation were presented.

Saitoh *et al.*, (2001) did not observe induction of *OGG1* expression in HeLa S3 cells treated with 2 mM HOCl. This highly toxic dose did however produce an approximately 4-fold increase in APE mRNA and protein 6 hours following treatment, as measured by RT-PCR and Western blotting. No evidence of repeat experiments was detailed and the quality of Western blots did not indicate that band intensity could be measured very accurately. Differing amounts of protein were loaded for Western blot analysis of the *OGG1*, *APE* and the house keeping gene α -tubulin, indicating that gels were loaded separately. The absence of an induction of *OGG1* at either mRNA or protein level, following exposure to such severe oxidative stress does however agree with the results in this thesis, which suggest that hOGG1 is in fact downregulated in an early response to oxidative stress following treatment with UVB. Further studies would be needed in order to confirm this however.

The experiments detailed here that did report modulation of *OGG1* mRNA were performed in whole animal studies. Such experiments are likely to produce differing responses to cell culture studies due to the complexity of mammalian systems. It should be noted that the peroxisome proliferators investigated by Rusyn *et al.*, (2000) produce little or no carcinogenic risk to humans.

Despite the decrease in Fpg-sensitive sites observed following vitamin C treatment (chapter 3), there was little evidence of repair modulation at the mRNA or protein levels of the repair factors investigated. It could be that vitamin C modulates DNA repair at a functional, rather than a transcriptional or translational level. This was investigated at a later stage (chapter 5).

Gifford *et al.*, (2000) investigated multi-probe ribonuclease protection assay analysis of mRNA levels for the *E.coli* oxidative DNA glycosylase genes under conditions of oxidative stress. Neither 10 μM H_2O_2 , 300 μM paraquat, 100 Gy of x-rays nor 50 μg nalidixic acid yielded more than a slight (two-fold) increase in the transcript levels for *fpg*, *mutY*, *nth* or *nei*. These genes did show increase in transcript levels when shifted from anaerobic to aerobic growth however. They also possessed higher transcript levels of DNA repair genes when in exponential growth phase compared to stationary phase. It was suggested that this might be due to the generation of both O_2^- and H_2O_2 by auto-oxidation of components of the respiratory chain. Cells are therefore experiencing more oxidative stress during exponential growth and so it makes sense to have higher levels of enzymes that repair oxidative DNA damage present during this time.

It is possible that the levels of endogenous base damage are so significant that high constitutive levels of the oxidative DNA glycosylases are necessary for genome maintenance. Thus, the increased levels of damage produced by treatment with oxidizing agents are low compared to the high level of background lesions. It may even be that cells in culture adapt to the extraordinarily high oxygen environment that they are maintained in by inducing DNA repair genes. Thus treatment with oxidising agents will be unable to further increase their cellular defences against such damage.

4.5.3 hHR23B & XPA protein expression

The NER factors hHR23B and XPA are both involved in the early damage recognition stages of nucleotide excision repair. It was thought that they might be subject to regulation in a system where an increased state of oxidative stress is induced and therefore the likelihood of an increase in oxidative DNA damage is possible. Modulation of XPA and hHR23B protein expression was not observed

following treatment with H₂O₂, UVB, HOCl or vitamin C using the Western blotting technique.

One study which did report a modulation of NER repair factors after exposure of normal human keratinocytes to UVB irradiation described a modest increase of a range of repair enzymes following treatment with 100 J/m² UVB (Maeda *et al.*, 2001). This was measured using the same ribonuclease protection assay kits as used in this study. Transcript levels were measured 4, 8 and 24 hours following treatment and duplicate ribonuclease protection assays were performed. Transcript levels at 4, 8 and 24 hours were compared to 'baseline' RNA samples that were extracted immediately following UVB treatment. At doses of 300 J/m² and 600 J/m² UVB mRNA transcript levels of all of the genes showed a decrease of between 10-60 %. In 300 J/m² treated cells this had returned to normal by 48 hours following treatment. Transcript levels in cells treated with 600 J/m² did not return to normal. From cell viability studies performed on the keratinocytes following exposure to UVB, it can be seen that by 72 hours following treatment, only 10% of the cells treated with 600 J/m² were still viable, indicating that a large amount of cell death was occurring. Following treatment with 300 J/m² there was only 60% survival, and following 100 J/m² UVB, 25% of the cells were non-viable. These figures show that cell viability was far less in this system than in the conditions that were investigated in this study. This could explain the differences seen in response to DNA damage responses, as could the use of a different cell type. Interestingly, the study went on to perform Western blotting using anti-hHR23B and anti-XPA antibodies. This unpublished data did not show any changes in protein levels reflective of the changes reported at mRNA level.

Recent evidence produced by studies into NER following DNA damage suggests that in this system translocation of repair factors to specific sites of damage may be of more importance than upregulation/down regulation (Fitch *et al.*, 2003; Wang *et al.*, 2003).

There is evidence that following damage to DNA by UV radiation, repair factors are recruited to the nuclear matrix (Balajee *et al.*, 1998; Kamiuchi *et al.*, 2002) and are not constitutive components as was once thought (Widlak & Rzeszowska-Wolny, 1999). The nuclear matrix is formed by chromatin organised into distinct

chromosomal loops by the specific attachment of DNA to an insoluble network of non-histone fibres. Immunofluorescence and Western blotting both indicated the enrichment of XPA, RPA, PCNA and the p62 and p89 subunits of the TFIIH transcription factor in the nuclear matrix of UV treated hamster cells (Balajee *et al.*, 1998). Recently, a CSB-dependent translocation of CSA to the nuclear matrix following both UVC irradiation and H₂O₂ treatment was reported in cells of human origin (Kamiuchi *et al.*, 2002).

The translocation of constitutive repair factors to points of damage may well reflect a more rapid response to DNA damage. This may be one explanation for the lack of a transcriptional or translational response to increased amounts of DNA damage reported in this thesis.

The lack of inducible DNA repair mechanisms shown in this study could in fact represent a protective system in these cells. It has been suggested that the over expression of DNA repair enzymes may in fact play an important role in the mechanism of action of carcinogens (e.g. peroxisome proliferators). For instance, polymerase β is normally expressed at low levels and has high infidelity in replicating DNA (Rusyn *et al.*, 2000). APE has other functions also, which if upregulated may produce a more problematic state for the cell than if left at ubiquitous levels. If only certain factors are modulated then DNA repair may upregulate unevenly. Imbalanced DNA repair could actually be both mutagenic and clastogenic, as during the repair process itself highly damaging DNA strand breaks are introduced. If further repair factors are not available to reassemble the DNA then a much greater consequence may result than from the initial damage. It is also true that premutagenic lesions can not become mutagenic without DNA replication, therefore an amount of DNA damage may be acceptable in cells that are not undergoing replication, and similarly in slowly replicating cells.

It is well documented that oxidative stress can trigger a battery of genes via the antioxidant responsive element (ARE) (Loft & Poulsen, 2000). Among the antioxidant inducible genes are those encoding antioxidant enzyme activities such as glutathione S-transferases (GSTs) and NAD(P)H:quinone oxidoreductase (NQO1);

active in detoxification of reactive substances such as oxygen radicals and redox cycling quinones. Enhanced expression of the antioxidant enzymes such as GSTs, γ -glutamylcysteine synthase and haem oxygenase as a response to oxidative stress has also been reported. These act as enzymatic scavengers for ROS (Martindale & Holbrook, 2002). It could be that such an ARE response is sufficient to deal with the oxidative stress being generated in some of the models being studied.

4.6 CONCLUSIONS

This chapter aimed to investigate the possibility of an adaptive response to oxidative stress produced in human cells via modulation of the DNA repair pathways involved in the repair of oxidative DNA damage. The main findings were:

- Little change in the BER genes *OGG1*, *TDG*, *APE*, *UDG*, *MPG*, *ENTG*, *RPA4* or *MGMT* after treatment with H₂O₂, UVB, HOCl or the antioxidant vitamin C determined using a ribonuclease protection assay.
- Little change in the NER genes *XPG*, *DDB1*, *XPC*, *XPF*, *RPAp70*, *DDB2*, *hHR23B*, *XPA*, *RPAp32*, *RPAp14*, *CSB*, *XPB*, *TFIIHp52*, *TFIIHp44*, *CSA*, *CDK7*, *CycH*, *TFIIHp34*, *ERCC1* or *XPD* following treatment with H₂O₂, UVB, HOCl or vitamin C using a ribonuclease protection assay.
- The optimisation of a Western blotting procedure for the detection of hHR23B, XPA, hOGG1, APE and the housekeeping gene β -actin.
- No significant changes in protein levels of hHR23B, XPA, hOGG1 or APE were induced in this system following exposure of human dermal fibroblasts to changes in cellular oxidative stress.

In the literature a number of studies have reported changes in mRNA and polypeptide levels of DNA repair enzymes after exposure to oxidative stress. Other reports have found a lack of any alterations in these repair factors. This study showed little modulation was found in this system. This chapter has focused on changes of gene expression in response to oxidative stress; studies have shown that DNA repair may not only be modulated at the gene level but that DNA repair activity as a whole could be altered in response to DNA damage. Further studies should investigate the possibility that DNA repair is regulated at activity level in response to DNA damage caused by increases in oxidative stress. Post-translational phosphorylation and translocation of repair factors are other areas worth investigating.

CHAPTER FIVE

DNA Repair Activity in Response to Oxidative Stress and in Breast Cancer

CHAPTER 5: DNA REPAIR ACTIVITY IN RESPONSE TO OXIDATIVE STRESS AND IN BREAST CANCER

5.1 INTRODUCTION

Oxidative stress arises in the cellular environment when the levels of ROS overwhelm the cells normal antioxidant defence mechanisms. As detailed in chapter 1, ROS can arise from both endogenous and exogenous sources and their effects on cellular organisms have been associated with a number of diseases including many forms of cancer, cardiovascular disease, chronic inflammation, neurodegenerative diseases and also the process of ageing.

In recent years the role of ROS in carcinogenesis has received much attention. ROS possess the three essential properties of all carcinogens: (i) they elicit permanent structural changes in DNA; (ii) they activate both cytoplasmic and nuclear signal transduction pathways; and (iii) they modulate the activity of stress proteins and stress genes that are involved in the regulation of key genes related to cell growth, differentiation and death (Kennedy *et al.*, 2003).

One of the major DNA base adducts produced by the reactions of ROS with DNA is the oxidation of guanine at the 8' position to form 8-oxoG. This species occurs in DNA either as a direct result of the oxidation of guanine bases already present in the DNA structure, or due to oxidation of guanine present in the intracellular nucleotide pool (particularly as 8-oxodGTP). This damaged guanine may then be incorporated into DNA during DNA replication.

8-oxoG is a useful biomarker of oxidative DNA damage, and can be used to estimate the carcinogenicity of ROS generating agents (Yamaguchi, *et al.*, 1996). Studies have reported that repair of this adduct can be induced following exposure to oxidative stress produced by ionising radiation (Bases *et al.*, 1992) and the renal and lung carcinogens ferric nitrilotriacetate (Yamaguchi *et al.*, 1996) and crocidolite asbestos respectively (Kim *et al.*, 2001). It has been suggested that the induction of this repair activity could be used as a biological marker of exposure to carcinogens and subsequent increases in levels of cellular oxidative stress.

8-oxodGTP, once incorporated from the nucleotide pool, can base pair with either adenine or cytosine and so is capable of producing A:T → G:C transitions as well as G:C → T:A transversions (Sekiguchi & Tsuzuki, 2002; Egashira *et al.*, 2002). The generally acknowledged theory that elevation of spontaneous mutations may be an early step in cancer progression, suggests that the presence of DNA base damage and generation of mutations would increase the likelihood of tumour occurrence; providing evidence for a role of DNA damage in carcinogenesis.

In order to combat the deleterious effects of oxidative base damage, a number of BER DNA glycosylases act to remove the non-bulky 8-oxoG adducts once they are incorporated into the DNA structure. However, the misincorporation of 8-OH-dGTP into DNA is prevented in human cells by human MutT homologue (hMTH1). This 8-oxo-dGTPase enzyme, hydrolyzes 8-OH-dGTP to 8-oxo-7,8-dihydrodeoxyguanosine monophosphate (8-OH-dGMP), which can then be eliminated from the cell, thus preventing misincorporation (**figure 5.1**). MTH1 has also been shown capable of acting on 2-hydroxydeoxyadenosine triphosphate (2-OHdATP), and actually hydrolyses this oxidised nucleotide more efficiently than the 8-OH-dGTP moiety (Fujikawa *et al.*, 1999; Egashira *et al.*, 2002; Sakai *et al.*, 2002).

A role for MTH1 in the prevention of carcinogenesis has been postulated. Sekiguchi & Tsuzuki (2002) reported that MutT deficient *E.coli* showed a 1000-fold higher frequency of A:T → G:C transitions than wild-type. Tsuzuki *et al.* (2001) discovered that MTH1 nullizygous mice lacked 8-oxodGTPase activity and were more susceptible than MTH1^{+/+} mice to cancers of the lung, liver and stomach.

Increased expression of hMTH1 at mRNA level has been measured in human renal cell carcinomas (Okamoto *et al.*, 1996), breast tumours (Wani *et al.*, 1998) and lung cancer tissue (Kennedy *et al.*, 2003) and at protein level in brain tumours (Iida *et al.*, 2001). One theory for this overexpression is that hMTH1 is induced in response to increased DNA damage resulting from oxidative stress generated as a by-product of increased cellular proliferation in cancerous cells.

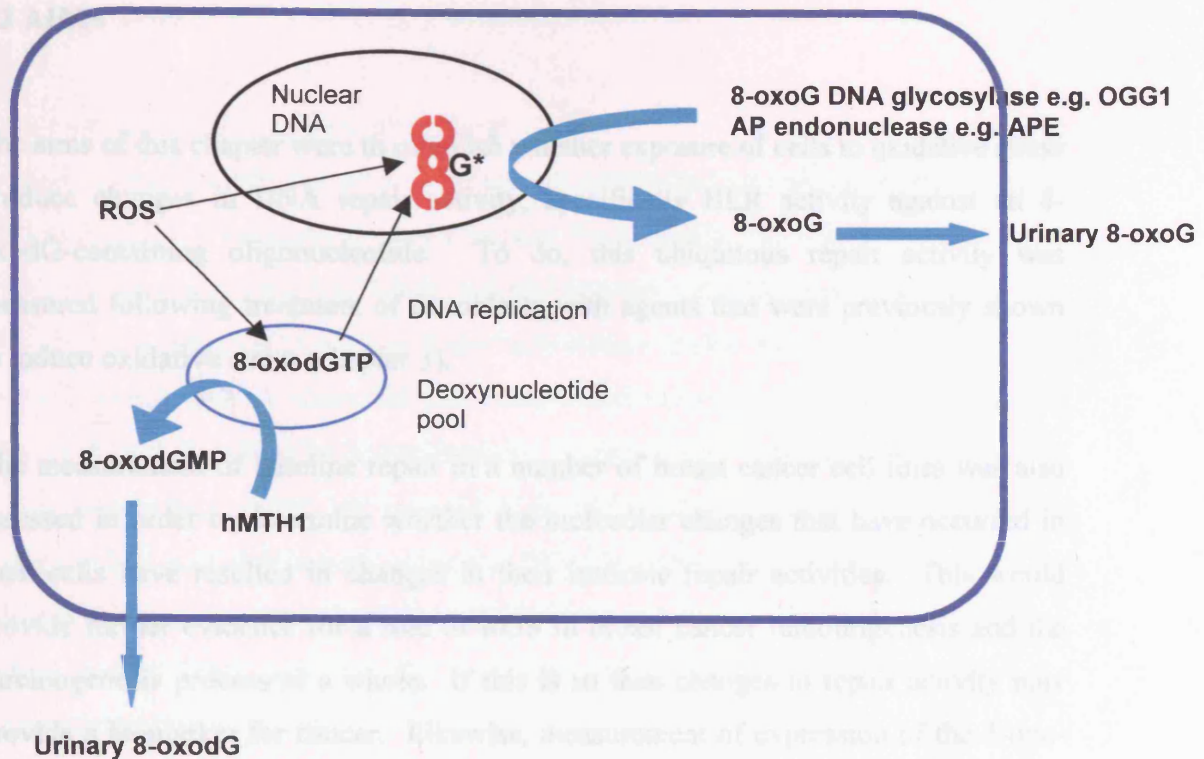


Figure 5.1: Schematic illustration of routes to remove and prevent 8-oxoguanine in nuclear DNA. Incorporation of 8-oxodGTP into nuclear DNA is prevented by its hydrolysis by hMTH1 to 8-oxodGMP in the nucleotide pool. 8-oxoG present in nuclear DNA is removed by actions of the BER enzymes OGG1 and APE. Abbreviations: 8-oxo-7,8-dihydrodeoxyguanosine triphosphate (8-oxodGTP), 8-oxo-7,8-dihydrodeoxyguanosine monophosphate (8-oxodGMP), human homologue of the MuT enzyme (hMTH1), 8-oxo-2'-deoxyguanosine (8-oxodG), 8-oxoguanine (8-oxoG), 8-oxoguanine glycosylase (OGG1).

Evidence reported in the literature suggests that the nucleotide pool sanitiser hMTH1 plays an important role in preventing the formation of base lesions in DNA that may be factors in the progression of carcinogenesis. The reports showing that this enzyme may be upregulated in response to oxidative stress and increased oxidative damage suggest that the measurement of this enzyme in tissues may provide a possible biomarker for rapidly proliferating cells and an indication of carcinogenesis.

5.2 AIMS

The aims of this chapter were to establish whether exposure of cells to oxidative stress produce changes in DNA repair activity, specifically BER activity against an 8-oxodG-containing oligonucleotide. To do, this ubiquitous repair activity was measured following treatment of fibroblasts with agents that were previously shown to induce oxidative stress (chapter 3).

The measurement of baseline repair in a number of breast cancer cell lines was also assessed in order to determine whether the molecular changes that have occurred in such cells have resulted in changes in their intrinsic repair activities. This would provide further evidence for a role of ROS in breast cancer tumourigenesis and the carcinogenesis process as a whole. If this is so then changes in repair activity may provide a biomarker for cancer. Likewise, measurement of expression of the 8-oxo-dGTPase gene, hMTH1, would provide more evidence for a role of ROS in carcinogenesis and also act as a biomarker for breast cancer susceptibility and cancer progression.

5.3 METHODS

5.3.1 Cell lines and treatment procedures

Normal dermal fibroblasts were isolated and maintained in culture as described in section 2.3.1.1. Treatments of approximately 5×10^6 cells with 400 μM and 800 μM H_2O_2 , 600 J/m^2 and 1200 J/m^2 UVB, 300 nM and 600 nM HOCl and 400 μM and 800 μM vitamin C were performed in 75 cm^2 cell culture flasks. Control cells were sham treated. At 4, 8 and 24 hours post treatment, flasks were removed from incubation at 37°C and cells detached by trypsinisation. After washing twice in sterile PBS, cell pellets were lysed in 50 μL ice-cold lysis buffer and stored at -80°C. Protein concentration was determined using the BCA Bradford based protein assay using BSA as standard (section 2.3.4.2). Following investigation of sufficient protein to detect endonuclease activity, 50 μg total cellular protein was used for the endonuclease nicking assay.

Breast cancer cell lines HBL 100, MCF-7, ZR-75.1, T47-D, MDA-MB-468, MDA-MB-231 and MDA-MB-436 were maintained in culture as described in section 2.3.1.1. Cell lysates were extracted as noted for normal dermal fibroblasts. mRNA for use in RT reactions was extracted as described in section 2.3.2.3. Briefly, cells were grown to 90% confluence, washed in 10 mL HBSS and lysed in 100 μL lysis binding buffer per 1×10^5 cells. 5 μL of 1 mg/mL proteinase K solution was added and lysates incubated at 37°C for 30 minutes before shearing DNA through a 21G and then 25G sterile needle, 3 to 5 times each. mRNA was isolated using oligo(dT)25 Dynabeads, resuspended in 30 μL DEPC treated water and stored at 4°C until RT reactions were performed.

5.3.2 Endonuclease nicking activity in dermal fibroblasts in response to oxidative stress

The endonuclease nicking assay (section 2.3.4.2) uses a radioactively labelled 8-oxodG containing 24mer oligonucleotide. Any 'nicking' activity can be detected by measuring the appearance of a ^{32}P -labelled 9mer oligonucleotide product and expressing this as a percentage of the total labelled oligonucleotides (24mer and 9 mer

product). An outline of the endonuclease nicking assay procedure is shown in **figure 5.2**.

Controls were included in each separate experiment to ensure that 9mer formation was due to specific nicking activity and not degradation of the 24mer during the oligonucleotide reaction. An undamaged oligonucleotide, of the same sequence as the 8-oxodG containing oligonucleotide, was used to show that nicking was only produced at damaged sites. Purified Fpg protein from *E.coli* was used to show whether different concentrations of enzyme would alter the efficiency of the nicking activity. Optimum time of incubation of oligonucleotide with cell lysate was assessed in a timecourse experiment and optimum amount of protein to be used in the assay was also assessed prior to analysis of samples.

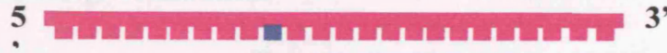
10 pmol 8-oxodG-containing oligonucleotide was end-labelled with [γ - 32 P] ATP (3000 Ci/mmol) with T4 polynucleotide kinase at 37°C for 30 minutes, as described in section 2.3.4.2. 10 pmol undamaged complimentary oligonucleotide was added and annealed by heating to 95°C for 10 minutes and then slowly cooled to room temperature. Any single-stranded oligonucleotide was then removed using the QIAquick[®] Nucleotide Removal Kit (section 2.3.4.2). Purified, labelled substrate was stored at -20°C until required for the oligonucleotide reaction.

Experiments investigated the optimal time for incubation of substrate with cellular lysate. The reaction was performed with 6 μ L (1 pmol) labelled substrate in a total reaction volume of 20 μ L. The amount of cell lysate used was dependent on total cellular protein concentration; optimal protein concentration (ranging from 20 to 50 μ g) was investigated.

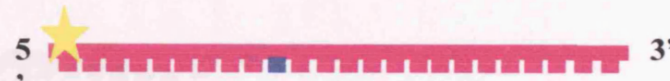
Reaction products were denatured in 10 μ L 3 \times denaturing buffer by heating to 95°C for 10 minutes and then cooled on ice for 5 minutes. Products were then resolved by 20% denaturing PAGE. The assay was performed in triplicate and mean and standard deviations of endonuclease nicking activity determined for each treatment using densitometric analysis of substrate and product bands by a β -Imaging Computing Densitometer (Molecular Dynamics) with MD ImageQuant software version 3.3.

8-oxo-dG oligonucleotide

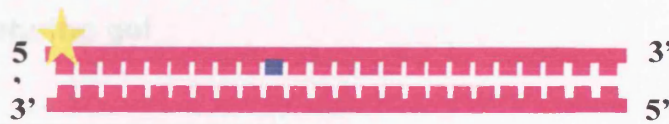
Expose to denaturing conditions



5' - end labelling



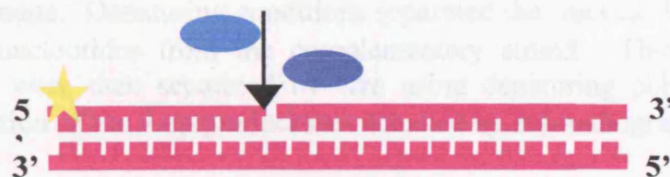
Annealing of oligonucleotide complimentary strand



Incubate with whole cell lysate



Nicking of 8-oxoguanine by OGG1 and APE



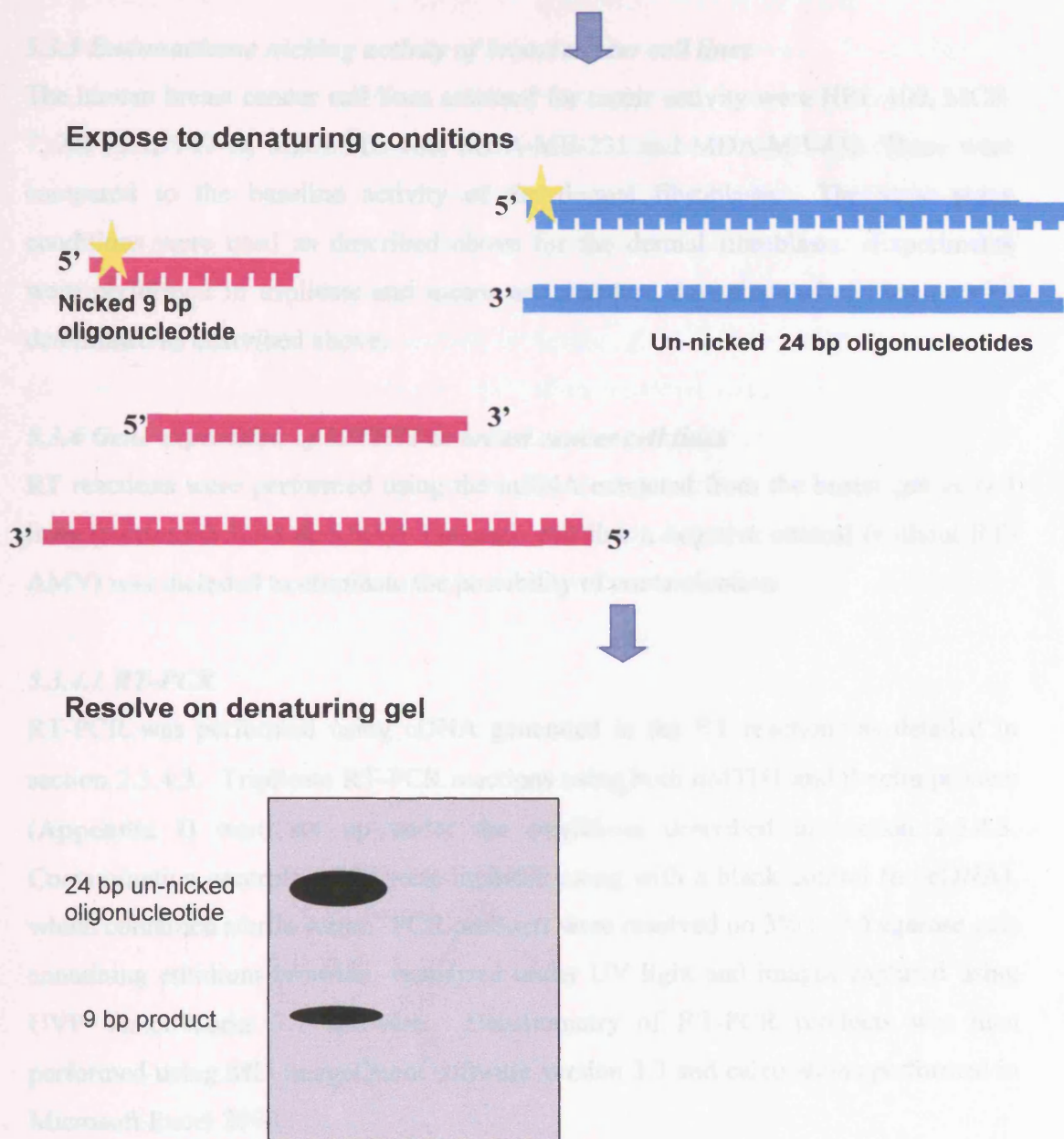


Figure 5.2: An overview of the endonuclease nicking assay. An 8-oxodG-containing 24 bp oligonucleotide was end labelled with [γ - 32 P] ATP. An undamaged complimentary oligonucleotide was annealed to produce a double-stranded DNA duplex, which was then incubated with whole cell lysate extracted from the cells under investigation. Repair proteins such as OGG1 (8-oxoguanine DNA glycosylase) and APE (AP endonuclease) 'nick' the substrate at the site of damage. Denaturing conditions separated the 'nicked' 9 bp product and 24 bp 'un-nicked' oligonucleotides from the complementary strand. These [γ - 32 P] ATP-labelled oligonucleotides were then separated by size using denaturing polyacrylamide gel electrophoresis and formation of the 9 bp product was detected by autoradiography.

5.3.3 Endonuclease nicking activity of breast cancer cell lines

The human breast cancer cell lines assessed for repair activity were HBL 100, MCF-7, ZR-75.1, T47-D, MDA-MB-468, MDA-MB-231 and MDA-MB-436. These were compared to the baseline activity of the dermal fibroblasts. The same assay conditions were used as described above for the dermal fibroblasts. Experiments were performed in triplicate and means and standard deviations of nicking activity determined as described above.

5.3.4 Gene expression of hMTH1 in breast cancer cell lines

RT reactions were performed using the mRNA extracted from the breast cancer cell lines (sections 2.3.2.3 & 5.3.1). For each cell line a negative control (without RT-AMV) was included to eliminate the possibility of contamination.

5.3.4.1 RT-PCR

RT-PCR was performed using cDNA generated in the RT reactions as detailed in section 2.3.4.3. Triplicate RT-PCR reactions using both hMTH1 and β -actin primers (**Appendix I**) were set up under the conditions described in section 2.3.4.3. Contamination controls (-RT) were included along with a blank control (no cDNA), which contained sterile water. PCR products were resolved on 3% (w/v) agarose gels containing ethidium bromide, visualised under UV light and images captured using UVP VisionWorks 3.1 software. Densitometry of RT-PCR products was then performed using MD ImageQuant software version 3.3 and calculations performed in Microsoft Excel 2000.

5.3.4.2 Quantitative real time RT-PCR analysis

Quantitative real-time RT-PCR analysis was performed using cDNA from the same mRNA used for RT-PCR analysis (section 5.3.4.1). Triplicate reactions of each sample were set up, along with a water control. MTH1 and β -actin primers were run simultaneously on the Cyclor for 40 cycles. A melt curve was also generated in order to investigate the formation of primer dimers. Real-time RT-PCR products were run on a 3% (w/v) agarose gel and visualised as for RT-PCR products, in order to confirm that the size of the PCR products corresponded to the predicted product size.

5.3.4.3 Designing of hMTH1 primers and sequencing of PCR products

Primers to hMTH1 mRNA were designed using Primer 3 software. To confirm the specificity of the hMTH1 primers, RT-PCR products were prepared for sequencing. Firstly, purification of the PCR products was performed using a QIAquick PCR Purification Kit (section 2.3.4.4). Sequencing reactions were then prepared using 3.5 pmol of either forward or reverse primer as appropriate, 8 μ L Big Dye and 2 μ L of the purified PCR product. Sequencing reactions were performed in a Progene thermal cycler under the conditions described in section 2.3.4.4 for a total of 35 cycles. Unincorporated Big Dye terminators were then removed using Centri-Sep columns (section 2.3.4.4). The remainder of the sequencing protocol was kindly performed by the Protein and Nucleic Acids Chemistry Laboratory (PNACL, University of Leicester) using a 377 ABI sequencer (section 2.3.4.4). Sequencing results were viewed and analysed using Chromus Version 1.45 software and BLAST 2.2.6 (section 2.3.6).

5.4 RESULTS

5.4.1 Optimisation of endonuclease nicking assay conditions

The endonuclease nicking assay offered a sensitive method for the detection of DNA glycosylase activity at 8-oxodG sites. This was used as an indicator of the repair capability of cells.

The ³²P-labelled oligonucleotide was firstly subjected to two concentrations of the purified *E.coli* Fpg protein (the working dilution was determined by experimentation), an enzyme that is known to nick 8-oxodG containing sites (**figure 5.3**). A very small amount (1.5%) of 9-mer product was formed with a 1/1000 dilution at baseline level. By two hours incubation at 37°C a concentration-dependent effect of the Fpg protein on 9mer formation could be seen. 1/1000 dilution showed 56% 9mer formation and 1/3000 a 29% 9-mer formation. After 4 hours of incubation 1/1000 had increased slightly to 58% 9-mer formation but 1/3000 dilution had dropped slightly to 20% 9mer formation (**figure 5.4**). The slowing down of the reaction was considered to indicate that one of the two substrates had reached saturation point i.e. no 8-oxodG was left for nicking, or not enough enzyme was present to nick the remaining 8-oxodG sites. The repair kinetics suggested that in the 1/1000 reaction the 8-oxodG was the limiting factor and that in the 1/3000 reaction the Fpg enzyme was the limiting factor.

The results showed that the nicking activity was caused by an enzymatic reaction, not just degradation and also that the 24mer was an appropriate substrate for this assay. This was shown by the lack of a 9mer product at 0 hours and increased 9mer formation with increased amount of Fpg protein.

Untreated dermal fibroblast cellular lysates were used to determine the optimal amount of total cellular protein to use in the assay (**figure 5.5 A**). 20 µg, 40 µg and 50 µg of total cellular protein, as measured using the Bradford assay, gave 3.8%, 4.2% and 5.2% 9mer formation respectively after 2 hours incubation with the 8-oxodG containing oligonucleotide (**figure 5.6**). It was decided to use 50 µg total cellular protein for all subsequent studies, as this amount gave the greatest amount of

product formation at this timepoint, which would allow greater sensitivity of product detection and therefore more reliable results.

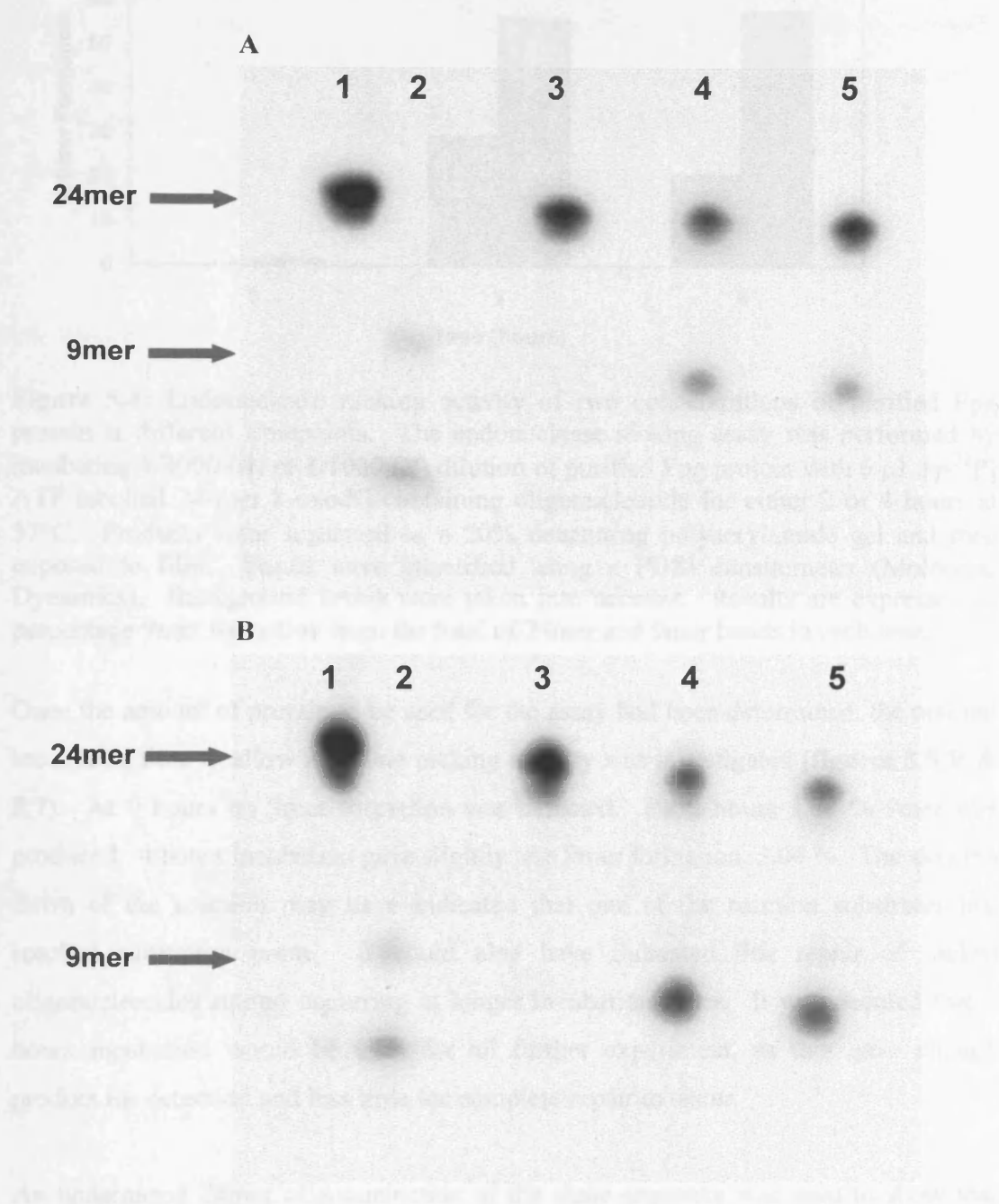


Figure 5.3: Endonuclease nicking assay with two concentrations of purified Fpg protein. A [γ - 32 P]-ATP labelled 8-oxodG-containing 24mer oligonucleotide was incubated with either (A) 1/3000 dilution of Fpg protein or (B) 1/1000 dilution of Fpg protein for 0, 2 or 4 hours at 37°C. The samples were resolved on a 20% denaturing polyacrylamide gel and 9mer product formation visualised by autoradiography. (A) Lane 1; 8-oxodG-containing 24mer marker. Lane 2; 9mer marker. Lanes 3-5; 8-oxodG-containing 24mer incubated with 1/3000 dilution Fpg protein for 0, 2 and 4 hours respectively. (B) Lane 1; 8-oxodG-containing 24mer marker. Lane 2; 9mer marker. Lanes 3-5; 8-oxodG-containing 24mer incubated with 1/3000 dilution Fpg protein for 0, 2 and 4 hours respectively.

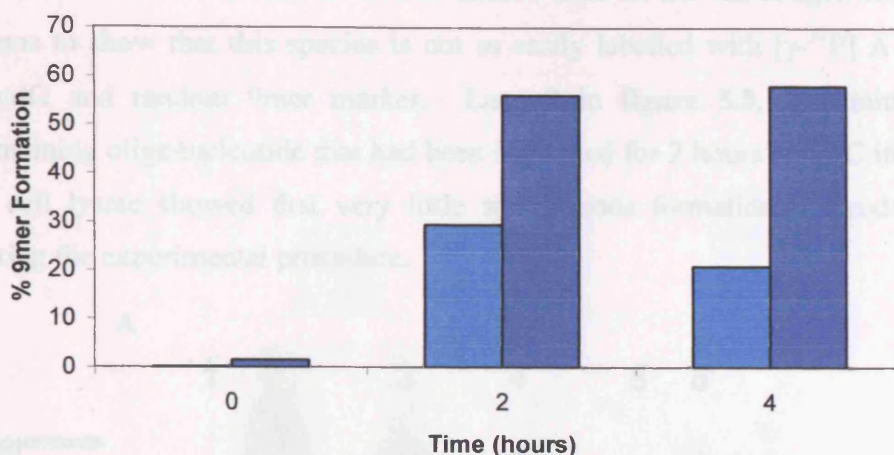


Figure 5.4: Endonuclease nicking activity of two concentrations of purified Fpg protein at different timepoints. The endonuclease nicking assay was performed by incubating 1/3000 (■) or 1/1000 (■) dilution of purified Fpg protein with 6 μ L [γ - 32 P] ATP labelled 24-mer 8-oxodG-containing oligonucleotide for either 2 or 4 hours at 37°C. Products were separated on a 20% denaturing polyacrylamide gel and then exposed to film. Bands were quantified using a PDSI densitometer (Molecular Dynamics). Background levels were taken into account. Results are expressed as percentage 9mer formation from the total of 24mer and 9mer bands in each lane.

Once the amount of protein to be used for the assay had been determined, the optimal incubation time to allow adequate nicking activity was investigated (**figures 5.5 B & 5.7**). At 0 hours no 9mer formation was detected. By 2 hours 4.04 % 9mer was produced. 4 hours incubation gave slightly less 9mer formation, 3.04 %. The slowing down of the reaction may have indicated that one of the reaction substrates had reached saturation point. It could also have indicated that repair of nicked oligonucleotides started occurring at longer incubation times. It was decided that 2 hours incubation would be used for all further experiment, as this gave enough product for detection and less time for complete repair to occur.

An undamaged 24mer oligonucleotide of the same sequence was used to show that nicking activity was specific to damaged sites (**figure 5.8**). No formation of products was seen when this oligonucleotide was incubated for 2 hours at 37°C with or without 50 μ g total cellular lysate from dermal fibroblasts. Several film exposures were developed showing that no 9mer formation was produced. The gel in **figure 5.8** was produced from a 10 minute exposure. Exposures of greater length than 10 minutes produced 8-oxodG oligonucleotide bands that were very saturated and distorted large

areas of the film. The lack of such an intense band for the undamaged oligonucleotide seems to show that this species is not as easily labelled with $[\gamma\text{-}^{32}\text{P}]$ ATP as the 8-oxodG and random 9mer marker. Lane 7 in **figure 5.8**, containing 8-oxodG-containing oligonucleotide that had been incubated for 2 hours at 37°C in the absence of cell lysate showed that very little spontaneous formation of product occurred during the experimental procedure.

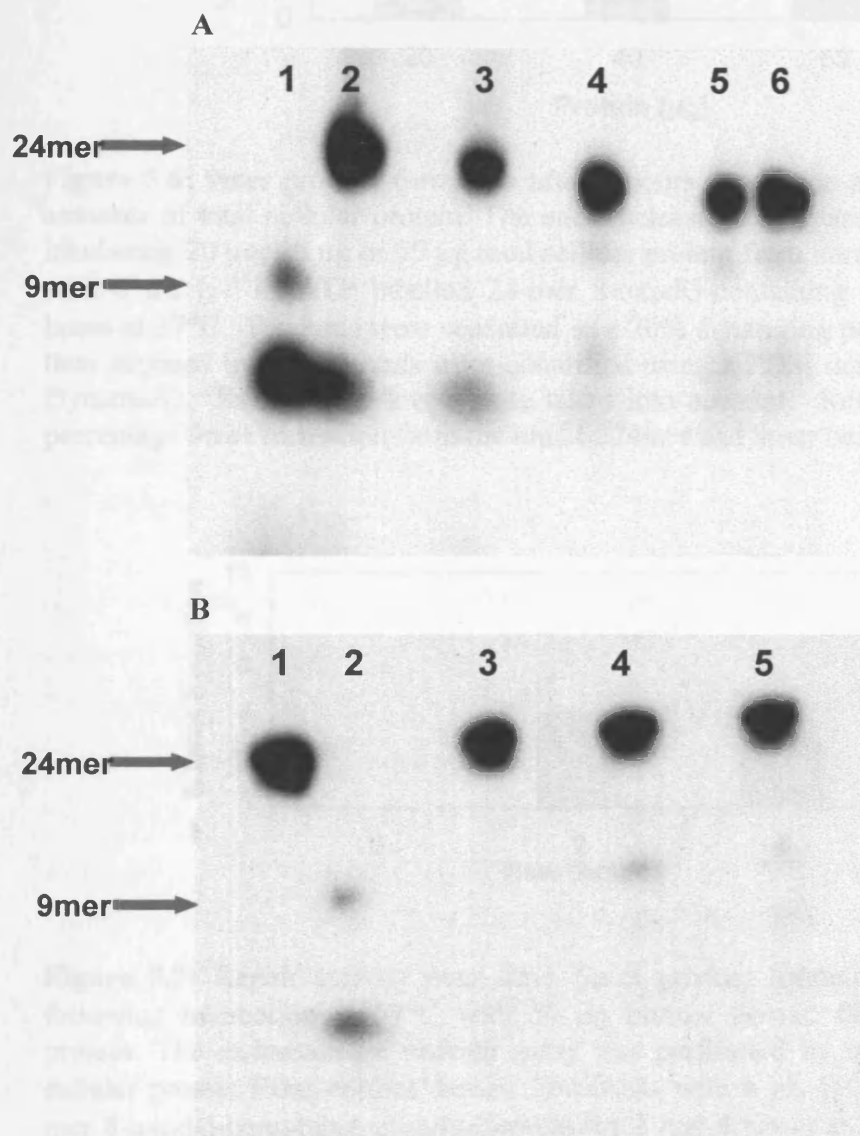


Figure 5.5: Endonuclease nicking assays to determine optimum concentration of cell lysate and incubation time for analysis of dermal fibroblast repair activity. **(A) Lane 1;** 9mer marker. **Lane 2;** 8-oxodG 24mer marker. **Lanes 3-6;** 8-oxodG containing oligo incubated for 2 hours with 0, 20, 40 and 50 μg total cellular lysate respectively. **(B) Lane 1;** 8-oxodG 24mer marker. **Lane 2;** 9mer marker. **Lanes 3-5;** 8-oxodG containing oligo incubated with 50 μg total cellular lysate for 0, 2 and 4 hours respectively.

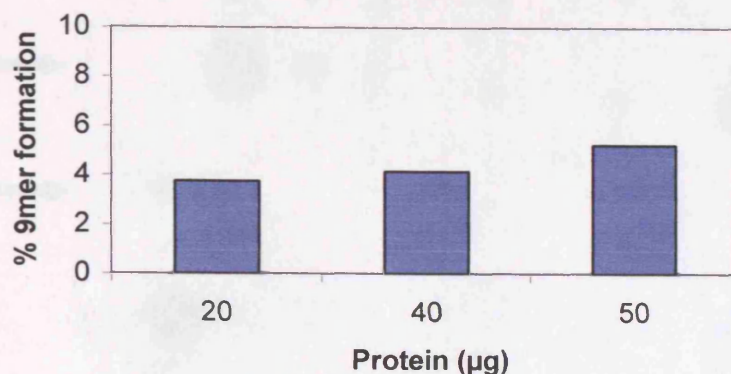


Figure 5.6: 9mer product formation after 2 hours incubation at 37°C with different amounts of total cellular protein. The endonuclease nicking assay was performed by incubating 20 µg, 40 µg or 50 µg total cellular protein from normal dermal fibroblasts with 6 µL [γ - 32 P] ATP labelled 24-mer 8-oxodG-containing oligonucleotide for 2 hours at 37°C. Products were separated on a 20% denaturing polyacrylamide gel and then exposed to film. Bands were quantified using a PDSI densitometer (Molecular Dynamics). Background levels were taken into account. Results are expressed as percentage 9mer formation from the total of 24mer and 9mer bands in each lane.

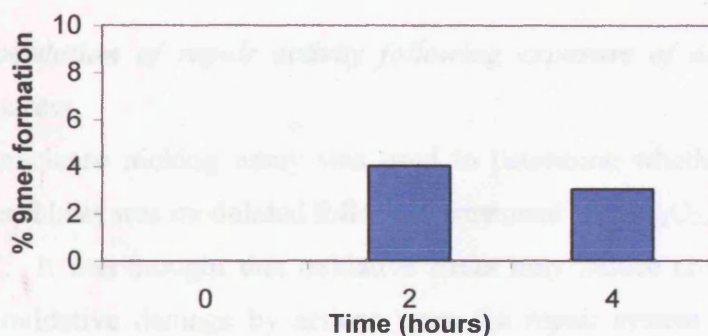


Figure 5.7: Repair activity over time. 9mer product formation at 2 and 4 hours following incubation at 37°C with 50 µg normal dermal fibroblast total cellular protein. The endonuclease nicking assay was performed by incubating 50 µg total cellular protein from normal dermal fibroblasts with 6 µL [γ - 32 P] ATP labelled 24-mer 8-oxodG-containing oligonucleotide for 2 and 4 hours at 37°C. Products were separated on a 20% denaturing polyacrylamide gel and then exposed to film. Bands were quantified using a PDSI densitometer (Molecular Dynamics). Background levels were taken into account. Results are expressed as percentage 9mer formation from the total of 24mer and 9mer bands in each lane.

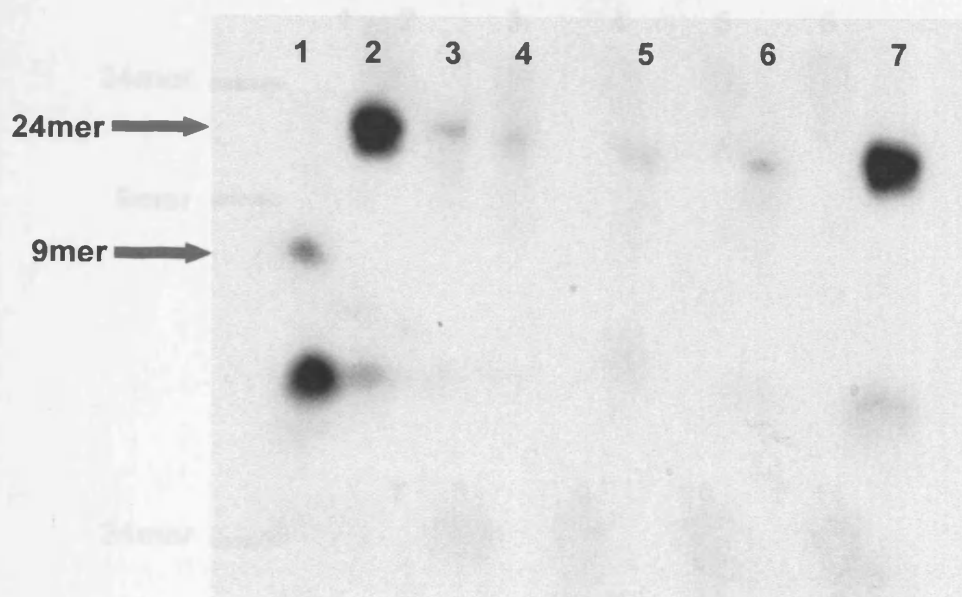


Figure 5.8: Lack of endonuclease nicking activity with undamaged 24mer oligonucleotide. **Lane 1;** 9mer marker. **Lane 2;** 24mer 8-oxodG containing-oligo marker. **Lane 3;** undamaged 24mer oligo marker. **Lanes 4-5;** undamaged oligo incubated with 50 µg total cellular lysate for 0 and 2 hours respectively. **Lane 6;** undamaged oligo incubated for 2 hours without cell lysate. **Lane 7;** 8-oxodG containing oligo incubated for 2 hours without cell lysate.

5.4.2 Modulation of repair activity following exposure of dermal fibroblasts to oxidative stress

The endonuclease nicking assay was used to determine whether repair activity of dermal fibroblasts was modulated following treatment with H₂O₂, HOCl, UVB and, or vitamin C. It was thought that oxidative stress may induce changes in the rates of repair of oxidative damage by actions upon the repair system as a whole and not merely by the modulation of individual repair factors at either mRNA or protein level, as investigated in chapter 4.

For each endonuclease nicking assay 50 µg total cellular protein was incubated for 2 hours at 37°C with 6 µL [γ -³²P] ATP labelled 8-oxodG-containing oligonucleotide, as determined by optimisation experiments detailed above (**figures 5.3 –5.8**).

The treatment of dermal fibroblasts with 400 µM and 800 µM H₂O₂ produced little change in repair activity at 4, 8 and 24 hours following treatment (**figures 5.9 & 5.10**).

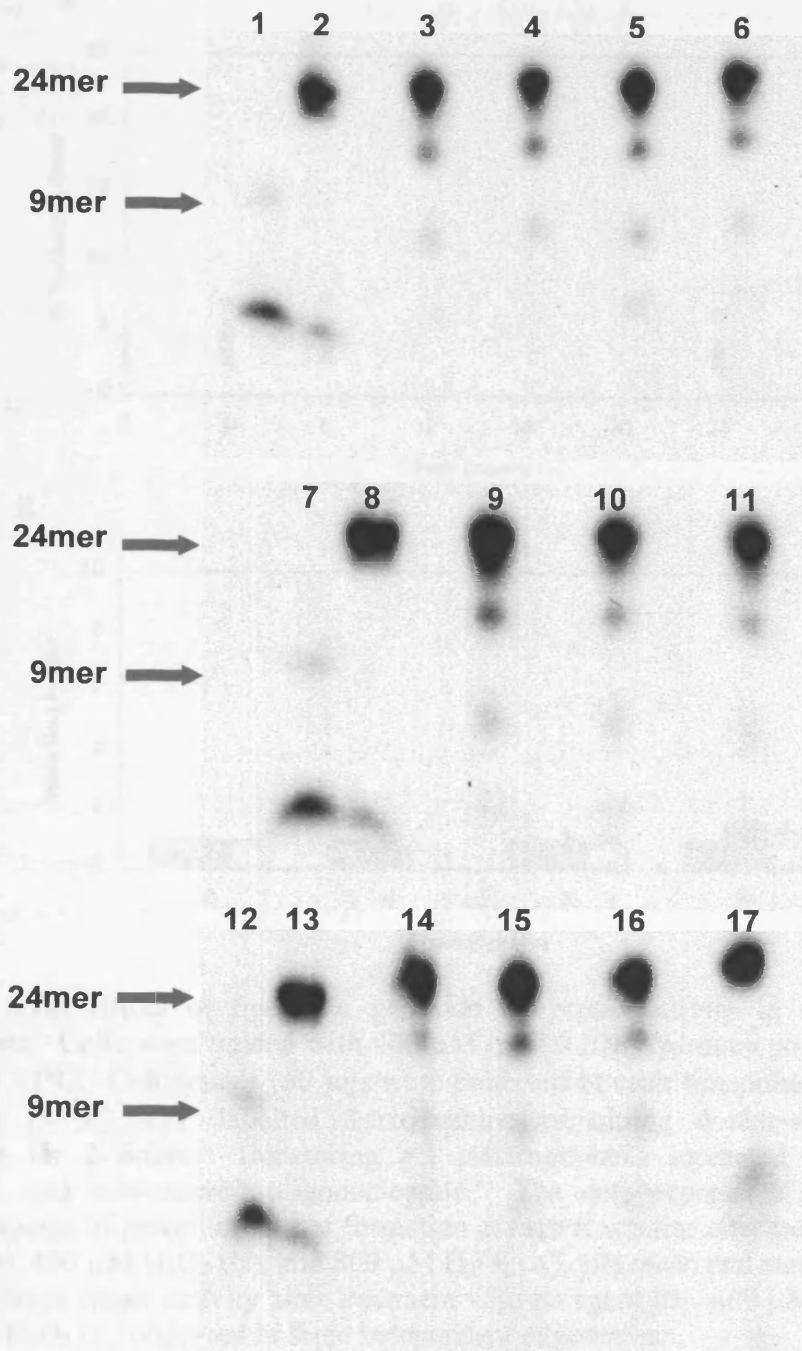


Figure 5.9: Endonuclease nicking activity of normal dermal fibroblast cell lysates following treatment with 400 μM and 800 μM H_2O_2 (using 50 μg protein in a 2 hour assay). **Lanes 1, 7 & 12;** 9mer marker. **Lanes 2, 8 & 13;** 8-oxodG 24mer marker. **Lanes 3-6;** Untreated dermal fibroblasts at 0, 4, 8 and 24 hours respectively. **Lanes 9-11;** Dermal fibroblasts treated with 400 μM H_2O_2 at 4, 8 and 24 hours post treatment respectively. **Lanes 14-16;** Dermal fibroblasts treated with 800 μM H_2O_2 at 4, 8 and 24 hours post treatment respectively. **Lane 17;** 8-oxodG containing 24mer incubated at 37°C for 2 hours without cell lysate.

Chapter 5: DNA repair activity in response to oxidative stress

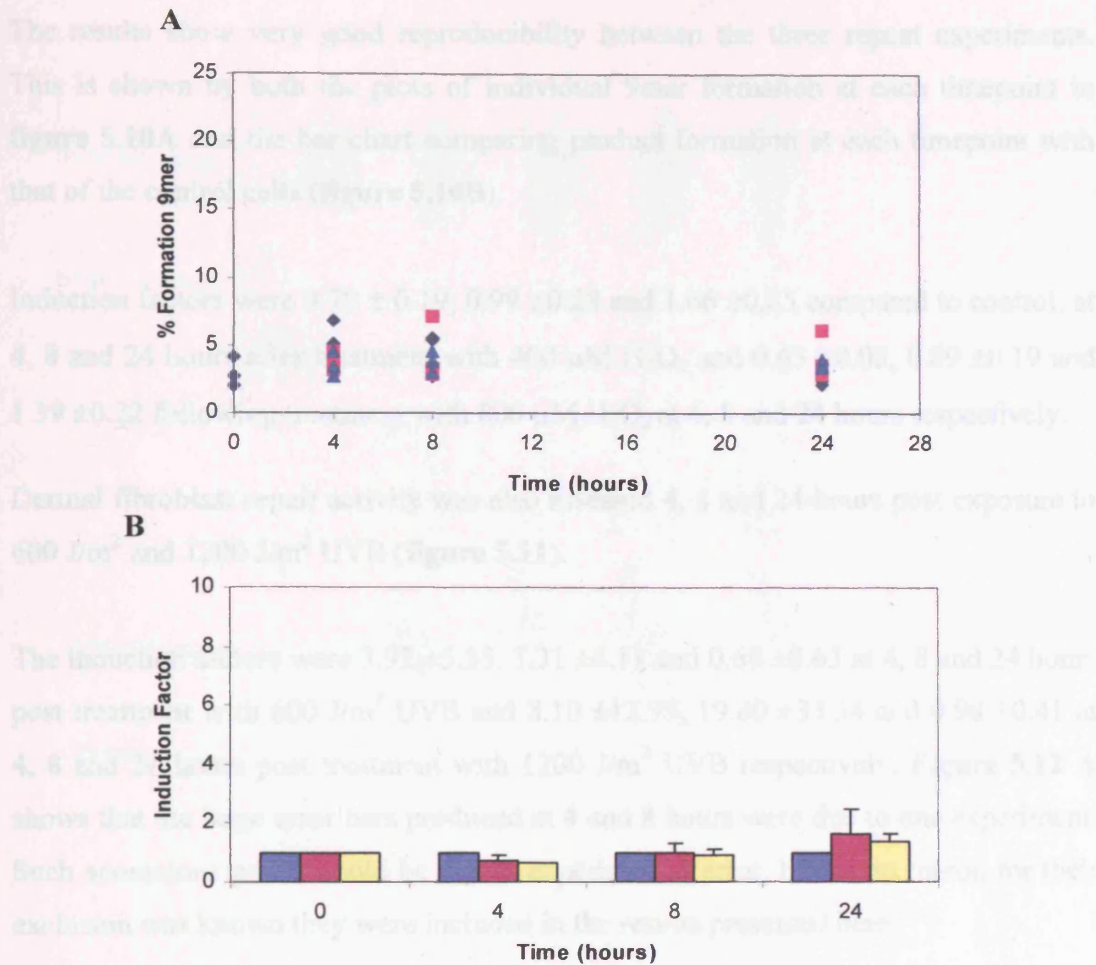


Figure 5.10: Effect of hydrogen peroxide on repair activity in normal dermal fibroblasts. Cells were treated with 400 μM or 800 μM hydrogen peroxide for 4-24 hours at 37°C. Cell lysates (50 μg) were collected at each timepoint and incubated with an [γ -³²P] ATP labelled 8-oxoguanine containing double-stranded repair substrate for 2 hours. Denaturing gel electrophoresis separated cleaved repair products and non-cleaved oligonucleotide. The data represents (A) individual measurements of percentage 9mer formation at each timepoint after treatment with no agent (♦), 400 μM H₂O₂ (■), and 800 μM H₂O₂ (▲). (B) mean and standard deviation of percentage repair activity after treatment with no agent (■), 400 μM H₂O₂ (■) and 800 μM H₂O₂ (■) observed in three independent experiments.

Chapter 5: DNA repair activity in response to oxidative stress

The results show very good reproducibility between the three repeat experiments. This is shown by both the plots of individual 9mer formation at each timepoint in **figure 5.10A** and the bar chart comparing product formation at each timepoint with that of the control cells (**figure 5.10B**).

Induction factors were 0.70 ± 0.19 , 0.99 ± 0.28 and 1.66 ± 0.85 compared to control, at 4, 8 and 24 hours after treatment with $400 \mu\text{M H}_2\text{O}_2$ and 0.63 ± 0.05 , 0.89 ± 0.19 and 1.39 ± 0.22 following treatment with $800 \mu\text{M H}_2\text{O}_2$ at 4, 8 and 24 hours respectively.

Dermal fibroblast repair activity was also assessed 4, 8 and 24 hours post exposure to 600 J/m^2 and 1200 J/m^2 UVB (**figure 5.11**).

The induction factors were 3.92 ± 5.35 , 3.31 ± 4.11 and 0.69 ± 0.63 at 4, 8 and 24 hours post treatment with 600 J/m^2 UVB and 8.10 ± 12.99 , 19.80 ± 33.34 and 0.98 ± 0.41 at 4, 8 and 24 hours post treatment with 1200 J/m^2 UVB respectively. **Figure 5.12 A** shows that the large error bars produced at 4 and 8 hours were due to one experiment. Such anomalous points could be due to experimental error, but as no reason for their exclusion was known they were included in the results presented here.

Repair activity was also assessed in dermal fibroblasts that had been treated with 300 nM and 600 nM HOCl for 4, 8 and 24 hours (**figure 5.13**). Results from three separate nicking assays are presented in **figure 5.14**.

There were no significant differences in repair activity produced in dermal fibroblasts by treatment with 300 nM or 600 nM HOCl at either 4, 8 or 24 hours post treatment. Product formation seemed a little more variable than seen with previous treatments but as control values varied slightly as well this must have been due to experimental procedure.

Induction factors were 1.65 ± 0.94 , 0.62 ± 0.59 and 0.59 ± 0.16 for 300 nM HOCl at 4, 8 and 24 hours respectively. Following treatment with 600 nM HOCl induction factors were 0.80 ± 0.64 , 1.01 ± 0.52 and 1.16 ± 0.35 at 4, 8 and 24 hours respectively.

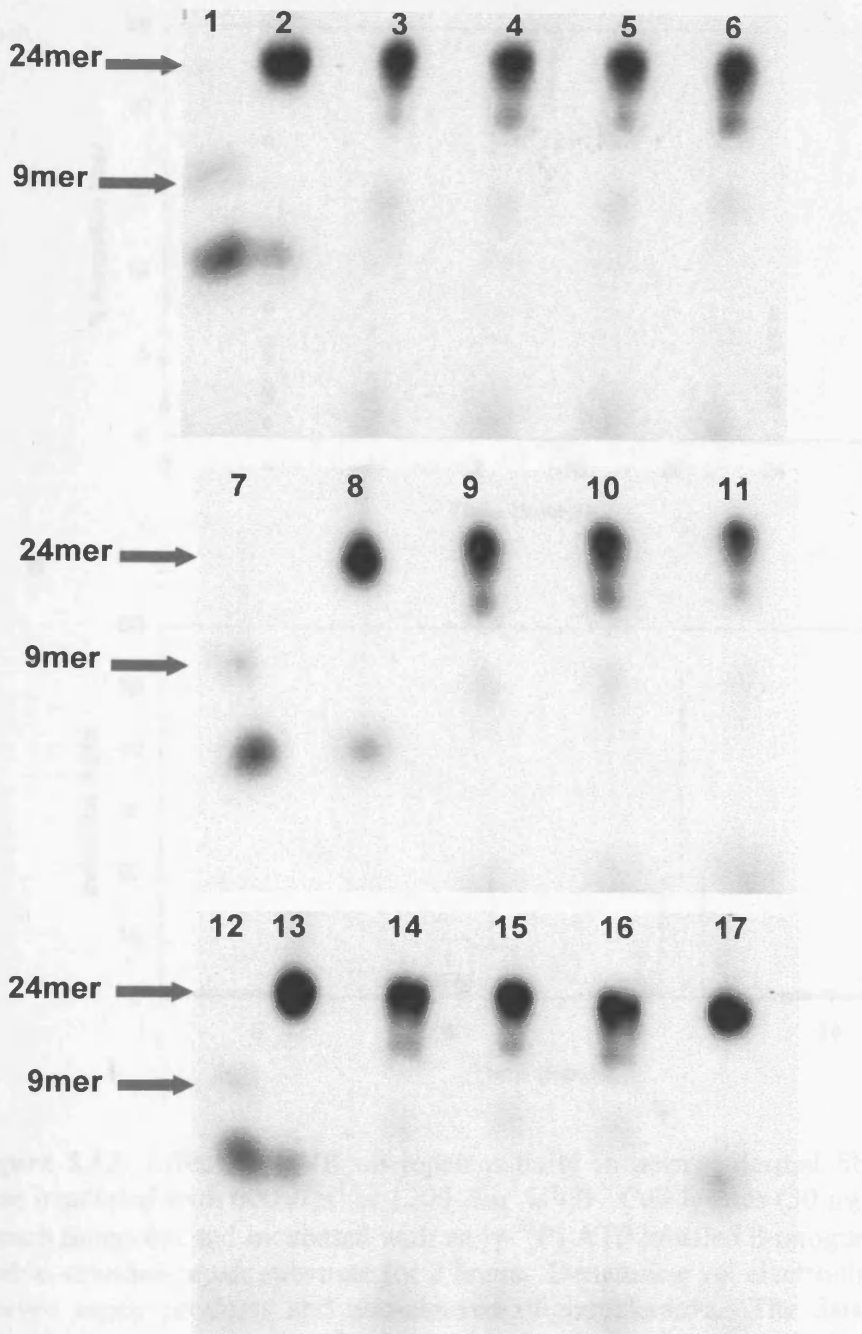


Figure 5.11: Endonuclease nicking activity of normal dermal fibroblast cell lysates following treatment with 600 J/m² and 1200 J/m² UVB (using 50 µg protein in a 2 hour assay). **Lanes 1, 7 & 12;** 9mer marker. **Lanes 2, 8 & 13;** 8-oxodG 24mer marker. **Lanes 3-6;** Untreated dermal fibroblasts at 0, 4, 8 and 24 hours respectively post sham treatment. **Lanes 9-11;** Dermal fibroblasts treated with 600 J/m² UVB at 4, 8 and 24 hours post irradiation. **Lanes 14-16;** Dermal fibroblasts treated with 1200 J/m² UVB at 4, 8 and 24 hours post irradiation. **Lane 17;** 8-oxodG containing 24mer incubated at 37°C for 2 hours

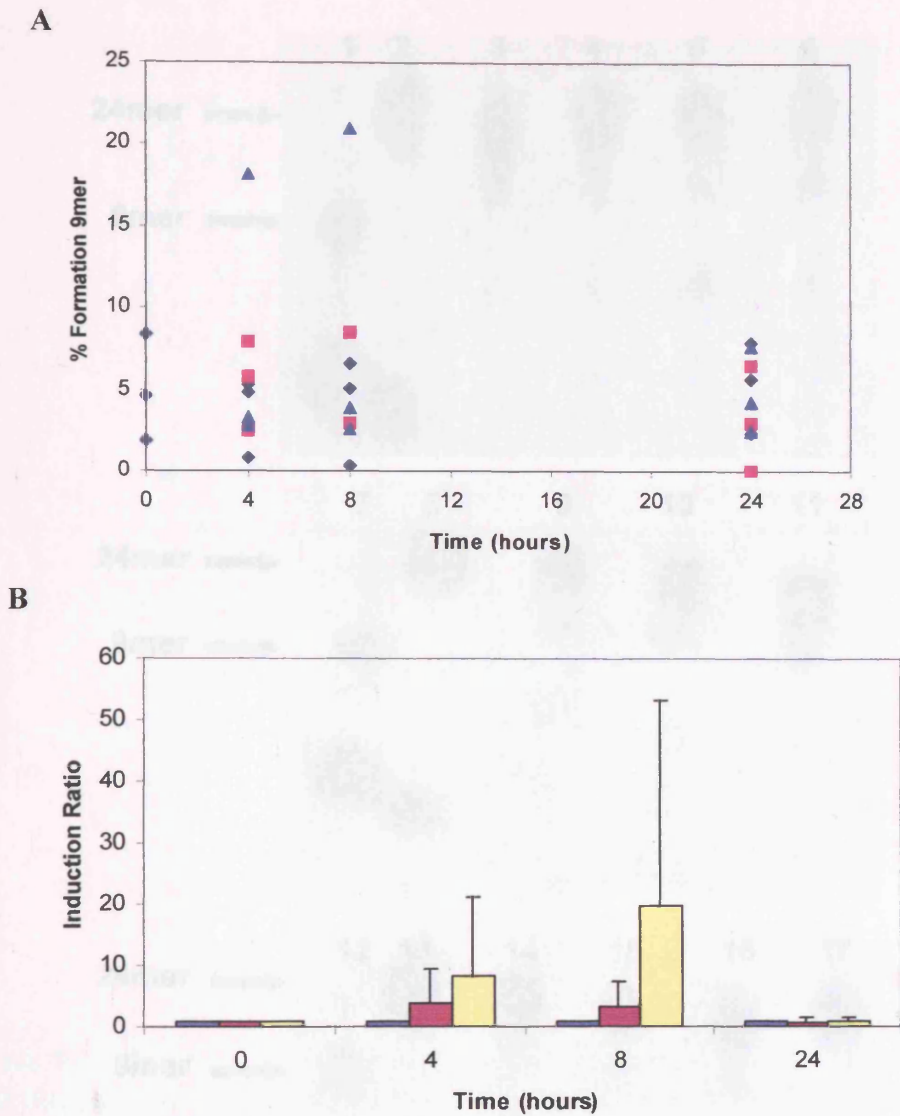


Figure 5.12: Effect of UVB on repair activity in normal dermal fibroblasts. Cells were irradiated with 600 J/m² or 1200 J/m² UVB. Cell lysates (50 µg) were collected at each timepoint and incubated with an [γ -³²P] ATP labelled 8-oxoguanine containing double-stranded repair substrate for 2 hours. Denaturing gel electrophoresis separated cleaved repair products and non-cleaved oligonucleotide. The data represents (A) individual measurements of percentage 9mer formation at each timepoint after treatment with no agent (◆), 600 J/m² UVB (■), and 1200 J/m² UVB (▲). (B) Mean and standard deviation of percentage repair activity after treatment with no agent (■), 600 J/m² UVB (■) and 1200 J/m² UVB (■) observed in three independent experiments.

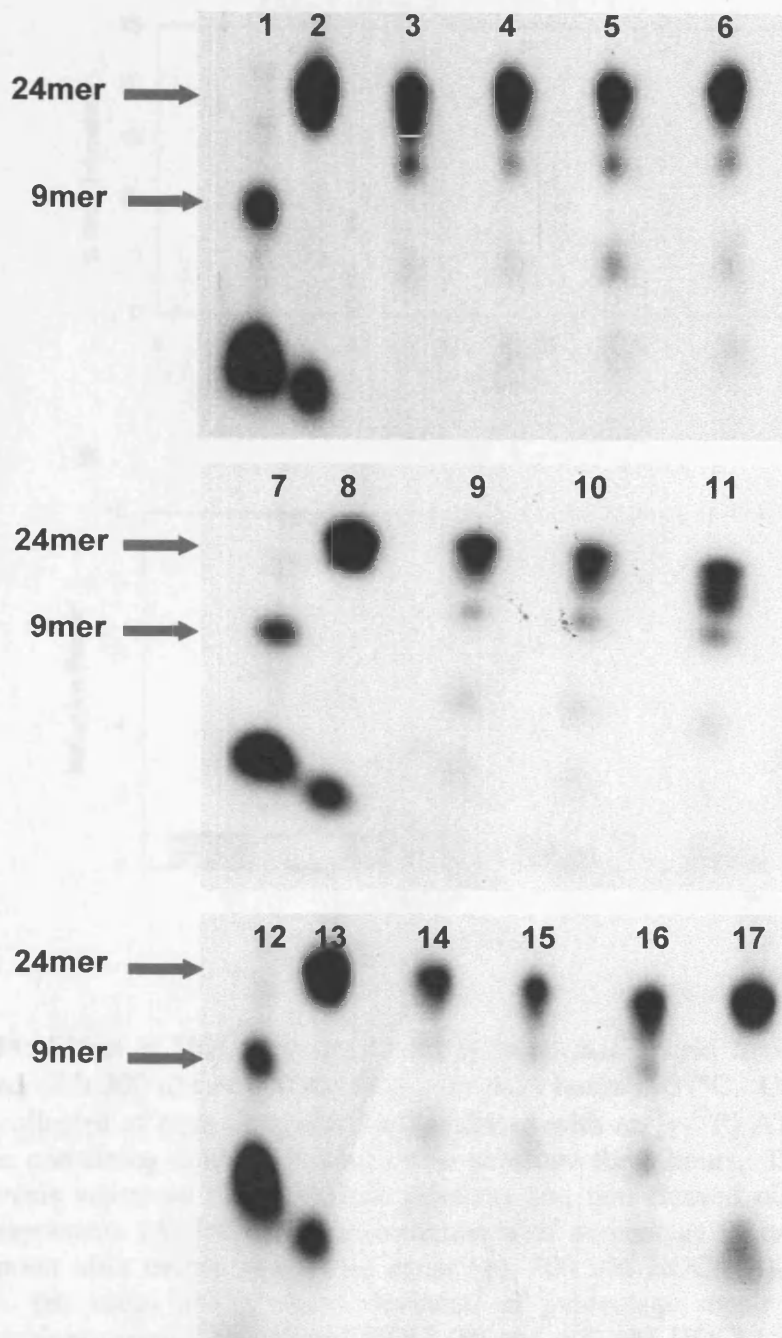


Figure 5.13: Endonuclease nicking activity of normal dermal fibroblast cell lysates following treatment with 300 nM and 600 nM HOCl (using 50 μ g protein in a 2 hour assay). **Lanes 1, 7 & 12;** 9mer marker. **Lanes 2, 8 & 13;** 8-oxodG 24mer marker. **Lanes 3-6;** Untreated dermal fibroblasts at 0, 4, 8 and 24 hours respectively. **Lanes 9-11;** Dermal fibroblasts treated with 300 nM HOCl at 4, 8 and 24 hours post treatment respectively. **Lanes 14-16;** Dermal fibroblasts treated with 600 nM HOCl at 4, 8 and 24 hours post treatment respectively. **Lane 17;** 8-oxodG containing 24mer incubated at 37°C for 2 hours without cell lysate.

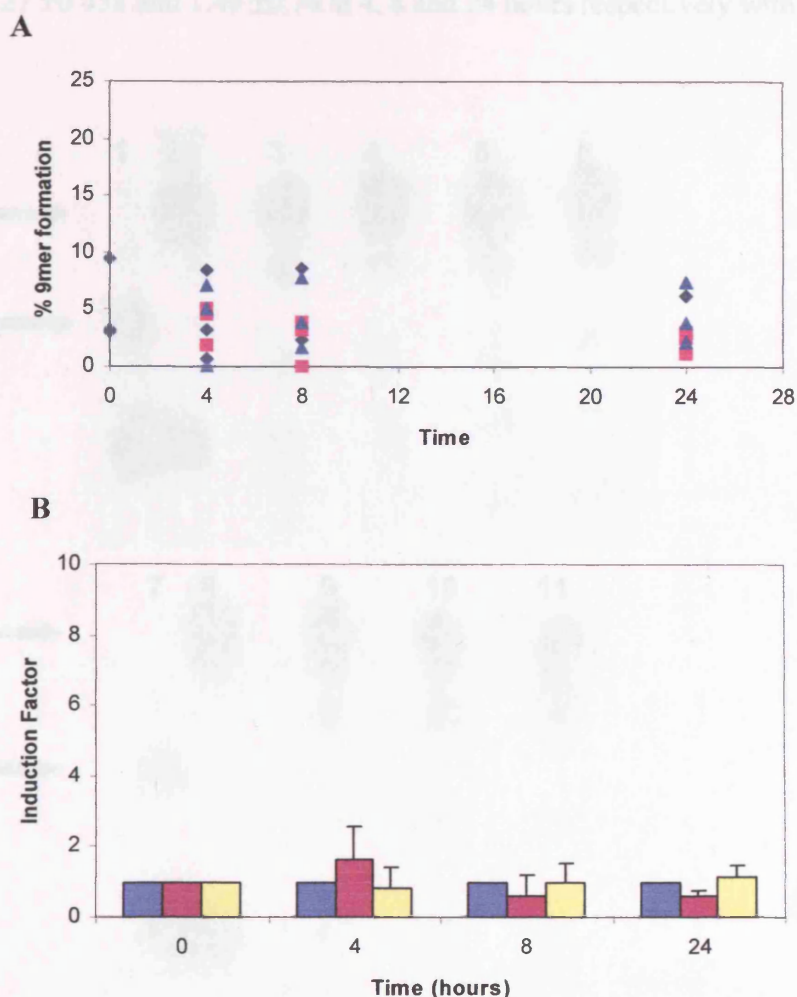


Figure 5.14: Effect of HOCl on repair activity in normal dermal fibroblasts. Cells were treated with 300 nM or 600 nM HOCl for 4-24 hours at 37°C. Cell lysates (50 µg) were collected at each timepoint and incubated with an [γ - 32 P] ATP labelled 8-oxoguanine containing double-stranded repair substrate for 2 hours. Denaturing gel electrophoresis separated cleaved repair products and non-cleaved oligonucleotide. The data represents (A) individual measurements of percentage 9mer formation at each timepoint after treatment with no agent (◆), 300 nM HOCl (■), and 600 nM HOCl (▲). (B) mean and standard deviation of percentage repair activity after treatment with no agent (■), 300 nM HOCl (■) and 600 nM HOCl (■) observed in three independent experiments.

Effects of vitamin C on repair activity are shown in **figure 5.15** and summarised in **figure 5.16**. Induction factors were calculated to be 2.18 ± 0.91 , 1.62 ± 0.99 and 1.29 ± 0.95 at 4, 8 and 24 hours respectively after treatment with 400 µM vitamin C and

2.45 ±1.19, 1.27 ±0.458 and 1.49 ±0.74 at 4, 8 and 24 hours respectively with 800 μM vitamin C.

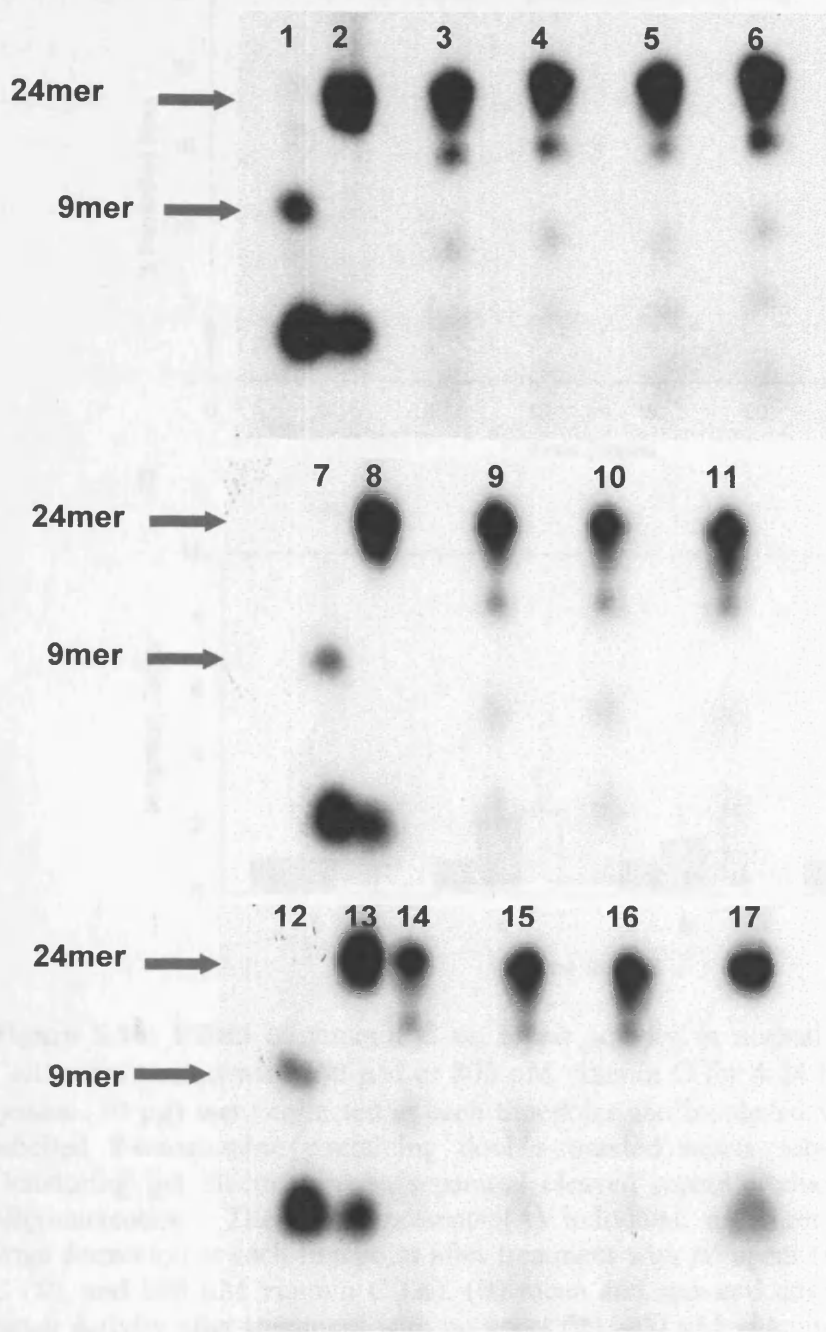


Figure 5.15: Endonuclease nicking activity of normal dermal fibroblast cell lysates following treatment with 400 μM and 800 μM vitamin C (using 50 μg protein in a 2 hour assay). **Lanes 1, 7 & 12;** 9mer marker. **Lanes 2, 8 & 13;** 8-oxodG 24mer marker. **Lanes 3-6;** Untreated dermal fibroblasts at 0, 4, 8 and 24 hours respectively. **Lanes 9-11;** Dermal fibroblasts treated with 400 μM vitamin C at 4, 8 and 24 hours post treatment respectively. **Lanes 14-16;** Dermal fibroblasts treated with 800 μM vitamin C at 4, 8 and 24 hours post treatment respectively. **Lane 17;** 8-oxodG containing 24mer incubated at 37°C for 2 hours without cell lysate.

Chapter 5: DNA repair activity in response to oxidative stress

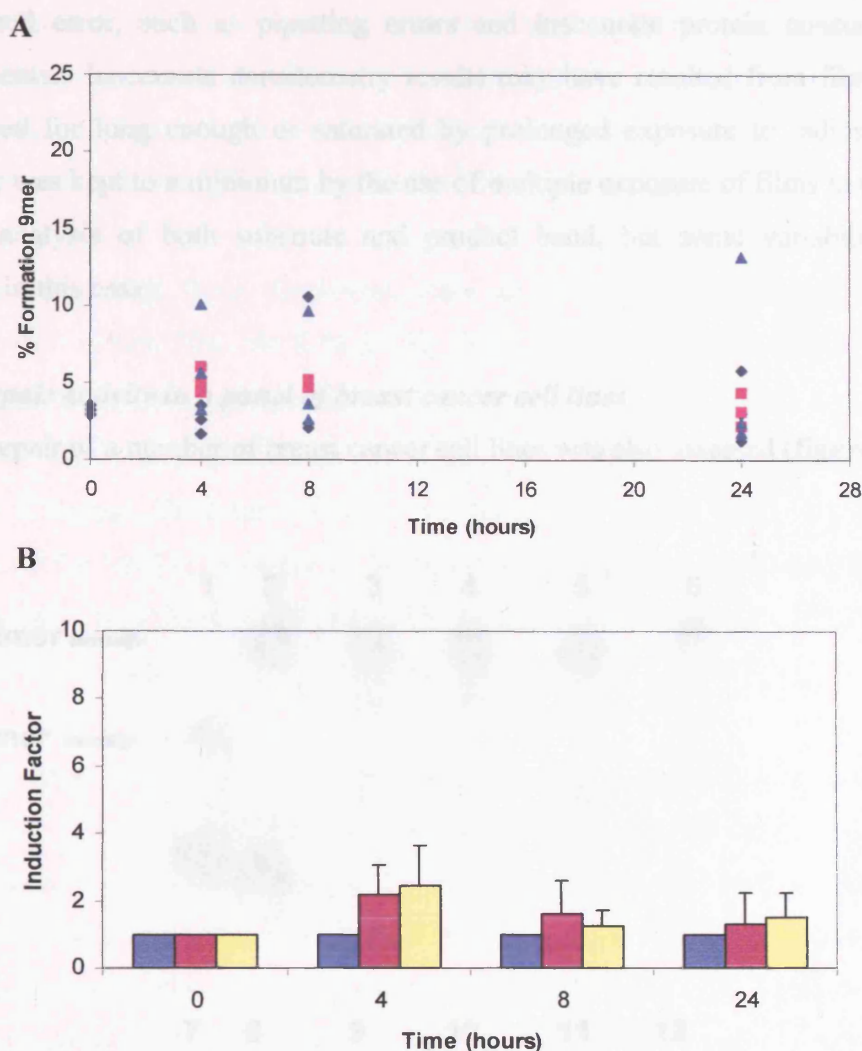


Figure 5.16: Effect of vitamin C on repair activity in normal dermal fibroblasts. Cells were treated with 400 μM or 800 μM vitamin C for 4-24 hours at 37°C. Cell lysates (50 μg) were collected at each timepoint and incubated with an [γ - ^{32}P] ATP labelled 8-oxoguanine containing double-stranded repair substrate for 2 hours. Denaturing gel electrophoresis separated cleaved repair products and non-cleaved oligonucleotide. The data represents (A) individual measurements of percentage 9mer formation at each timepoint after treatment with no agent (◆), 400 μM vitamin C (■), and 800 μM vitamin C (▲). (B) mean and standard deviation of percentage repair activity after treatment with no agent (■), 400 μM vitamin C (■) and 800 μM vitamin C (■) observed in three independent experiments.

Statistically significant changes in endonuclease nicking activity were not observed following treatment of dermal fibroblasts with either doses of vitamin C, although a slight trend for increased activity is noticeable in **figure 5.16 B**, with both 400 μM and 800 μM .

The few anomalous points in the results presented above were most likely to be due to experimental error, such as pipetting errors and inaccurate protein concentration measurements. Inaccurate densitometry results may have resulted from film either not exposed for long enough or saturated by prolonged exposure to radioactivity. Such error was kept to a minimum by the use of multiple exposure of films to provide sensitive analysis of both substrate and product band, but some variability was inevitable in this assay.

5.4.3 Repair activity in a panel of breast cancer cell lines

Baseline repair of a number of breast cancer cell lines was also assessed (figure 5.17).

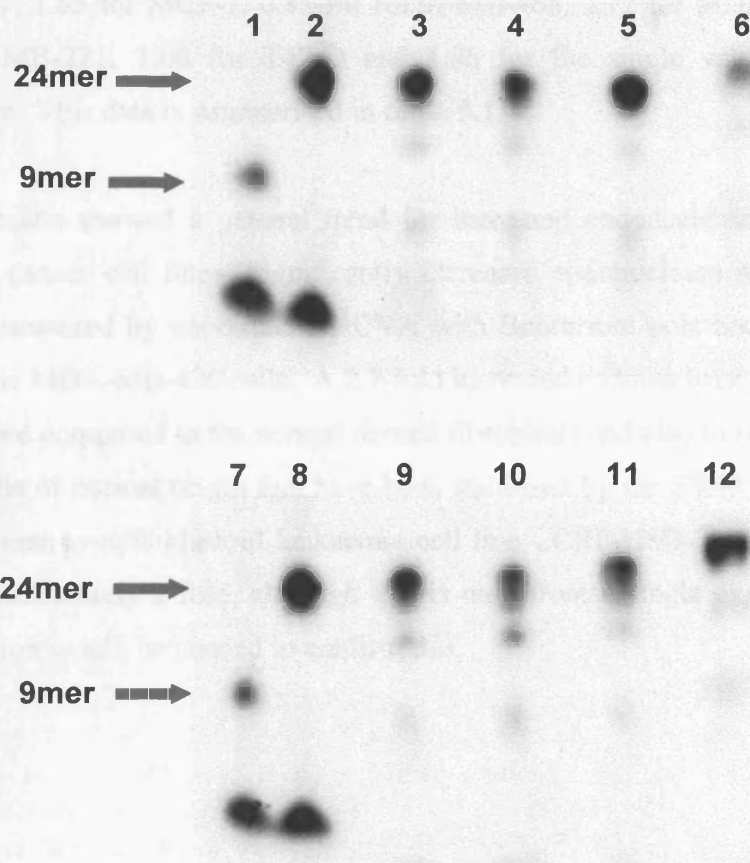


Figure 5.17: Endonuclease nicking activity of breast cancer cell lysates (using 50 μ g protein in a 2 hour assay). **Lanes 1 & 7;** 9mer marker. **Lanes 2 & 8;** 8-oxodG substrate. **Lane 3;** dermal fibroblast. **Lane 4;** HBL 100. **Lane 5;** ZR75.1. **Lane 6;** MCF-7. **Lane 9;** MDA-MB 468. **Lane 10;** MDA-MB 436. **Lane 11;** MDA-MB 231. **Lane 12;** T47-D.

Chapter 5: DNA repair activity in response to oxidative stress

The endonuclease nicking assay with breast cancer cell lines was performed in triplicate (**figure 5.18**). The same conditions were used as for the dermal fibroblasts. Dermal fibroblasts were included in the experiments in order to compare repair activities and to act as a level of comparison between cells of normal origin. HBL 100 are cells of normal origin that contain the SV40 virus genome.

Mean percentages of 9mer formation were as follows: NDF (normal dermal fibroblast) 5.57 ± 0.49 , HBL100 5.78 ± 0.76 , ZR75.1 7.28 ± 1.47 , MCF-7 9.17 ± 1.66 , MDA-MB-468 4.73 ± 0.64 , MDA-MB-436 15.13 ± 4.86 , MDA-MB-231 4.01 ± 2.61 , T47-D 6.00 ± 2.62 and CCRF-HSB-2 10.90. The relative induction factors, as compared to dermal fibroblast activity were therefore, 1.04 for HBL 100, 1.31 for ZR75.1, 1.65 for MCF-7, 0.85 for MDA-MB-468, 2.72 for MDA-MB-436, 0.72 for MDA-MB-231, 1.08 for T47-D and 1.96 for the single value of CCRF-HSB-2 activity. This data is summarised in **table 5.1**.

The results showed a general trend for increased endonuclease nicking activity in breast cancer cell lines. Significantly increased endonuclease nicking activity ($p < 0.05$, measured by univariate ANOVA with Bonferroni post hoc test) was observed with the MDA-MB-436 cells. A 2.7-fold increased endonuclease nicking activity was observed compared to the normal dermal fibroblasts and also to HBL 100 cells, which are cells of normal origin that have been stabilised by the SV40 virus. Interestingly, the human lymphoblastoid leukaemia cell line CCRF-HSB-2 also showed induction of approximately 2-fold, although this is only from a single experiment and further repetition would be needed to confirm this.

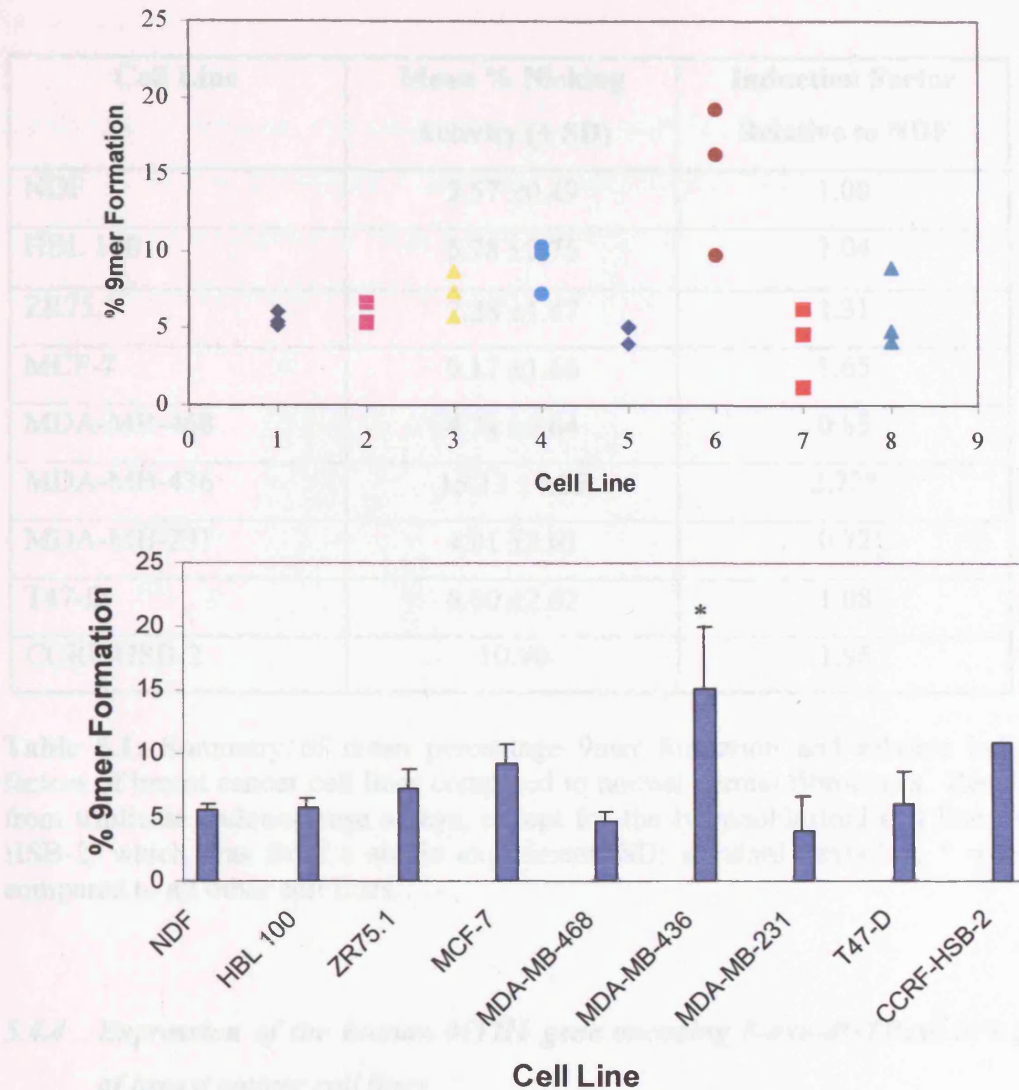


Figure 5.18: Baseline repair activity in a panel of 7 breast cancer cell lines was assessed using the endonuclease nicking assay. Cell lysates (50 μ g) were collected from proliferating cells and incubated with an [γ - 32 P] ATP labelled 8-oxoguanine containing double-stranded repair substrate for 2 hours. Denaturing gel electrophoresis separated cleaved repair products and non-cleaved oligonucleotide. The data represents (A) individual measurements of percentage 9mer formation for each cell line; normal dermal fibroblast (NDF) (\blacklozenge), HBL 100 (\blacksquare), ZR75.1 (\blacktriangle), MCF-7 (\bullet), MDA-MB 468(\blacklozenge), MDA-MB 436 (\bullet), MDA-MB 231 (\blacksquare) and T47-D (\blacktriangle). (B) Mean and standard deviation of percentage repair activity observed in three independent experiments with each breast cancer cell line and a single experiment with the lymphoblastoid cell line CCRF-HSB-2. * Significantly different to all except MCF-7 endonuclease repair activity ($p < 0.05$). Analysed using one-way ANOVA with Bonferroni post hoc analysis.

Cell Line	Mean % Nicking Activity (\pm SD)	Induction Factor Relative to NDF
NDF	5.57 \pm 0.49	1.00
HBL 100	5.78 \pm 0.76	1.04
ZR75.1	7.28 \pm 1.47	1.31
MCF-7	9.17 \pm 1.66	1.65
MDA-MB-468	4.74 \pm 0.64	0.85
MDA-MB-436	15.13 \pm 4.86	2.72*
MDA-MB-231	4.01 \pm 2.61	0.72
T47-D	6.00 \pm 2.62	1.08
CCRF-HSB-2	10.90	1.96

Table 5.1: Summary of mean percentage 9mer formation and relative induction factors of breast cancer cell lines compared to normal dermal fibroblasts. Results are from triplicate endonuclease assays, except for the lymphoblastoid cell line CCRF-HSB-2, which was from a single experiment. SD; standard deviation. * = $p < 0.05$ compared to all other cell lines.

5.4.4 Expression of the human MTH1 gene encoding 8-oxo-dGTPase in a panel of breast cancer cell lines

5.4.4.1 RT-PCR

RT-PCR was performed with cDNA prepared from mRNA extracted from each of the cell lines using oligo d(T) beads. Three separate RT-PCR reactions were set up for both MTH1 primers and the housekeeping gene, β -actin. Products were run on 3% (w/v) agarose gels and imaged under UV light. Representative RT-PCR gels are shown (**figure 5.19**).

Bands observed following RT-PCR with the hMTH1 primers were in agreement with the predicted product size of 273 bp (**figure 5.19**). hMTH1 bands were produced with

all cell lines, showing that mRNA expression of this enzyme is ubiquitous in these breast cancer cell lines.

Densitometry analysis was performed on gels captured by UVP VisionWorks 3.1 software using a β -Imaging Computing Densitometer. The band intensities for hMTH1 were normalised to those for β -actin and relative expression levels calculated by comparison to dermal fibroblast expression. Results are presented in **figure 5.20**.

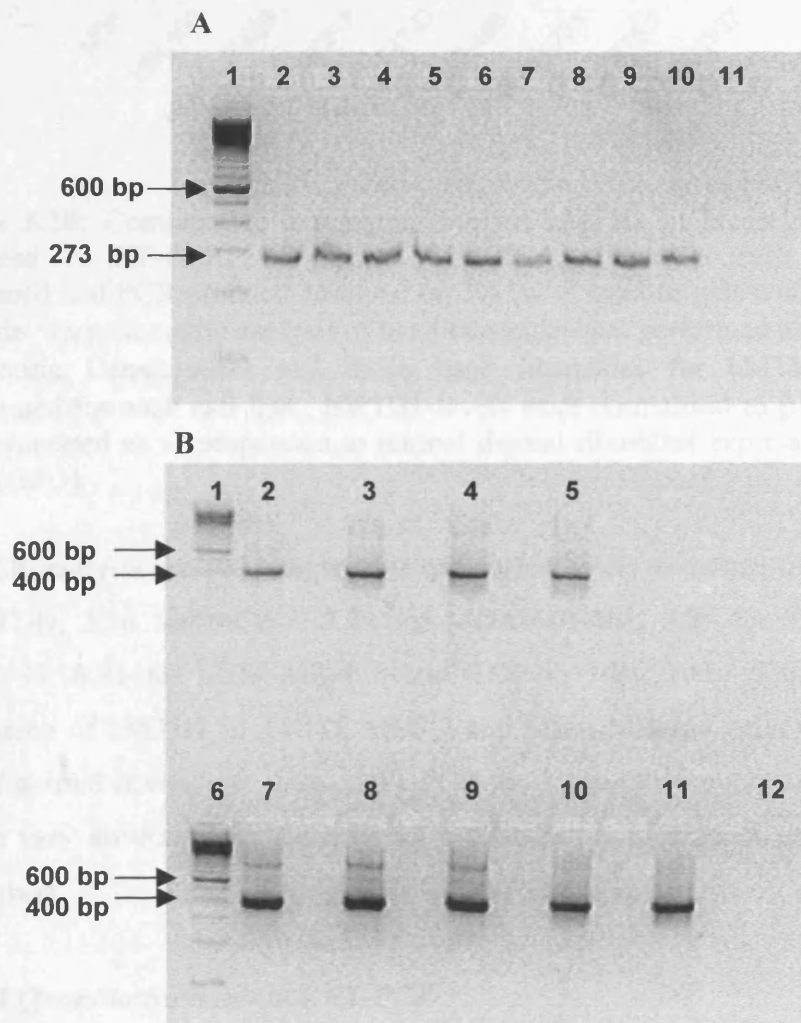


Figure 5.19: RT-PCR analysis of hMTH1 (A) and β -actin (B) in breast cancer cell lines. (A) Lane 1; 100 bp DNA ladder. Lanes 2-11; PCR products from T47-D, MCF-7, MDA-MB-468, MDA-MB-231, ZR75.1, HCC1937, MDA-MB-436, HBL 100, dermal fibroblast and water negative control respectively. (B) Lanes 1 & 6; 100 bp DNA ladder. Lanes 2-5; HCC1937, MDA-MB 436, HBL 100, T47-D. Lanes 7-12; ZR75.1, MCF-7, MDA-MB-468, MDA-MB-231, dermal fibroblast and water negative control respectively.

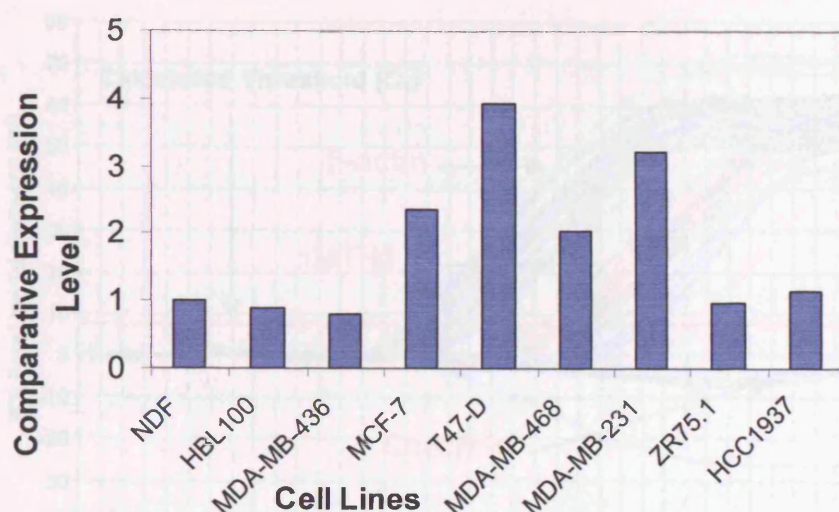


Figure 5.20: Comparative expression level of hMTH1 in breast cancer cell lines measured by RT-PCR. Triplicate RT-PCR reactions for each cell line were performed and PCR products resolved on 3% (w/v) agarose gels containing ethidium bromide. Densitometric analysis of band intensities was performed using a β -Imaging Computing Densitometer and mean band intensities for hMTH1 and β -actin determined for each cell line. hMTH1 levels were normalised to β -actin levels and then expressed as a comparison to normal dermal fibroblast expression. Values are means (n=3).

RT-PCR analysis showed comparative expression levels to dermal fibroblasts of 3.93 for T47-D, 2.36 for MCF-7, 3.23 for MDA-MB-468, 0.99 for ZR75.1, 1.14 for HCC1937, 0.81 for MDA-MB-436 and 0.88 for HBL 100. This suggested that expression of hMTH1 in T47-D, MCF-7 and MDA-MB-468 cells was greater than that of dermal fibroblasts. Use of RT-PCR for comparative expression analysis may not be very accurate because it is not a quantitative method of measuring mRNA expression.

5.4.4.2 Quantitative Real-time RT-PCR

Real-time RT-PCR provides a much more sensitive and quantitative approach to measuring the expression level of genes in a sample of cDNA. **Figure 5.21** shows the real-time RT-PCR formation of products against cycle number and **figure 5.22** shows the melt curve generated in order to investigate the formation of primer dimers.

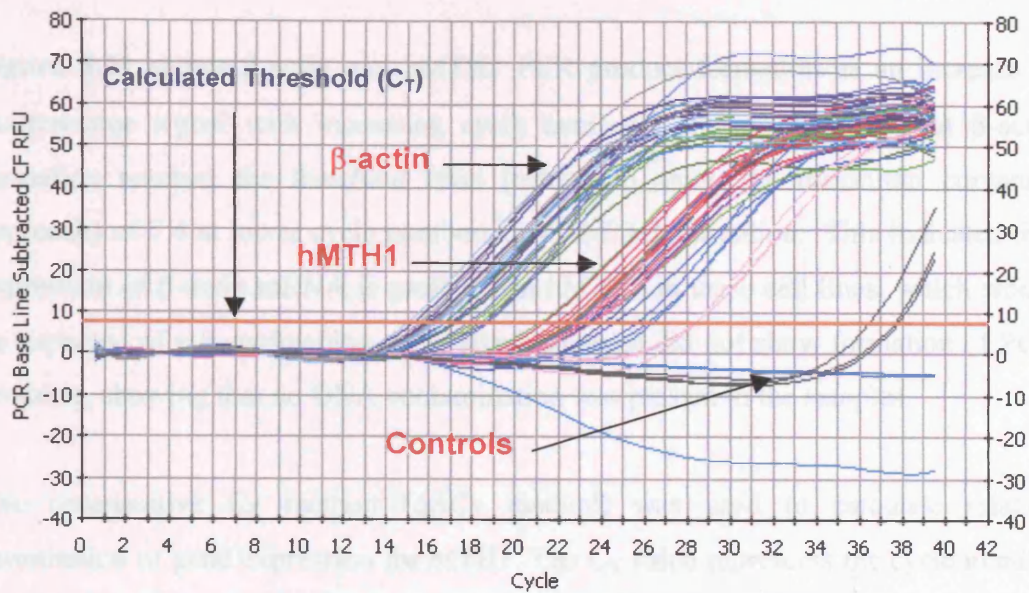


Figure 5.21: Quantitative real-time RT-PCR analysis of hMTH1 and β -actin mRNA expression in breast cancer cell lines. Reactions were set up in triplicate for both hMTH1 and β -actin using 5 pmol forward and reverse primers and cDNA as template. Mastermixes were used to limit errors of pipetting. Samples were subjected to 40 cycles of 95.0°C for 30 seconds, 60.0°C for 30 seconds and 72.0°C for 30 seconds, following initial denaturation at 95.0°C for 3 minutes to activate the hot-start enzyme, iTaq™ DNA polymerase. Data was collected by the iCycler iQ system (Bio-Rad Laboratories) and viewed in Microsoft Word. Arrows indicate formation of β -actin and hMTH1 PCR products with increasing cycle number and lack of formation of PCR products in control samples lacking cDNA.

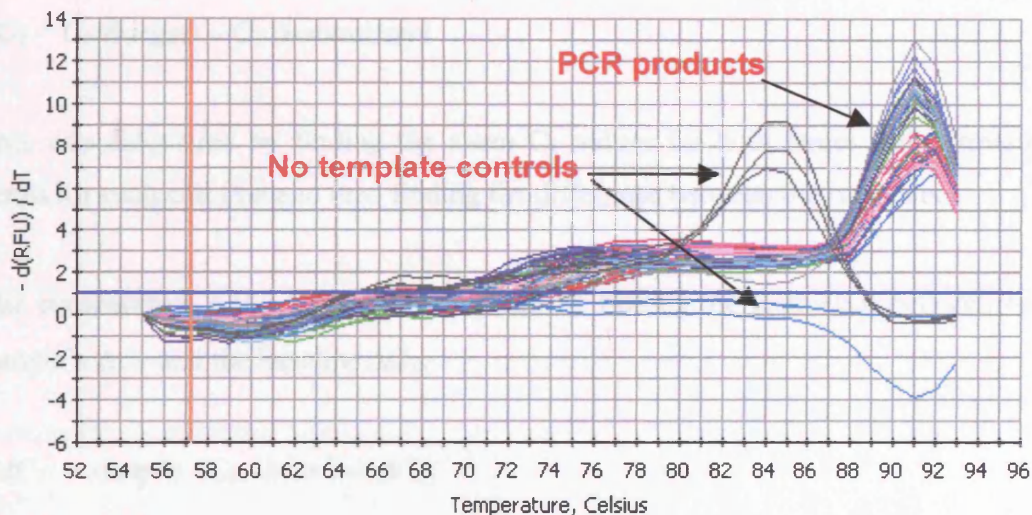


Figure 5.22: Melt curve generated from quantitative real-time RT-PCR analysis of MTH1 and β -actin mRNA expression in breast cancer cell lines. Analysis was performed on the same samples as in **figure 5.21**. Following RT-PCR, products were heated to 95.0°C to examine the existence of primer dimer formation. No primer dimer peak was detected.

Figure 5.21 shows β -actin and hMTH1 PCR product formation as an increase in fluorescence signal with increasing cycle number. It was observed that β -actin formation reached the threshold level (calculated using the maximum curvature approach) of 7.4 at lower cycle numbers than hMTH1 formation. This indicated that expression of β -actin mRNA is greater than hMTH1 in these cell lines, which would be expected of a housekeeping gene. Blank samples did not show formation of PCR products, showing that no DNA contamination was present in the samples.

The comparative C_T method ($\Delta\Delta C_T$ method) was used to calculate relative quantitation of gene expression for MTH1. The C_T value represents the cycle number at which formation of the PCR product in the sample reaches the calculated threshold of fluorescence signal. In this experiment the calculated threshold, as determined by the iCycler iQ system software, was 7.4. The level of this threshold was set above that of the baseline level in order to eliminate any baseline variation.

The calculations for the quantitation started with finding the difference (ΔC_T) between the C_T values of the target (MTH1) and the normalizer gene (β -actin).

$$\Delta C_T = C_T(\text{target}) - C_T(\text{normalizer})$$

This was calculated by finding the mean C_T values for both target and normalizer genes for each cell line and then finding the difference between the two values.

The comparative $\Delta\Delta C_T$ was then calculated by finding the difference between each sample's ΔC_T and the baseline ΔC_T .

$$\Delta\Delta C_T = \text{sample } \Delta C_T - \text{baseline } \Delta C_T$$

The dermal fibroblast ΔC_T was chosen as the reference (baseline) for each comparison to be made to. If the baseline was actually the minimum level of expression then the $\Delta\Delta C_T$ values would be negative, if expression is increased in some samples and

Chapter 5: DNA repair activity in response to oxidative stress

decreased in others then the $\Delta\Delta C_T$ values would be a mixture of negative and positive.

To transform the $\Delta\Delta C_T$ values to absolute values, the following formula was used:

$$\text{Comparative expression level} = 2^{-\Delta\Delta C_T}$$

The results are tabulated in **table 5.2**. The comparative expression levels presented in **table 5.2** are also presented graphically in **figure 5.23**.

Cell Line	Mean C_T MTH1	Mean C_T β -actin	ΔC_T	$\Delta\Delta C_T$	Comparative expression level
Dermal fibroblasts	26.03	18.33	7.70	0.00	1.00
HBL 100	23.33	15.63	7.70	0.00	1.00
MDA-MB-436	23.60	16.73	6.87	-0.83	1.78
MCF-7	22.53	15.87	6.67	-1.03	2.05
T47-D	22.57	16.70	5.87	-1.83	3.56
MDA-MB-468	22.13	15.90	6.23	-1.47	2.76
MDA-MB-231	23.33	17.20	6.13	-1.57	2.96
ZR75.1	23.17	17.67	5.50	-2.20	4.59
HCC1937	28.33	22.47	5.87	-1.83	3.56

Table 5.2: Calculations of comparative expression levels of MTH1 in breast cancer cell lines produced by quantitative real-time RT-PCR analysis. Reactions were performed in triplicate, using cDNA as template and subjected to 40 cycles on the iCycler iQ system. Calculated threshold (C_T) values for each PCR product were determined by the iCycler iQ system software. Mean C_T values were determined for MTH1 and β -actin in all cell lines and the relative gene expression of MTH1 was calculated using the comparative C_T method ($\Delta\Delta C_T$) as described in the text, using β -actin gene expression as a normalizer value. Dermal fibroblast MTH1 gene expression was taken as baseline and all other cell lines were compared to it.

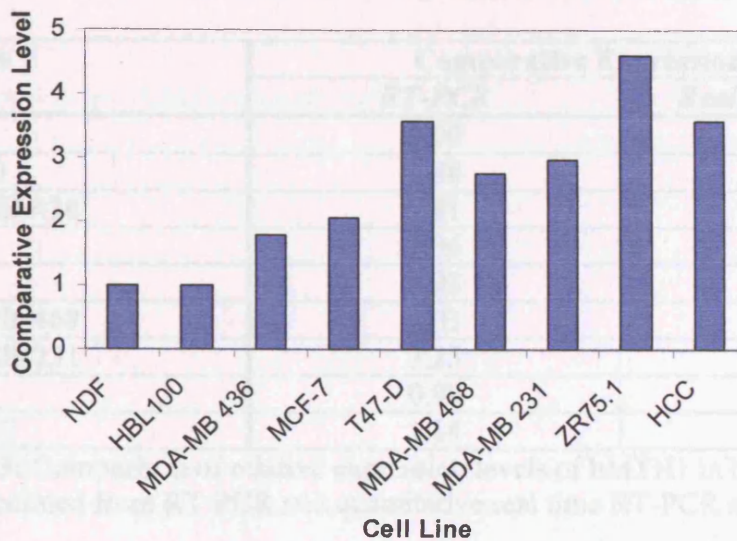


Figure 5.23: Comparative expression levels of MTH1 in breast cancer cell lines as measured by quantitative real-time RT-PCR analysis. Reactions were performed in triplicate, using cDNA as template and subjected to 40 cycles on the iCycler iQ system. Calculated threshold (C_T) values for each PCR product were determined by the iCycler iQ system software. Mean C_T values were determined for MTH1 and β -actin in all cell lines and the relative gene expression of MTH1 was calculated using the comparative C_T method ($\Delta\Delta C_T$) as described in the text, using β -actin gene expression as a normalizer value. Dermal fibroblast MTH1 gene expression was taken as baseline and all other cell lines were compared to it. Values are the result of one experiment.

The comparative analysis showed that all breast cancer cell lines except HBL 100, which is a cell line of normal origin that contains the SV40 virus genome, possessed higher expression levels of the MTH1 gene compared to dermal fibroblasts. HBL 100 cells were calculated to have the same expression level for hMTH1 as the dermal fibroblasts. Other cell lines were calculated as having expression levels of 1.78 (MDA-MB-436), 2.05 (MCF-7), 3.56 (T47-D), 2.76 (MDA-MB-468), 2.96 (MDA-MB-231), 4.59 (ZR75.1) and 3.56 (HCC1937).

The comparative expression levels calculated from the quantitative real-time RT-PCR analysis and those calculated from RT-PCR analysis are compared in **table 5.3**.

Cell Line	Comparative Expression Level	
	<i>RT-PCR</i>	<i>Real Time RT-PCR</i>
NDF	1.00	1.00
HBL 100	0.88	1.00
MDA-MB-436	0.81	1.78
MCF-7	2.36	2.05
T47-D	3.93	3.56
MDA-MB-468	2.03	2.76
MDA-MB-231	3.23	2.96
ZR75.1	0.99	4.59
HCC1937	1.14	3.56

Table 5.3: Comparison of relative expression levels of hMTH1 in breast cancer cell lines calculated from RT-PCR and quantitative real time RT-PCR analysis.

Table 5.3 showed that the two methods gave fairly comparative levels of hMTH1 mRNA expression in most of the breast cancer cell lines that were investigated. However, two of the cell lines in which expression levels were quite different between the two techniques were ZR75.1 and HCC1937, with expression levels as measured by RT-PCR of 0.99 and 1.14, respectively, and as measured by real time RT-PCR, 4.59 and 3.56, respectively. The MDA-MB-436 cell line also showed different expression levels between the two techniques, of 0.81 and 1.78 by RT-PCR and quantitative real time RT-PCR analysis, respectively. However, the difference between the two values is not as striking as for the other two cell lines. HCC1937 produced a band of low intensity for RT-PCR, perhaps making densitometric analysis more inaccurate. There was also lower expression of the housekeeping gene β -actin in the HCC1937 cells, suggesting that a smaller yield of mRNA was obtained from the cells.

Sequencing of RT-PCR product to check for specificity

Products produced from HBL 100 and ZR75.1 cDNA were purified of residual dNTP's and enzymes, and then sent to PNAFL (University of Leicester) for sequencing using ABI BigDye terminator sequencing chemistry. Unincorporated dye terminators were removed by DyeEx columns and the resulting products analysed on an ABI 377 Sequencer. Sequencing chromatograms are reproduced in **Appendix III**.

Chapter 5: DNA repair activity in response to oxidative stress

The sense and anti-sense sequence of the PCR products were checked against the gene sequence for MTH1 using BLAST 2.2.6 software and found to be 100% homologous to the published gene sequences.

5.5 DISCUSSION

The aim of this chapter was to establish whether changes in levels of cellular oxidative stress can modulate responses to increased DNA damage produced by such an oxidative challenge. The response was assessed at both functional repair level and also by measurement of gene expression of an enzyme known to prevent incorporation of damaged bases into DNA.

The repair activity of dermal fibroblasts, before and after exposure to ROS and the antioxidant vitamin C, was measured using an endonuclease nicking assay. Repair activities were also assessed in a number of breast cancer cell lines, as it has been stated that levels of oxidative damage may increase in breast cancer. The use of the DNA repair enzyme hMTH1 (human MutT homologue) as a potential biomarker of oxidative stress has been suggested due to reports of its enhanced expression in a number of cancers. Expression of this gene at mRNA level was assessed in breast cancer cell lines. Any alteration in expression would provide evidence for a possible adaptive response of cells exposed to cellular oxidative stress resulting from increased cellular proliferation and other sources of ROS.

An endonuclease nicking assay was established to measure repair activity and expression of hMTH1 at mRNA level was assessed in a number of cell lines using PCR techniques. The findings from these experiments are discussed below.

5.5.1 Endonuclease nicking activity in response to oxidative stress in dermal fibroblasts

The ability of whole cell extracts to detect and excise an 8-oxodG-containing oligonucleotide was used to assess changes in repair activity following treatment of dermal fibroblasts with the following agents; H₂O₂, UVB, HOCl and vitamin C.

The endonuclease nicking assay measured the ability of cellular lysates to perform 8-oxoG glycosylase/AP lyase activities on an 8-oxodG-containing 24mer oligonucleotide. Chung *et al.*, (1991) first used such an approach in order to establish the presence of an enzyme in *E.coli* that specifically removed 8-oxoG from 8-oxoG:C pairs in double-stranded DNA. This enzyme was later identified as Fpg. Yamamoto

Chapter 5: DNA repair activity in response to oxidative stress

et al., (1992) established the ubiquitous presence of such endonuclease activity in mammalian cells.

The 8-oxoG-containing 24mer oligonucleotide was firstly end-labelled with [γ - ^{32}P]-ATP and then annealed to a complementary oligonucleotide to form a double-stranded substrate. The DNA glycosylase OGG1, and the AP endonuclease, APE, present in mammalian cells, will only recognise and act upon damaged sites in double-stranded DNA. Once the 8-oxoG site was recognised, the glycosylase catalysed hydrolytic cleavage of the N-glycosyl bond linking the base to the sugar, if the glycosylase also possessed lyase activity (hOGG1 does) then the backbone may be cleaved 5' to the damaged site. Alternatively lyase activity may be performed by the AP endonuclease (e.g. hAPE), which would generate a single nucleotide gap.

Upon exposure to denaturing conditions, the double-stranded structure was disrupted, releasing an end-labelled 9 base pair fragment from any substrates that have been 'nicked' and intact end-labelled 24 base pair oligonucleotides from substrate that has not been acted upon by the repair enzymes. Subsequent separation of the 24mer and 9mer end-labelled oligonucleotides by denaturing polyacrylamide gel electrophoresis and detection by autoradiography allowed the formation of 9mer product to be detected. Calculation of the amount of 9mer produced as a percentage of total product and substrate highlighted any changes in endonuclease nicking activity between samples; samples possessing a higher activity formed a higher percentage of product.

Optimal conditions for measurement of endonuclease activity were established. Incubation of the damaged oligonucleotide with purified Fpg protein from *E.coli* showed a concentration dependent increase in nicking activity. Further experiments established that using an incubation time of 2 hours at 37°C with 50 μg total cellular protein was sufficient for 9mer formation and detection, without saturation of the amount of substrate. An undamaged oligonucleotide of the same sequence as the 8-oxoG-containing 24mer was used to show that nicking activity was specific to the damaged site and so product formation was relative to repair activity. As an additional control, 8-oxoG-containing oligonucleotide was incubated without cell

Chapter 5: DNA repair activity in response to oxidative stress

lysate in all experiments to show that 9mer formation was not produced by degradation of the 24mer during the oligonucleotide reaction and subsequent sample handling. The appearance of the repair product with a slightly different size than the 9mer marker may have been due to the position of excision of the 8-oxoG species.

Experiments with dermal fibroblasts exposed to the ROS and ROS generators H₂O₂, HOCl and UVB over a 24 hour time period showed little change in endonuclease nicking activity. Results published in the literature show a 2.6-fold increased repair activity measured in human lung alveolar epithelial cells exposed to the lung carcinogen crocidolite asbestos at 18 hours post treatment (Kim *et al.*, 2001). Yamaguchi *et al.*, (1996) observed a similar 3-fold increased repair activity in rat kidney following administration of the renal carcinogen ferric nitrilotriacetate. You *et al.*, (2000) reported a modest 2-fold increase in activity in ischemic-reperfused hearts of rats. However, in contrast, Tsurudome *et al.*, (1999) observed a 25% decrease in repair activity in rat lungs exposed to diesel exhaust particles over a time course of 2 hours to 2 days following exposure.

A number of different approaches have also measured changes in repair activity following exposure of cells to oxidising agents; Ramana *et al.*, (1998) reported an approximate 2-fold induction of endonuclease activity in a single experiment following exposure of HeLa cells to 130 nM HOCl. They used a 43mer duplex oligonucleotide containing a tetrahydrofuran residue at position 31. Grösch *et al.*, (1998) used a radiolabelled double-stranded 35mer oligonucleotide which contained uracil at a defined position in the sequence. The uracil was removed from the oligonucleotide with uracil DNA glycosylase (UDG), to generate a single AP site in the duplex before incubation with protein extracted from cells treated with 300 µM H₂O₂. Results showed a slightly increased rate of product formation with treated cell extract than control, but there was no evidence of repeat experiments. In an attempt to repeat the studies of Ramana *et al.*, (1998), Hsieh *et al.*, (2001) reported no increase in APE endonuclease activity. A very small increase in APE redox activity in combination with PKC activity was observed though, leading to the suggestion that APE may be regulated by phosphorylation.

Chapter 5: DNA repair activity in response to oxidative stress

It could be that the DNA sequence surrounding the damaged site has an impact on DNA repair efficiency. Hirano *et al.*, (2001) investigated the effect of 6 different sequences of 8-oxoG-containing oligonucleotides on the rate of repair. They observed up to 10-fold differences in repair activity between the different substrates when incubated with crude extracts of rat liver and kidney, suggesting that repair systems may act with sequence specificity on damaged DNA. If this was so then it could be that the sequence used in this study does not attract as much repair activity as sequences used in other investigations, and so is not subject to as much regulation. The lack of modulation of repair activity observed in the dermal fibroblasts may also have been due to the cell-type being studied. Cappelli *et al.*, (2000) report that 8-oxoG is poorly repaired in human fibroblasts compared to uracil and AP sites.

Little has been reported in the literature of the effects of antioxidants, such as vitamin C, on endonuclease nicking activity. The results presented in this thesis suggest a slight trend for increased endonuclease nicking activity following treatment with vitamin C, most noticeably at 4 hours post treatment. A possible correlation with the decrease in Fpg-sensitive sites (i.e. oxidative damage) observed with the alkaline unwinding assay (chapter 3), would indicate that vitamin C may act to induce BER activity, and thus reduce the number of Fpg-sensitive sites present in DNA. Despite the lack of a statistically significant change in endonuclease nicking activity, this would be a good area for further investigations into the role of antioxidants in DNA repair mechanisms.

Together with the results from chapter 4, this data suggested that repair was not modulated by increased oxidative stress in dermal fibroblasts. This could be due to the fact that repair in this system was already at its maximal level as cells may already have been experiencing significant levels of oxidative stress. Repair may have been modulated in response to cell culture conditions. Cells in culture are exposed to approximately 21% oxygen; whereas the actual concentration that cells are exposed to *in vivo* is calculated to be around 6%. The use of incubators with low oxygen content are being investigated and may provide interesting answers to modulation of repair activity dependent upon oxygen tension.

Chapter 5: DNA repair activity in response to oxidative stress

As discussed in the previous chapter, increasing repair activity may not be advantageous in these cells. If upregulated unevenly then the balance of repair may be disturbed and more dangerous damage i.e. strand breaks, could be induced. This would be possible in a situation where strand breaks were not subject to efficient DNA synthesis and ligation, as performed by DNA polymerases and DNA ligases (Kaina *et al.*, 1993; Cerda *et al.*, 1998).

Only modest induction of repair activity is reported in the literature (maximum is 3-fold) and many of the studies reporting modulation of repair activity have been performed with *in vivo* animal studies. Such different approaches are likely to have different findings compared to investigations with *in vitro* mammalian cells. Direct comparisons can therefore not effectively be made, only used as suggestions of possible DNA repair regulation.

5.5.2 Endonuclease nicking activity in breast cancer cell lines

The endonuclease nicking assay was also used to compare the baseline repair activities of 7 human breast tumour cell lines with control cell lines, in order to determine whether repair of oxidative damage to DNA may be altered in breast cancer. Any changes could be as a result of the pathological condition or as a causative factor in disease progression.

The results indicated that MDA-MB-436 breast cancer cell lines possessed a significant 2.7-fold increased repair activity compared to that of the dermal fibroblasts used as a control. Repair activities in the other breast cancer cell lines, although elevated in MCF-7 cells (which possess low metastatic potential), were not significantly different to that of the dermal fibroblasts. Interestingly, similar repair activities to the dermal fibroblasts were measured in the HBL 100 cell line. These cells are of normal origin but have been immortalised by the introduction of the SV40 viral genome. The MDA-MB-468 and MDA-MB-231 cells, derived from high-grade breast tumours with high metastatic potential, showed a trend for repair activities similar, if not decreased to those of the control cells.

Mambo *et al.*, (2002) investigated the repair of 8-oxoG and thymine glycol (Tg)-containing oligonucleotides in two different breast cancer cell lines, MCF-7 and

Chapter 5: DNA repair activity in response to oxidative stress

MDA-MB-468. Their aim was to investigate the role that oxidative DNA damage may play in breast cancer, following reports that 8-oxoG levels are increased in breast cancer tissue compared to normal surrounding tissue (Malins & Haimanot, 1991). They found a slightly lower 8-oxoG incision rate in MCF-7 cells compared to MDA-MB-468 cells with a lower mitochondrial repair activity in cancer cells compared to their control non-cancer lymphoblastoid cell line CRL 2337 and normal human mammary epithelial cells, AG11134. In this thesis, total cellular MCF-7 repair activity was found to be slightly elevated compared to control cells. It would have been interesting to measure nuclear and mitochondrial repair activity separately in this study to see if there was any correlation with metastatic potential of the cell types and mitochondrial repair activity.

Cerda *et al.*, (1998) investigated the expression of N-methylpurine-DNA glycosylase (MPG) in breast cancer. This protein primarily removes N-alkylpurine damage resulting from alkylating attack by methylating agents but is also capable of acting upon 8-oxoG (Bessho, *et al.*, 1993) and hypoxanthine (Saparbaev & Laval, 1994). MPG mRNA was found to be enhanced by up to 24-fold in breast cancer tumour cells compared to normal surrounding tissue and by 2-fold, 5-fold and 7-fold in MDA-MB-231, MCF-7 and T47-D breast cancer cell lines investigated using Northern blotting. Protein levels were also increased 3-fold and 6-fold in T47-D and MCF-7 cells respectively. Activity against an ethenoadenine-containing oligonucleotide was found to be 4.5-fold increased in T47-D and MCF-7 cells compared to MDA-MB-231 and MCF10A (an immortalised, non-transformed breast epithelial cell line). They suggest that this was either due to overexpression of this gene contributing to breast cancer development through imbalanced repair, or that elevated repair may be utilised as a protective mechanism by breast cancer cells in response to elevated levels of DNA adducts found in breast cancer tissue (Malins & Haimanot, 1991).

Kondo *et al.*, (2000) found increased hOGG1 expression and 8-oxoG specific endonuclease activity in response to increased 8-oxodG levels in human colorectal carcinoma tissue. Their findings that 8-oxodG levels did not differ between early and advanced stage cancers together with the fact that hOGG1 expression and activity increased with clinical stage of colorectal carcinoma suggests that carcinoma cells adjust to levels of oxidative stress by modulating their repair activity. The results in

this study may provide evidence that some breast cancer cell lines may also react in this way.

5.5.3 Expression of hMTH1 in breast cancer cell lines

Expression of the nucleotide pool sanitiser, hMTH1, was measured in a range of human breast cancer cell lines using RT-PCR and quantitative real time RT-PCR, in an attempt to discover whether regulation of this gene was altered in cancer cells. hMTH1 mRNA was found to be expressed in all of the cell lines tested.

Both RT-PCR and quantitative real time RT-PCR suggested that expression of the hMTH1 gene was increased in a number of breast cancer cell lines when compared to that of expression in dermal fibroblasts. The RT-PCR technique, which is not as sensitive or quantitative as real time RT-PCR, showed 2.0, 2.4, 3.2 and 3.9-fold increased expression of hMTH1 mRNA in MDA-MB-468, MCF-7, MDA-MB-231 and T47-D cells respectively. Quantitative real time RT-PCR analysis, which offered a much more sensitive method of detection, showed enhanced hMTH1 mRNA expression in all of the breast cancer cell lines. The relative expression of the SV40 immortalised HBL 100 cell lines was identical to that of the dermal fibroblasts, suggesting that increased hMTH1 expression may be due to the transformations undergone in the other cells to make them cancerous.

The smallest induction of hMTH1 measured in the breast cancer cell lines was 1.8-fold in the MDA-MB-436 cells. Interestingly this is the one cell line that showed significantly enhanced nicking activity in the endonuclease nicking assay discussed previously. One conclusion which could be drawn from this would be the possibility that the increased 8-oxoG repair potential of these cells may mean that enhanced expression of hMTH1 is not necessary to limit the effects of 8-oxoG damage. This would agree with the results of Kennedy *et al.*, (1998) who showed an inverse linear correlation between the amount of 8-oxodG in DNA of lung cancer cell lines and their expression of hMTH1 mRNA. These results may imply that upregulation of the hMTH1 gene protects the integrity of the cancer cell DNA by preventing misincorporation of 8-oxodGTP into DNA, thereby reducing the detectable level of 8-oxodG. The results of Okamoto *et al.*, (1994, 1996) also agree with this theory. They

found that hMTH1 mRNA expression increased with clinical stage of renal cell carcinoma whilst 8-oxodG levels remained constant.

It would be interesting to measure the levels of 8-oxodG in the breast cancer cell lines that have been used in this study, especially as significantly elevated levels of 8-oxodG have been measured in carcinomas of the breast (Malins & Haimanot, 1991) and elevated DNA damage has been associated with increased breast cancer risk (Smith *et al.*, 2003). This would establish whether there is an inverse relationship between the levels of 8-oxodG and hMTH1 expression in breast cancer cell lines. Measurement of hMTH1 protein levels and 8-oxodGTP hydrolysis would also show whether mRNA expression level of hMTH1 is related to functional protein level.

Changes in the endonuclease nicking activity in breast cancer cells provides further evidence for an adaptive response to increased oxidative stress caused by increased cellular proliferation in cancer cells. Data from this and other studies suggest that the transformations that make a cell cancerous induce it to proliferate rapidly, generating greater levels of endogenous ROS as a by-product of increased aerobic metabolism. This increase in ROS levels will produce more oxidative DNA damage and DNA repair and so expression of factors that limit the effects of such damaging species will be modulated accordingly. Further work is needed to confirm such a mechanism, but if this theory is true then measurements of oxidative DNA damage and expression of factors subject to regulation may provide future biomarkers for the progression and aggressiveness of cancers and also possibly highlight potential gene targets for chemoprevention.

5.5 CONCLUSIONS

This chapter investigated responses to changes in oxidative stress in dermal fibroblasts and a panel of breast cancer cell lines. The major conclusions to be drawn from this section were:

- The endonuclease nicking activity of dermal fibroblasts and breast cancer cell lines could be detected using a radiolabelled 24mer oligonucleotide containing 8-oxoG.
- Dermal fibroblast endonuclease nicking activity was not modulated by exposure to different concentrations of the ROS and ROS generators H₂O₂, HOCl and UVB, which were shown to induce oxidative DNA damage (chapter 3).
- A slight trend for increased endonuclease nicking activity was observed following exposure of dermal fibroblasts to the antioxidant vitamin C, which was previously shown to decrease oxidative DNA damage (chapter 3). A possible role for vitamin C in upregulation of BER requires further investigation.
- Significantly increased endonuclease nicking activity was detected in the MDA-MB-436 breast cancer cell line compared to dermal fibroblasts, but not in the other breast cancer cell lines investigated.
- Semi-quantitative RT-PCR analysis showed expression of the nucleotide pool sanitiser, hMTH1, in all of the breast cancer cell lines under investigation and suggested that expression in MDA-MB-468, MCF-7, MDA-MB-231 and T47-D cell lines may be enhanced compared to dermal fibroblasts and the immortalised HBL 100 cell line.
- Sensitive quantitative real time RT-PCR analysis suggested an increased expression of hMTH1 mRNA in all breast cancer cell lines investigated but further work is needed to confirm this.

Chapter 5: DNA repair activity in response to oxidative stress

- Enhanced endonuclease nicking activity in MDA-MB-436 cells corresponded to relatively low expression of hMTH1 mRNA in these breast cancer cell lines compared to the others under investigation. This may suggest that modulation of hMTH1 expression is regulated depending on the repair capability of cells, or vice versa. Further work is needed to confirm this.

CHAPTER SIX

General Discussion and Future Work

CHAPTER 6: GENERAL DISCUSSION AND FUTURE WORK

6.1 GENERAL DISCUSSION

The focus of this thesis was to study the effects of changes in cellular oxidative stress on the regulation of DNA repair mechanisms. An *in vitro* model system was established in cultured human fibroblasts to allow measurement of gene and protein modulation, together with repair activity, following treatment with ROS, ROS generators and also an antioxidant. Further work centred on possible molecular changes in breast tumour cells in response to oxidative stress generated during the process of carcinogenesis. The intrinsic repair of the oxidative lesion 8-oxoG and mRNA expression of the nucleotide pool sanitiser *hMTH1* were measured in order to establish whether increased oxidative stress in cancer cells results in adaptive responses.

6.1.1 *Establishing an in vitro model to study oxidative stress*

Initial experiments involved determining a suitable *in vitro* model for studies of gene and protein modulation in response to oxidative stress. Human dermal fibroblasts obtained from mammary reduction and primary lymphocytes obtained from separation of peripheral blood were investigated for their suitability to be used in studies presented in this thesis.

The primary lymphocytes were obtained in a much lower yield than the dermal fibroblasts and without mitogenic stimulation were not maintained in culture for long periods of time. For the number of cells required for this study, multiple batches of lymphocytes would have been needed. Obtaining primary lymphocytes requires invasive methods, and if the same individual is not available then interpatient variations may affect experimental results. The dermal fibroblasts were obtained from one patient and easy to maintain in culture. Excess fibroblasts were stored in liquid nitrogen, ensuring that sufficient cells for all of the planned studies were available. Interpatient variations were therefore avoided. Storage of fibroblasts also allowed cells of similar passage to be used for all investigations. This was important as cells may undergo selective adaptation for molecular changes that give them advantageous cellular growth in the artificial cell culture conditions. The fibroblasts

also produced greater yields of RNA, which was an important factor for investigations into gene regulation via measurement of mRNA transcript levels.

The three oxidising agents, H₂O₂, HOCl and UVB, were chosen because of their physiological relevance. Each is known to induce cellular oxidative DNA damage (Epe, 1995; Kawanishi *et al.*, 2001). It was important to determine concentrations or doses of these agents that would induce oxidative stress and/or DNA damage whilst also not resulting in high levels of cytotoxicity. Doses were also kept within ranges that may be encountered *in vivo* during exposure to an oxidative insult, in order to mimic the DNA damage response as near to *in vivo* conditions as possible. Many of the studies reporting regulation of repair pathways in response to UV irradiation use the physiologically irrelevant UVC wavelength (254 nm) (Hwang *et al.*, 1999; Fitch *et al.*, 2003) and many do not state exactly which wavelengths of UV irradiation are being used (Adimoolam & Ford, 2002). In this study care was taken to use the physiologically relevant UVB wavelength (290-320 nm).

The treatments produced little decrease in cellular viability but were shown to induce structural changes in DNA as measured by the induction of specific oxidative lesions sensitive to the bacterial Fpg protein and also by induction of single- and double-strand breaks in DNA. Vitamin C was shown to decrease the number of Fpg-sensitive sites present in cellular DNA.

6.1.2 Modulation of BER and NER in response to oxidative stress

The use of a ribonuclease protection assay allowed the simultaneous measurement of multiple gene transcripts in a single sample, thus limiting intersample variations. The multi-probe sets chosen, allowed regulation of both BER and NER pathways to be studied as a whole system, rather than just concentrating on single repair factors.

In the studies performed in this thesis, a significant decrease in *hOGG1* transcript level was observed following oxidative stress induced by UVB irradiation at 8 hours post treatment. By 24 hours post treatment, transcript levels had returned to baseline level. Other statistically significant changes in transcript level were measured in *ENTG* (more commonly *hNTH1*), *MGMT*, *RPA4*, *TDG* and *hHR23B* following UVB irradiation; *DDB1* following vitamin C treatment; *XPB* following H₂O₂ treatment and

RPA14 following treatment with HOCl. However, these very small, though statistically significant changes, were not thought to be biologically relevant.

A number of important BER and NER factors, in addition to hOGG1, were chosen to study at protein level, as any adaptive response may be mediated via translational mechanisms rather than transcriptional regulation. Immunodetection of the BER factors hAPE and hOGG1 did not show any significant modulation of protein levels. Similarly, the NER factors hHR23B and XPA, which are important at the early stages of NER, did not show any regulation at protein level in response to the treatments of H₂O₂, HOCl, UVB or vitamin C over the chosen time period.

Establishment of the endonuclease nicking assay allowed 8-oxoG excision to be measured. The use of purified Fpg protein demonstrated that increased incision activity was measurable by this method. Repair activity, which could be subject to posttranslational regulation independent of mRNA and protein levels, did not show any statistically significant modulation following treatment with any of the agents, although a slight trend for increased repair activity was produced following vitamin C treatment. Combined with the decrease in Fpg-sensitive sites present in DNA following vitamin C treatment, this may establish a possible area for future investigation.

The results presented here thus provide evidence for a lack of significant modulation of BER and NER following oxidative stress in human dermal fibroblasts. Other studies have also reported a lack of repair modulation in response to oxidative stress generated by agents such as H₂O₂ in myeloid leukaemia cells (Hsieh *et al.*, 2001) and rat lung cells (Fung *et al.*, 1998) and HOCl in HeLa cells (Saitoh *et al.*, 2001). Evidence presented to the contrary in CHO cells (Grösch *et al.*, 1998), HeLa cells and lung fibroblasts (Ramana *et al.*, 1998), rat tissue (Tsurudome *et al.*, 1999; Rusyn *et al.*, 2000) and epithelial (A549) cells (Kim *et al.*, 2001) highlights the complexity of studying such responses. Modulation of repair responses may be cell type dependent and cell cycle dependent. This highlights the importance of exact regulation of experimental conditions.

The work in this thesis was designed to follow on from published reports detailing an adaptive response to oxidative damage generated by agents such as H₂O₂ and HOCl in cultured human cells (e.g. Ramana *et al.*, 1998; Saitoh *et al.*, 2001). As discussed in previous chapters, such studies were performed in different cell types and mainly with different concentrations of treatment. Additionally, cell confluence is not reported for all studies. It is therefore difficult to make direct comparisons but in the model used in this thesis, any adaptive response to these treatments is not co-ordinated through transcriptional or translational modulation of BER or NER pathways. It is also plausible that initial reports may have been misleading; the lack of supportive reports in recent years indicates that such findings are not as inherently produced as it was first imagined. Recently, studies investigating the DNA repair response have centred on the phosphorylation of repair factors (Hsieh *et al.*, 2001) and translocation to sites of DNA damage (Balajee *et al.*, 1998; Frossi *et al.*, 2002; Kamiuchi *et al.*, 2002; Fitch *et al.*, 2003; Wang *et al.*, 2003).

Cell type and cell cycle effects may be important in the regulation of DNA repair genes in response to oxidative stress. Gifford *et al.*, (2000) showed that in *E.coli* progressing from log-phase growth to stationary phase, transcript levels of the *fpg*, *mutY*, *nei* and *nth* glycosylase genes were decreased. The same four genes were increased after cells were shifted from anaerobic to aerobic growth. This data, although in *E.coli*, suggests not only that cell growth stage may be important in expression of repair genes but also that such genes may be induced in response to oxidative stress generated by the presence of oxygen. This lends further weight to the idea that cells in culture may already be exposed to higher levels of oxygen than experienced *in vivo* and have already maximally adapted gene expression of proteins involved in limiting the effects of oxidative stress.

Reasons for a lack of any adaptive response may also be explained if baseline repair is sufficient to deal with the damage being induced, as is suggested for *S.cerevisiae* (Birrell *et al.*, 2002). It may also be the case that other systems, such as the antioxidant responsive element are able to deal with any temporarily increased oxidative insults.

The lack of modulation of excision repair in response to increased oxidative stress may also be a protective mechanism. Cells overexpressing the *MPG* gene (a DNA glycosylase which acts upon alkylated purine bases) were found to exhibit increased chromosomal damage and gene mutations (Kaina *et al.*, 1993), suggesting that if downstream repair factors such as apurinic endonucleases are not also modulated, an imbalance in the repair machinery may result, leading to an increased number of apurinic sites and strand breaks and ultimately resulting in genomic instability (Cerdeira *et al.*, 1998).

One thing that was not investigated in these studies was the effect of cellular proliferation on these DNA repair pathways. It is well known that DNA repair is linked to cell cycle regulation. In fact hNEIL1 has been shown to be strongly dependent upon the S phase of the cell cycle (Hazra *et al.*, 2002) and thus may be involved in replication associated repair. Perhaps the lack of modulation observed in this study is reflective of the stage of the cell cycle that the cells were in at the time of oxidative insult. In order to replicate conditions, all experiments were performed with cells of approximately 80% confluence. It may be that by the time the cells had reached such confluence, the rate of cellular proliferation was slowing down and so the need to repair DNA that is not undergoing DNA replication was not essential. Any DNA damage which is produced at this time may be left unrepaired until the next time the cell undergoes mitosis, unless the damage is sustained in an active gene, where in theory, NER-TCR should be performed (Mitra *et al.*, 2002). These studies did not show any changes in TCR associated genes when measured with the ribonuclease protection assay but it would be interesting to use immunodetection in order to assess whether protein levels of the TCR factors CSA and CSB are modulated under such conditions.

In studies using mouse 'knockouts' for single DNA glycosylases involved in BER, the rate of mutation has been much less than expected (Klungland *et al.*, 1999). This has led to suggestions of the multi-functionality of this system, i.e. if a single repair factor is absent then others will be utilised to process the damage without much loss in repair efficiency. The existence of multiple DNA glycosylases, all with different substrate preferences but also the ability to process numerous types of damage, suggests that this is the cells own way to cope with 'mopping up' excess damage such

as induced during this investigation. Recently, *csb(-)/ogg1(-)* double knockout mice were shown to accumulate with age several fold higher levels of oxidised purine modifications in hepatocytes, splenocytes and kidney cells (Osterod *et al.*, 2002). The same group also reported virtually absent global repair of oxidative DNA base modifications induced by photosensitization in *csb(-)/ogg1(-)* immortalised embryonic fibroblasts. The generation of further 'double knockout' systems, deficient in two or more DNA repair related genes, either within the same pathway or across different pathways, may provide more information about how repair pathways are coordinated in order to process oxidative DNA damage.

6.1.3 DNA repair and carcinogenesis

The endonuclease nicking assay detected significantly increased nicking activity in the breast cancer cell line MDA-MB-436 compared to activity in human dermal fibroblasts used as a control. Further investigation would be needed to establish whether this is as a response to increased oxidative stress generated in cancerous cells due to poorly regulated cellular functions and increased cellular proliferation. A correlation between metastatic potential of the breast cancer cell lines and their repair activity was suggested, however, the MDA-MD-436 cells possess a high metastatic potential and therefore the theory that a high metastatic potential may be related to decreased ability to repair oxidative DNA damage leading to genomic instability can not be corroborated.

RT-PCR and quantitative real-time RT-PCR analysis revealed that the nucleotide pool sanitiser *hMTH1* was expressed in all of the breast cancer cell lines used in this investigation. Increased expression of *hMTH1* mRNA, compared to the dermal fibroblast control, was detected in MDA-MB-468, MCF-7, MDA-MB-231 and T47-D cell lines when measured by RT-PCR analysis. The more sensitive method of quantitative real-time RT-PCR showed enhanced *hMTH1* expression in all of the breast cancer cell lines. It would be interesting to measure *hMTH1* protein levels and activity in these cells in order to establish whether the increase in transcript level is translated into functional protein.

Interestingly, the enhanced nicking activity in MDA-MB-436 cells corresponded to the lowest expression of *hMTH1* mRNA of all the cell lines investigated. This may

suggest that the modulation of *hMTH1* expression be regulated depending upon the repair capability of a cell or vice versa. Increases in *hMTH1* transcript have also been reported in lung cancer cell lines (Kennedy *et al.*, 1998), lung cancer carcinomas (Kennedy *et al.*, 2003), breast tumour cells (Wani *et al.*, 1998) and renal cell carcinomas (Okamoto *et al.*, 1996). These results imply that upregulation of the *hMTH1* gene may be a protective mechanism employed by cancerous cells to limit the effects of oxidative lesions in their DNA (Kennedy *et al.*, 1998; 2003). This would need further investigation but suggests that cancerous cells may respond to increased oxidative stress generated during the carcinogenesis process by adapting their repair of oxidative lesions.

The preliminary results in this thesis add further evidence for the use of hMTH1 as a molecular marker for oxidative stress and carcinogenesis. Further work is needed to confirm whether such increased expression is due to increased oxidative stress.

When analysing the results of *in vitro* experiments it is very important to bear in mind that such a system does not accurately reflect *in vivo* conditions; where biochemical and physical interactions between cells are important for the function of the organism as a whole. Studying individual DNA repair systems will not reflect the interplay of all of these pathways as they are present in a living organism.

6.2 FUTURE WORK

Further work to complement the studies in this thesis is discussed below:

6.2.1 Modulation of BER and NER in response to oxidative stress

The ribonuclease protection assay and Western blotting showed that any adaptive response to oxidative stress is not mediated via modulation of repair factors at gene transcript or protein levels in this model system. It would however, be interesting to perform studies in which cells are grown in reduced oxygen, to better mimic *in vivo* conditions, and then exposed to ROS.

Further work could also concentrate more on posttranslational mechanisms, such as phosphorylation events and corresponding modulation of interrelated pathways. The translocation of repair proteins within the cell to sites of damage may also be of importance, and could be studied using Western blotting and confocal microscopy techniques. One way to study this would be to treat the cells with the appropriate damaging agent, before fixing onto microscope slides and incubating with the appropriate immunofluorescence-labeled antibody raised against the protein being investigated. Confocal microscopy could then be used to observe the location of the protein within the cell. When this is compared to untreated control cells any response mediated via translocation of the protein may be identified. Such a mechanism would reflect a much more rapid and sensitive way of detecting and repairing increased DNA damage.

Separate investigations of DNA repair in nuclear and mitochondria would also be interesting, particularly as repair of mitochondrial oxidative lesions has been shown to be altered in breast cancer cell lines (Mambo *et al.*, 2002). Cell lines deficient in multiple repair factors could be used to highlight factors important in the co-ordination of the repair response to oxidative damage.

6.2.2 Measuring responses to oxidative stress in cancer cells

A continuation of this work would involve the use of immunodetection to detect hMTH1 protein in the breast cancer cell lines and compare expression to that of a control. The enzyme activity should also be measured and compared to control cells.

Chapter 6: General discussion & future work

It would also be interesting to look at other DNA repair systems known to process oxidative DNA damage (such as BER and TCR-NER) in these breast tumour cells to see if these are similarly upregulated using quantitative real-time RT-PCR.

Learning more about the efficiency and fidelity of these protective mechanisms may provide us with important tools for the prevention of cancer and degenerative disorders where oxidative DNA damage is implicated. It will also allow the establishment of treatments for diseases where a lack of function of one of these key proteins is responsible, possibly in the form of gene therapy.

The identification of molecular markers that would allow the detection of diseases at an early stage would be highly beneficial and allow the best possible prognosis for affected individuals.

APPENDIX I Design of hMTH1 primer sequences

Primer	Start site	Length (bases)	T _m (°C)	Sequence
Forward	284	20	57.94	TGCAAGAAGGAGAGAC CATC
Reverse	556	20	58.00	TCTGAAGCAGGAGTGG AAAC

T_m = Annealing temperature

Product size: 273 bp

hMTH1 mRNA sequence (accession code: AB025241)

GAAAAGCGCGCGCGGGGATTCCAGGAGTCGTGGTTTCTTGCCTTGATGTA
 CTGGAGCAATCAGATCACACGGCGGCTTGGAGAGTGAGTGCAAGGTTTTA
 TGAGTGGAATTAGCCCTCAGCAGATGGGGGAGCCAGAAGGCAGTTGGAG
 TGGGAAGAACCCAGGGACCATGGGCGCCTCCAGGCTCTATACCCTGGTGC
 TGGTCCTGCAGCCTCAGCGAGTTCTCCTGGGCATGAAAAAGCGAGGCTTC
 GGGGCCGGCCGGTGGAAATGGCTTTGGGGGCAAAGTGCAAGAAGGAGAGA
 CCATCGAGGATGGGGCTAGGAGGGAGCTGCAGGAGGAGAGCGGTCTGAC
 AGTGGACGCCCTGCACAAGGTGGGCCAGATCGTGTTTGAGTTCGTGGGCG
 AGCCTGAGCTCATGGACGTGCATGTCTTCTGCACAGACAGCATCCAGGGG
 ACCCCCGTGGAGAGCGACGAAATGCGCCCATGCTGGTTCCAGCTGGATCA
 GATCCCCTTCAAGGACATGTGGCCCGACGACAGCTACTGGTTTCCACTCCT
 GCTTCAGAAGAAGAAATTCACGGGTA CTCAAGTTCAGGGTTCAGGACA
 CCATCCTGGACTACACTCCGCGAGGTGGACACGGTCTAGCGGGAGCCC
 AGGGCAGCCCCTGGGCAGGAGACGTGGCTGCTGAACAGCTGCAAACCAT
 CTTACCTGGGGGCATTGAGTGGCGCAGAGCCGGGTTTCATCTGGAATTA
 ACTGGATGGAAGGGAAAATAAAGCTATCTAGCGGTGAAAAA

Sequence size: 788

Forward primer

Reverse primer

APPENDIX II

Raw data from densitometric analysis of ribonuclease protection assay (Example)

hBER-1 400 μ M H₂O₂

Sample	1				2				3			
	OGG1	GAPDH	ratio/GAPD	ratio/con	OGG1	GAPDH	ratio/GAPD	ratio/con	OGG1	GAPDH	ratio/GAPD	ratio/con
Control 0 hrs	1986.8	17295	0.115	1.000	2313.3	14500	0.160	1.000	1312.7	11600	0.11	1.00
Control 8 hrs	2295.9	20828	0.110	1.000	3949.6	17769	0.222	1.000	1536.7	11610	0.13	1.00
Control 24 hrs	1770.6	13880	0.128	1.000	1977.5	15750	0.126	1.000	1491.3	11287	0.13	1.00
400 μ M H ₂ O ₂ 8 hrs	1563.6	25001	0.063	0.567	2688.4	17334	0.155	0.698	976.4	10438	0.09	0.71
400 μ M H ₂ O ₂ 24 hrs	2021.8	20597	0.098	0.769	2631.9	17921	0.147	1.170	184.1	8469.8	0.02	0.16
	TDG	GAPDH	ratio/GAPD	ratio/con	TDG	GAPDH	ratio/GAPD	ratio/con	TDG	GAPDH	ratio/GAPD	ratio/con
Control 0 hrs	1475.1	17295	0.085	1.000	1645.4	14500	0.113	1.000	353.5	11600	0.03	1.00
Control 8 hrs	1290.3	20828	0.062	1.000	2762.7	17769	0.155	1.000	445.1	11610	0.04	1.00
Control 24 hrs	1222.1	13880	0.088	1.000	1516.8	15750	0.096	1.000	527.5	11287	0.05	1.00
400 μ M H ₂ O ₂ 8 hrs	1235.6	25001	0.049	0.798	2889.6	17334	0.167	1.072	353.2	10438	0.03	0.88
400 μ M H ₂ O ₂ 24 hrs	1414.8	20597	0.069	0.780	1753.8	17921	0.098	1.016	53.6	8469.8	0.01	0.14
	APE	GAPDH	ratio/GAPD	ratio/con	APE	GAPDH	ratio/GAPD	ratio/con	APE	GAPDH	ratio/GAPD	ratio/con
Control 0 hrs	4375.3	17295	0.253	1.000	3941.3	14500	0.272	1.000	2021.4	11600	0.17	1.00
Control 8 hrs	5680.6	20828	0.273	1.000	7871.2	17769	0.443	1.000	2030.2	11610	0.17	1.00
Control 24 hrs	3393.1	13880	0.244	1.000	3285.4	15750	0.209	1.000	2085.7	11287	0.18	1.00
400 μ M H ₂ O ₂ 8 hrs	3938.4	25001	0.158	0.578	6410.4	17334	0.370	0.835	1426.2	10438	0.14	0.78
400 μ M H ₂ O ₂ 24 hrs	4681.1	20597	0.227	0.930	5628.1	17921	0.314	1.505	794.2	8469.8	0.09	0.51
	UDG	GAPDH	ratio/GAPD	ratio/con	UDG	GAPDH	ratio/GAPD	ratio/con	UDG	GAPDH	ratio/GAPD	ratio/con
Control 0 hrs	2366.7	17295	0.137	1.000	2557.3	14500	0.176	1.000	1189.9	11600	0.10	1.00
Control 8 hrs	2685.9	20828	0.129	1.000	4624.1	17769	0.260	1.000	1261.1	11610	0.11	1.00
Control 24 hrs	1637.3	13880	0.118	1.000	2252.3	15750	0.143	1.000	1265.8	11287	0.11	1.00
400 μ M H ₂ O ₂ 8 hrs	1941.4	25001	0.078	0.602	3194.6	17334	0.184	0.708	901.5	10438	0.09	0.80
400 μ M H ₂ O ₂ 24 hrs	2204.7	20597	0.107	0.907	3058.1	17921	0.171	1.193	302.1	8469.8	0.04	0.32

	MPG	GAPDH	ratio/GAPD	ratio/con	MPG	GAPDH	ratio/GAPD	ratio/con	MPG	GAPDH	ratio/GAPD	ratio/con
Control 0 hrs	3198.6	17295	0.185	1.000	3133	14500	0.216	1.000	3160.7	11600	0.27	1.00
Control 8 hrs	5230.2	20828	0.251	1.000	6499.8	17769	0.366	1.000	3063.3	11610	0.26	1.00
Control 24 hrs	3014.9	13880	0.217	1.000	2076.1	15750	0.132	1.000	3048.1	11287	0.27	1.00
400 µM H₂O₂ 8 hrs	1924.4	25001	0.077	0.307	4267.2	17334	0.246	0.673	2134.3	10438	0.20	0.77
400 µM H₂O₂ 24 hrs	3980.5	20597	0.193	0.890	4960.1	17921	0.277	2.100	906.62	8469.8	0.11	0.40
	ENTG	GAPDH	ratio/GAPD	ratio/con	ENTG	GAPDH	ratio/GAPD	ratio/con	ENTG	GAPDH	ratio/GAPD	ratio/con
Control 0 hrs	2030.2	17295	0.117	1.000	2044.2	14500	0.141	1.000	1645.1	11600	0.14	1.00
Control 8 hrs	2374.8	20828	0.114	1.000	2975.2	17769	0.167	1.000	1889.2	11610	0.16	1.00
Control 24 hrs	1732.1	13880	0.125	1.000	2025.8	15750	0.129	1.000	1719	11287	0.15	1.00
400 µM H₂O₂ 8 hrs	1331.6	25001	0.053	0.467	2468.4	17334	0.142	0.850	1334.2	10438	0.13	0.79
400 µM H₂O₂ 24 hrs	1533.2	20597	0.074	0.596	2358.7	17921	0.132	1.023	314.23	8469.8	0.04	0.24
	RPA4	GAPDH	ratio/GAPD	ratio/con	RPA4	GAPDH	ratio/GAPD	ratio/con	RPA4	GAPDH	ratio/GAPD	ratio/con
Control 0 hrs	1990.6	17295	0.115	1.000	1938.4	14500	0.134	1.000	1515.9	11600	0.13	1.000
Control 8 hrs	2442.3	20828	0.117	1.000	2401	17769	0.135	1.000	1713.2	11610	0.15	1.000
Control 24 hrs	1859.1	13880	0.134	1.000	1837.8	15750	0.117	1.000	1675.2	11287	0.15	1.000
400 µM H₂O₂ 8 hrs	1700.4	25001	0.068	0.580	2133.6	17334	0.123	0.911	1010.5	10438	0.10	0.656
400 µM H₂O₂ 24 hrs	2506.8	20597	0.122	0.909	2032.9	17921	0.113	0.972	194.52	8469.8	0.02	0.155
	MGMT	GAPDH	ratio/GAPD	ratio/con	MGMT	GAPDH	ratio/GAPD	ratio/con	MGMT	GAPDH	ratio/GAPD	ratio/con
Control 0 hrs	1420.1	17295	0.082	1.000	2282.4	14500	0.157	1.000	440.2	11600	0.04	1.000
Control 8 hrs	1198.6	20828	0.058	1.000	3929.5	17769	0.221	1.000	592.3	11610	0.05	1.000
Control 24 hrs	1323.9	13880	0.095	1.000	2096.6	15750	0.133	1.000	583.3	11287	0.05	1.000
400 µM H₂O₂ 8 hrs	986.37	25001	0.039	0.686	2929	17334	0.169	0.764	340.9	10438	0.03	0.640
400 µM H₂O₂ 24 hrs	1478.4	20597	0.072	0.752	2990.8	17921	0.167	1.254	81.4	8469.8	0.01	0.186
	L32	GAPDH	ratio/GAPD	ratio/con	L32	GAPDH	ratio/GAPD	ratio/con	L32	GAPDH	ratio/GAPD	ratio/con
Control 0 hrs	13818	17295	0.799	1.000	16222	14500	1.119	1.000	11277.3	11600	0.97	1.000
Control 8 hrs	16090	20828	0.773	1.000	22299	17769	1.255	1.000	11641.2	11610	1.00	1.000
Control 24 hrs	10612	13880	0.765	1.000	12072	15750	0.766	1.000	13448.1	11287	1.19	1.000
400 µM H₂O₂ 8 hrs	31251	25001	1.250	1.618	17705	17334	1.021	0.814	9958.3	10438	0.95	0.951
400 µM H₂O₂ 24 hrs	16160	20597	0.785	1.026	17289	17921	0.965	1.259	6364.2	8469.8	0.75	0.631

Summary of ratios to GAPDH and control sample

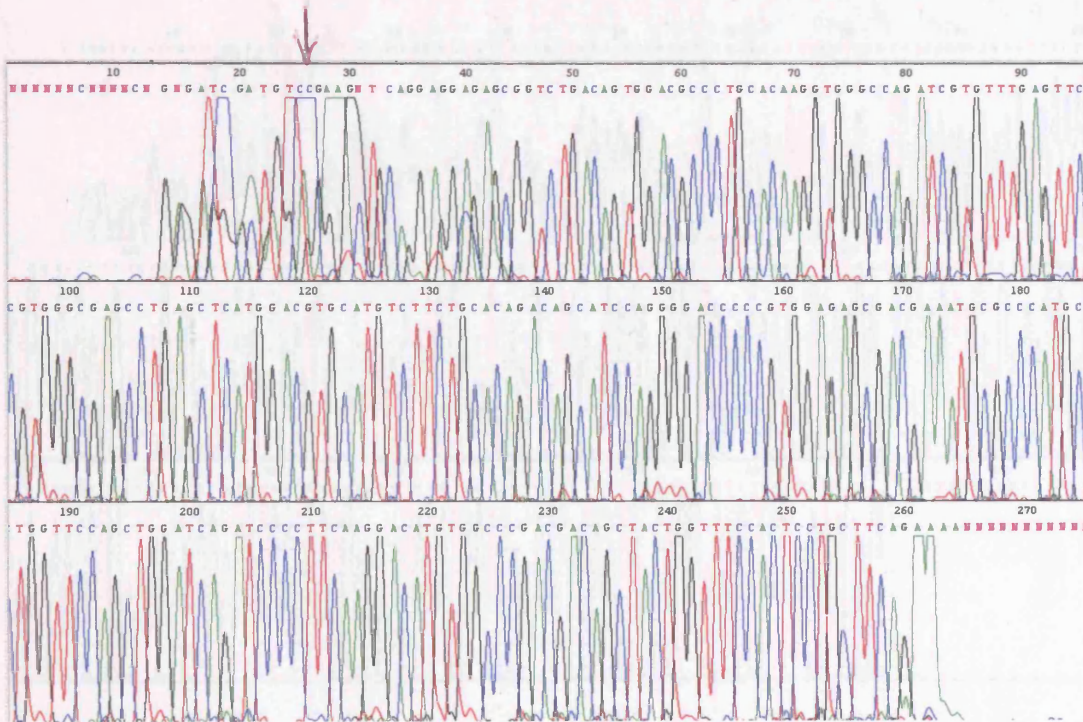
		MEANS								
		OGG1	TDG	APE	UDG	MPG	ENTG	RPA4	MGMT	L32
Control	1	1.000	1.000	1.000	1.000	1.000	1.000	1.000	1.000	1.000
	2	1.000	1.000	1.000	1.000	1.000	1.000	1.000	1.000	1.000
	3	1.000	1.000	1.000	1.000	1.000	1.000	1.000	1.000	1.000
	mean	1.000								
	SD	0.000								
8 hrs H₂O₂	1	0.707	0.882	0.781	0.795	0.775	0.785	0.656	0.640	0.951
	2	0.698	1.072	0.835	0.708	0.673	0.850	0.911	0.764	0.814
	3	0.567	0.798	0.578	0.602	0.307	0.467	0.580	0.686	1.618
	mean	0.657	0.917	0.731	0.702	0.585	0.701	0.716	0.697	1.128
	SD	0.078	0.141	0.136	0.097	0.246	0.205	0.173	0.063	0.430
24 hrs H₂O₂	1	0.164	0.135	0.507	0.318	0.396	0.244	0.155	0.186	0.631
	2	1.170	1.016	1.505	1.193	2.100	1.023	0.972	1.254	1.259
	3	0.769	0.780	0.930	0.907	0.890	0.596	0.909	0.752	1.026
	mean	0.701	0.644	0.981	0.806	1.129	0.621	0.678	0.731	0.972
	SD	0.506	0.456	0.501	0.446	0.876	0.390	0.455	0.534	0.317
means										
		OGG1	TDG	APE	UDG	MPG	ENTG	RPA4	MGMT	L32
Control		1.000								
8 hrs H₂O₂		0.657	0.917	0.731	0.702	0.585	0.701	0.716	0.697	1.128
24 hrs H₂O₂		0.701	0.644	0.981	0.806	1.129	0.621	0.678	0.731	0.972
SD										
		OGG1	TDG	APE	UDG	MPG	ENTG	RPA4	MGMT	L32
Control		0.000								
8 hrs H₂O₂		0.078	0.141	0.136	0.097	0.246	0.205	0.173	0.063	0.430
24 hrs H₂O₂		0.506	0.456	0.501	0.446	0.876	0.390	0.455	0.534	0.317

APPENDIX III

hMTH1 PCR product sequencing data

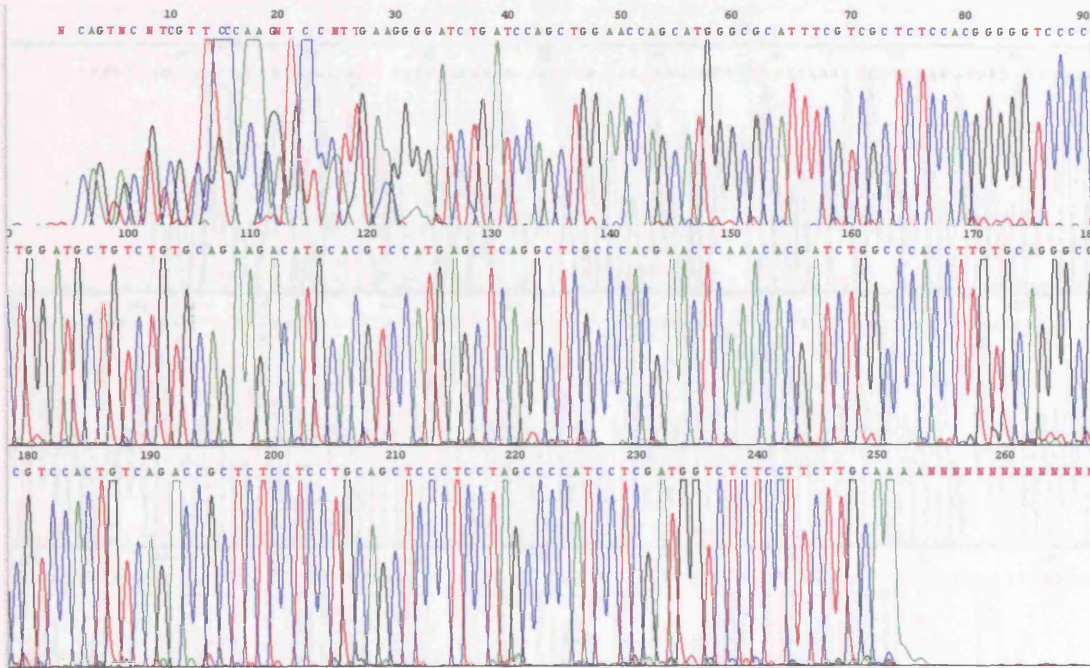
A. HBL 100 hMTH1 sense sequence exported from chromatogram file

CAGGAGGAGAGCGGTCTGACAGTGGACGCCCTGCACAAGGTGGGCCAGATCGTGTTT
 GAGTTCGTGGGCGAGCCTGAGCTCATGGACGTGCATGTCTTCTGCACAGACAGCATC
 CAGGGGACCCCGTGGAGAGCGACGAAATGCGCCCATGCTGGTTCCAGCTGGATCAG
 ATCCCCTTCAAGGACATGTGGCCCGACGACAGCTACTGGTTTCCACTCCTGCTTCAG
 AA



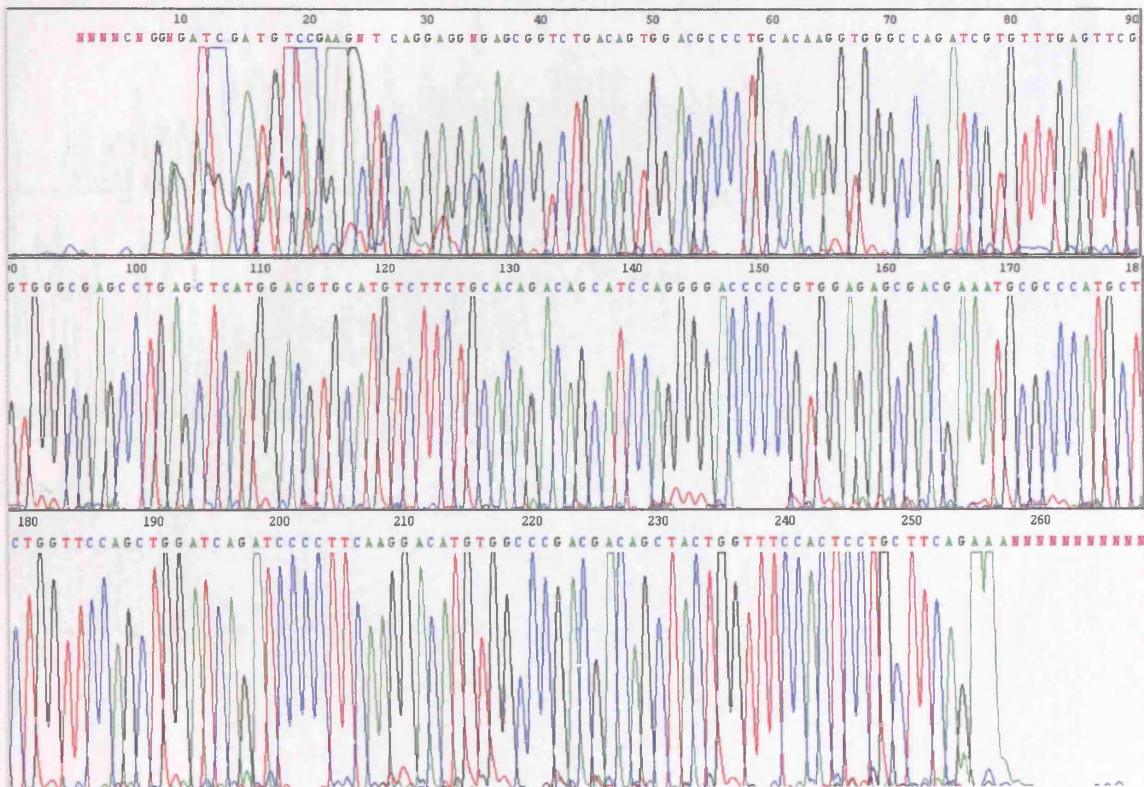
B. HBL 100 hMTH1 anti-sense sequence exported from chromatogram file

TTGAAGGGGATCTGATCCAGCTGGAACCAGCATGGGCGCATTTCGTGCTCTCCACG
GGGGTCCCCTGGATGCTGTCTGTGCAGAAGACATGCACGTCCATGAGCTCAGGCTCG
CCCACGAACCTCAAACACGATCTGGCCCACCTTGTGCAGGGCGTCCACTGTCAGACCG
CTCTCCTCCTGCAGCTCCCTCCTAGCCCCATCCTCGATGGTCTCTCCTTCTTGCA



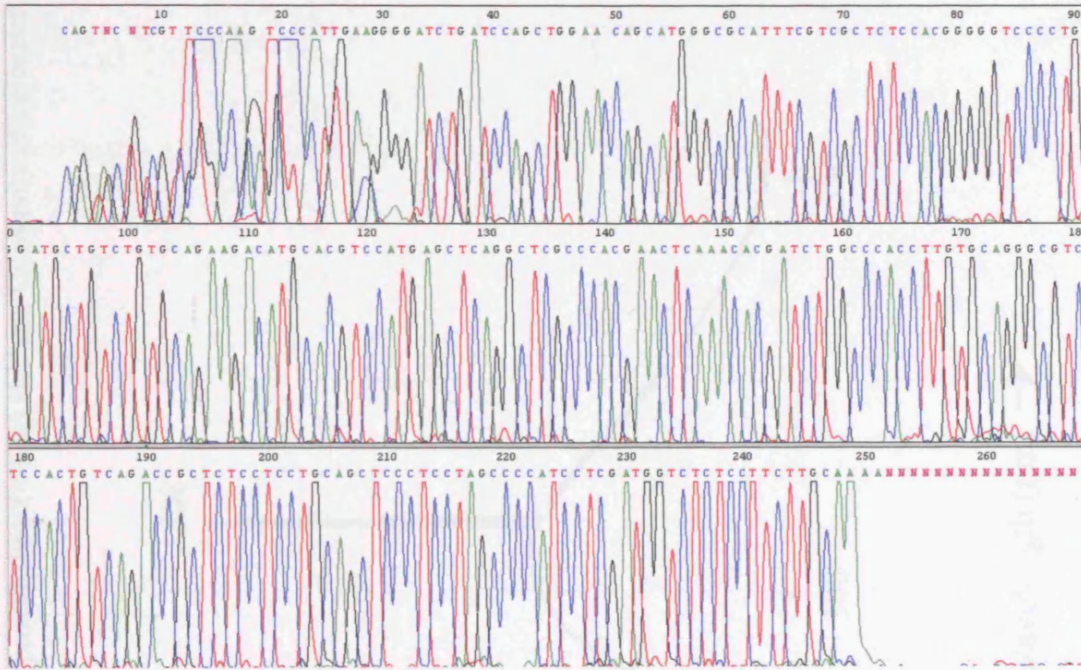
C. ZR-75.1 hMTH1 sense sequence exported from chromatogram file

CAGGAGGNGAGCGGTCTGACAGTGGACGCCCTGCACAAGGTGGGCCAGATCGTGTTT
 GAGTTCGTGGGCGAGCCTGAGCTCATGGACGTGCATGTCTTCTGCACAGACAGCATC
 CAGGGGACCCCCGTGGAGAGCGACGAAATGCGCCCATGCTGGTTCCAGCTGGATCAG
 ATCCCCTTCAAGGACATGTGGCCCGACGACAGCTACTGGTTTCCACTCCTGCTTCAG
 AA



D. ZR-75.1 hMTH1 anti-sense sequence exported from chromatogram file

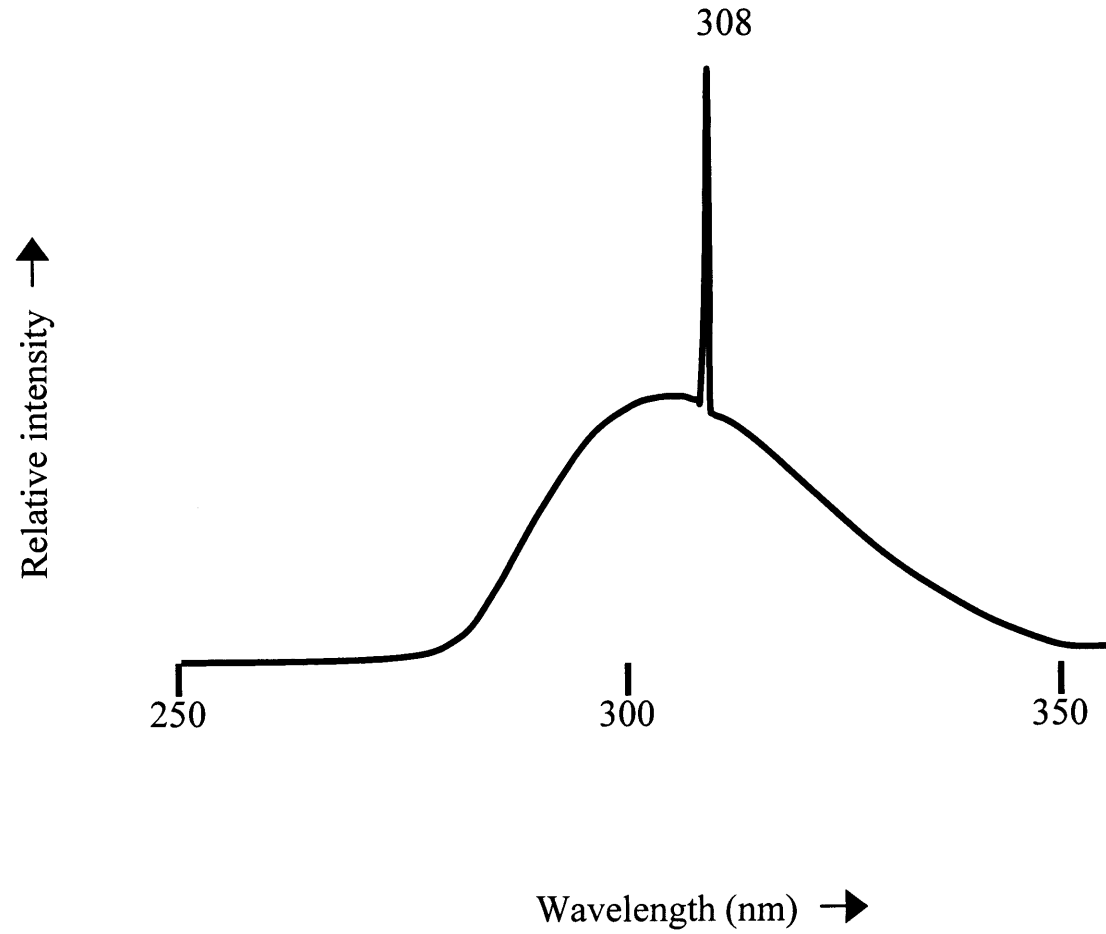
TTGAAGGGGATCTGATCCAGCTGGAAC-AGCATGGGCGCATTTCGTGCTCTCCACG
 GGGGTCCCCTGGATGCTGTCTGTGCAGAAGACATGCACGTCCATGAGCTCAGGCTCG
 CCCACGAACTCAAACACGATCTGGCCCACCTTGTGCAGGGCGTCCACTGTCAGACCG
 CTCTCCTCCTGCAGCTCCCTCCTAGCCCCATCCTCGATGGTCTCTCCTTCTTGCA



APPENDIX IV

Emission spectrum of UVB lamp

(provided by Dr Karl Herbert, University of Leicester, Leicester, UK).



APPENDIX V

Communications arising from this thesis

Phillips SEE and Herbert KE. Effects of oxidative stress on nucleotide excision repair and base excision repair in human primary fibroblasts. Gordon Research Conference: Mammalian DNA Repair, California, USA (2003).

Herbert KE, Phillips SE, Goodrem P, Hastings R and Shaw J. ROS and repair of oxidative DNA damage in primary human fibroblasts and breast cancer cell lines. Society for Free Radical Biology and Medicine (2003).

REFERENCES

- Adelman R, Saul RL and Ames BN (1988). Oxidative damage to DNA: relation to species metabolic rate and life span. *Proc Natl Acad Sci USA*. **85(8)**: 2706-8
- Adimoolam, S. and Ford, JM (2002). p53 and DNA damage-inducible expression of the xeroderma pigmentosum group C gene. *Proc Natl Acad Sci USA*. **99(20)**: 12985-12990
- Akman SA, O'Connor TR and Rodriguez-H (2000). Mapping oxidative DNA damage and mechanisms of repair. *Reactive Oxygen Species: From Radiation to Molecular Biology. Annals New York Academy Sci.* **899**: 88-102
- Ames BN (1989). Endogenous DNA damage as related to cancer and aging. *Mutat Res.* **214(1)**: 41-6
- Balajee AS, May A and Bohr VA (1998). Fine structural analysis of DNA repair in mammalian cells. *Mutat Res.* **404(1-2)**: 3-11
- Bases R., Franklin WA, Moy T and Mendez F (1992). Enhanced excision repair activity in mammalian cells after ionizing radiation. *Int J Rad Biol.* **62(4)**: 427-441
- Batty DP and Wood RD (2000). Damage recognition in nucleotide excision repair of DNA. *Gene.* **241(2)**: 193-204
- Beckman KB and Ames BN (1997). Oxidative decay of DNA. *J Biol Chem.* **272(32)**: 19633-19636
- Bernstein C, Bernstein H, Payne CM and Garewal H (2002). DNA repair/pro-apoptotic dual-role proteins in five major DNA repair pathways: fail-safe protection against carcinogenesis. *Mutat Res.* **511**: 145-178
- Bessho T, Roy R, Yamamoto K, Kasai H, Nishimura S, Tano K and Mitra S (1993). Repair of 8-hydroxyguanine in DNA by mammalian N-methylpurine-DNA glycosylase. *Proc Natl Acad Sci USA.* **90**: 8901-8904
- Birrell GW, Brown JA, Wu HI, Giaever G, Chu AM, Davis RW and Brown JM (2002). Transcriptional response of *Saccharomyces cerevisiae* to DNA-damaging agents does not identify the genes that protect against these agents. *Proc. Natl. Acad. Sci. USA.* **99(13)**: 8778-8783
- Boiteux S and Laval J (1997). Repair of oxidized purines in DNA. *Base Excision Repair of DNA Damage. I. D. Hickson, Landes Bioscience.* 31-44.
- Bouziane M, Miao F, Bates SE, Somsouk L, Sang B-C, Denissenko M and O'Connor TR (2000). Promoter structure and cell cycle dependent expression of the human methylpurine-DNA glycosylase gene. *DNA Repair.* **461(1)**: 15-29

References

- Brinkley P (2003). Repairing BRCA1 science. *The Scientist*. www.the-scientist.com
[<http://www.biomedcentral.com/news/20030618/04>]
- Cadet JM, Berger M, Douki T and Ravanat JL (1997). Oxidative damage to DNA: Formation, measurement and biological significance. *Rev Physiol Biochem Pharmacol*. **131**: 1-87
- Cadet J, Douki T, Pouget J-P and Ravanat J-L (2000). Singlet oxygen DNA damage products: formation and measurement. *Met Enzymol*. **319**: 143-53
- Cappelli E, Degan P and Frosina G (2000). Comparative repair of the endogenous lesions 8-oxo7,8-dihydroguanine (8-oxoG), uracil and abasic site by mammalian cell extracts: 8-oxoG is poorly repaired by human cell extracts. *Carcinogenesis*. **21(6)**: 1135-1141
- Cappelli E, Hazra T, Hill JW, Slupphaug G, Bogliolo M and Frosina G (2001). Rates of base excision repair are not solely dependent on levels of initiating enzymes. *Carcinogenesis*. **22(3)**: 387-393
- Cerda SR, Turk PW, Thor AD and Weitzman SA (1998). Altered expression of the DNA repair protein, *N*-methylpurine-DNA glycosylase (MPG), in breast cancer. *FEBS Letts*. **431**: 12-18
- Chakrabarti R, Kundu S, Kumar S and Chakrabarti R (2000). Vitamin A as an enzyme that catalyzes the reduction of MTT to formazan by vitamin C. *J Cell Biochem*. **80**: 133-138
- Chaudhry MA, Dedon PC, Wilson DM, Demple B and Weinfeld M (1999). Removal by human apurinic/apyrimidinic endonuclease 1 (Ape 1) and *Escherichia coli* exonuclease III of 3'-phosphoglycolates from DNA treated with neocarzinostatin, calicheamicin, and gamma-radiation. *Biochem Pharmacol*. **57(5)**: 531-538
- Chung MH, Kasai H, Jones DS, Inoue H, Ishikawa H, Ohtsuka E and Nishimura S (1991). An endonuclease activity of *Escherichia coli* that specifically removes 8-hydroxyguanine residues from DNA. *Mutat Res*. **254**: 1-12
- Cooke MS, Evans MD, Podmore I, Herbert KE, Mistry N, Mistry P, Hickenbotham PT, Hussieni A, Griffiths HR and Lunec J (1997). Novel repair action of vitamin C upon *in vivo* oxidative DNA damage. *FEBS Letts*. **363**: 363-367
- Cooke MS, Evans MD, Herbert KE and Lunec J (2000). Urinary 8-oxo-2'-deoxyguanosine--source, significance and supplements. *Free Rad Res*. **32(5)**: 381-97
- Cooke MS, Evans MD, Dizdaroglu M and Lunec J (2003). Oxidative DNA damage: mechanisms, mutations and disease. *FASEB J*. **17(10)**: 1195-1214

References

- Cooper PK, Nouspikel T, Clarkson SG and Leadon SA (1997). Defective transcription-coupled repair of oxidative base damage in Cockayne syndrome patients from XP group G. *Science*. **275**: 990-993
- de Boer J and Hoeijmakers JHJ (2000). Nucleotide excision repair and human syndromes. *Carcinogenesis*. **21(3)**: 453-60
- de Laat WL, Jaspers NGJ and Hoeijmakers JHJ (1999). Molecular mechanism of nucleotide excision repair. *Genes & Develop*. **13**: 768-765
- Dianov G, Bischoff C, Piotrowski J and Bohr VA (1998). Repair pathways for processing of 8-oxoguanine in DNA by mammalian cell extracts. *J Biol Chem*. **273(50)**: 33811-6
- Dianov GL, Jensen BR, Kenny MK and Bohr VA (1999). Replication protein A stimulates proliferating cell nuclear antigen dependent repair of abasic sites in DNA by human cell extracts. *Biochem*. **38(34)**: 11021-11025
- Dizdaroglu M, Karahalil B, (1999). Excision of products of oxidative DNA base damage by human NTH1 protein. *Biochem*. **38**: 243-246
- Dizdaroglu M, Jaruga P, Birincioglu M and Rodriguez H (2002). Free radical-induced damage to DNA: Mechanisms and measurement. *Free Rad Biol Med*. **32(11)**: 1102-1115
- Egashira A, Yamauchi K, Yoshiyama K, Kawate H, Katsuki M, Sekiguchi M, Sugimachi K, Maki H and Tsuzuki T (2002). Mutational specificity of mice defective in the MTH1 and/or the MSH2 genes. *DNA Repair*. **1(11)**: 881-893
- Eide L, Luna L, Gustad EC, Henderson PT, Essigmann JM, Demple B and Seeberg E (2001). Human endonuclease III acts preferentially on DNA damage opposite guanine residues in DNA. *Biochem*. **40**: 6653-6659
- Epe B (1995). DNA damage profiles induced by oxidizing agents. *Rev Physiol Biochem Pharmacol*. **127**: 223-249
- ESCODD (2000). Comparison of different methods of measuring 8-oxoguanine as a marker of oxidative DNA damage. *Free Rad Res*. **32(4)**: 333-341
- ESCODD (2002). Comparative analysis of baseline 8-oxo-7,8-dihydroguanine in mammalian cell DNA, by different methods in different laboratories, an approach to consensus. *Carcinogenesis*. **23(12)**: 2129-2133
- ESCODD (2003). Measurement of DNA oxidation in human cells by chromatographic and enzymic methods. *Free Rad Biol Med*. **34(8)**: 1089-1099
- Evans AR, Limp-Foster M and Kelley MR (2000). Going APE over ref-1. *Mutat Res*. **461**: 83-108

References

- Fitch ME, Cross IV and Ford JM (2003). p53 responsive nucleotide excision repair gene products p48 and XPC, but not p53, localize to sites of UV-irradiation-induced DNA damage, in vivo. *Carcinogenesis*. **24(5)**: 843-850
- Floyd RA (1990). Role of oxygen free radicals in carcinogenesis and brain ischemia. *FASEB J*. **4(9)**: 2587-97
- Francis MA and Rainbow AJ (1999). UV-enhanced reactivation of a UV-damaged reporter gene suggests transcription-coupled repair is UV-inducible in human cells. *Carcinogenesis*. **20(1)**: 19-26
- Ford JM and Hanawalt PC (1997). Expression of wild-type p53 is required for efficient global genomic nucleotide excision repair in UV-irradiated human fibroblasts. *J Biological Chem*. **272(44)**: 28073-28080
- Friedberg EC (1996). Relationships between DNA repair and transcription. *Annu Rev Biochem*. **65**: 15-42
- Frosina G, Fortini P, Rossi O, Carrozzino F, Raspaglio G, Cox LS, Lane DP, Abbondandolo A and Dogliotti E (1996). Two pathways for base excision repair in mammalian cells. *J Biol Chem*. **271(16)**: 9573-9578
- Frossi B, Tell G, Spessotto P, Colombatti A, Vitale G and Pucillo C (2002). H₂O₂ induces translocation of APE/Ref-1 to mitochondria in the Raji B-cell line. *J Cellular Physiol*. **193**: 180-186
- Fujikawa K, Kamiya H, Yakushiji H, Fujii Y, Nakabeppu Y and Kasai H (1999). The oxidized forms of dATP are substrates for the human MutT homologue, the hMTH1 protein. *J Biol Chem*. **274(26)**: 18201-18205
- Fung H, Kow YW, Van Houten B, Taatjes D, Hatahet Z, Janssen YMW, Vacek P, Faux S and Mossman BT (1998). Asbestos increases mammalian AP-endonuclease gene expression, protein levels, and enzyme activity in mesothelial cells. *Cancer Res*. **58**: 189-194
- Gaiddon C, Moorthy NC and Prives C (1999). Ref-1 regulates the transactivation and pro-apoptotic functions of p53 in vivo. *EMBO J*. **18(20)**: 5609-5621
- Gifford CM, Blaisdell JO and Wallace SS (2000). Multiprobe RNase protection assay analysis of mRNA levels for the Escherichia coli oxidative DNA glycosylase genes under conditions of oxidative stress. *J Bacteriol*. **182(19)**: 5416-5424
- Gowen LC, Avrutskaya AV, Latour AM, Koller BH and Leadon SA (1998). BRCA1 required for transcription-coupled repair of oxidative DNA damage. *Science*. **281**: 1009-1012

References

- Gowen LC, Avrutskaya AV, Latour AM, Koller BH and Leadon SA (2003). **Retraction****. *Science*. 300: 1657**
- Gros L, Saparbaev MK and Laval J (2002). Enzymology of the repair of free radicals-induced DNA damage. *Oncogene*. **21**: 8905-8925
- Grösch S, Fritz G and Kaina B (1998). Apurinic endonuclease (Ref-1) is induced in mammalian cells by oxidative stress and involved in clastogenic adaptation. *Cancer Res*. **58(19)**: 4410-4416
- Hadi MZ and Wilson DM (2000). Second human protein with homology to the Escherichia coli abasic endonuclease exonuclease III. *Environ Mol Mutagenesis*. **36**: 312-324
- Hainaut P, Hernandez T, Robinson A, Rodriguez-Tome P, Flores T, Hollstein M, Harris CC and Montesano R (1998). IARC database of p53 gene mutations in human tumours and cell lines: updated compilation, revised formats and new visualisation tools. *Nuc Acids Res*. **26(1)**: 205-213
- Halliwell B and Gutteridge JMC (1990). Role of free radicals and catalytic metal ions in human disease: an overview. *Met Enzymol*. **186**: 1-85
- Hanawalt PC (1994). Transcription-coupled repair and human disease. *Science*. **266**: 1957-1958.
- Hanawalt PC (1995). DNA repair comes of age. *Mutat Res*. **336(2)**: 101-113
- Hanawalt PC (2002). Subpathways of nucleotide excision repair and their regulation. *Oncogene*. **21**: 8949-8956
- Harrison L, Ascione AG, Wilson DM and Demple B (1995). Characterization of the promoter region of the human apurinic endonuclease gene (APE). *J Biol Chem*. **270(10)**: 5556-5564
- Hartwig A, Dally H and Schlepegrell (1996). Sensitive analysis of oxidative DNA damage in mammalian cells: use of the bacterial Fpg protein in combination with alkaline unwinding. *Toxicol Lett*. **88**: 85-90
- Hartwig A (1998). Assessment of oxidative DNA damage by the frequency of formamidopyrimidine glycosylase (FPG) sensitive DNA lesions. *DNA & free radicals: techniques, mechanisms & applications*. OICA International, UK.
- Hazra TK, Izumi T, Boldogh I, Imhoff B, Kow YW, Jaruga P, Dizdaroglu M and Mitra S (2002). Identification and characterization of a human DNA glycosylase for repair of modified bases in oxidatively damaged DNA. *Proc Natl Acad Sci USA*. **99(6)**: 3523-3528

References

- Hazra TK, Izumi T, Kow YW and Mitra S (2003). The discovery of a new family of mammalian enzymes for repair of oxidatively damaged DNA, and its physiological implications. *Carcinogenesis*. **24(2)**: 155-157
- Helbock HJ, Beckman KB, Shigenaga MK, Walter PB, Woodall AA, Yeo HC and Ames BN (1998). DNA oxidation matters: the HPLC-electrochemical detection assay of 8-oxo-deoxyguanosine and 8-oxo-guanine. *Proc Natl Acad Sci USA*. **95**: 288-293
- Helbock HJ, Beckman KB and Ames BN (1999). 8-Hydroxydeoxyguanosine and 8-hydroxyguanine as biomarkers of oxidative DNA damage. *Met Enzymol*. **300**: 156-166
- Henle ES and Linn S (1997). Formation, prevention, and repair of DNA damage by iron hydrogen peroxide. *J Biol Chem*. **272(31)**: 19095-19098
- Hickson ID (1997). General introduction to DNA base excision repair. *Base excision repair of DNA damage*. Landes Bioscience.
- Hilbert TP, Chaung W, Boorstein RJ, Cunningham RP and Teebor GW (1997). *J Biol Chem*. **272(10)**: 6733-6740
- Hirano T, Hirano H, Yamaguchi R, Asami S, Tsurudome Y and Kasai H (2001). Sequence specificity of the 8-hydroxyguanine repair activity in rat organs. *J Radiat Res*. **42**: 247-254
- Hoeijmakers JH (2001). Genome maintenance mechanisms for preventing cancer. *Nature*. **411**: 366-374
- Hsieh MM, Hegde V, Kelley MR and Deutsch WA (2001). Activation of APE/Ref-1 redox activity is mediated by reactive oxygen species and PKC phosphorylation. *Nucleic Acids Res*. **29(14)**: 3116-3122
- Hwang BJ, Ford JM, Hanawalt PC and Chu G (1999). Expression of the p48 xeroderma pigmentosum gene is p53-dependent and is involved in global genomic repair. *Proc Natl Acad Sci USA*. **96(2)**: 424-428
- Iida T, Furuta A, Kawashima M, Nishida J, Nakabeppu Y and Iwaki T (2001). Accumulation of 8-oxo-2'-deoxyguanosine and increased expression of hMTH1 protein in brain tumors. *Neuro-oncol*. **3(2)**: 73-81
- Ischenko AA and Saporbaev MK (2002). Alternative nucleotide incision repair pathway for oxidative DNA damage. *Nature*. **415**: 183-187

References

- Izumi T, Hazra TK, Boldogh I, Tomkinson AE, Park MS, Ikeda S and Mitra S (2000). Requirement for human AP endonuclease 1 for repair of 3' blocking damage at DNA single-strand breaks induced by reactive oxygen species. *Carcinogenesis*. **21(7)**: 1329-1334
- Janićijević A, Sugasawa K, Shimizu Y, Hanaoka F, Wijgers N, Djurica M, Hoeijmakers JHJ and Wyman C (2003). DNA bending by the human damage recognition complex XPC-HR23B. *DNA Repair*. **2**: 325-336
- Jaruga P and Dizdaroglu M (1996). Repair of products of oxidative base damage in human cells. *Nucleic Acids Res*. **24**: 1389-1394
- Kaina B, Fritz G and Coquerelle T (1993). Contribution of O⁶-alkylguanine and N-alkylpurines to the formation of sister chromatid exchanges, chromosomal aberrations and gene mutations: new insights gained from studies of genetically engineered mammalian cells. *Environ Mol Mutagen*. **22(4)**: 283-292
- Kamiuchi S, Saijo M, Citterio E, de Jager M, Hoeijmakers JHJ and Tanaka K (2002). Translocation of Cockayne syndrome group A protein to the nuclear matrix: Possible relevance to transcription-coupled DNA repair. *Proc Natl Acad Sci USA*. **99(1)**: 201-206
- Kawanishi S, Hiraku Y and Oikawa S (2001). Mechanism of guanine-specific DNA damage by oxidative stress and its role in carcinogenesis and aging. *Mutat Res*. **488(1)**: 65-76
- Kielbassa C, Roza L and Epe B (1997). Wavelength dependence of oxidative DNA damage induced by UV and visible light. *Carcinogenesis*. **18(4)**: 811-816
- Kennedy CH, Cueto R, Belinsky SA, Lechner JF and Pryor (1998). Overexpression of hMTH1 mRNA: a molecular marker of oxidative stress in lung cancer cells. *FEBS Lett*. **429**: 17-20
- Kennedy CH, Pass HI, Mitchell JB (2003). Expression of human MuT homologue (hMTH1) protein in primary non-small-cell lung carcinomas and histologically normal surrounding tissue. *Free Rad Biol Med*. **34(11)**: 1447-1457
- Kim H-N, Morimoto Y, Tsuda T, Ootsuyama Y, Hirohashi M, Hirano T, Tanaka I, Lim Y, Yun I-G and Kasai H (2001). Changes in DNA 8-hydroxyguanine levels, 8-hydroxyguanine repair activity, and hOGG1 and hMTH1 mRNA expression in human lung alveolar epithelial cells induced by crocidolite asbestos. *Carcinogenesis*. **22(2)**: 265-269
- Klungland A and Lindahl T (1997). Second pathway for completion of human DNA base excision-repair: reconstitution with purified proteins and requirement for Dnase IV (FEN1). *EMBO J*. **16(11)**: 3341-3348

References

- Klungland A, Rosewell I, Hollenbach S, Larsen E, Daly G, Epe B, Seeberg E, Lindahl T and Barnes D (1999). Accumulation of premutagenic DNA lesions in mice defective in removal of oxidative base damage. *Proc Natl Acad Sci USA*. **96(23)**: 13300-5
- Kondo S, Toyokuni S, Tanaka T, Hiai H, Onodera H, Kasai H and Imamura M (2000). Overexpression of the hOGG1 gene and high 8-hydroxy-2'-deoxyguanosine (8-OHdG) lyase activity in human colorectal carcinoma: regulation mechanism of the 8-OHdG level in DNA. *Clin Cancer Res*. **6(4)**: 1394-4000
- Kreklau EL, Limp-Foster M, Liu N, Xu Y, Kelley MR and Erickson LC (2001). A novel fluorometric oligonucleotide assay to measure O6-methylguanine DNA methyltransferase, methylpurine DNA glycosylase, 8-oxoguanine DNA glycosylase and abasic endonuclease activities: DNA repair status in human breast carcinoma cells overexpressing methylpurine DNA glycosylase. *Nucleic Acids Res*. **29(12)**: 2558-2566
- Krokan HE, Nilsen H, Skorpen F, Otterlei M and Slupphaug G (2000). Base excision repair of DNA in mammalian cells. *FEBS Lett*. **476(1-2)**: 73-7
- Langen RCJ, Korn SH and Wouters EFM (2003). ROS in the local and systemic pathogenesis of COPD. *Free Rad Biol Med*. **35(3)**: 226-235
- Leadon SA (1999). Transcription-coupled repair of DNA damage: unanticipated players, unexpected complexities. *Am J Hum Genet*. **64**: 1259-1263
- Lengauer C, Kinzler KW, and Vogelstein B (1998). Genetic instabilities in human cancers. *Nature*. **396**: 643-649
- Le Page F, Kwoh EE, Avrutskaya A, Gentil A, Leadon SA, Sarasin A and Cooper PK (2000). Transcription-coupled repair of 8-oxoGuanine: requirement for XPG, TFIIH and CSB and implications for Cockayne syndrome. *Cell*. **101**: 159-171
- Li DL, Zhang W, Zhu J, Chang P, Sahin A, Singletary E, Bondy M, Hazra T, Mitra S, Lau SS, Shen J and DiGiovanni J (2001). Oxidative DNA damage and 8-hydroxy-2'-deoxyguanosine DNA glycosylase/apurinic lyase in human breast cancer. *Mol Carcinogenesis*. **31**: 214-223
- Loft S and Poulsen HE (1996). Cancer risk and oxidative DNA damage in man. *J Mol Med* **74(6)**: 297-312
- Loft S and Poulsen HE (1999). Markers of oxidative damage to DNA: antioxidants and molecular damage. *Met Enzymol*. **300**: 166-84
- Loft S and Poulsen HE (2000). Antioxidant intervention studies related to DNA damage, DNA repair and gene expression. *Free Rad Res*. **33**: S67-83

References

- Lunec J, Holloway KA, Cooke MS, Faux S, Griffiths HR and Evans MD (2002). Urinary 8-oxo-2'-deoxyguanosine: Redox regulation of DNA repair in vivo? *Free Rad Biol Med.* **33(7)**: 875-885
- Maeda T, Chua PPS, Chong MT, Sim ABT, Nikaido O and Tron VA (2001). Nucleotide excision repair genes are upregulated by low-dose artificial ultraviolet B: Evidence of a photoprotective SOS response? *J Investigative Dermatol.* **117(6)**: 1490-1497
- Malins DC. and Haimanot R (1991). Major alterations in the nucleotide structure of DNA in cancer of the female breast. *Cancer Res.* **51**: 5430-5432
- Mambo E, Nyaga SG, Bohr VA and Evans MK (2002). Defective repair of 8-hydroxyguanine in mitochondria of MCF-7 and MDA-MB-468 human breast cancer cell lines. *Cancer Res.* **62**: 1349-1355
- Marenstein DR, Ocampo MTA, Chan MK, Altamirano A, Basu AK, Boorstein RJ, Cunningham RP and Teebor GW (2001). Stimulation of human endonuclease III by box-binding protein 1 (DNA-binding protein B). *J Biol Chem.* **276(24)**: 21242-21249
- Marenstein DR, Chan MK, Altamirano A, Basu AK, Boorstein RJ, Cunningham RP and Teebor GW (2003). Substrate specificity of human endonuclease III (hNTH1). *J Biol Chem.* **278(11)**: 9005-9012
- Margison GP, Povey AC, Kaina B and Santibáñez Koref M F (2003). Variability and regulation of O6-alkylguanine-DNA alkyltransferase. *Carcinogenesis.* **24(4)**: 625-635
- Marnett LJ (2000). Oxyradicals and DNA damage. *Carcinogenesis.* **21(3)**: 361-70
- Martindale JL and Holbrook NJ (2002). Cellular responses to oxidative stress: signaling for suicide and survival. *J Cell Physiol.* **192**: 1-15
- Martinet W, Knaapen MWM, De Meyer GRY, Herman AG and Kockx MM (2002). Elevated levels of oxidative DNA damage and DNA repair enzymes in human atherosclerotic plaques. *Circulation.* **106**: 927-932
- Martins EAL. and Meneghini R (1990). DNA Damage and lethal effects of hydrogen-peroxide and menadione in chinese hamster-cells - distinct mechanisms are involved. *Free Rad Biol Med.* **8(5)**: 433-440
- Matsumoto Y, Zhang Q-M, Takao M, Yasui A and Yonei (2001). *Escherichia coli* Nth and human hNTH1 DNA glycosylases are involved in removal of 8-oxoguanine from 8-oxoguanine/guanine mispairs in DNA. *Nucl Acids Res.* **29(9)**: 1975-1981
- May P and May E (1999). Twenty years of p53 research: structural and functional aspects of the p53 protein. *Oncogene.* **18**: 7621-7636

References

- McCullough AK, Dodson ML and Lloyd RS (1999). Initiation of base excision repair: glycosylase mechanisms and structures. *Annu Rev Biochem.* **68**: 255-285
- McKay BC, Ljungman M and Rainbow AJ (1999). Potential roles for p53 in nucleotide excision repair. *Carcinogenesis.* **20(8)**: 1389-1396
- Mendez F, Sandigursky M, Kureekattil RP, Kenny MK, Franklin WA and Bases R (2003). Specific stimulation of human apurinic/apyrimidinic endonuclease by heat shock protein 70. *DNA Repair.* **2**: 259-271
- Michiels C, Minet E, Mottet D and Raes M (2002). Regulation of gene expression by oxygen: NF- κ B and HIF-1, two extremes. *Free Rad Biol Med.* **33(9)**: 1231-1242
- Mistry P and Herbert KE (2003). Modulation of hOGG1 DNA repair enzyme in human cultured cells in response to pro-oxidant and antioxidant challenge. *Free Rad Biol Med.* **35(4)**: 397-405
- Mitra S, Izumi T, Boldogh I, Bhakat KK, Hill JW and Hazra TK (2002). Choreography of oxidative damage repair in mammalian genomes. *Free Rad Biol Med.* **33(1)**: 15-28
- Nakabeppu Y (2001). Molecular genetics and structural biology of human MuT homolog, MTH1. *Mutat Res.* **477**: 59-70
- Nigg EA (1995). Cyclin-dependent protein kinases: key regulators of the eukaryotic cell cycle. *Bioessays.* **17(6)**: 471-480
- Nilsen H and Krokan HE (2001). Base excision repair in a network of defence and tolerance. *Carcinogenesis.* **22(7)**: 987-998
- Nouspikel T and Hanawalt PC (2002). DNA repair in terminally differentiated cells. *DNA Repair.* **1(1)**: 59-75
- Offer HR, Wolkowicz R, Matas D, Blumenstein S, Livneh Z and Rotter V (1999). Direct involvement of p53 in the base excision repair pathway of the DNA repair machinery. *FEBS Lett.* **450(3)**: 197-204
- Offer H, Zurer I, Banfalvi G, Reha'k M, Falcovitz A, Milyavsky M, Goldfinger N and Rotter V (2001). p53 Modulates base excision repair activity in a cell cycle- specific manner after genotoxic stress. *Cancer Res.* **61(1)**: 88-96
- Okamoto K, Toyokuni S, Uchida K, Ogawa O, Takeenewa J, Kakehi Y, Kinoshita H, Hattori-Nakakuki Y, Hiai H and Yoshida O (1994). Formation of 8-hydroxy-2'-deoxyguanosine and 4-hydroxy-2-nonenal-modified proteins in human renal-cell carcinoma. *Int J Cancer.* **58(6)**: 825-829

References

- Okamoto K, Toyokuni S, Kim WJ, Ogawa O, Kakehi Y, Arao S, Hiai H and Yoshida O (1996). Overexpression of human mutT homologue gene messenger RNA in renal-cell carcinoma: evidence of persistent oxidative stress in cancer. *Int J Cancer*. **65(4)**: 437-441
- Osterod M, Larsen E, Le Page F, Hengstler JG, Van Der Horst GT, Klunghand I and Epe B (2002). A global DNA repair mechanism involving the Cockayne syndrome B (CSB) gene product can prevent the in vivo accumulation of endogenous oxidative DNA base damage. *Oncogene*. **21(54)**: 8232-8239
- Otterlei M, Warbrick E, Nagelhus TA, Haug T, Slupphaug G, Akbari M, Aas PA, Steinsbekk K, Bakke O and Krokan HE (1999). Post-replicative base excision repair in replication foci. *EMBO J*. **18(13)**: 3834-3844
- Pflaum M, Kielbassa C, Garmyn M and Epe B (1998). Oxidative DNA damage induced by visible light in mammalian cells: extent, inhibition by antioxidants and genotoxic effects. *Mutat Res*. **408**: 137-146
- Prasad R, Lavrik OI, Kim S-J, Kedar P, Yang X-P, Berg BJV and Wilson SH (2001). DNA polymerase beta -mediated long patch base excision repair. *J Biol Chem*. **276(35)**: 32411-32414
- Ramana CV, Boldogh I, Izumi T and Mitra S (1998). Activation of apurinic/aprimidinic endonuclease in human cells by reactive oxygen species and its correlation with their adaptive response to genotoxicity of free radicals. *Proc Natl Acad Sci USA*. **95(9)**: 5061-5066
- Ravanat JL, Douki T, Duez P, Gremaud E, Herbert K, Hofer T, Lasserre L, Saint-Pierre, Favier A and Cadet J (2002). Cellular background level of 8-oxo-7,8-dihydro-2'-deoxyguanosine: an isotope based method to evaluate artefactual oxidation of DNA during its extraction and subsequent work-up. *Carcinogenesis*. **23(11)**: 1911-1918
- Reardon JT, Bessho T, Kung HC, Bolton PH and Sancar A (1997). *In vitro* repair of oxidative DNA damage by human nucleotide excision repair system: Possible explanation for neurodegeneration in Xeroderma pigmentosum patients. *Proc Natl Acad Sci USA*. **94(17)**: 9463-9468
- Rusyn I, Denissenko MF, Wong VA, Butterworth BE, Cunningham ML, Upton PB, Thurman RG and Swenberg JA (2000). Expression of base excision repair enzymes in rat and mouse liver is induced by peroxisome proliferators and is dependent upon carcinogenic potency. *Carcinogenesis*. **21(12)**: 2141-2145
- Saitoh T, Shinmura K, Yamaguchi S, Tani M, Seki S, Murakami H, Nojima Y and Yokota (2001). Enhancement of OGG1 protein AP lyase activity by increase of APEX protein. *Mutat Res*. **486**: 31-40

References

- Sakai Y, Furuichi M, Takahashi M, Mishima M, Iwai S, Shirakawa M and Nakabeppu Y (2002). A Molecular Basis for the Selective Recognition of 2-Hydroxy-dATP and 8-Oxo-dGTP by Human MTH1. *J Biol Chem.* **277(10)**: 8579-8587
- Sancar A (1994). Mechanisms of DNA excision repair. *Science.* **266**: 1954-6
- Sancar A (1996). DNA excision repair. *Annu Rev Biochem.* **65**: 43-81
- Saparbaev M and Laval J (1994). Excision of hypoxanthine from DNA containing dIMP residues by the Escherichia coli, yeast, rat and human alkylpurine DNA glycosylases. *Proc Natl Acad Sci USA.* **91**: 5873-5877
- Sekiguchi M. and Tsuzuki T (2002). Oxidative nucleotide damage: consequences and prevention. *Oncogene.* **21(58)**: 8895-8904
- Shimoda R, Nagashima M, Sakamoto M, Yamaguchi N, Hirohashi S, Yokota J and Kasai H (1994). Increased formation of oxidative DNA damage, 8-hydroxyguanine, in human livers with chronic hepatitis. *Cancer Res.* **54(12)**: 3171-3172
- Smith TR, Miller MS, Lohman KK, Case LD and Hu JJ (2003). DNA damage and breast cancer risk. *Carcinogenesis.* **24(5)**: 883-889
- Stevnsner T, Nyaga S, de Souza-Pinto NC, van der Horst GT, Gorgels TG, Hogue BA, Thorslund T and Bohr VA (2002). Mitochondrial repair of 8-oxoguanine is deficient in Cockayne syndrome group B. *Oncogene.* **21(57)**: 8675-8682
- Therrien J-P, Drouin R, Baril C and Drobetsky EA (1999). Human cells compromised for p53 function exhibit defective global and transcription-coupled nucleotide excision repair, whereas cells compromised for pRb function are defective only in global repair. *Proc Natl Acad Sci USA.* **96(26)**: 15038-15043
- Tsuchimoto D, Sakai Y, Sakumi K, Nishioka K, Sasaki M, Fujiwara T and Nakabeppu (2001). Human APE2 protein is mostly localized in the nuclei and to some extent in the mitochondria, while nuclear APE2 is partly associated with proliferating cell nuclear antigen. *Nucl Acids Res.* **29(11)**: 2349-2360
- Tsurudome Y, Hirano T, Yamato H, Tanaka I, Sagai M, Hirano H, Nagata N, Itoh H and Kasai H (1999). Changes in levels of 8-hydroxyguanine in DNA, its repair and OGG1 mRNA in rat lungs after intratracheal administration of diesel exhaust particles. *Carcinogenesis.* **20(8)**: 1573-1576
- Tsuzuki T, Egashira A, Igarashi H, Iwakuma T, Nakatsuru Y, Tominaga Y, Kawate H, Nakao K, Nakamura K, Ide F, Kura S, Nakabeppu Y, Katsuki M, Ishikawa T and Sekiguchi M (2001). Spontaneous tumorigenesis in mice defective in the MTH1 gene encoding 8-oxo-dGTPase. *Proc Natl Acad Sci USA.* **98(20)**: 11456-11461

References

- Tuo J, Müftüoğlu M, Chen C, Jaruga P, Selzer RR, Brosch RM, Rodriguez H, Dizdaroglu M and Bohr VA (2001). The Cockayne syndrome group B gene product is involved in general genome base excision repair of 8-hydroxyguanine in DNA. *J Biol Chem.* **276(49)**: 45772-45779
- Tuo J, Chen C, Zeng X, Christiansen M and Bohr VA (2002). Functional crosstalk between hOgg1 and the helicase domain of Cockayne syndrome group B protein. *DNA repair.* **1**: 913-927
- Vidal AE, Hickson ID, Boiteux S and Radicella JP (2001). Mechanism of stimulation of the DNA glycosylase activity of hOGG1 by the major human AP endonuclease: bypass of the AP lyase activity step. *Nucl Acids Res.* **29(6)**: 285-1292
- Vogel U, Dybdahl M, Frenz G and Nexø BA (2000). DNA repair capacity: inconsistency between effect of over-expression of five NER genes and the correlation to mRNA levels in primary lymphocytes. *Mutat Res.* **461**: 197-210
- Volkert MR and Landini P (2001). Transcriptional responses to DNA damage. *Current Opinion Microbiol.* **4**: 178-185
- Wang Q, Zhu QZ, Wani MA, Wani G, Chen J and Wani AA (2003). Tumour suppressor p53 dependent recruitment of nucleotide excision repair factors XPC and TFIIH to DNA damage. *DNA Repair.* **2**: 483-499
- Wani G, Milo GE and D'Ambrosio (1998). Enhanced expression of the 8-oxo-7,8-dihydrodeoxyguanosine triphosphate gene in human breast tumour cells. *Cancer Lett.* **125**: 123-130
- Wani MA, Zhu QZ, El-Mahdy M and Wani AA (1999). Influence of p53 tumor suppressor protein on bias of DNA repair and apoptotic response in human cells. *Carcinogenesis.* **20(5)**: 765-772
- Whitehouse CJ, Taylor RM, Thistlethwaite A, Zhang H, Karimi-Busheri F, Lasko DD, Weinfeld M and Caldecott KW (2001). *Cell.* **104(1)**: 107-117
- Widlak P and Rzeszowska-Wolny (1999). Nuclear matrix and nucleotide excision repair: damage-recognition proteins are not constitutive components of the nuclear matrix. *Gene Ther Mol Biol.* **4**: 275-284
- Wilson DM and Thompson LH (1997). Life without DNA repair. *Proc Natl Acad Sci USA.* **94(24)**: 12754-12757
- Wilson DM and Barsky D (2001). The major human abasic endonuclease: formation, consequences and repair of abasic lesions in DNA. *Mutat Res.* **485**: 283-307
- Wittschieben BØ and Wood RD (2003). DDB complexities. *DNA Repair.* **2**: 1065-1069

References

- Wood RD (1999). DNA damage recognition during nucleotide excision repair in mammalian cells. *Biochimie*. **81(1-2)**: 39-44.
- Wood RD, Mitchell M, Sgouros J and Lindahl T (2001). Human DNA repair genes. *Science*. **291**: 1284-1289
- Xanthoudakis S and Curran T (1992). Identification and characterization of Ref-1, a nuclear protein that facilitates AP-1 DNA-binding activity. *EMBO J*. **11(2)**: 653-665
- Xanthoudakis S, Miao G, Wang F, Pan YC and Curran T (1992). Redox activation of Fos-Jun DNA binding activity is mediated by DNA repair enzyme. *EMBO J*. **11(9)**: 3323-3325
- Xanthoudakis S, Miao G and Curran T (1994). The redox and DNA-repair activities of Ref-1 are encoded by nonoverlapping domains. *Proc Natl Acad Sci USA*. **91**: 23-27
- Yamaguchi R, Hirano T, Asami S, Chung M-H, Sugita A and Kasai H (1996). Increased 8-hydroxyguanine levels in DNA and its repair activity in rat kidney after administration of a renal carcinogen, ferric nitrilotriacetate. *Carcinogenesis*. **17(11)**: 2419-2422
- Yamamoto F, Kasai H, Bessho T, Chung M-H, Inoue H, Ohtsuka E, Hori T and Nishimura S (1992). Ubiquitous presence in mammalian cells of enzymatic activity specifically cleaving 8-hydroxyguanine-containing DNA. *Jpn J Cancer Res*. **83**: 351-357
- Yao KS, Xanthoudakis S, Curran Y and O'Dwyer PJ (1994). Activation of AP-1 and of a nuclear redox factor, Ref-1 in the response of HT29 colon cancer cells to hypoxia. *Mol Cell Biol*. **14(9)**: 5997-6003
- Ye N, Bianchi MS, Bianchi NO and Holmquist GP (1999). Adaptive enhancement and kinetics of nucleotide excision repair in humans. *Mutat Res*. **435**: 43-61
- You H-J, Kim G-T, Kim Y-H, Chun Y-S, Park J, Chung M-H and Kim M-S (2000). Increased 8-hydroxyguanine formation and endonuclease activity for its repair in ischemic-reperfused hearts of rats. *J Mol Cell Cardiol*. **32**: 1053-1059
- Zienolddiny S, Ryberg D and Haugen A (2000). Induction of microsatellite mutations by oxidative agents in human lung cancer cell lines. *Carcinogenesis*. **21(8)**: 1521-1526